

University of New Hampshire

University of New Hampshire Scholars' Repository

Master's Theses and Capstones

Student Scholarship

Fall 2009

Temperature moderation in a coastal coldwater stream a study of surface water, groundwater and hyporheic zone interaction

Danna Butler Truslow

University of New Hampshire, Durham

Follow this and additional works at: <https://scholars.unh.edu/thesis>

Recommended Citation

Truslow, Danna Butler, "Temperature moderation in a coastal coldwater stream a study of surface water, groundwater and hyporheic zone interaction" (2009). *Master's Theses and Capstones*. 499.
<https://scholars.unh.edu/thesis/499>

This Thesis is brought to you for free and open access by the Student Scholarship at University of New Hampshire Scholars' Repository. It has been accepted for inclusion in Master's Theses and Capstones by an authorized administrator of University of New Hampshire Scholars' Repository. For more information, please contact Scholarly.Communication@unh.edu.

TEMPERATURE MODERATION IN A COASTAL COLDWATER
STREAM

A STUDY OF SURFACE WATER, GROUNDWATER AND
HYPORHEIC ZONE INTERACTION

BY

DANNA BUTLER TRUSLOW
BA/BS Geology/Hydrology
University of New Hampshire
1978/1982

THESIS

Submitted To The University Of New Hampshire
In Partial Fulfillment of
the Requirements for the Degree of

Master of Science

in

Hydrology

September, 2009

UMI Number: 1472085

INFORMATION TO USERS

The quality of this reproduction is dependent upon the quality of the copy submitted. Broken or indistinct print, colored or poor quality illustrations and photographs, print bleed-through, substandard margins, and improper alignment can adversely affect reproduction.

In the unlikely event that the author did not send a complete manuscript and there are missing pages, these will be noted. Also, if unauthorized copyright material had to be removed, a note will indicate the deletion.

UMI[®]

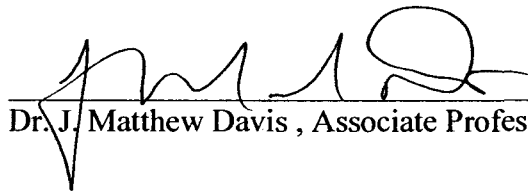
UMI Microform 1472085
Copyright 2009 by ProQuest LLC
All rights reserved. This microform edition is protected against
unauthorized copying under Title 17, United States Code.

ProQuest LLC
789 East Eisenhower Parkway
P.O. Box 1346
Ann Arbor, MI 48106-1346

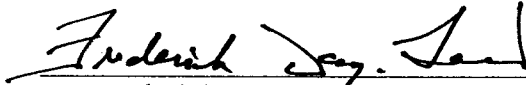
This thesis has been examined and approved.



Thesis Director, Jennifer M. Jacobs, Associate Professor of Civil Engineering



Dr. J. Matthew Davis , Associate Professor of Hydrogeology



Dr. Frederick Day-Lewis, Geophysicist, US Geological Survey

6/10/2009
Date

DEDICATION

I dedicate my thesis to my family. My parents, Thomas Grattan Butler and Margaret Hatch Butler, taught me the love of learning and encouraged curiosity. Our trips and adventures exploring the natural world inspired my chosen field. My husband Bill Truslow and children Hannah and Sam Truslow have patiently supported my pursuit of research and an advanced degree at an advanced age.

ACKNOWLEDGEMENTS

Thanks to my thesis advisor, Dr. Jennifer Jacobs, for her unflagging patience and encouragement and hours of fieldwork, number crunching and reviewing, and to Dr. Matt Davis for sharing his expertise in groundwater, field work and heat flow modeling and assistance with field equipment. Dr. Fred Day-Lewis, of US Geological Survey (USGS) gave generously of his time and expertise, and he provided the geophysical and fiber-optic instrumentation that made such a difference to the project.

Thanks to the USGS, Geophysical Branch in Storrs, CT and geophysicist Carole Johnson for providing the field instrumentation and devoting many days of field work during the geophysical and FODTS field campaigns. Landowners Phillip and Gail Sanborn gave unrestricted access to their land for this research, and without it, the work would not have been accomplished. Thanks for mowing and moving the electric fence, too.

Thanks to Dr. Joseph Licciardi for his field visit and assistance with site geomorphology. Thanks to Drs. Tom Ballestero and Rob Roseen for providing mini-piezometers, flumes, and data loggers for the 2007 field campaigns. Dr. David Burdick loaned the Lasermark survey equipment for several days of field work. Thanks to the NCALM group at University of Florida and University of California at Berkeley for choosing this project for seed grant funding. Thanks

particularly to Michael Sartori and Sidney Schofield at NCALM, Florida, for completing the fieldwork and data processing when I really needed it and kindly responding to my multiple inquiries.

Finally, thanks for the hours of field work and analysis assistance by Sam Truslow, Ellen Douglas, Dan Coons, Gary LeMay, Kerry Schorzman, George Fowler, Pallavi Mittal, Hwan Hee Han, Ram Ray, Lee Friess, Matt Farfour, John Reed, and John Duncan.

TABLE OF CONTENTS

DEDICATION	iii
ACKNOWLEDGEMENTS	iv
LIST OF TABLES.....	ix
LIST OF FIGURES.....	xi
ABSTRACT	xvi
CHAPTER 1	1
INTRODUCTION	1
Introduction	1
The hyporheic zone	2
Biogeochemistry and the hyporheic zone.....	4
Ecological functions of the hyporheic zone	5
Stream geomorphology and the hyporheic zone	5
Influences on stream temperature.....	7
Subsurface heat flow and stream temperature	8
Regions of hyporheic zone and stream temperature research	10
Measuring hyporheic zone extent and flux.....	12
Heat as a tracer of subsurface flow	15
Hyporheic flow modeling	17
Hyporheic corridors.....	19
Research objectives	20
CHAPTER 2	25
SITE DESCRIPTION AND SETTING.....	25
Site description.....	25
Land use	25
Riparian canopy	26
Hydrologic setting	27
Surface water	27
Groundwater.....	29
Geologic setting.....	30
CHAPTER 3	37
METHODOLOGY	37
Research approach.....	37
Field methods.....	39
Introduction.....	39
Geomorphic surveys and measurements.....	41

Streambed depth measurements	44
Pebble counts.....	45
Meteorologic data collection	45
Tree canopy measurements	46
Hydrologic measurements.....	47
Stream flow.....	47
Groundwater levels.....	49
Stream/hyporheic zone gradients.....	49
Temperature measurements	51
Hobo temperature data loggers.....	52
Mini-piezometers thermocouples.....	55
Fiber-Optic Distributed Temperature Sensor Survey.....	57
Topographic LIDAR mapping	60
Data analysis and evaluation methods.....	62
Graphical analyses.....	62
ArcGIS and ArcHydro analysis.....	62
Hydraulic gradient calculations.....	65
Statistical analysis.....	65
Temperature amplitude analysis.....	66
Time stability analyses.....	66
Heat budget calculations	69
Heat budget modeling	75
Modeled sub-reaches.....	76
Model data.....	76
Estimation of flux component temperature change.....	81
Sensitivity analysis.....	82
CHAPTER 4	91
RESULTS.....	91
Introduction	91
Catchment geomorphology	91
Stream gradients and depths of streambed alluvium.....	92
Catchment surficial geology.....	96
Stream cross sections and stream classification.....	99
Stream flow.....	103
Measured stream flow.....	103
Digital elevation model flow stream flow analysis.....	105
Experimental results	110
Weather conditions.....	110
Tree canopy density.....	112
Hyporheic temperature amplitude analysis.....	112
Streambed hydraulic potential.....	113
WHB stream water temperatures.....	119
Wednesday Hill Brook sub-reach descriptions	128
Designation of sub-reaches.....	128

Reach 1	129
Reach 2	132
Reach 3	136
Reach 4	140
Reach 5	144
Reach 6	149
Study reach summary	152
Time stability analysis.....	154
Heat budget model.....	158
Heat budget simulation.....	162
Small scale heat budgets – Reach 1a and 2a.....	170
Summary of heat budget modeling.....	174
Sensitivity analysis	175
CHAPTER 5	238
DISCUSSION	238
Introduction	238
Spatial and temporal distribution of temperature	239
Vertical hyporheic extent and hyporheic exchange coefficients	241
Geomorphology and stream temperature.....	243
Catchment influences on stream temperature.....	245
Stream channel morphology and stream temperature.....	247
Heat budget modeling	250
FODTS surveys for stream hydrology and temperature research.....	255
Data deficiencies and additional data needs	257
Streamflow measurement and ArchHydro analysis.....	257
Vertical hydraulic gradient data	257
Floodplain and valley geomorphology.....	259
Recommendations for stream temperature measurement	259
Coldwater stream habitat and groundwater.....	261
Section 6.....	264
CONCLUSIONS	264
References Cited	268
Appendix A - Data Tables	280
Appendix B – Additional graphics.....	296

LIST OF TABLES

Table		Page
Table 3-1	Measurement device installation details and locations	84-87
Table 3-2	Mini-piezometer installation details and locations	87-89
Table 3-3	Estimated thermal conductivity values base on Streambed material properties	73
Table 3-4	Modeling steps used to estimate heat budget contributions in sub-reaches	79
Table 4-1	Stream characteristics and Rosgen stream classification	102
Table 4-2	Tributary delineation and streamflow estimates – ArchHydro analysis	107
Table 4-3	Estimate of diffuse discharge from box valley and floodplain – ArchHydro analysis	109
Table 4-4	Amplitude of diurnal temperature measurements in Wednesday Hill Brook and streambed, Lee, NH	113
Table 4-5	Mean vertical hydraulic gradients at piezometers – August 17 to October 14, 2007	115
Table 4-6	Monitoring well construction details	116
Table 4-7	Summary statistics – groundwater temperatures	117
Table 4-8	Summary statistics for stream temperatures measured with Hobo dataloggers	123
Table 4-9	Preliminary tributary, seep and spring temperatures – August 14, 2007	125
Table 4-10	Summary statistics for tributaries	126
Table 4-11	Summary of sub-reach 1 stream characteristics	130

Table		Page
Table 4-12	Summary of sub-reach 2 stream characteristics	133
Table 4-13	Summary of sub-reach 3 stream characteristics	138
Table 4-14	Summary of sub-reach 4 stream characteristics	142
Table 4-15	Summary of sub-reach 5 stream characteristics	145
Table 4-16	Summary of sub-reach 4 stream characteristics	150
Table 4-17	Summary of streambed conduction at piezometers	161
Table 4-18a	Results of heat budget modeling – Reach 1	163
Table 4-18b	Results of heat budget modeling – Reach 2	164
Table 4-18c	Results of heat budget modeling – Reach 4	166
Table 4-18d	Results of heat budget modeling – Reach 5	167
Table 4-19	Stream temperature change and discharge values due to advective and non-advective heat sources	169
Table 4-20	Results of heat budget modeling – Reach 1a and 2a	172

LIST OF FIGURES

Figure	Page
Figure 1-1 The hyporheic zone and catchment hydrology	23
Figure 1-2 Hyporheic flow path lengths and residence times	24
Figure 2-1 Site location map, Wednesday Hill Brook in Lee, NH	34
Figure 2-2 Wednesday Hill Brook watershed area	35
Figure 2-3 Surficial geologic map of the Wednesday Hill Brook study Area	36
Figure 3-1 Location of measurement devices on Wednesday Hill Brook in Lee, NH	90
Figure 4-1 Upper study reaches	178
Figure 4-2 Middle valley study reaches	179
Figure 4-3 Lower valley study reaches	180
Figure 4-4 Longitudinal profile and sediment depths on study reach	181
Figure 4-5 Pebble counts of streambed sediments at 100-meter reaches	182
Figure 4-6 Streambed electrical conductance and streambed sediment depths in study reach	183
Figure 4-7 Stream cross-section at 145, 165, and 167 m a, b and c	184
Figure 4-7 Stream cross section at 237, 334 and 512 m d, e & f	185
Figure 4-8a Valley cross-section at 200 and 453 m	186

List of Figures (continued)

Figure		Page
Figure 4-8b	Valley cross-section at 200 and 453 m	187
Figure 4-9	Stream flow measurements on study reach August to October 2007	188
Figure 4-10	Stream flow measurements on study reach August to October 2008	189
Figure 4-11	Sub catchment and streams	190
Figure 4-12	Stream flow accumulation – sinks unfilled filled - calculated using ArchHydro tools on LiDAR DEM	191
Figure 4-13a	Air Temperature during field campaigns – August to October, 2007	192
Figure 4-13 b	Precipitation and relative humidity during field campaigns – August to October 2007	193
Figure 4-13c	Wind speeds during field campaigns – August to October 2007	194
Figure 4-13d	Solar and net radiation during field campaigns – August to October 2007	195
Figure 4-14a	Vertical hydraulic gradients at mini-piezometers 167 to 336 m, August to October 2007	196
Figure 4-14b	Vertical hydraulic gradients at mini-piezometers 370 to 634 m, August to October 2007	197
Figure 4-15	Monitoring well field temperatures – August and September 2007	198
Figure 4-16	Monitoring well field temperatures – 2005 to 2007	199
Figure 4-17	Average FO-DTS temperature measurements along the study reach showing log dam temperature spikes, August 22 to August 29, 2007	200

List of Figures (continued)

Figure		Page
Figure 4-18	Average FO-DTS temperature measurements and standard deviations along study reach – edited August 22 to August 29, 2007	201
Figure 4-19	Average FO-DTS temperature measurements and standard deviations from both field campaigns along study reach – edited, August to October 2007	202
Figure 4-20	Reach 1 - box and whisker plots of stream temperature measurements 75 m to 634 m, August to September 2007	203
Figure 4-21	Mean Temperature vs. Standard deviation, FODTS and Hobo stream temperature measurements, Wednesday Hill Brook in Lee, NH	204
Figure 4-22	Stream temperatures in the Upper study reach 75 to 276 m. August to September 2007	205
Figure 4-23	Stream temperatures in the middle study reach 294 to 372 m August to September 2007	206
Figure 4-24	Stream temperature measurements from the middle study reach 413 to 445 m August to September 2007	207
Figure 4-25	Stream temperature measurements in the lower study reach 461 to 491 m August to September 2007	208
Figure 4-26	Stream temperature measurements from the lower study reach 518 to 634 m August to September 2007	209
Figure 4-27	Tributaries and data logger locations plotted on FC-07-1 FO-DTS temperature trend line	210
Figure 4-28	Tributary temperatures August to September 2007	211
Figure 4-29	Reach 2 - box and whisker plot of mini-piezometer temperatures 167 and 171 m,	212
Figure 4-30	Stream and hyporheic zone temperatures at 237 m, August to September 2007	213

List of Figures (continued)

Figure		Page
Figure 4-31	Amplitudes of diurnal temperature fluctuation – stream and streambed temperatures	214
Figure 4-32	Reach 3 - box and whisker plot of mini-piezometer temperatures - 257, 268, 276, 293 and 295 m	215
Figure 4-33	Stream and hyporheic zone temperatures at 257 m, August to September 2007	216
Figure 4-34	Stream and hyporheic zone temperatures at 268 m, August to September 2007	217
Figure 4-35	Stream and hyporheic zone temperatures at 276 m, August to September 2007	218
Figure 4-36	Stream and hyporheic zone temperatures at 293 m, August to September 2007	219
Figure 4-37	Reach 4 - box and whisker plot of mini-piezometer Temperatures, 334 and 336 m,	220
Figure 4-38	Stream and hyporheic zone temperatures at 336 m, August to September 2007	221
Figure 4-39	Stream and hyporheic zone temperatures at 370 m, August to September 2007	222
Figure 4-40	Stream and hyporheic zone temperatures at 372 m, August to September 2007	223
Figure 4-41	Reach 5 - box and whisker plot of mini-piezometer temperatures, 413 to 443 m	224
Figure 4-42	Reach 5 - box and whisker plot of mini-piezometer temperatures, 461 to 491 m,	225
Figure 4-43	Reach 5 - box and whisker plot of mini-piezometer temperatures, 510 to 634 m,	226

List of Figures (continued)

Figure		Page
Figure 4-44	Mean relative differences in FODTS temperature along study reach, August 22 to August 28, 2007	227
Figure 4-45	Mean relative difference in FODTS temperature along study reach without armored reach, August 22 to 29, 2007	228
Figure 4-46	Mean relative difference distribution of temperature classified by reach	229
Figure 4-47	Mean relative difference distribution of temperature classified by D50 streambed sediment grain size	230
Figure 4-48	Mean relative difference distribution of temperature classified by streambed morphology	231
Figure 4-49	Non-advective and advective components of stream temperature heat budget	232
Figure 4-50	Non-advective heat flux at 336 m 8/22 to 8/29/2007	233
Figure 4-51	Temperature change by mechanism and reach	234
Figure 4-52	Groundwater and tributary discharge estimates – heat budget model	235
Figure 4-53	Modeled temperature change in Wednesday Hill Brook due to advective and non-advective heat fluxes – Reach 1a and 2a	236
Figure 4-54	Heat budget model sensitivity analysis - Thermal conductivity, hyporheic zone temperature and hyporheic exchange coefficient	237

ABSTRACT

TEMPERATURE MODERATION IN A COASTAL COLDWATER STREAM

A STUDY OF SURFACE WATER, GROUNDWATER AND HYPORHEIC ZONE INTERACTION

by

Danna Butler Truslow

University of New Hampshire, September 2009

A fiber-optic distributed temperature sensor (FODTS) survey was conducted along a 520 m reach of Wednesday Hill Brook (WHB) in Lee, NH, a first order tributary to the Lamprey River. These data were supplemented by stream and streambed temperature and vertical hydraulic gradient data collection at 35 piezometers, and continuous and periodic measurement of tributary, stream, and groundwater temperatures and streamflow. An under-canopy weather station provided on-site meteorologic data, and a LiDAR survey provided high definition land surface topographic data for interpretation of geomorphology. A heat budget model was developed and used to estimate the advective components of heat flow to and from the stream.

The FODTS survey describes a stream that experiences a late summer mean temperature drop of over 2°C within the first 150 m and a sustained temperature

of less than 13.5°C in the lower 350 m. Multiple local variations in temperature are detected in the lower portion of the reach. Streambed temperatures and hydraulic gradient data suggest that vertical hyporheic exchange is predominantly found in the upper 200 m. Exchange penetrates to 20 cm in most of the reach but is greater than 40 cm in a few locations and plays a large role in temperature reduction.

Groundwater discharge in these upper reaches is also substantial and is focused in spring brook discharge areas. A substantial sand and gravel deposit of late glacial origin (Birch, 1989) discharges along the base of the western hillslope near its contact with overlying marine silt and clay (Goldsmith, 1990). A shallow bedrock bowl suggested by an EM survey also underlies this upper catchment area. The bedrock lip coincides with valley constriction and a sudden change in stream direction. Vertical hyporheic exchange decreases downstream.

Exchange is most active at instream log and debris dams in the lower reaches. Groundwater discharge along preferential flow pathways is prevalent in this lower catchment area.

A heat budget analysis quantifies non-advective influences, net radiation, convection, evaporation, friction and streambed conduction, and advective influences, hyporheic exchange and tributary and groundwater discharge.

Temperature gains within 4 sub reaches were dominated by net radiation, which

accounted for nearly 50% of heat gain. Convection and evaporation (condensation) made up most of the remaining heat gain. Friction was an insignificant influence. Tributaries added modest heat gains in the lower reaches. Heat losses were dominated by hyporheic exchange (50 to 85%) and groundwater discharge (14 to 40%) in the upper reaches with tributary discharge and streambed conduction making up the balance of heat loss. In the middle and lower reaches, groundwater discharge accounted for 56% of heat loss with streambed conduction making up 37 to 44%. Hyporheic exchange did not provide heat loss in the middle reach and accounted for only 6% of the heat loss in the lower reach.

Two localized zones of significant heat loss were identified in the upper 150 m of stream. Here, groundwater and tributary discharge were focused at the outflow of two spring brooks flowing from the western valley. The influences of hyporheic exchange and streambed conduction are maximized where these tributary/groundwater discharge points cool both the stream and the streambed. On a smaller scale, this same symbiotic cooling effect is active in the lower reach where zones of preferential flow discharge cool groundwater to the stream. In this study reach, vertical hyporheic exchange provides the greatest cooling mechanism and groundwater discharge is the underlying temperature control.

The temperature delineation made possible by the FODTS stream temperature provided the resolution needed to define focused groundwater discharge and hyporheic cooling zones. This detailed temperature survey tool may re-define our understanding of groundwater discharge regimes. The research also demonstrates the importance of small-scale geomorphic features and hydrologic mechanisms in low order and headwater streams and underscores their value in supporting fresh water ecosystems, nutrient cycling and water resource protection.

CHAPTER 1

INTRODUCTION

Introduction

Streams and rivers contain 0.02% of the world's available freshwater resources with wetlands, lakes and groundwater making up the remaining 99.98% percent (Winter et al., 1998). Though they are a small percentage of the world's total fresh water, streams are a visible reminder of the natural world even in an urbanized setting. Yet, streams cannot be defined only by the water flowing at the surface. An important zone of storage and flow can surround these streams and can add two to three times to the total volume of available stream flow (Harvey and Wagner, 2000). This zone, the hyporheic zone, provides a critical hydrologic, biological and biogeochemical environment for stream systems (Brunke and Gonser, 1998).

Streams flow from high to lower elevation and, depending on streambed materials and stream gradient, develop a step-pool, riffle-pool, or plane bed morphologic pattern (Leopold et al., 1972). In the hyporheic zone, water also moves from high to low head through the pore spaces in streambed materials. Flowing stream water typically moves into the hyporheic zone at riffles and steps then returns to the stream at pools and other depressions. This dynamic

hydrologic interface located beneath and adjacent to streams allows shallow groundwater and stream water to exchange along flow paths centimeters to tens of meters in length (Bencala, 1993; Harvey and Wagner, 2000). Streambed topography, water surface gradient, hydraulic conductivity, bed roughness, groundwater contribution, and hydraulic gradient control the exchange of water between the stream and streambed (Vaux, 1968; Harvey and Wagner, 2000; Stonestrom and Constantz, 2003; Storey et al., 2003, Anderson et al., 2005; Grieg et al., 2007).

The hyporheic zone

In the context of the research presented here, the “hyporheic zone” refers to the region beneath and adjacent to a stream where *active* exchange of water between the stream and subsurface is occurring. As reviewed by Woessner (2000), stream and river floodplain systems are influenced by groundwater flow from surrounding upland areas, groundwater flow within a floodplain, near-stream groundwater discharge, and hyporheic zone flow. The groundwater-surface water-hyporheic system is a “single resource” (Winter et al., 1998) with transfer of water between them taking place on multiple scales. Figure 1-1 illustrates the relationship of the hyporheic zone to the other groundwater and stream system components.

The hyporheic zone can vary horizontally and vertically over time due to changes in streamflow and relative groundwater contribution to the zone. Storey et al. (2003) found that changes in baseflow throughout the year could change small scale hyporheic flux around riffles and pools and that changing hydraulic conductivity due to temperature change, changes in stream stage, and aquifer discharge could combine to reduce hyporheic exchange flux by 10 to 30 times. Harvey and Bencala (1993) also saw changes in hyporheic extent and flux due to precipitation events and resulting interflow to streams.

Stream and hyporheic zone environments can be described much like a biological community, patchy and diverse, with flow, chemical conditions, temperature, and streambed morphology changing over short distances laterally, vertically, and longitudinally. This heterogeneity leads to diverse biological communities with multiple ecotones and an active biogeochemical environment (Poole, 2002).

The hyporheic zone literature includes descriptions and analysis of the chemical, biological, and physical processes active in this linked stream and groundwater system. Since the earliest studies of the hyporheic zone, interstitial flow, and salmonid spawning habitat (Vaux, 1962, 1968), hyporheic research documents the unique characteristics of this zone, described below, as compared to

streams, riparian zones, and hillslopes (Bencala, 1993; Hakenkamp et al., 1993; Vallett, 1993; Boulton et al., 1998; Woessner, 2000; Findlay, 2005).

Biogeochemistry and the hyporheic zone

Nutrient transformation and retention, movement of dissolved oxygen, and solute transport are biogeochemical processes that occur in the hyporheic zone and can modify stream water chemistry and influence biological activity (Findlay, 1995, Chestnut and McDowell, 2000; Hall et al., 2002). The transformation of nitrogen and carbon from organic matter in the hyporheic zone are nutrients of particular interest in coastal New Hampshire (NHDES, 2009) where nitrogen is the limiting nutrient. The contact of slower moving interstitial water in the streambed with biologically and chemically rich sediments enhances stream biogeochemical activity (Harvey and Wagner, 2000). Sediment scale and reach scale biogeochemical mechanisms in the hyporheic zone can have a significant impact on nutrient and dissolved oxygen availability which, in turn, affects biological activity (Boulton et al., 1998; Lautz and Siegel, 2006). Dissolved oxygen can move into the hyporheic zone from stream water inflow. Hyporheic flow from areas of these oxic to anoxic zones over short distances (sediment scale) provides the conditions for nutrient transformation. The available dissolved nutrients then affect biological activity in the hyporheic zone and the stream as water returns to the stream (reach scale) (Harvey and Wagner, 2000).

Ecological functions of the hyporheic zone

Stream and streambed biomass and ecological functions are also closely tied to exchange between streams and groundwater (Hendricks, 1993; Brunke and Gonser, 1997; Boulton et al., 1998). The hyporheic zone provides refuge for many aquatic organisms including spawning and larval habitat for invertebrates and fish (Vaux, 1968; Hakenkamp et al., 1993; Valett, 1993; Dent et al., 2000). Microbes and periphyton are abundant in the hyporheic zone (Findlay, 2005). The availability of nutrients, oxygen, and interstitial flow in exchange zones is linked to the abundance of hyporheic dwellers (Hendricks, 1993; Dent et al., 2000). Macrophytes, fish and stream dwelling mammals can also modify the hyporheic zone to optimize their habitat (Hendricks and White, 1988; Grieg, 2007). Fish, especially salmonids, require thermally cool and stable areas for spawning and development (Powers et al., 1999; Ebersole, 2003).

Stream geomorphology and the hyporheic zone

Streambed physical characteristics and stream geomorphology play a major role in the lateral and vertical extent of hyporheic flow and the rate of flux into and out of the streambed (Harvey and Bencala, 1993; Kashahara and Wondzell, 2003; Anderson et al., 2005). In early studies of stream water and streambed exchange, Vaux (1968) found that when downwelling stream water enters the

porous streambed it is initially turbulent, but below this turbulent zone it behaves according to Darcy's law of flow in porous media (Freeze and Cherry, 1979). Vaux (1968) developed a laboratory simulation of streambed flow in convex, linear, and concave longitudinal profiles (the idealized geometry of the streambed along the slope of downstream flow). He demonstrated that downwelling, or movement of stream water into the streambed, occurred in a convex profile. A concave profile yields upwelling (flow back to the stream) at the break in slope, and a flat streambed segment yielded neither upwelling nor downwelling flow.

Vaux (1968) also showed that a sigmoid streambed surface, where two breaks in streambed slope occur, creates downwelling at the positive slope break and upwelling at the negative break. This sigmoid surface closely approximates the riffle run pool or step run pool morphology common in streams. Finally, he showed that a partially penetrating impermeable barrier, which is analogous to the presence of a natural rock or log dam, creates a vertically variable downwelling and upwelling pattern. The mechanism of stream/streambed exchange flow is analogous to larger scale patterns of groundwater recharge and discharge due to land surface topography as described by Toth (1963) and Freeze and Witherspoon (1967).

Influences on stream temperature

Natural influences on stream temperature include shading (solar radiation), rainfall, air temperature, groundwater discharge, hillslope hydrology, and hyporheic exchange (Poole and Berman, 2001; Webb and Zhang, 2004).

Manmade influences include several major factors including impoundment, water withdrawals and returns, runoff, and land use. Urbanization, agriculture and forestry practices have all been found to affect stream temperature through the disturbance of hydrologic processes, streambed modification and canopy removal (Poole and Berman, 2001; Webb and Zhang, 2004).

Johnson (2004) and Story et al. (2003) both found that although canopy shading was important, streambed characteristics and hyporheic flow significantly affected diurnal and longitudinal stream temperature changes along a reach.

Biologists and fisheries managers have also long recognized the importance of stream temperature to fish populations. Both groundwater and hyporheic exchange have been identified as major factors in the maintenance of coldwater habitats for species such as salmon and trout (Power et al., 1999, Tetzlaff et al., 2005). Chu et al. (2008) developed a geographic information systems (GIS) model for Ontario fisheries that links sustainable coldwater fish habitat and geology and which recognizes the importance of groundwater contribution to coldwater streams.

Subsurface heat flow and stream temperature

Groundwater contribution to and hyporheic exchange within a streambed influences stream temperature temporally and spatially. Heat, like water, flows by advection and conduction (Anderson, 2005). Streams respond quickly to conduction of heat from the air and solar radiation as well as advection of heat from precipitation, runoff, and point sources. Stream water temperatures vary widely, diurnally and annually, in response to these heat sources (Lapham, 1989; Stonestrom and Constantz, 2003; Johnson, 2004; Hatch et al., 2007). In contrast, subsurface and groundwater temperatures are more stable and are generally close to the average annual air temperature (Lapham, 1989; Brunke and Gonser, 1997; Malard et al., 2001).

Hyporheic zone temperatures reflect the mixing (through advection and conduction) of heat between the surface water and groundwater flowing into and out of the hyporheic zone. In summer, surface waters can be cooled by discharge of cooler groundwater, but can also be cooled by heat conduction from the stream to the streambed due to temperature gradients and streambed material properties. During the winter, heat conduction and groundwater discharge can warm surface water as heat flows from the warmer streambed and

groundwater discharge (Cozzetto et al., 2006). In summary, hyporheic exchange and streambed heat conduction can strongly influence stream temperature.

The temperature distribution within a stream and streambed also plays an important role in stream ecological function processes (White, 1993; Winter et al., 1998; Stonestrom and Constantz, 2003, Hannah et al., 2004). Cool stream temperatures help oxygen remain in solution and available for respiration and nutrient transformation (Vaux, 1968; Hendricks and White, 1991; Brown et al., 2005). The temperature of interstitial water in streambeds has been directly related to the diversity and abundance of hyporheic zone dwellers (Fowler and Death, 2001; Malard et al., 2001). Recent work by Grieg et al. (2007) shows a direct relationship between the growth of salmonid embryos and intragravel (hyporheic zone) temperatures.

While hyporheic exchange generally moderates stream temperature (Johnson, 2004), temperature differences between water in the stream and hyporheic zone, also provide a cooling mechanism. These differences depend on streambed material properties, stream geomorphology and the degree of tree canopy shading (Evans and Petts, 1997; Webb and Zhang, 1999; Poole and Berman, 2001; Franken et al., 2001; Alexander and Cassie, 2003; Story et al., 2003; Johnson, 2004). Stream segments restored to increase groundwater discharge

and hyporheic exchange were found to have more moderate temperatures than unrestored reaches (Loheide and Gorelick, 2006). Even in periods of low flow or no flow, these restored reaches had cooler subsurface water flowing in the hyporheic zone.

The importance of stream morphology and streambed characteristics to stream temperature distribution was also explored in an evaluation of stream temperatures before and after forest clear cutting in the Pacific Northwest (Story et al., 2003). They found that stream temperature changes after clear cutting were not consistent among stream segments and suggested further study of hyporheic temperature and exchange with respect to stream temperature moderation. In northeast Oregon, stream temperature heterogeneity or patchiness due to variations in streambed morphology was found to be important to salmonid habitat. Increased temperature patchiness increased rainbow trout populations in the study area (Ebersole, 2001).

Regions of hyporheic zone and stream temperature research

Hyporheic zone research in North America has largely been conducted in the west and north central regions. There are also several centers of research along the east coast. Awareness of hyporheic zone function and dynamics resulted from fisheries studies conducted to understand stream conditions necessary for salmonid spawning and survival. Studies in other coastal and Great Lakes states

and provinces followed. Research into hyporheic dynamics, habitat and biogeochemistry has also been completed in several Rocky Mountain States since the 1980's. Biogeochemical studies of nutrient and solute flux in the hyporheic zone followed this initial work and are more geographically distributed especially where anthropogenic influences (agriculture, urbanization, mineral extraction) influence stream chemistry.

Outside of New England, established and developing centers of research into hyporheic zone dynamics, biology, and biogeochemistry are located in Alaska (Vaux, 1962; 1968; Edwardson et al., 2005), the Pacific Northwest (Kashahara and Wondzell, 2003; Ebersole et al., 2003; Johnson, 2004; Moore et al., 2005a, 2005b; Gooseff et al., 2005), California (Bencala et al., 1984a, 1984b; Hatch et al., 2006; Loheide and Gorelick, 2006), Rocky Mountain States (Vallett et al., 1990; Poole and Berman, 2001; Constantz et al., 1994; Ryan and Boufadel, 2006; Wroblecky et al., 1998; Gooseff et al., 2007; Lautz and Fanelli, 2008), Michigan (Hendricks and White, 1988; Hendricks and White, 1991), Ontario (Franken et al., 2001; Storey et al., 2003; Conant, 2004; Marshall et al., 2007), and the southeastern Appalachians (Castro and Hornberger, 1991; Roberts et al., 2007).

In New England, hyporheic zone research has been conducted at Hubbard Brook Experimental Forest (HBEF) in the White Mountains of New Hampshire and in eastern Massachusetts within the Ipswich and Parker River watersheds. HBEF is a Long Term Ecological Research (LTER) site focusing on precipitation, soil and stream chemistry. The impact of acid rain on soil, surface water and groundwater and nutrient cycling has been studied extensively there (Hall et al., 2002; Findlay, 2005). The hyporheic zone work at HBEF is an outgrowth of stream nutrient studies and streambed processes. Similarly, in coastal Massachusetts, interest in anthropogenic nutrient sources, and their fate and transport is motivating hyporheic zone research (Peterson et al., 2001; Thouin, 2008; NHRRC, 2009). Recent studies in central Massachusetts revealed that hyporheic flow zones sustained headwater stream habitats and wetland ecology especially when surface water was seasonally absent from the stream or wetland (Collins et al., 2007). Hyporheic flow zones were found to connect intermittent stream reaches, which suggests that broader protection of these habitat linkages is important.

Measuring hyporheic zone extent and flux

Hyporheic zone flow path lengths generally range from centimeters to tens of meters (Harvey and Wagner, 2000). Hyporheic zone depths are estimated to be centimeters to meters depending on sediment characteristics (Castro and

Hornberger, 1990; Harvey and Wagner, 2000). The exchange between the stream to streambed and back to the stream can vary from seconds to months to years depending on the depth of flow paths (Harvey and Wagner, 2000; Kashahara and Wondzell, 2003; Lautz and Siegel, 2006). Flow path length and residence time ranges are illustrated in Figure 1-2.

Gross flux and hyporheic zone extent is measured in the field using conservative solute tracers (Harvey and Bencala, 1993), in-situ streambed chemistry (Hendricks and White, 1991), seepage meters (Harvey and Wagner, 2000), and temperature (Hendricks and White, 1988; Constantz and Stonestrom, 2003; Hatch, et al., 2006; Loheide and Gorelick; 2006). Measurements of hydraulic head, hydraulic conductivity, and stream flow using wells, piezometers, weirs and flumes also provide valuable vertical and horizontal hydraulic information on hyporheic zone extent, flux, and interaction between alluvial, hillslope, and regional groundwater systems.

Bencala et al. (1984b) attributed flow through the streambed to hydraulic head differences caused by streambed gradients. Using floodplain and streambed piezometer and soluble stream tracers, he documented areas of outflow from the streambed. This, and subsequent tracer work, defined the zone of transient

stream storage as the flow area through the hyporheic zone and dead zone storage in the stream and the streambed (Harvey and Wagner, 2000).

Conservative tracer studies have been widely used to measure the residence time and exchange rate of stream water in the hyporheic zone and to determine areas of downwelling and upwelling. Stream/hyporheic zone area ratios have also been determined based in these studies (Triska et al., 1989; Castro and Hornberger, 1991; Harvey and Bencala, 1993; Harvey et al., 1996; Chestnut and MacDowell, 2000; Hall et al., 2002; Cozzetto et al., 2006; Gooseff et al. 2007). Conservative tracers such as chloride or bromide or non-conservative solutes such as nitrate or phosphate are also used to estimate flow in streams versus flow in the hyporheic zone (or hyporheic zone uptake) based on dissolved constituent breakthrough curves. Although hyporheic exchange rate is also a factor, generally, the longer the tail of the breakthrough curve, the larger the hyporheic zone or dead zone (Harvey and Wagner, 2000, Lautz and Siegel, 2006).

Harvey and Bencala (1993) and Castro and Hornberger (1991) used tracers in combination with hydrologic information from wells to describe the hyporheic flow beneath and lateral to alluviated streams and demonstrated that topography is a major driver of hyporheic flow. Harvey and Wagner (2000) illustrated the

limitations of the tracer method to determine hyporheic residence time due to streambed roughness and morphology (Figure 1.2). In summary, they related streambed conditions to the length of flow paths and residence time that could reasonably be measured,

Fluvial geomorphologic measurements and streambed sediment characteristics have also been used to characterize hyporheic zone fluxes and residence times (Vaux, 1968; Kashahara and Wondzell, 2003; Anderson et al. 2005; Gooseff et al. 2005; Lautz and Siegel, 2006). These field studies are often combined with analytical or numerical modeling to determine hyporheic zone extent and flow characteristics. The influence of stream geomorphologic complexity on hyporheic flow patterns and river ecology was documented by Wright et al. (2005) and Poole et al. (2006). Hendricks and White (1988) documented hyporheic flow in Michigan within and around *Chara* mounds, beaver dams and lamprey nests using temperature measurements and solute concentrations.

Heat as a tracer of subsurface flow

Heat has been used as a tracer in surface water/ground water interaction studies for many years (Stallman, 1965; Lapham, 1989; Sophocleus, 2002; Constantz and Stonestrom, 2003; Anderson, 2005). Heat measurement techniques have also been applied in hyporheic zone flow evaluations. In-situ temperature

measurements can estimate the horizontal and/or vertical extent of the hyporheic zone. Streambed temperatures are measured using thermistors or thermocouples (Hendricks and White, 1991; White, 1993; Hendricks, 1993; Conant, 2004; Hatch et al., 2006; Loheide and Gorelick, 2006; Constantz, 2008). Two-dimensional measurements of stream and streambed temperatures are made using fiber optic and remote imagery (Loheide and Gorelick, 2006; Selker et al., 2006, Lowry et al., 2007).

Conant (2004) used temperature measurements in wells and piezometers, installed in the riparian zone and riverbed, to determine where contamination was seeping into the hyporheic zone based on temperature contrasts. Hatch et al. (2006) and Keery et al. (2006) estimated streambed seepage using a time series analysis of diurnal temperature fluctuations measured in the stream and streambed. These continuous temperature measurements were made using regularly spaced thermistors installed in streambed wells. The lag time between the stream and streambed temperatures at different depths, the amplitude of temperature changes and periodicity were used to estimate streambed seepage rates.

Loheide and Gorelick (2006) combined thermal infrared imagery and thermistor point measurements of stream and streambed temperatures to estimate

groundwater discharge and hyporheic zone discharge of restored versus unrestored stream sections. Selker et al. (2006) used fiber optic technology to continuously measure stream and lakebed temperatures along a kilometer of fiber optic cable. From these data, they were able to identify areas of groundwater discharge at the streambed/stream and lakebed interface. Delineation of groundwater discharge to Great Bay in New Hampshire was accomplished using thermal infrared imagery (Roseen, 2002). Groundwater seepage to an estuary on Cape Cod was also measured using fiber optic temperature measurement technology. Traditional bed seepage measurements corroborated the fiber optic analysis results (Henderson et al., 2009).

Hyporheic flow modeling

Hyporheic zone modeling is used to understand the influence of bedforms, stream geomorphology, and adjacent land use on hyporheic flow. Although numerical flow modeling was not used in the Wednesday Hill Brook study, the relationship between stream geomorphology and hyporheic flow is important to understanding degree of hyporheic exchange along the study reach.

The USGS finite difference model, MODFLOW (McDonald and Harbaugh, 1988) can be used to simulate hyporheic flow. Field study data were related to stream morphologic patterns and hyporheic zone exchange in mountain streams in

Oregon (Kashahara and Wondzell, 2003; Anderson et al., 2005; Gooseff et al., 2005), Montana (Gooseff et al., 2007) and Wyoming (Lautz and Siegel, 2006).

Kashahara and Wondzell (2003) used MODFLOW to determine the relative importance of geomorphic features to hyporheic exchange in a second and fifth order stream. The second order stream was steep and generally followed a step-pool morphology. The fifth order stream was more sinuous and the gradient more gradual. Step-pool sequences were found to be the largest driver of hyporheic flow in the second order stream. In the fifth order stream, sinuosity was important but through a sensitivity analysis it was determined that the removal of riffles decreased hyporheic flux by 50% while the removal of sinuosity reduced hyporheic flux by only 25% (Kashahara and Wondzell, 2003).

Gooseff et al. (2007) used MODFLOW to relate the hyporheic zone residence time to the geomorphic characteristics of urban, agricultural, and reference streams. They demonstrated that the more complex geomorphology of the reference streams led to longer residence times and greater hyporheic zone complexity. It can be inferred that the shallow depth of permeable bed sediments in the urban and agricultural streams led to lower hyporheic zone exchange as well.

Lautz and Siegel (2006) studied vertical and lateral hyporheic zone flux using a combination of field instrumentation, tracer studies and MODFLOW modeling. A contaminant transport module, MT3D, was also used to simulate the depth of the hyporheic zone along a 320 m reach of stream in Wyoming. Their findings showed that log and debris dams had the greatest influence on vertical flux into and out of the streambed. The dams produced the greatest depth of hyporheic zone penetration and areas downstream from complex meanders showed limited vertical hyporheic flux.

In summary, modeling studies are able to link the importance of bedforms (pool-step-riffle, pool-riffle-step, beaver dams and log dams), average water surface concavity, and the relative sizes of these stream features to hyporheic zone upwelling and downwelling lengths, depth, and volume.

Hyporheic corridors

Vanotte et al. (1980) proposed the river continuum concept in which the hydrology and the morphologic pattern of rivers from the headwaters to twelfth order streams are related to biotic assemblages and nutrient transfer. This model illustrates the relative importance of physical features to river ecology and has allowed stream systems to be placed in a well-defined physical context.

Stanford and Ward (1993) proposed the hyporheic corridor concept and related

the development of the hyporheic zone from the steep headwater stream to the coastal plain along a continuum. This also demonstrates “the landscape-level importance of hyporheic zones and processes” to stream and river ecology (Stanford and Ward, 1993). From a geomorphic perspective, the concept also illustrates that although the hyporheic zone may be discontinuous along a stream or river system, the evolution of and linkages between the hyporheic zone and stream are important to the overall function of stream and river systems. This supposition was supported by recent work in a Massachusetts tributary stream where discontinuous surface flows in small headwater streams were linked in the subsurface by hyporheic zones in periods of low stream flow (Collins et al., 2007). This continuity allowed for the survival of stream-dependent biological communities when the stream itself was not flowing.

Research objectives

This research was conducted to gain a better understanding of the stream temperature dynamics and hyporheic zone exchange characteristics of a coastal New England stream. The research combined temperature, hydrologic, geophysical, and geomorphologic measurements along a 520 m reach of Wednesday Hill Brook in Lee New Hampshire in order to answer the following questions:

- What are the vertical extent and exchange characteristics of the hyporheic zone?
- What is the temperature regime of the Wednesday Hill Brook study reach?
- What is the relationship between catchment and stream geomorphology and temperature variations in the stream and streambed?

Several hypotheses were formed based on the literature review and initial interpretation of the local geologic setting:

- Stream and streambed temperature patterns will provide a direct indication of hyporheic flow patterns.
- Summertime stream and streambed temperatures at riffles will be relatively warmer and indicate areas of downwelling. Stream and streambed temperatures at pools will be relatively cooler due to hyporheic upwelling.
- The upper portions of the reach will be dominated by tributary and groundwater influence and the downstream portion will be largely influenced by hyporheic zone exchange.
- Groundwater discharge to the stream has an important influence on stream temperature.
- Summer stream temperatures will increase downstream along the study reach due to slower streamflow movement and greater net radiation input.

- The hyporheic zone is more extensive in the lower reach where the sand and gravel bed thickens and limited in the upper reach where the streambed is armored.

Until recently, the importance of headwater streams and first and second order streams to the overall watershed and downstream river health has received minimal attention. Now it is recognized that these streams play a critical role in the maintenance of water quality, moderate temperatures and biological integrity. Thus, it is important to understand stream dynamics on multiple scales. This detailed hydrologic study of Wednesday Hill Brook, a first order coastal stream, seeks to enhance our understanding of how hyporheic zone and streambed processes influence stream temperature moderation which, in turn, impacts stream ecology and biogeochemistry in the subject stream and the wider coastal watershed.

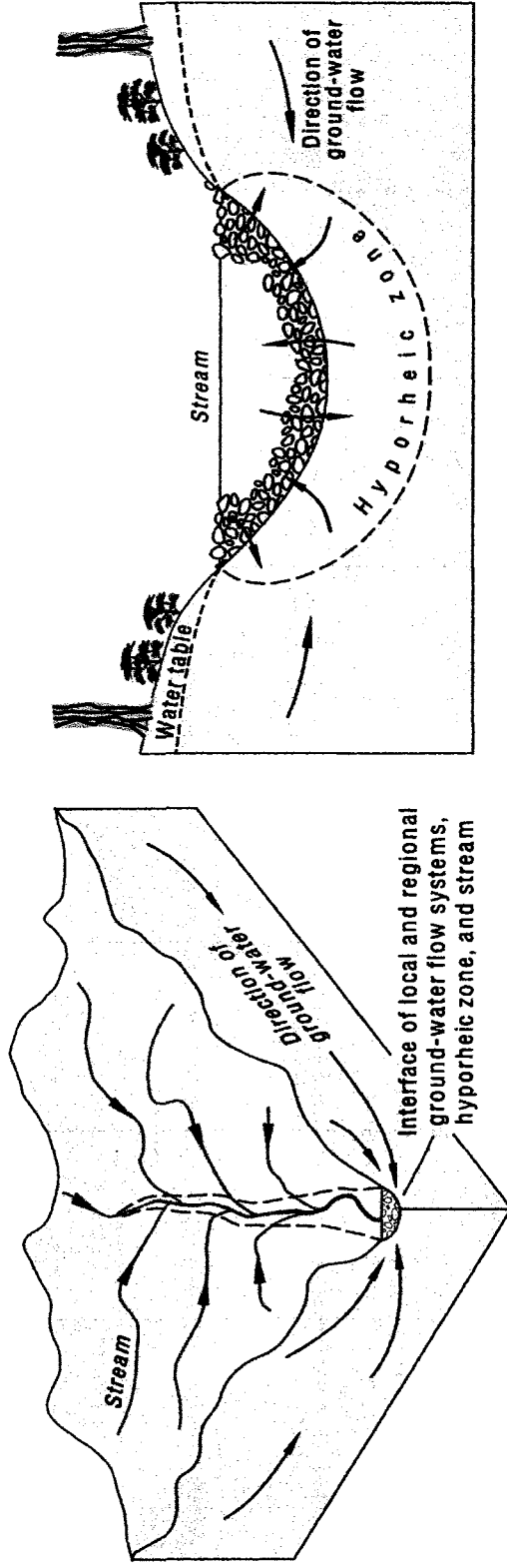


Figure 1-1 The hyporheic zone and its relationship to catchment hydrology (Winter et al., 1998)

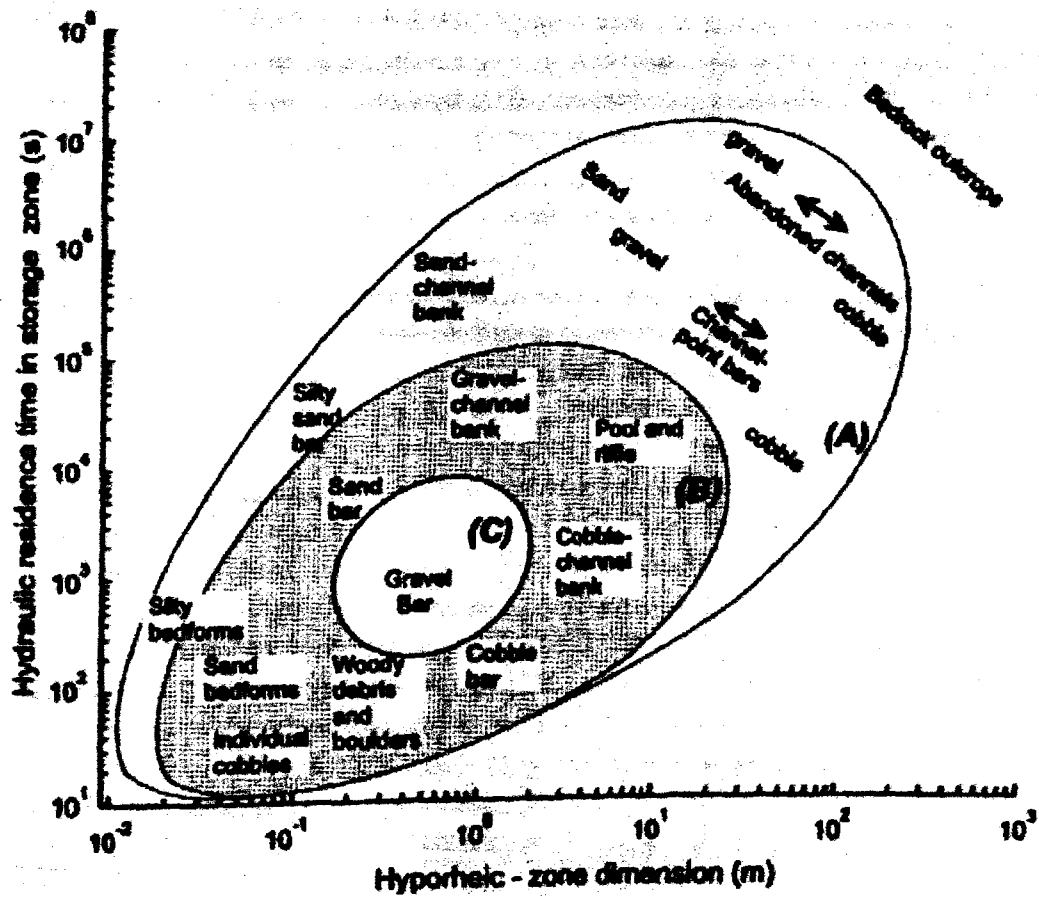


Figure 1-2 Hyporheic flow path lengths and residence times (Harvey and Wagner, 2000)

CHAPTER 2

SITE DESCRIPTION AND SETTING

Site description

The research site is located in the Wednesday Hill Brook (WHB) watershed in Lee, New Hampshire (Rockingham County) and is part of the larger Lamprey River Watershed. The study reach begins where Wednesday Hill Road crosses the stream and extends downstream 520 m (Figure 2-1). Approximately 400 m beyond the end of the study reach, the stream enters the Lamprey River.

Land use

The study reach is within a large unfragmented parcel of land which contains the stream, pasture, cornfield, woodland, and a house and barn complex. The stream is near the eastern boundary of this land (Figure 2-1). The parcel is owned by Phillip Sanborn and is protected by a conservation easement held by the Town of Lee. The house and barn are more than 200 m to the west of the stream. The land parcel is narrow at the upper reach of the study site and widens downstream. Immediately abutting the land near the top of the reach are residential developments with widely spaced homes. Three of these homes are approximately 100 m from the stream but there is generally a wide riparian

corridor along the stream and the stream valley has not been encroached upon by the developments. The homes have individual septic systems and have deep bedrock wells for their water supply. South of these homes, open space woodlands associated with the eastern development provide a large buffer for both WHB and the Lamprey River. To the west, woodland, cornfields and grazing land owned by Phillip Sanborn make up the lower portion of the watershed.

The watershed area above the study reach begins north of Route 155 where school and public buildings are located. This part of the watershed contains several closely spaced housing tract developments but also has considerable open field and forest.

Riparian canopy

The vegetation in the stream valley is primarily hemlock and yellow birch canopy within the first 300 m reach of the study catchment and transitions to red maple, cherry and birch as the floodplain widens. The herbaceous and shrub layer is minimal in the upper 300 m of the study catchment and becomes denser downstream as the canopy changes to a larger percentage of smaller diameter deciduous trees. This downstream area was cleared for grazing in the past, but has re-grown over the past 40 years. Tree canopy densities measured in August 2007 are reviewed in Results.

Hydrologic setting

Surface water

WHB is a first order stream that drains to the Lamprey River just downstream of the Lee Hook Road Bridge. The watershed area is approximately 1.5 square kilometers (km²) and is a sub-watershed of the larger Lamprey River Watershed, which covers 479 km² (NHWRRRC, 2009a). Figure 2-2 is a topographic map showing the watershed boundaries and the study reach location. The stream flows northeast to southwest in the first 150 m of the reach then turns south until it enters the Lamprey River.

Stream gauging at the culvert at Wednesday Hill Brook has been ongoing since 2005 (Davis, personal communication, 2007). The US Geological Survey maintains a stream flow gage at Packers Falls on the Lamprey River, approximately 5 km downstream of the confluence of Wednesday Hill Brook with the Lamprey River. Continuous or daily flow measurements have been measured at this location since 1934 (USGS, 2008).

The study reach begins where the stream passes through a 1.2 m corrugated metal culvert under Wednesday Hill Road. This large culvert has created a plunge pool below it that is about 1.5 m deep during periods of high stream flow.

In this upper portion of the study reach, the stream occupies a narrow, steep-sided stream valley.

Beyond the plunge pool, the bedforms in the stream follow a step-pool morphology for approximately 100 m below the road crossing. In the first 60 m of the study reach, steps and cascades are made up of boulders, cobbles and possibly bedrock outcrops. In the next 40 m, steps and cascades have formed from woody debris and logs that have fallen due to stream bank erosion and storm flow. Below this point, step-riffle-pool, riffle-pool, and riffle-step-pool morphology dominate stream morphology to the end of the study reach and log dams are frequent.

Spring-fed brooks, small wetlands and seeps are common throughout the study reach. Several of these brooks appear to flow throughout the year. However, flow is often not within a visible streambed but in a covered channel that flows below tree roots and within a permeable zone of sand and cobbles that contain these channels. Wetlands have formed near the base of the valley walls and peat deposits were formed from the long-term plant decomposition and sediment accumulation in these small wetlands. The stream valley walls remain steep until the 300 m mark where a broad floodplain has developed adjacent to the stream. This floodplain area is still bounded by valley walls that are steep, but not as high

as in the upper study reach. The floodplain in this area widens to about 50 m and broadens to over 100 m near the confluence with the Lamprey River.

Wetlands are common in the floodplain areas especially close to valley walls.

Groundwater

The USGS Hydrologic Atlas for the Lamprey River Area (Moore, 1990)

characterizes the deltaic deposit that forms the western hillslope as having a transmissivity of less than 4.6 m^2 per day. Groundwater is mapped as flowing from this upland deposit to the south and east towards the stream.

Several hydrologic and biogeochemical studies have been or are being carried out in the WHB area or on the nearby Lamprey River. University of New Hampshire utilizes the Lamprey River as a hydrologic observatory as part of ongoing research within the Departments of Natural Resources, Earth Science and Civil Engineering (NHWRRRC, 2009b). The studies completed in the WHB watershed to date have been related to water quality evaluations and nutrient biogeochemical evaluations (Blumberg, 2002; Traer, 2007; NHWRRRC, 2009a).

Ten riparian zone wells were installed as part of the Blumberg research in 2003. Five of these wells are within the study reach. These wells are approximately 1 m deep and are installed within 1 m of the stream bank. In 2004, 13 monitoring wells were installed adjacent to the stream between the 110 and 120 m stations.

These wells are 0.5 to 1.0 m deep and are installed between the western stream valley wall and the stream. These wells were installed to better understand the nutrient dynamics within the watershed. The wells and the stream water are regularly sampled for a range of organic and inorganic parameters as well as temperature and water levels. Research on nitrous oxide gas production within the stream is also ongoing at WHB (DiFranco, personal communication, 2009).

Groundwater levels in the monitoring well field are generally above land surface suggesting a vertically upward flow gradient. Upward flow is most pronounced at the toe of the steep western hillslope and moderates with proximity to the stream. Small peat-filled wetlands are common at the toes of both the western and eastern hillslope further suggesting groundwater discharge to the riparian zone in these areas. Several significant groundwater seeps crop out just above the stream bank at 190, 230, and 250 m downstream from the culvert.

Geologic setting

The bedrock in the lower WHB area is the Calef member of the Eliot Formation (Lyons et al., 1997) and is a dark gray phyllite. The boulders, cobbles and gravel in the streambed in the upper 70 m of the study reach are largely made up of this rock type. There are imbedded boulders or possibly bedrock outcrops at several locations along the reach from the culvert to about 70 m downstream as well.

There are also several riffles, 156 and 298 m downstream, that may result from bedrock being close to the stream bottom where this phyllite is the dominant source material. Beyond the downstream limit of the study reach, an area of bedrock is exposed in the streambed. The Eliot Formation is also exposed along the Lamprey River where the brook enters the river.

Delcore and Koteff (1989), Koteff et al. (1989), Goldsmith (1990a), and Goldsmith (1990b) mapped the surficial geology of the WHB watershed at the 7.5-minute quadrangle scale. The materials above bedrock in this area are all derived from glacial advance, glacial melt waters, from advancing seas after deglaciation, or by recent stream deposition of these re-worked glacial materials.

The flat-topped deposit in the western upland area of the WHB watershed is mapped as stratified sand and gravel (Qge). This is a delta-like deposit formed as the ice sheet decayed and retreated (Figure 2-3). This and similar deposits have been interpreted as ice contact marine deltas (Birch, 1980). Birch (1980) found that similar deltaic features formed along bedrock ridges. Upper Wednesday Hill Brook above the study reach is very linear and parallel to the edge of this deltaic deposit. This may explain the linearity of this upper reach area.

The upland area east of the stream is made up of glacial till. This poorly sorted mix of clay, silt, sand, gravel and cobbles (Qt and Qtt) was deposited in front of or beneath advancing glacial ice. The top of Wednesday Hill is made up of glacial till and is likely to be a small drumlin.

Surrounding the till and the deltaic deposits at lower elevations are two members of the Presumpscot formation, a marine sand (Qps) and marine silt and clay (Qpc). The marine sand deposits were formed by near shore wave action that eroded and re-shaped the glacial sand and gravels. The materials are generally less than 3 m thick and interfinger with the marine silt and clay.

The depth and character of these marine sand deposits were characterized by Eller (2006) using seismic and ground penetrating radar surveys at the UNH Burley Demeritt Farm, Lee and Camp Hedding and Camp Lee, Epping, NH. Birch (1989) also completed seismic refraction surveys and resistivity surveys to describe the marine transgression and deglaciation history of the area. Eller (2006) found that the marine sands were thickest in the Lamprey River valley in the area near WHB west to Epping, New Hampshire.

The marine silt and clay is found at lower elevations in the stream valley. It is characteristically dense bluish clay interfingered with small layers of sand near its

contact with the marine sand deposits. This material appears to underlie much of study reach.

Alluvial gravel, sand and silt (Qal) has been deposited from stream erosion and re-deposition where the floodplain widens at 300 m downstream and continues downstream to where WHB enters the Lamprey River. A more detailed geologic description that is based on fieldwork and LiDAR analysis is included in the Results section.

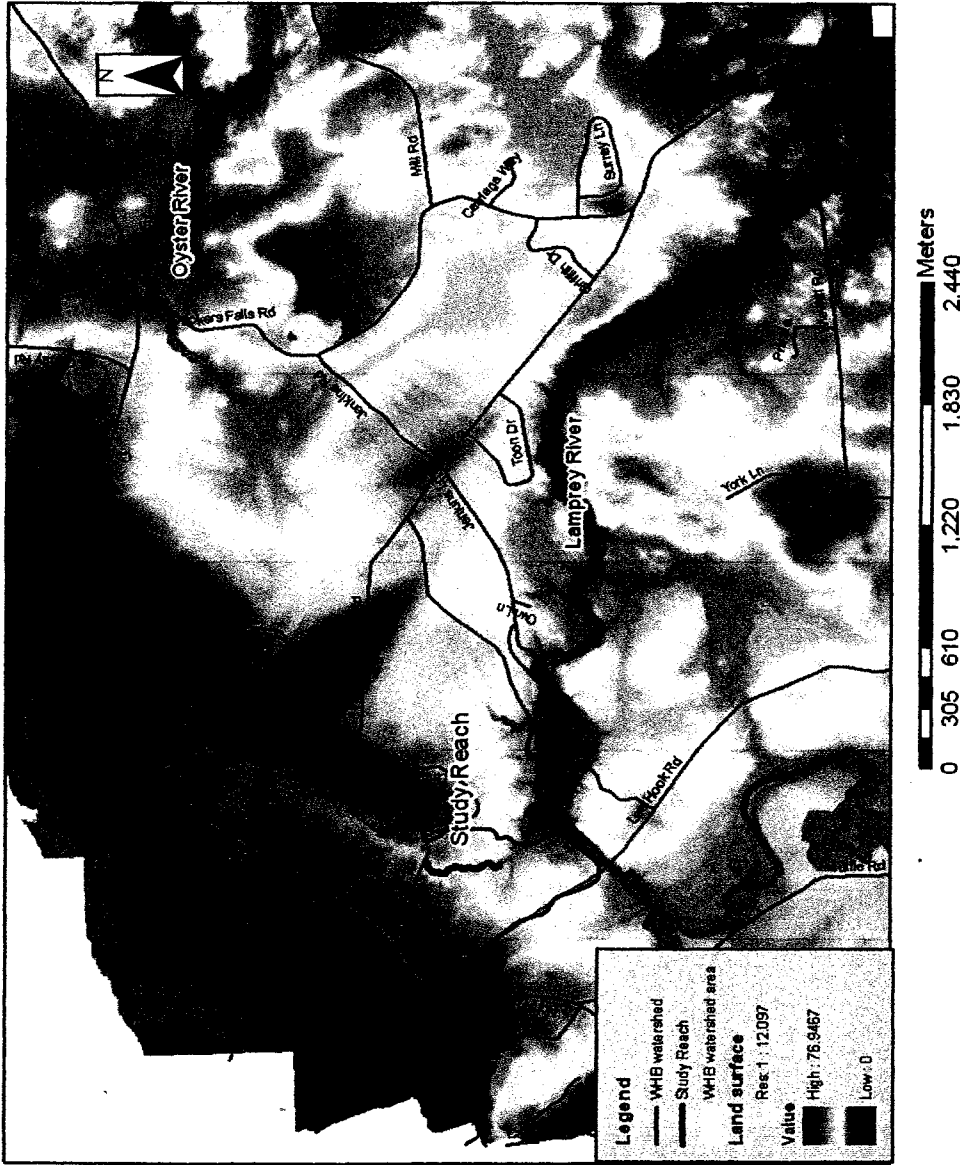


Figure 2-1 Site location map
 Wednesday Hill Brook in Lee, NH
 Hill shade topography from LiDAR imagery
 provided by NCALM,
 roads from NHGRANIT GIS database

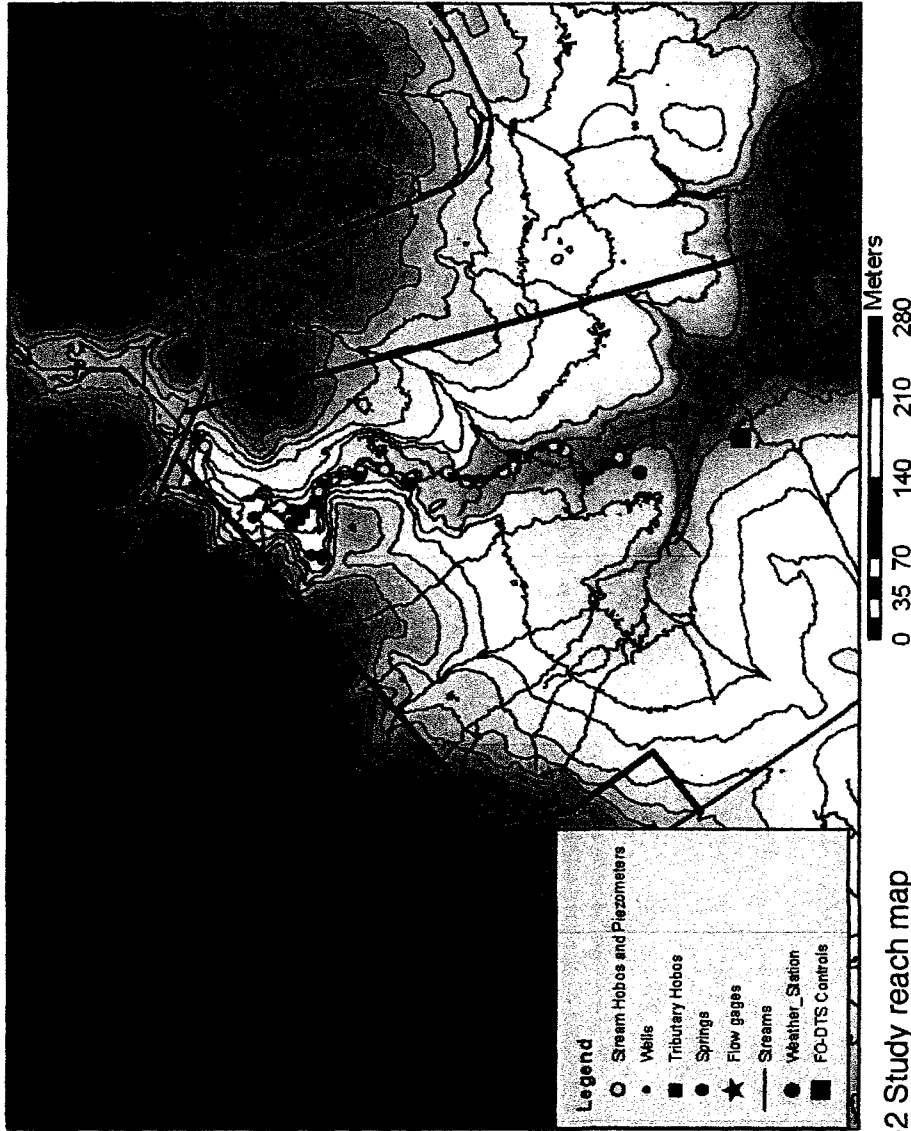


Figure 2-2 Study reach map
 Wednesday Hill Brook in Lee, NH
 Hillshade topography from LiDAR imagery provided by NCALM,
 roads from NHGRANIT GIS database

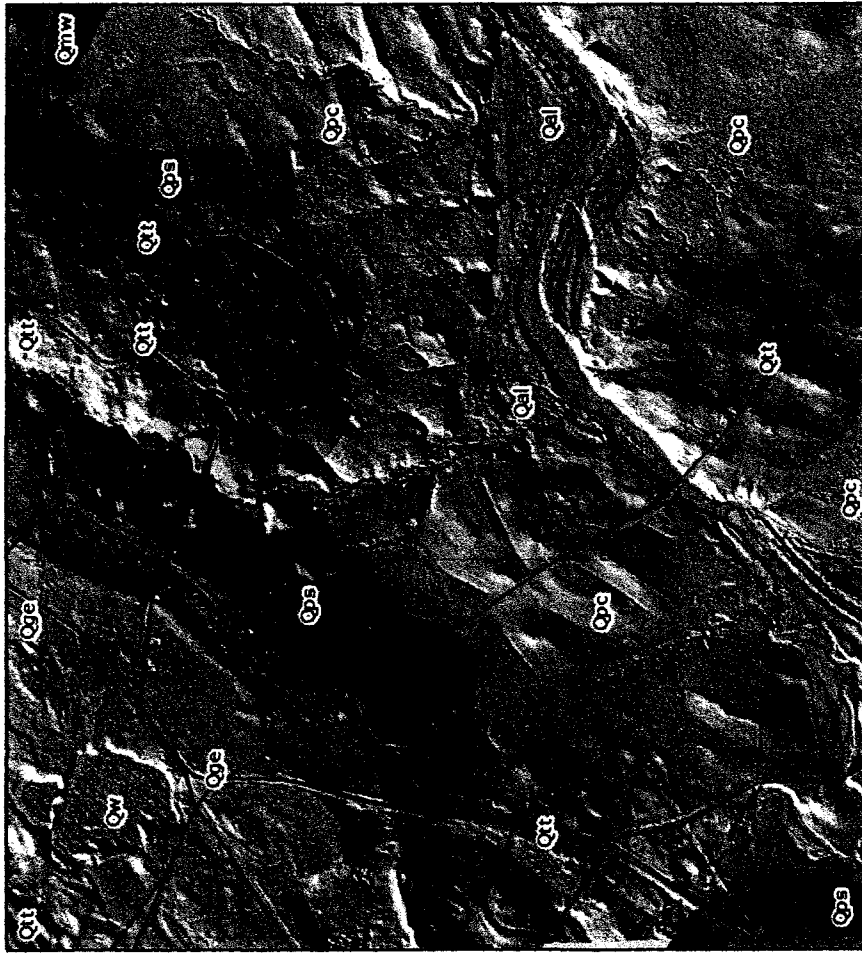


Figure 2-3 Surficial geologic map
 Wednesday Hill Brook in Lee, NH
 Hill shade topography from LIDAR imagery provided by NCALM; surficial geology from
 NHGRANIT GIS database

CHAPTER 3

METHODOLOGY

Research approach

Fieldwork focused on characterizing the geomorphology of the stream and catchment area, the stream hydraulics and the temperature dynamics of the air, stream, streambed, groundwater, and tributaries. Several assumptions were made about the near surface geology and hydrology of the stream in formulating the field program. The 520 m study reach was chosen because it represented a segment where bed materials are conducive to allowing hyporheic exchange and stream gradients and variations in morphology could potentially influence the pattern of hyporheic flow.

The conceptual model of the study reach was developed after preliminary field measurements. It assumes that the vertical extent of the hyporheic zone is limited to the sand and gravel dominated streambed that is generally less than 1 m thick within the study reach. This streambed is underlain by marine silt and clay. This combination provides a potential hyporheic zone that is limited by the depth of the streambed sand and gravel. Hyporheic exchange therefore can occur in this zone and in adjacent alluvial materials, but is assumed to not

penetrate the underlying marine silt and clay. Storey et al.'s (2003), streambed hydraulic conductivity and hyporheic extent model results support this assumption.

Geophysical and physical measurements of streambed depth, sediment size and stream geomorphic characterization techniques were carried out to further define catchment geomorphology. LiDAR was also flown and results were analyzed to precisely assess catchment topographic and surface flow characteristics.

In order to characterize hyporheic exchange and groundwater discharge using heat as a tracer, a contrast between temperature in the stream and groundwater temperature was required. Late summer and early fall were chosen to take advantage of these conditions.

A range of temperature instrumentation was used for this study. The USGS Geophysical Branch in Storrs, CT provided equipment for and supported the Fiber Optic Distributed Temperature Sensor (FODTS) measurements. The FODTS provided high-resolution stream temperature measurement along the study reach. Because hyporheic exchange is largely driven by streambed topography and the composition of the streambed, multiple riffle and pool features were chosen for discrete stream and streambed temperature

measurement. Mini-piezometers installed in streambed alluvium measured hydraulic head between the stream and streambed. Piezometers were also equipped with thermocouple wire to measure streambed temperatures at regular depth intervals. Hobo™ thermistors were used to measure stream and streambed temperatures for comparison with the FODTS and thermocouple measurements and to measure temperature in existing catchment monitoring wells and small tributaries that flowed to the stream.

The experimental data were analyzed graphically and statistically to understand catchment and hyporheic flow dynamics. High-resolution LiDAR digital elevation model (DEM) data were analyzed to define catchment morphology and to characterize streamflow and subsurface flow characteristics. Finally, time stability analysis and heat budget modeling were used to characterize heat flow and to quantify the individual components of stream temperature moderation.

Field methods

Introduction

Preparation, fieldwork, and preliminary data collection on the WHB study reach began in April 2007 and continued until November 2008. Initial work included establishing the study reach extent, marking longitudinal stream stations and completing an earth conductivity survey. Stream morphology surveys,

streambed depth probes and preliminary temperature measurements followed this initial work.

The majority of temperature and hydrologic data used for this research was collected during two field campaigns. Although much of the instrumentation was installed prior to the first campaign, the majority of data collection occurred simultaneously with the FODTS data collection, August 22 to August 28, 2007 (FC-07-1) and September 25 to October 9, 2007 (FC-07-2). During this field deployment, mini-piezometers fitted with thermocouple sensors, Hobo™ thermistor dataloggers, an FODTS survey unit, a weather station, and a flume were installed and data collected. Much of this equipment either remained in place or was re-deployed from late September through early October 2007 to collect additional temperature and hydrologic data.

To fill identified data gaps, supplemental temperature, geomorphic and hydrologic data were collected between April 2008 and September 2008. A LiDAR survey was conducted in November 2008. Figure 2-2 shows the study reach and the locations of the instrumentation and measurement points. Figures 4-1, 4-2 and 4-3 are enlarged segments of the study reach that show detailed topography, geomorphic features and cross section locations.

Geomorphic surveys and measurements

Stream stations

On April 13, 2007, stream station flags were placed along WHB from the culvert at Wednesday Hill Road to the mouth of the stream at the Lamprey River. Metal and plastic pin flags labeled with distance in meters from the Wednesday Hill Road crossing were placed at regular intervals and at major stream features to guide planned experiment positioning and for general reference. An optical rangefinder was used to measure the distances between points.

A fiber optic cable was installed in the stream thalweg to collect stream temperature measurements in the study reach. The instrumentation and installation details for these measurements are described in a following section. Field notes were taken during the cable installation to cross correlate field station measurement stations with cable stations. The cable sheath is labeled with sequential meter markings. Cable meter locations (plus or minus 0.5 m) were noted in the field book at flagged stream stations, at major stream features, and at Hobo and piezometer locations. All instrumentation and data are referenced to these cable locations. Table 3-1 lists instrument installation details referenced to both stream station and cable station locations.

Geophysical survey

On April 14, 2007, measurements of the apparent electrical conductivity of the shallow subsurface were made using a Geonics EM-31 unit. This instrument uses electromagnetic induction to estimate shallow earth conductivity to a depth of less than 6 m. Apparent conductivity is measured in mmhos/m.

Measurements were made at the centerline of the stream every 50 m, at every stream station measurement flag, and at significant hydrologic or geomorphic features along the length of the stream. Some measurements were also made within tributaries and seep areas. The observed value was recorded at the stream station location. The data are included in Appendix A.1.

Longitudinal profiles

A detailed longitudinal profile, from the culvert to about 400 m downstream, was conducted during July and August 2008. An elevation of 30 m above mean sea level was assumed at the centerline of Wednesday Hill Road at the stream crossing. Temporary benchmarks (TBM's) were established along the stream using either wooden hub stakes driven into the ground or galvanized metal spikes driven into sturdy streamside trees. The elevations of these TBM's were transferred downstream from the assumed elevation at Wednesday Hill Road using a Lasermark self-leveling rotary laser level and detector rod.

Longitudinal distance was determined using a measurement tape laid out along the stream bank near the bankfull position. These distances were also checked against the existing stream station flags to allow for reasonable correspondence of measurements. Significant changes in elevation and morphology were noted and measured in the longitudinal survey. The streambed elevation was measured at the deepest point of the stream (thalweg). At most locations the elevation of the water surface was also recorded. LiDAR topographic data, collected in November 2008 were also used to augment the field-collected longitudinal profile information and to convert these assumed elevations to surveyed elevations.

Stream cross sections

Six bank-to-bank stream cross sections were surveyed at selected mini-piezometer locations. Cross sections were completed primarily to evaluate stream geomorphology and hydrologic metrics. A Lasermark self-leveling rotary laser level and detector rod was used to complete the survey. Measurements were made at bankfull, thalweg, and at elevation changes along the cross section. Water surface elevations were also measured at each cross section.

Two valley-wide cross sections were also surveyed to provide elevation data for earth resistivity surveys. These surveys were completed with a Leica Total

Station theodolite. Elevations were measured at significant breaks in slope and hillslope features along a 70 m section at station 211 m and along a 65 m section at station 461 m. The locations of these cross sections are shown on Figures 4-1 to 4-3. LiDAR topography was used to augment the cross section location data and obtain reference elevations.

Streambed depth measurements

Over most of the study reach, the streambed is made up of cobbles, gravels, sand and silt that overlie a marine silt and clay deposit. This alluvial material makes up the streambed and potential hyporheic zone. To assess the depth and general sediment character of the streambed, a series of probes and depth measurements were made to determine the depth of this zone. A 1.8 m long, 4 mm diameter steel rod was used to probe the streambed. The probe was advanced to a point where either bed "refusal" resistance was reached or it was determined that the underlying silt and clay boundary was reached. These measurements were made at over 200 locations along the study reach and where detailed information about streambed geometry was needed.

Log dam and woody debris dam geometries were also measured using a combination of sediment depth probes and height measurements. The heights of the log dam above the streambed, both upstream and downstream of the log feature, were recorded. The data from the probes and dam measurements were

incorporated into the longitudinal profile for two-dimensional characterization of the streambed.

Pebble counts

Pebble counts were completed to characterize streambed surface sediments (Rosgen, 1996). One hundred sediment grains were selected along each of five 100 m reaches. One sediment grain was selected at each footstep along the reach and the median grain diameter of the grain was measured to the nearest millimeter. Silt and clay sized particles were not measured but assessed by tactile analysis. Cobbles and boulders that rose above the stream surface were characterized by measuring the distance that the grain protruded above the waterline. A grain size frequency distribution curve was developed for each reach.

Meteorologic data collection

An under-canopy weather station was installed on August 17, 2007 at the downstream limit of the study reach (Figure 3-1). This unit included a Kipp & Zonen CNR1 LI-COR 200x net radiometer for measurement of net radiation. Solar radiation was measured using a LI200X silicon pyranometer by Licor. A Vaisala HMP-45C unit measured relative humidity and air temperature. Relative humidity and temperature values were collected at 1.5 m above ground surface.

Wind speed and direction were measured at 2.0 m above ground surface using a RM Young CS-800-L anemometer. Each of these instruments was wired to a Campbell Scientific CR10x data logger for continuous measurement of weather data. Data were sampled every 15 minutes from August 17 to October 8, 2007. Two tipping bucket rain gages (CS-615) were installed. One was located at the weather station. The other was placed in a cornfield above the canopy at approximately 200 m from the stream.

Tree canopy measurements

A Model A spherical densiometer was used to measure the percent canopy cover in the stream using the method described by Lemmon (1956). Thirty-five measurements were made at stream station flags and at piezometer locations on August 20, 2007. The densiometer was held at chest level and the percent cover in each of the four cardinal directions was estimated by counting the shaded grids in that quadrant. The four directional coverage values at each measurement locations were converted to percentages then averaged to determine percent canopy cover at that location.

Hydrologic measurements

Stream flow

The stream flow or discharge of the stream was measured at the upper limit of the study reach at Wednesday Hill Road and at the end of the reach at approximately 520 m downstream. These measurements were made to determine the overall gain or loss of discharge along the reach.

The upstream measurement system was designed and installed by Dr. Davis and graduate student M. Frades in 2005. A Campbell Scientific SR-50 ultrasonic measurement unit equipped with an air temperature probe to correct for variations in the speed of sound due to temperature is installed above a hole in the culvert at Wednesday Hill Road. The unit measures the distance to the water surface near the culvert outflow. A conversion is then applied to the measurement based on Manning's equation for flow to determine the discharge at the culvert. Distance measurements are made every 15 minutes and recorded using a Campbell Scientific CR510. The data were downloaded regularly until early October 2007 when the SR-50 transducer failed. The unit was re-installed in June 2008 after the SR-50 was repaired.

Stream flow was measured downstream using a Parshall Flume. A one-inch (2.54 cm) flume was installed for the initial field mobilization (FC-2007-1) but the flume proved to be too small. It was replaced by a two-inch (5.08 cm) flume in September 2007. Both flumes were equipped with a stilling well. A Global Water pressure transducer and dedicated data logger was installed in the stilling well. Water levels were automatically measured every 15 minutes from August 23 to September 12, when a heavy rain undermined the flume. The 5.08 cm flume was installed on September 28 and remained in place until the end of the field campaign on October 7, when another heavy rain event dislodged the larger flume. The flume was then removed and the data loggers were downloaded and removed. Significant effort was made to prevent flow bypass around the stream bank edges in both installations, but some leakage did occur at the edges and at the flume mouth.

Pressure transducer water levels in the flume stilling well were converted to streamflow discharge by developing a rating curve. Both the 2.54-cm and 5.08-cm flumes were equipped with level markings at the outflow. These markings were read daily and the level of the transducer at the time of level reading was related to discharge by statistical regression. This fit was then applied to the flow-rating curve for the flumes developed by the manufacturer to estimate the final discharge value.

Groundwater levels

A series of 3.8 cm PVC wells were installed by the UNH Water Resource Research Center in 2005 to measure shallow groundwater levels and water quality. The well locations are shown in Figure 3-1 and Appendix B. Water levels were measured at the monitoring wells in the upper portion of the study reach on August 22, 2007 and again on November 16, 2007. Water levels were measured from the top of the PVC well casing using a YSI TLC meter to the nearest hundredth of an inch. These measurements were then converted to meters. Elevations measured by previous researchers were used to determine the relative elevation of the water table.

Stream/hyporheic zone gradients

Twenty five (25) mini piezometers were installed in the streambed to collect streambed hydraulic potential and streambed temperatures at several depths. Piezometers were constructed of clear 0.64 cm diameter rigid acrylic tubing. The bottom 2 cm of the piezometers was slotted several times then wrapped with a geotextile fabric to prevent fine sediment from entering the bottom and slots. In addition, the piezometers were equipped with thermocouple wire at two or more depths to measure streambed temperatures. The thermocouple wire installation and measurement are further described in a following section.

Piezometers were installed by inserting the piezometer into a slightly larger galvanized pipe then placing a nylon washer plug at the bottom of the pipe before advancing it into the streambed. The pipe was advanced into the streambed in a vertical orientation using a five-pound maul until the streambed alluvium depth was reached. This depth had been previously measured using a probe as described above. Once at the prescribed depth, the pipe was gently pulled back, leaving the nylon plug and piezometer in place. The sandy sediment filled in the small annulus created by the pipe. Native clay from a downstream location was used at the stream surface to seal the piezometer installation.

Water levels were measured 19 times at most locations throughout the two field campaigns. The height of the stream above the streambed was measured to the nearest millimeter and the height of the water level in the piezometer above the streambed was also measured to the nearest millimeter. Several piezometers were damaged during strong storms in September and October 2007. The remaining piezometers were removed on October 14, 2007.

Piezometers were located at significant geomorphic stream features along the study reach. Table 3-1 lists the stream station position and depth of each piezometer. In several locations, piezometer pairs were installed in adjacent

riffles and pools to gather contrasting temperature distributions and hydraulic gradient information. Several additional piezometers were installed during FC-07-1 at locations where temperature anomalies were noted by the FODTS survey.

Temperature measurements

Temperature measurements were made in the stream, streambed, tributaries, and groundwater wells throughout both field campaigns. These late summer stream and groundwater temperature measurements provide the contrast needed to evaluate heating from solar radiation and to capture temperature differences between groundwater discharge and tributary discharge.

Stream temperature was measured continuously during the two field campaigns using a fiber optic distributed temperature sensor along the length of the study reach. Stream temperatures were measured using Hobo thermistor data loggers at selected point locations during the field season. Finally, stream temperatures were measured using a hand-held thermocouple thermometer at piezometer locations.

Streambed temperatures were measured at selected locations using both Hobos and thermocouple sensors attached to the mini-piezometers. Tributary temperatures were measured with Hobos and with the handheld thermocouple thermometer. Well water temperatures were measured using Hobos installed at the bottom of the well.

Hobo temperature data loggers

Temperature measurements of stream water, streambed, tributaries and groundwater were measured using Onset Computer Corporation Hobo™ UA-00-64 Pendant data loggers (Hobos). These thermistor sensors measure temperature to an accuracy of 0.47°C at 25°C. Temperatures are resolved to 0.10°C at 25°C and the loggers have 64K memory. They are waterproof at the depth and temperature range of this study site (Onset Computer Corporation, 2008).

Prior to installation of the Hobos, calibration testing was completed on those units owned by the researchers to determine the range and variability of the units to be used during the field campaigns. The Hobos were placed in a 40°C water bath for two hours. A thermocouple wire was also periodically measured as a temperature check. The temperatures measured by the Hobos were not significantly different. The Hobo testing results are included in Appendix B. Some of the Hobos used during the two field campaigns were provided by the

USGS. These units were not tested but were assumed to fall into the same range of variability as those tested in the initial calibration.

The Hobos were programmed to collect temperature measurements every 15 minutes throughout the study period. Table 3-1 lists the locations and vertical position of Hobos within the study reach. Stream temperature Hobos were placed in a 15 cm section of 3.8 cm PVC pipe and fastened to the stream bottom at the thalweg using a 25 cm galvanized spike. At tributaries, Hobos were installed using the PVC pipe sleeve and spike, and were also tied off to a nearby tree or sapling with nylon masonry cord.

Most streambed piezometers were installed to 20 cm below the stream surface (bss) by pushing the Hobo into the streambed using a small PVC pipe. At one location, the Hobo could only be installed to 15 cm bss. The subsurface Hobo data loggers were tied to masonry cord, which was fastened to a stake or tree at the edge of the stream, or to the spike fastening the surface water Hobo to the streambed.

Hobos installed in wells were tied with masonry cord. A galvanized washer was attached to the cord near the Hobo to keep the Hobo at the bottom of the well. The cord was tied off at the top of the well so that it could be easily recovered.

Drainage features that had a well-defined channel and contained flowing water at the time of the preliminary survey were considered tributaries. Features where a spring was present within several meters of the stream and was flowing at the time of the first measurements were called springs and areas of more diffuse discharge where the stream bank was saturated or even contained minor flow channels were considered seeps. The springs and seeps usually discharged to the surface more than a meter above the streambed and tributaries entered the stream at less than 0.5 m above the streambed.

Continuous measurements were taken at four tributaries and one seep over a portion of the 2007 field season. Chosen prior to the FODTS survey, these points were thought to represent tributary conditions along the brook. The tributaries were measured at points less than 5 m from their confluence with the brook.

After reviewing 2007 field data, several other tributaries were chosen for continuous measurement using Hobo dataloggers. Two tributaries measured in

2007 were also measured in 2008 to provide a cross calibration between years. Means were calculated over the time period of interest for the two years and a relationship between average temperatures by ratio was developed. The 2008 means were adjusted to better match 2007 temperatures using this ratio prior to application in modeling and analysis.

Mini-piezometers thermocouples

Mini-piezometers were fitted with thermocouple wire to measure streambed temperatures at two or more depths. Multiple streambed temperature measurements were collected at regular intervals and at selected riffles and pools to understand heat flow from the stream surface into the hyporheic zone. Piezometer locations are shown in Figure 3-1 and installation details are listed in Table 3-2.

Type T thermocouple (TC) wire (sensors) manufactured by Omega Engineering, Inc. was used for the installations. This thermocouple type was used, as it is most accurate at the expected temperature range in an aqueous environment. The lower centimeter of wire was stripped of its plastic casing; the wires twisted to provide contact, and then dipped in liquid plastic to protect the wires. The wire was then attached to the piezometers using electrical tape at several depths and

the wire was left free at the top of the piezometer for measurement with a handheld thermometer (Omega Engineering Model HH23).

The TC sensors were installed at the bottom of the piezometer to measure the temperature at the base of the stream alluvium and at 20 cm below the streambed. Where possible one or two additional TC sensors were placed at regular intervals between these two depths depending on the streambed thickness.

Most of the TC piezometers were installed prior to the first field campaign. Their locations were chosen based on stream morphology. During the first field campaign, a number of temperature anomalies were detected along the study reach with the FODTS survey. Once identified, additional mini piezometers fitted with TC wire were installed at these locations to understand the streambed hydraulic and temperature gradient.

At five piezometer locations, TC wire was connected to Campbell Scientific data loggers to allow for continuous data collection over the field campaigns. One piezometer installed at the 237 m riffle was equipped with four TC sensors. The other four piezometers were paired. At the 370 m location one piezometer of the

pair was installed in a riffle and one in an adjacent downstream pool. Each of these piezometers had sensors at four depths. The pair at 510 and 512 m was also installed in an adjacent riffle and pool feature and had sensors at four depths on each piezometer. Campbell Scientific 510S data loggers were used for data collection at 237 m and at the 370 m pair. Campbell Scientific data logger thermistors were also used at these locations to assure temperature accuracy. At the 510 and 512 m location, a data logger and multiplexer were used to accommodate the thermocouple sensors. No data logger thermistor was utilized at this location.

Fiber-Optic Distributed Temperature Sensor Survey

The temperature of the streambed surface was measured along the study reach with a fiber-optic distributed temperature sensor (FODTS) system. This method employs the use of laser light propagation and measurement of backscatter along a standard telecommunication fiber-optic cable (Henderson et al., 2009). FODTS is emerging as a powerful technology for hydrologic investigations, enabling 1-m spatial resolution and 0.01C temperature resolution depending on measurement configuration (Selker et al., 2006). Most commercially available systems used in hydrology are based on analysis of Raman backscatter. The ratio of intensity between the Raman Stokes (temperature independent) and anti-Stokes (temperature dependent) components allows for measurement of temperature (Selker et al., 2006). Temperature measurements are localized to

intervals of cable using the principle of optical time-domain reflectometry (OTDR), which is based on a time-of-flight calculation given by the speed of light in the cable. For this experiment, a Lios Technology OTS20P 2000/4000 was used. This instrument uses optical frequency domain reflectometry (OFDR), which is similar in concept to OTDR, except that backscatter is analyzed in the frequency domain. The LIOS Technology software Charon_02 controls the data collection, performs the OFDR analysis, and outputs temperature along the cable.

The FODTS measurements were performed in collaboration with the U.S. Geological Survey (USGS), Office of Ground Water, Branch of Geophysics, which provided the LIOS system for data collection. A laptop computer controlled the Lios OTS20P 2000/4000 and a Honda generator was used to power the unit over the two field campaigns. A locking steel job box was used to contain and protect the computer and LIOS unit during deployment. Approximately 540 m of “military/tactical” 62.5 micron telecommunication fiber in a 4.5-mm PVC jacket, manufactured by AFL was installed at the streambed surface or at approximately 2 cm below the streambed in the thalweg, depending on the size and character of the streambed materials. In the cobble and boulder section at the upper limit of the reach, the cable was secured to the stream bottom using cobbles and boulders from the stream and with galvanized steel washers attached to the cable with elastics. In areas of softer streambed sediment, the cable was buried to about 2 cm below the streambed and fastened to the stream bottom by

pushing the attached washers into the streambed at depth below the cable. The cable entered the stream at about 10 m downstream from the culvert outflow at Wednesday Hill Road. At the downstream end of the reach, the cable came out of the water at about 510 m, just upstream of the flume. The location of the LIOS control unit during the field campaigns is shown on Figure 3-1.

Where large log dams crossed the stream, the cable was brought out of the water above the log dam and then returned to the streambed at the downstream end of the log dam. Because of these in-stream obstructions and the variability of the streambed versus the bankfull stream edge, the cable distance is 40 m greater than the 500 m downstream distances measured with the rangefinder. The cable length is marked at one m intervals. This allowed for accurate distance correlation along the stream. All obstructions (log and debris dams, etc.) where the cable came out of the water and stream features were noted during cable installation and referenced to the cable distance markings and stream station flags where possible. Between the first and second field campaigns, the cable was left in the stream and the job box remained on site. Rodents chewed the cable in multiple locations where the cable ran over land from the stream to the job box. The cable was repaired prior to the second field campaign and adjustments made to the cable length parameters as needed for data analysis.

Topographic LIDAR mapping

On November 11, 2008, the study area was flown to collect detailed topographic data. LiDAR, Light Detection and Ranging, data were collected using an Optech Gemini Airborne laser Terrain Mapper (ALTM) mounted in a twin-engine Cessna Skymaster airplane. The National Center for Aerial and Laser Mapping (NCALM) provided the equipment, conducted the aerial survey, and processed all raw data as described below as part of an NCALM seed research grant awarded in January 2008.

The ALTM was flown at approximately 600 m (2000 ft) above ground level (AGL). The pulse-rate frequency was 70 KHz; the scan angle was +/- 20 degrees with +/- 3 degrees cut off during processing, so the useable swath was 366 m wide. There was 100% overlap in flight lines resulting in a swath spacing of 183 m.

Thirty-two overlapping swaths were flown to collect data over a 42.5 km² area. Approximately 4 km² of this area encompasses the WHB watershed. Up to four range measurements (returns) are recorded per laser pulse, including the first and last. The first stop range will often be at or near the top of the canopy, while the last stop can be either top, mid-canopy, or at or near the ground. Good leaf-off conditions during the flight ensured better penetration than heavy summer canopy.

Both the horizontal and vertical positions of the LiDAR point cloud were fixed relative to the National CORS network (NGS, 2008). Two temporary NCALM GPS reference stations were established for this survey: one was located at the Portsmouth International Airport at Pease, and the other was within the project site at the UNH campus. All NCALM GPS observations were logged at a 1-second rate and were submitted to the NGS on-line processor OPUS with solution files attached. NCALM GPS equipment consisted of ASHTECH (Thales Navigation) Z-Extreme receivers, with choke ring antennas (Part# 700936.D) mounted on 1.5 m fixed-height tripods.

Final point spacing (including overlap swaths) was approximately 9 points per m². Data points were gridded by NCALM using Surfer (Golden Software) with a kriging algorithm to produce a digital elevation model (DEM) at 1 m horizontal spacing. The precision of the LiDAR vertical point cloud data was approximately 5 to 10 cm +/- 1 cm while horizontal precision was 0.11 m. In addition to DEM's, data were delivered in point cloud (LAS) format classed as ground or non-ground for further analysis. The data were provided in units of m with UTM Zone 19 coordinates. The vertical datum used was NAVD88 (using geoid model Geoid03), and the horizontal datum used was NAD83 (CORS96) (EPOCH:2002.0000).

Data analysis and evaluation methods

Graphical analyses

Time series of air, groundwater, surface water and the hyporheic zone data were evaluated graphically using Microsoft Excel to illustrate diurnal and longer-term changes. Excel bar charts were also used to represent hydraulic gradients, diurnal temperature amplitudes, and stream and groundwater fluxes.

Box and whisker plots were plotted using Sigma Plot to illustrate temperature data. Sigma Plot was also used to generate basic statistics for Hobo data and TC data collected at piezometers.

Pebble count data were graphed with Excel to show cumulative grain size distribution and to determine the median grain size diameter of streambed surface material for each reach (Rosgen, 1996). Stream longitudinal profiles and cross sections were illustrated graphically using Excel to determine the characteristic channel and valley shape (Rosgen, 1996).

ArcGIS and ArcHydro analysis

Base maps were developed using NHGRANIT geographic information systems (GIS) data imported into ArcGIS. Data sets used included NH Roads, NH Flow

(stream centerlines) surficial geology and NHGS bedrock depths. LiDAR DEM data provided by NCALM were analyzed using Spatial Analyst Surface contour tools to provide land surface contours. Detailed streamflow and flow accumulation analyses were conducted using the ArcHydro GIS tools (Maidment, 2002).

The LiDAR digital elevation model (DEM) data were used to estimate surface flow paths using several ArcHydro utility tools (Maidment, 2002). The stream flow analysis has several steps prior to flow path calculation. One step fills sinks or holes in the topographic data that dead end flow paths. Some of these dead ends are actual topographic features (wetlands, depressions, ponds) while others just represent limitations in the coverage of topographic point data. These features are typically filled by ArcHydro for initial flow analysis to allow for more efficient stream flow routing.

Stream definition analysis using the unfilled data was used to infer groundwater discharge in the reach by summing the contribution from the dead-ended flow paths in the box valley and in the western floodplain area. These were compared against expected surface flow amounts and groundwater contributions to evaluate heat budget modeling.

The ArcHydro analysis of filled point data was used to define drainage pathways. A minimum of 5,000 pixels (5,000 m² of contribution area) was chosen to define a flow path. The main stem of WHB and significant tributaries were defined with this analysis method.

The number of contributing pixels for each defined flow path is stored in the attribute data for the stream definition layer. These data were queried in order to determine the contributing area for each of the defined tributaries as well as the WHB main stem.

The streamflow flow from each of the tributaries and at points along WHB stream was then calculated. The ratio of average measured flow at the upstream gage and upstream contributing area was then multiplied by the tributary or sub-reach contributing area to provide an estimate of the tributary streamflow values. The sub-reach flow values were estimated by dividing the difference between the downstream and upstream flow by the percent difference between downstream and upstream contributing areas.

The longitudinal elevation profile of the WHB study reach and its tributaries was determined using several methods. The ArcGIS profile tool was used to roughly estimate the elevation changes. Elevations were compared to the field-surveyed

data. The estimated elevations completed during the field survey were modified to match the LiDAR topographic survey elevations. Catchment cross sections were also generated using this method to define watershed geomorphology.

Hydraulic gradient calculations

The following formula was used to calculate the vertical hydraulic potential of the streambed at piezometers.

$$i_v = \left(h_{stream} - h_{streambed} \right) / d_{streambed} \quad (1)$$

where i_v is vertical hydraulic potential (dimensionless), h_{stream} is the height of stream water above streambed surface (cm) and $h_{streambed}$ is the height of water in piezometer above streambed surface (cm), and $d_{streambed}$ is the depth of the piezometer (cm) below the streambed surface.

Statistical analysis

Temperature data were analyzed statistically. Temperature histograms were graphed to determine distribution characteristics. These analyses were carried out using JMP 7.0.2 statistical software. Mean, standard deviation, maximum and minimum temperatures from the FODTS data were analyzed using a Matlab program (Day-Lewis, personal communication). Sigma Plot was used to develop basic statistics and box and whisker plots for Hobo data logger data and thermocouple data collected at piezometers.

Temperature amplitude analysis

An analysis of percent amplitude between the stream and streambed temperatures was conducted at stream/streambed hobo pairs and at continuously measured piezometer locations 237, 370 and 372 m. The 72-hour period from August 26 to 29, 2007 was used for this analysis as the average diurnal temperature change was constant compared to the temperatures measured before or after and it coincided with the FODTS survey. The average amplitude of diurnal temperature change (maximum temperature minus minimum temperature) for these three days was calculated for the stream and 20 cm streambed at each location where these measurements were concurrently measured. The average streambed temperature amplitude was divided by the average stream temperature amplitude then multiplied by 100 to arrive at the percent amplitude of the streambed compared to the stream. Based on Silliman et al., (1995), amplitude percentages greater than 10% were interpreted to imply advection or hyporheic flow at these locations.

Time stability analyses

Time stability analyses (TSA) were conducted on the FODTS stream temperature data collected during FC-07-1. A Matlab program was written to conduct the analysis. TSA has been used to evaluate time-invariant characteristics of soil moisture in agricultural and mountainous settings (Jacobs et al., 2004, Brocca et al., 2008). These soil characteristics include slope, soil type, and vegetation type. The stream characteristics dominant grain size, reach morphology and

mean sediment depth were evaluated against time stability of the stream temperature data set.

Preliminary temperature data analyses revealed that there is great longitudinal variability in stream temperature upstream to downstream and significant temperature changes by location. The TSA was applied to WHB to determine time if its stream temperature is time invariant.

The stream temperature mean and standard deviation for each measurement point along the cable over the entire study period were calculated as:

$$\bar{T}_i = \frac{1}{n_t} \sum_{t=1}^{n_t} T_{t,i} \quad (2)$$

$$\sigma_i = \sqrt{\frac{1}{n_t - 1} \sum_{t=1}^{n_t} (T_{t,i} - \bar{T}_i)^2} \quad (3)$$

where \bar{T}_i is the mean temperature at sampling point i ($^{\circ}\text{C}$), σ_i is the standard deviation in temperature at each sampling interval, i is the sampling point along the FODTS cable, n_t is the total number of measurements taken at each location, t is the sample time, and $T_{t,i}$ is the stream temperature at each measurement point (i) at each sampling interval t ($^{\circ}\text{C}$).

The time stability analysis was completed first for the entire study reach, then for a smaller portion of the study reach that eliminated the armored reach (approximately the first 100 m). The reach mean was calculated for each sample time as

$$\bar{T}_t = \frac{1}{n_t} \sum_{i=1}^{n_t} T_{i,t} \quad (4)$$

where n_t is the total number of measurements made at each time t .

The mean relative difference ($\bar{\delta}_t$) and variance of the mean relative difference ($\sigma(\bar{\delta}_t)^2$) in temperature are given by

$$\bar{\delta}_t = \frac{1}{n_t} \sum_{i=1}^{n_t} \left(\frac{T_{i,t} - \bar{T}_t}{\bar{T}_t} \right) \quad (5)$$

$$\sigma(\bar{\delta}_t)^2 = \frac{1}{n_t - 1} \sum_{i=1}^{n_t} \left(\frac{T_{i,t} - \bar{T}_t}{\bar{T}_t} - \bar{\delta}_t \right)^2 \quad (6)$$

The mean relative difference at each temperature measurement point along the cable is the point's bias with respect to the reach mean and expresses whether the point is cooler or warmer than the average reach temperature. The variance is the absolute variability of that difference at the sampling point.

Distribution and statistical differences among TSA values based on stream characteristics were conducted by distribution analysis and means testing against zero. Both JMP7™ and Sigma Plot were used to conduct these analyses.

Heat budget calculations

A heat budget was developed to determine the physical factors causing observed heating and cooling along sub sections of the study reach. The overall heat budget quantifies the advective and non-advective heat exchange to and from the study reach. The non-advective terms were evaluated using methods described by Webb and Zhang (1997, 1999), Story et al. (2003) and Johnson (2004). The advective terms were adapted from methods in Story et al. (2003) and Cozzetto et al. (2006). The model period was the first field campaign (FC-07-1) from August 21 to August 28, 2007. The mean temperatures and discharge measured during this period were used for the heat budget model. Because no precipitation occurred during FC-07-1, a precipitation heat term was not included. The heat budget equation calculates the change in temperature at the downstream cross section of a reach based on the heat transfer across the control volume of the reach at steady state where

$$Q_{ds}T_{ds} = Q_{us}T_{us} + L\beta[H_{netrad} - H_{evap} - H_{conv} - H_{cond} + H_{fr}] + L[q_{gw}T_{gw} + q_{hyp}(T_{hyp} - T_{us})] + \sum_{i=1}^n Q_{trib,i}T_{trib,i} - \left[\frac{S_{end}T_{end} - S_{start}T_{start}}{\Delta t} \right] \quad (7)$$

The left hand side of the equation is the downstream heat flow out of the subreach. On the right hand side, the first term is the upstream heat flow boundary condition, the second term is the non-advective heat flow, the third term is the diffuse advective heat flow and the fourth is the heat flow due to point sources. The fifth term accounts for the change of heat in storage between the beginning and end of the heat budget analysis period.

Q_{us} and Q_{ds} are the streamflows at the upstream and downstream reach cross sections, respectively, and T_{us} and T_{ds} are the stream temperatures at the upstream and downstream cross section, respectively.

The non-advective components of the heat budget are contained in the second term. L is the reach length, the unit heat capacity, β , is w/C where w is the average stream width (m) and C is the heat capacity of water ($4.18 \times 10^6 \text{ J m}^{-3} \text{ }^\circ\text{C}^{-1}$). H_{netrad} is net radiation (W m^{-2}), H_{evap} is the evaporative energy flux (W m^{-2}), H_{conv} is the convective energy flux (W m^{-2}), H_{cond} is *streambed* conduction (W m^{-2}), and H_{fr} is the heat flux due to streambed friction.

Net radiation was directly measured at the WHB weather station throughout the 2007 field season. Corrections to net radiation for direct solar radiation are often made (Webb and Zhang, 1999), but since the WHB stream corridor has an 85% average canopy cover and direct radiation occurs only from 11:00 to 14:00, no correction was made for direct radiation.

Evaporative energy flux is estimated by

$$H_{evap} = E_v L_v \rho_w \quad (8)$$

where E_v is the evaporation rate (mm day^{-1}), L_v is latent heat of vaporization ($\text{J g}^{-1} \text{ } ^\circ\text{C}^{-1}$), and ρ_w is the density of water (g m^{-3}) at $25 \text{ } ^\circ\text{C}$. The evaporation rate was estimated with the Penman empirical equation (Chow et al., 1988).

$$E_v = 0.165(0.8 + U/100)^* (e_w - e_a) \quad (9)$$

where U is the wind speed at 2 m above the stream surface (km day^{-1}), e_w is saturated vapor pressure at the surface water temperature (T_w), and e_a is air vapor pressure (mbar) calculated from saturated vapor pressure at the air temperature (T_a) and relative humidity.

The latent heat of vaporization ($^\circ\text{C J}^{-1} \text{ g}^{-1}$) is estimated as a function of air temperature

$$L_v = 2454.9 - 2.366 T_a \quad (10)$$

where T_a ($^{\circ}\text{C}$) is the air temperature.

Convective energy flux, H_{conv} , or sensible heat flux was estimated using the Bowen ratio (Bowen, 1926) and evaporative heat flux (Webb and Zhang, 1999) as

$$H_{conv} = \left\{ \left[0.61P(T_w - T_a) / (e_w - e_a) \right] / 1000 \right\} H_{evap} \quad (11)$$

where P is atmospheric pressure (970 mbar).

Streambed conduction, H_{cond} , is estimated as

$$H_{cond} = K \left(\frac{dT}{dh} \right) \quad (12)$$

where K is thermal conductivity of streambed materials ($\text{J m}^{-1}\text{s}^{-1}\text{ }^{\circ}\text{C}^{-1}$), dT is the temperature difference between the streambed surface and streambed at 20 cm below the stream surface (bss), and dh is the distance between the streambed surface and streambed (20 cm).

K was estimated based on streambed characteristics derived from the pebble count data, streambed probes and field observations. Streambed characteristics were

compared to a relationship, illustrated in Lapham (1989), between dry bulk density of sediment and thermal conductivity. A range of values from 1.8 for silty clay to $2.8 \text{ J m}^{-1}\text{s}^{-1} \text{ }^\circ\text{C}^{-1}$ for coarse gravel was used (Table 3-3). Because streambed temperatures were measured at 20 cm below stream surface and at the bottom of the streambed, conduction values were calculated for both intervals. The streambed temperatures measured at piezometers between August 20 and 29th were averaged to provide stream temperature, streambed temperature at 20 cm and streambed temperature at the base of the streambed. Gradients and streambed conduction were then calculated from these values.

Table 3-3 Estimated thermal conductivity values based on streambed material properties (Lapham, 1989), Wednesday Hill Brook in Lee, NH

Pebble count reach (m)	D50 grain size (mm)	Bed material type	Estimated thermal conductivity $K (\text{J m}^{-1}\text{s}^{-1} \text{ }^\circ\text{C}^{-1})$
0 - 100	80	Cobbles and gravel	2.8
100 - 200	20	Fine to coarse gravel	2.6
200 - 300	7	Fine gravel	2.2
300 - 400	0.8	Sand and fine gravel	2.0
400 - 500	0.4	Silt, clay and sand	1.8

H_{fr} is the heat energy from fluid friction ($W m^{-2}$) given by Theurer et al. (1984) as

$$H_{fr}=9805(Q_{us}/w) S \quad (13)$$

where s is the slope of the channel ($m m^{-1}$).

The third term in equation 7 is the diffuse advective heat flux from groundwater and hyporheic exchange. Here, q_{gw} is the groundwater flux to the stream ($m^2 s^{-1}$), T_{gw} is the temperature of the groundwater ($^{\circ}C$) and T_{hyp} is the average temperature of the hyporheic zone ($^{\circ}C$). q_{hyp} is the hyporheic flux per meter ($m^2 s^{-1}$) and is estimated following Harvey and Wagner (2000) as

$$q_{hyp}=\alpha A \quad (14)$$

where α is the exchange coefficient (s^{-1}), the rate at which stream water is exchanged with water in storage, and A is the cross sectional area of the stream (m^2).

The fourth term describes the point sources of heat discharge to the stream. Here, $Q_{trib, i}$ is the estimated discharge of a tributary i entering the reach, $T_{trib, i}$ is the temperature of that tributary, and n is the number of tributaries.

For this study, the heat budget equation is applied over a time period, Δt , with average flux values over that period. The fifth term of equation 7 is the change in heat storage over the study period. T_{start} and T_{end} are the starting and ending water

temperatures averaged over the length of the reach ($^{\circ}\text{C}$), respectively. S_{start} and S_{end} are the volume of water in the reach at the beginning and end of the study period, respectively, and Δt is the length of the study period(s). The stream volume was calculated using the mean stream width and depth and the reach length.

Heat budget modeling

The heat budget model developed for WHB was used to estimate and understand the advective contribution of heat to the stream from groundwater discharge, hyporheic exchange and tributary discharge. The temperatures of the stream, the hyporheic zone, groundwater, and tributaries were known, but the tributary and groundwater discharge values and hyporheic exchange rate were not directly measured. The general approach was to use a water balance to estimate the total groundwater and tributary inflow in a reach. Once these inputs were constrained, the heat budget was used to estimate the hyporheic exchange.

In order to calculate the downstream reach temperature, equation 6 was re-arranged to solve for T_{ds} from known values and a reasonable estimate of unknowns, Q_{gw} , Q_{hyp} , and Q_{trib} . Unknowns were adjusted to satisfy the water balance for the reach and to match the observed downstream temperature (T_{ds}).

Modeled sub-reaches

The study reach was divided into sub-reaches that reflect distinct hydrologic or geomorphic conditions as discussed in Chapter 4. Four sub-reaches were chosen for modeling. The following sections describe the model parameters and the methods used to constrain the remaining model input data.

Model data

FC-07-1, the 6.9-day campaign in August 2007, was chosen for modeling efforts.

Reach averaged FODTS temperatures were used to determine T_{start} and T_{end} .

Location averaged FODTS temperatures were used to determine T_{us} and the target T_{ds} . The reach volume was determined from mean stream width, depth and length.

The values for wind speed at 2 m, air temperature and relative humidity, used in the non-advective heat calculations, were measured by the WHB weather station and surface water temperature estimates were from the continuous Hobo thermistor measurements. The average net radiation measured at the weather station during FC-07-1 was used for model input at all reaches. Evaporative and convective fluxes were calculated at 75 m using stream temperatures from the upper reaches. Evaporative and convective fluxes calculated at 336 m and 486 m were used for Reaches 4 and 5, respectively. Heat flux due to friction was estimated using streamflow estimates and stream dimensions for each reach.

The streambed temperature gradients (dT/dz) were derived from stream and hyporheic zone temperatures measured using Hobo data loggers or mini-piezometers equipped with thermocouple wires. The 20 cm streambed depth measurement was used to provide consistency among values. Locations for streambed conduction calculations were initially chosen where there was a minimal hydraulic gradient between the stream and streambed to minimize the influence of hyporheic exchange on this component of heat budget calculations. Streambed conduction was then calculated at all locations where stream and streambed temperatures were concurrently measured. Streambed conduction values used for reach modeling were based on the average of streambed conduction values located within that reach.

Reach 1 and 2 groundwater temperatures for modeling were an average of the temperatures measured at the monitoring well field. Reach 4 and 5 groundwater temperatures were estimated from seep and deep streambed temperatures measured in each reach. Tributary temperatures were based on average values from the individual tributaries measured during August 2007 or the corrected August 2008 data. Hyporheic zone temperatures were based on average values of either the piezometer or the Hobo temperatures measured at 20 cm bss in that reach during FC-07-1.

The upstream streamflow value used for reach 1 was the average discharge for the study period at the culvert streamflow gage. The target downstream discharge value at the end of each study reach was estimated based on the catchment area estimates derived from ArchHydro analysis of the WHB watershed at each subreach as described in the previous ArchHydro section.

Table 3-4 Modeling steps used to estimate heat budget contributions in sub-reaches, Wednesday Hill Brook in Lee, NH.

Simulation	Description	Energy balance or water balance ?	Water balance additions	Approach
1	Non advective contributions only	Neither	None	Downstream temperature predicted with non-advective flux components only
2	Tributary contribution at average temperatures only	Energy	Tributary discharge	Tributary discharge increased until measured downstream temperature matched
3	Groundwater contribution at average temperatures only	Energy	Groundwater discharge	Groundwater flux increased until measured downstream temperature matched
4	Hyporheic exchange at average temperatures only	Energy	None	Hyporheic exchange rate increased until measured downstream temperature matched
5	Groundwater and tributary discharge at average temperatures only	Water	Tributary discharge & groundwater discharge	Tributary discharge estimated from Archydro and groundwater discharge increased to achieve water balance
6	Groundwater and tributary discharge and hyporheic exchange at average temperatures	Water and energy	Tributary discharge & groundwater discharge	Tributary discharge estimated from Archydro, groundwater discharge increased to target downstream streamflow value, then hyporheic exchange increased to match measured downstream temperature

The input of non-advective heat flow, groundwater heat discharge, tributary heat discharge and hyporheic heat exchange were first considered individually, and then jointly to determine that contribution necessary to match the observed downstream temperature for each reach. The analysis was conducted using a series of six simulations to understand the relative importance of the heat sources (Table 3-4).

First, the model was applied using only the non-advective heat fluxes.

In simulations 2, 3 and 4, the non-advective heat was combined with a single advective term. In simulation 5, the groundwater and tributary flow rates necessary to satisfy the reach water balance were calculated. These rates were used to determine the resultant temperature.

In simulation 6, the tributary and groundwater discharge values were combined with hyporheic exchange to estimate the downstream temperature. The hyporheic exchange coefficient was adjusted until the modeled downstream temperature matched the observed value.

A small-scale heat budget (reach 1a and reach 2a) was also completed to better define significant local temperature change mechanisms in the immediate vicinity of tributary 1W and 2W. A reach that was 20 m long, 10 m upstream and 10 m

downstream, was analyzed surrounding the large observed mean temperature declines at these two tributaries. A large zone of permeable streambed material thought to carrying substantial groundwater to the stream was noted at both tributaries. Further estimates and verification of this groundwater contribution were made based on estimated permeability, area of the contributing zone of groundwater and hydraulic conductivity of the tributary streambed material. Reach flows were adjusted by assuming that the majority of flow for the larger sub reach (1 or 2) was entering the stream at the tributary. The hyporheic flux was then modified to match the observed average temperature downstream of the tributary in that reach. Some modifications to the larger sub-reach models were then made based on these finer scale calculations.

Estimation of flux component temperature change

The final reach water and energy balance values were used to determine each heat flux component's contribution to the reach temperature change. The temperature change for advective components is

$$\Delta T_{comp} = \frac{(Q_{us}T_{us} + Q_{comp}T_{comp})}{Q_{us} + Q_{comp}} - T_{us} \quad (16)$$

where ΔT_{comp} is the temperature change in the sub reach due to the heat flow from the component, Q_{comp} is the discharge value for the component of heat

flow, and T_{comp} is the temperature of the flow component. These advective components included groundwater, tributary and hyporheic discharge. For hyporheic exchange, there is no added streamflow and Q_{comp} is zero. For the starting and ending temperature flow component, Q_{comp} was estimated as the sub reach stream volume divided by Δt .

For the non-advective components, the relationship is

$$\Delta T_{comp} = \frac{(Q_{us}T_{us} + L\beta H_{comp})}{Q_{us}} - T_{us} \quad (17)$$

where H_{comp} is the heat flux due to net radiation, evaporation, convection, streambed conduction or friction.

Sensitivity analysis

Sensitivity of the model to changes in three parameters, the hyporheic exchange coefficient (α), streambed sediment thermal conductivity (K) and the stream-streambed thermal gradient used to calculate hyporheic flux (dT) was completed for each reach. The final simulation, including both advective and non-advective heat fluxes, was used as the baseline for the analysis. Each of the parameters was varied up to two times greater than the modeled parameter value and to half the value or zero while all other parameter values were held constant. For thermal conductivity, the physically based range for K of 1.6 to 3.2 J m⁻¹s⁻¹ °C⁻¹ was used

rather than doubling or halving the parameter. Modeled parameter values used for the sensitivity analysis were graphically compared to the absolute value of the resultant temperature changes ($T_{\text{modeled}} - T_{\text{observed}}$).

Table 3-1 Location of Hobo thermistors in study reach
 Wednesday Hill Brook in Lee, NH

FODTS Cable Station (m)	Station (m from WH Road)	Purpose	Description	Vertical Position	Date Installed (2007)	Collection Interval
75	10 (1)	Calibration	step	stream	23-Aug (3)	15 min
171	93 (1)	Calibration	pool	stream	23-Aug (2)	15 min
237	147 (1)	Streambed profile	riffle	stream	21-Aug (2)	15 min
257	158 (1)	Streambed profile	riffle	stream	25-Aug (2)	15 min
257	158 (1)	Streambed profile	riffle	20 cm bss	25-Aug (2)	15 min
268	168 (1)	Streambed profile	riffle	20 cm bss	25-Aug (2)	15 min
268	168 (1)	Streambed profile	riffle	stream	25-Aug (3)	15 min
276	176 (1)	Streambed profile	pool	20 cm bss	25-Aug (2)	15 min
276	176 (1)	Streambed profile	pool	stream	25-Aug (2)	15 min
293	198 (1)	Calibration	riffle	stream	23-Aug (2)	15 min
293	198	Streambed profile	riffle	20 cm bss	17-Aug (2)	15 min
336	229.5	Streambed profile	riffle	20 cm bss	17-Aug (2)	15 min
336	229.5	Streambed profile	riffle	stream	17-Aug (2)	15 min

bss – below stream surface (1) USGS Hobo (2) Removed 8-28 to 9-01-07 (3) Removed 9-07 to 9-11-09

Table 3-1 Location of Hobo thermistors in study reach
Wednesday Hill Brook in Lee, NH

FODTS Cable Station (m)	Station (m from WH Road)	Purpose	Description	Vertical Position	Date Installed (2007)	Collection Interval
370	250 (1)	Streambed profile	riffle	stream	21-Aug (2)	15 min
372	251.5 (1)	Streambed profile	pool	stream	21-Aug (2)	15 min
413	298 (1)	Streambed profile	riffle	stream	25-Aug (2)	15 min
413	298 (1)	Streambed profile	riffle	15 cm	25-Aug (2)	15 min
416	300 (1)	Calibration	riffle	stream	22-Aug (2)	15 min
430	312 (1)	Streambed profile	run	stream	25-Aug (2)	15 min
433	315 (1)	Streambed profile	pool	20 cm bss	25-Aug (2)	15 min
443	325	Streambed profile	pool	stream	17-Aug (2)	15 min
443	325	Streambed profile	pool	20 cm bss	17-Aug (2)	15 min
461	340	Streambed profile	riffle	stream	17-Aug (2)	15 min
461	340	Streambed profile	riffle	20 cm bss	17-Aug (2)	15 min

bss – below stream surface (1) USGS Hobo (2) Removed 8-28 to 9-01-07 (3) Removed 9-07 to 9-11-09

Table 3-1 Location of Hobo thermistors in study reach
Wednesday Hill Brook in Lee, NH

FODTS Cable Station (m)	Station (m from WH Road)	Purpose	Description	Vertical Position	Date Installed (2007)	Collection Interval
480	360	Streambed profile	rifle	stream	17-Aug (2)	15 min
480	360	Streambed profile	rifle	20 cm bss	17-Aug (2)	15 min
486	365	Streambed profile	pool	stream	17-Aug (2)	15 min
486	365	Streambed profile	pool	20 cm bss	17-Aug (2)	15 min
491	370	Streambed profile	rifle	stream	17-Aug (2)	15 min
491	370	Streambed profile	rifle	20 cm bss	17-Aug (2)	15 min
510	388	Streambed profile	rifle	stream	22-Aug (2)	15 min
512	390 (1)	Streambed profile	pool	stream	22-Aug (2)	15 min
525	400 (1)	Calibration Streambed profile	run	stream	22-Aug (2)	15 min
525	400	Streambed profile	run	20 cm bss	17-Aug (2)	15 min
634	500 (1)	Calibration Streambed profile	pool	stream	22-Aug (2)	15 min
634	500	Streambed profile	pool	20 cm bss	17-Aug (3)	15 min

bss -- below stream surface (1) USGS Hobo (2) Removed 8-28 to 9-01-07 (3) Removed 9-07 to 9-11-09

Table 3-1 Location of Hobo thermistors in wells and tributaries, Wednesday Hill Brook in Lee, NH

FODTS Cable Station (m)	Station (m from WH Road)	Purpose	Description	Vertical Position	Date Installed (2007)	Collection Interval
196	110-124	Groundwater, Riparian zone	Well L1A-11	1 m bls	11-Aug (1)	15 min
197	110-124	Groundwater, Riparian zone	Well L1A-42	1 m bls	11-Aug (1)	15 min
198	110-124	Groundwater, Riparian zone	Well L1A-22	1 m bls	11-Aug (1)	15 min
199	110-124	Groundwater, Riparian zone	Well L1A-01	1 m bls	11-Aug (1)	15 min
199	110-124	Groundwater, Riparian zone	Well L1A-02	1 m bls	11-Aug (1)	15 min
199	110-124	Groundwater, Riparian zone	Well L1A-12	1 m bls	11-Aug (1)	15 min
201	110-124	Groundwater, Riparian zone	Well L1A-23	1 m bls	11-Aug (1)	15 min
210	124	Tributary temps	Tributary-West	2 cm bss	17-Aug (2)	15 min
225	132	Tributary temps	Tributary-West	2 cm bss	17-Aug (2)	15 min
290	190	Tributary temps	Tributary-West	2 cm bss	19-Aug (2)	15 min
368	250	Tributary temps	Seep - West	2 cm bss	17-Aug (2)	15 min
481	362	Tributary temps	Tributary - East	2 cm bss	17-Aug (2)	15 min
617	484	Tributary temps	Tributary-West	2 cm bss	17-Aug (2)	15 min

bls – below land surface
 bss – below stream surface

(1) Removed 11-08-2007

(2) Removed between 9-7 and 9-11-07

Table 3-2 Location of mini-piezometers in stream
Wednesday Hill Brook in Lee, NH

FODTS Cable Station (m)	Station (meters from WH Road)	Purpose	Sensor	Description	Vertical Position	Date Installed (2007) (1)	Collection Interval
167	88	Streambed profile	TC - hand	rifle	bottom, 20 cm bss	18-Aug	1-2 x per day
171	93	Streambed profile	TC - hand	pool	bottom, 20 cm bss	18-Aug	1-2 x per day
237	147	Streambed profile	TC-dedicated	rifle	4 level	18-Aug	1 minute
257	158	Streambed profile	TC - hand	rifle	3 level	28-Aug	1-2 x per day
268	168	Streambed profile	TC - hand	run	4 level	29-Aug	1-2 x per day
276	176	Streambed profile	TC - hand	pool	4 level	29-Aug	1-2 x per day
292	196.9	Streambed profile	TC - hand	rifle	bottom, 20 cm bss	18-Aug	1-2 x per day
295	199.5	Streambed profile	TC - hand	pool	bottom, 20 cm bss	18-Aug	1-2 x per day
334	228	Streambed profile	TC - hand	rifle	bottom, 20 cm bss	18-Aug	1-2 x per day
336	229.5	Streambed profile	TC - hand	pool	bottom, 20 cm bss	18-Aug	1-2 x per day
370	250.4	Streambed profile	TC-dedicated	rifle	4 level	18-Aug	15 minute
372	251.5	Streambed profile	TC-dedicated	pool	4 level	18-Aug	15 minute

bss – below stream surface
TC-hand – thermocouple, measured by hand, TC-dedicated – thermocouple, measured by data
logger (1) Removed 10-14-07

Table 3-2 Location of mini-piezometers in stream , Wednesday Hill Brook in Lee, NH

FODTS Cable Station(m)	Station (m from WH Road)	Purpose	Sensor	Description	Vertical Position	Date Installed (2007) (1)	Collection Interval
413	298	Streambed profile	TC - hand	riffle	3 level	27-Aug	1-2 x /day
422	308	Streambed profile	TC - hand	run	3 level	27-Aug	1-2 x /day
430	312	Streambed profile	TC - hand	run	3 level	27-Aug	1-2 x /day
433	315	Streambed profile	TC - hand	pool	3 level	29-Aug	1-2 x /day
443	325	Streambed profile	TC - hand	riffle	bottom, 20 cm bss	18-Aug	1-2 x per day
461	340	Streambed profile	TC - hand	riffle	bottom, 20 cm bss	18-Aug	1-2 x per day
480	360	Streambed profile	TC - hand	riffle	bottom, 20 cm bss	18-Aug	1-2 x per day
486	365	Streambed profile	TC - hand	pool	bottom, 20 cm bss	18-Aug	1-2 x per day
491	370	Streambed profile	TC - hand	riffle	bottom, 20 cm bss	18-Aug	1-2 x per day
510	388	Streambed profile	TC-dedicated	riffle	4 level	21-Aug	15 minute
512	390	Streambed profile	TC-dedicated	pool	4 level	21-Aug	15 minute
525	400	Streambed profile	TC - hand	pool	bottom, 20 cm bss	18-Aug	1-2 x per day
634	500	Streambed profile	TC - hand	riffle	bottom, 20 cm bss	18-Aug	1-2 x per day

bss – below stream surface TC-hand – thermocouple, measured by hand, TC-dedicated – thermocouple, measured by data logger (1) Removed 10-14-07

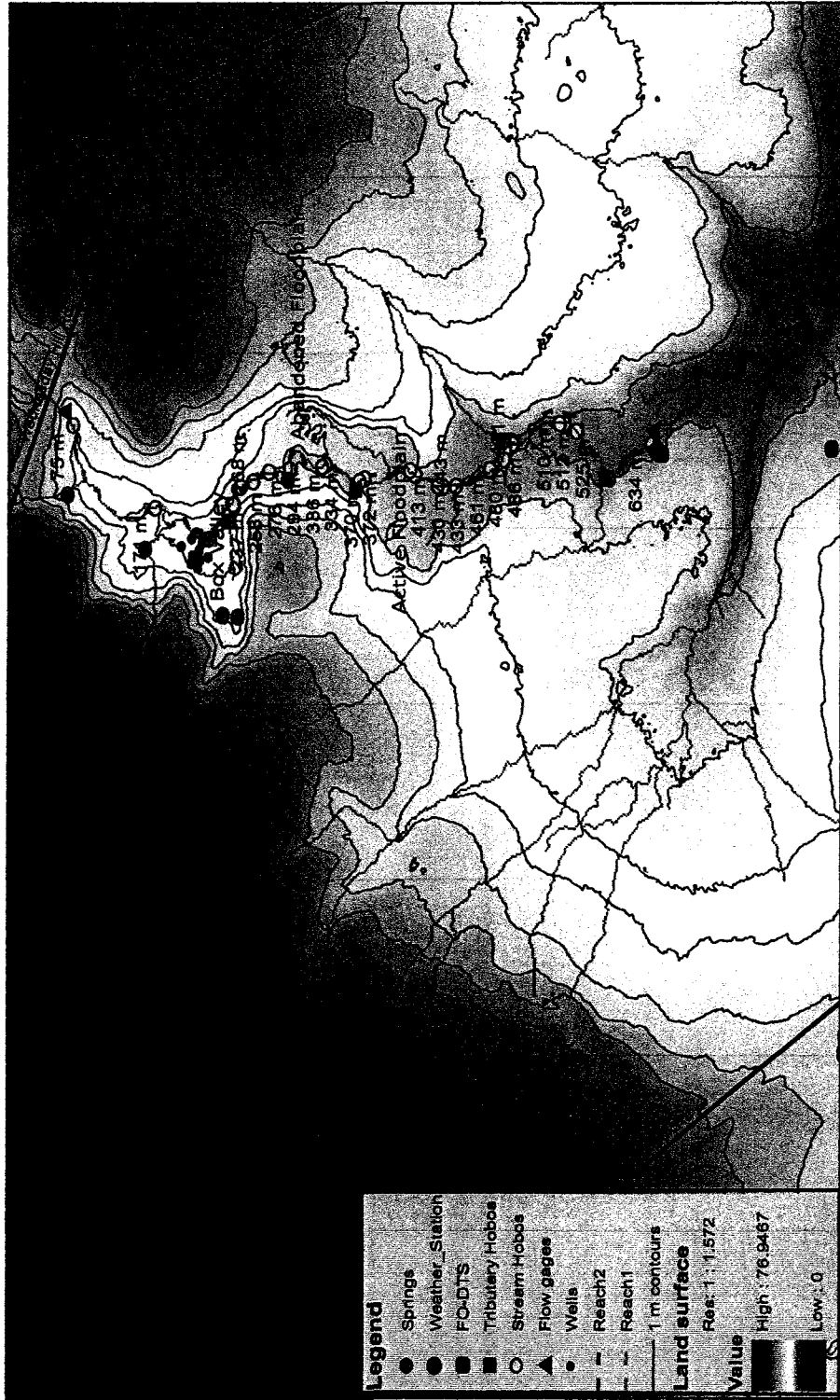


Figure 3-1 Location of field instrumentation in the Wednesday Hill Brook study reach Lee, NH. Topography developed from LiDAR imagery provided by National Center for Airborne Laser Mapping

CHAPTER 4

RESULTS

Introduction

In this section, a catchment-wide discussion of geomorphology and hydrology is presented, followed by the experimental results. The results are subdivided into broad study reach measurements and sub-reach specific results. Reach measurements include weather station observations, stream temperatures, and groundwater temperatures. Sub-reach results examine the streambed temperatures collected at multiple depths and stream temperature moderation processes. The results of the time stability analysis and heat budget modeling for four of the sub-reaches conclude this chapter.

Catchment geomorphology

The site map (Figure 3-1) illustrates the variety of valley and stream features within the watershed and along the 520 m study reach. Figures 4-1, 4-2 and 4-3 provide sub-catchment details of the study reach and feature land surface topography at 0.5 m contours provided by the LiDAR mapping.

Overall the WHB watershed is long and narrow (Figure 2-1). The stream is nearly linear in the reach above Wednesday Hill Road and flows northeast to southwest. About 150 m downstream of the road, the stream changes to a southerly flow direction and is much less linear than the upper area (Figure 4-1).

This flow pattern suggests that there may be underlying bedrock structural control in the upper drainage area. Adjacent catchments also appear to be controlled by underlying structure with a similar trend.

Stream gradients and depths of streambed alluvium

The longitudinal profile of WHB from the culvert to 400 m downstream (Figure 4-4) illustrates the changing stream gradient and streambed sediment thickness along the study reach. The profile shows the streambed elevation at the thalweg and the water surface elevation and, where available, displays the measured depths of streambed sediments. A table of streambed depth measurements is included in Appendix A.1.

Within the first 16 m of the study reach, the stream gradient averages 5% then moderates to an average slope of 3% at approximately 165 m. The upper reach follows a step-pool morphology. Boulders, cobbles and bedrock make up the majority of the streambed sediments and the streambed is less than 20 cm deep. Several spring brooks enter the stream from the west at 110 and 126 m and a large seepage area exists near the toe of the western slope between 135 and 155 m. The bed materials are somewhat armored or imbricated due to the stream energy created at the culvert plunge pool and the relatively steep gradient of the reach.

Between 185 and 200 m, the gradient moderates to 0.5%. The streambed morphology is largely riffle-pool with some log dams creating step-pool features. At approximately 185 m, a major spring brook enters the stream from the west. Here, a small delta has formed at the mouth of the spring brook. There are two logdams immediately upstream of this confluence. The gradient moderates further from 200 to 235 m where the average gradient is 0.3%. Several spring brooks enter the stream from the box valley to the west (210 and 225 m) and carry coarse sediment from the hillslope. The streambed depth in this section increases to more than 60 cm in most areas. In the area between 165 and 235 m there is a broad valley, with steep-sided valley walls to the east and west, but the stream is somewhat entrenched at this location and it appears that the floodplain is minimally active.

At 245 m, a large log dam creates a 1 m high cascade. The stream begins a tight meander just upstream of this log dam then makes another change of direction from east to southeast between 230 and 280 m. The stream is constricted within a narrows with steep hill slopes at this change in stream direction. Above the log dam, sediment has accumulated to 85 cm, but just downstream of the constriction the streambed depths decrease to less than 20 cm. Downstream of the large log dam a series of smaller log and debris dams create an area of step-pool features between 265 and 285 m. The average gradient in this reach (245

to 285 m) is 3.8%. Sediment has accumulated to over 90 cm behind the smaller log dams, but is variable overall.

Between 285 and 395 m, a series of meanders have formed. The gradient is 0.5% and the streambed material is generally deep and varies between 20 to 40 cm in riffles and up to 90 cm in pools. Many seeps and small springs enter the stream from the western hillslope and a considerable wetland is present on the floodplain that forms the eastern stream bank. The stream is entrenched in this area and the floodplain is no longer active.

At about 410 m, a small step has formed at the stream bend. Over a 10 m reach the gradient steepens to 1.7% then moderates to less than 1.0% at 525 m. In the section with the steeper gradient, the sediment is less than 20 cm deep but deepens considerably downstream where it is trapped behind log dams and debris dams. Multiple small spring brooks enter the stream from the west but are hidden at the surface beneath tree roots and vegetation. Sediment deposits and sediment turbulence at the confluence with the brook provide evidence of these tributaries' contribution. The greatest streambed depth in the study reach (156 cm) was measured at the bottom of a deep pool near 512 m.

Below 540 m the streambed thins dramatically and clay is exposed at riffles and along straight runs. Sediment has accumulated at bars and pools but to depths of less than 30 cm.

Pebble counts

Figure 4-5 shows a graph of pebble count data by reach. Data are included in Appendix A.2. The first 100 m of stream is made up largely of cobbles, boulders and possibly bedrock. The d50 (median grain size diameter) is 80 mm (medium cobbles) with little silt and clay fraction.

The reach from 180 to 295 m exhibits a coarse grain size distribution with the 40 mm d50. This clast size is considered to be large gravel. There is also a large percentage of fine to coarse sand as well as fine gravels with very little silt and clay. In this reach, streambed sediment depths increase to over 60 cm.

Sediment in the next 100 m reach (295 to 410 m) is much finer with a d50 of 7 mm – fine gravel. Coarse sand and finer grain sizes make up less than 30% of the sediment in this reach.

The d50 between 410 and 525 m decreases nearly an order of magnitude to 0.8 mm, indicating medium to coarse sand. This reach contains less than 10% of sediment in the gravel to cobble sized fraction and less than 3% silt and clay. At the end of the study reach (525 to 635 m) the d50 grain size is 0.25 mm

indicating medium to fine sand. The silt and clay fraction, 30%, is much greater than in upstream sections . As is typical of a stream, which changes from a fairly steep to a moderate gradient, grain size decreases with gradient due largely to a decrease in stream energy and sediment transport. In the case of WHB, the dominant grain size is also small in the lowest reach because marine silt and clay deposits are exposed at the streambed below 555 m.

Catchment surficial geology

Field observations generally support the reconnaissance level USGS mapping work shown on Figure 2-3. Some refinement was suggested by site fieldwork and by the site's high-resolution LiDAR topography (Figures 4-1 to 4-3). Re-defining the surficial geologic contacts is outside the scope of this research, but some site observations are relevant to defining the catchment-scale hydrology, which is the subject of this research.

The marine sand terrace, which laps onto the glacial till to the east and the deltaic sand and gravel deposit to the west, is draped over steep hill slopes that dominate the upper 300 m of the study reach. In this area, groundwater seeps and springs are prevalent. The steep hill slopes and squared off western valleys may be a result of an erosional process known as groundwater sapping (Licciardi, 2008, personal communication). These features are known as box canyons in the western United States. Since the features formed on these hill slopes are much more subtle, they will be referred to as box valleys.

Springs appear near the toe of these steep hill slopes where the permeable outwash and marine sand deposits contact underlying marine silt and clay. Springs begin and sustain many of the tributary streams in the study reach and allow sand and gravel to be carried away from the spring towards the stream. This process promotes slope undercutting and slumping along the valley walls. Slumping erodes the valley near the base of the slope and forms the box valley geometry. The sediment transport provided by these spring brooks carries well sorted, coarse streambed materials to WHB.

The USGS mapping of the area suggests widespread silt and clay within the stream valley in the upper study reach, but alluvium from groundwater sapping and tributary discharge and formation of peat and wetland deposits near groundwater seeps and in the floodplains masks the presence of these deposits at the surface. At several locations in the lower study reach, clay is exposed in the streambed and stream cut walls. Stream alluvium is deposited in the floodplain that has been formed downstream of 250 m. The floodplain deposits extend downstream to the confluence of the stream with the Lamprey River where evidence of sediment deposition from WHB is apparent for several hundred meters downstream along both the northern and southern river banks.

The character of the streambed sediments changes from angular phyllite boulders, cobbles and gravel derived from the Eliot Formation in the upper reaches to the sub-rounded to well rounded oxidized cobbles, gravels and sand typical of a deltaic or outwash deposit to fine sand, silt and clay. A plot of streambed material depth (open circles) and streambed apparent electrical conductivity or EM (solid squares) (Figure 4-6) suggests that EM provides a rough measure of the relative depth of streambed sediment and the presence of clay in streambed sediments. Clay and silt materials were observed in stream cuts at various locations and predominate the streambed materials downstream of 420 m. At 420 m, the streambed sediments thin considerably and EM also increases rapidly. The moderate high and low anomalies in EM values upstream of this rapid increase may indicate that clay is present within the range of the instrument, 6 m, but is not a dominant constituent of streambed or alluvial materials adjacent to the stream. This is also supported by the increase in clay and silt sized sediment with distance downstream.

Another subsurface feature that can be interpreted from the EM survey is the presence of shallow bedrock beneath the streambed. Between 110 and 150 m downstream from the culvert, EM values drop from 38 to 3 umhos/cm and then increase steeply again to 75 umhos/cm at 230 m. The lowest EM value in this trough roughly corresponds to the 250 m station on the FODTS cable. This location corresponds to the area where the stream direction changes and the valley decreases to its narrowest point. Birch (1980) found that many outwash deltas, like

the one just to the west at Lee center, coincide with bedrock ridges. The change in stream direction and the EM trough suggest that this might be a bedrock high beneath the streambed and could represent the location where WHB breaches its structural control.

Stream cross sections and stream classification

Six stream channel cross sections at 145, 165, 172, 237, 334 and 512 m and two valley wide cross sections at 200 and 453 m illustrate the overall shape of the streambed and catchment (Figures 4-7 a-f and Figures 4-8 a and b). Locations of cross section locations are shown on Figure 4-1, 4-2 and 4-3.

Measurements of stream gradient, channel sediment makeup, bankfull width, and bankfull depth as well as ratios of these measurements were used to broadly classify stream segments according to the Rosgen stream classification system (Rosgen and Silvey, 1998). An overall guide to these stream classifications is reproduced in Appendix A.3. Table 4-1 summarizes these findings. The upper 80 m of stream is moderately entrenched and is classified as a B3 stream. The B represents the plan form and cross sectional shape created by the stream and 3 represents the median streambed sediment size. Cross sections at 145 and 165 m illustrate the typical stream cross sections for this stream type. Underlying bedrock structure often controls these high gradient streams (Rosgen and Silvey, 1998).

The increasing sediment supply from spring brooks and surrounding valley materials and the decreasing stream gradient creates a G stream type for the stretch between 165 and 200 m. The stream cross-section at 165 and 171 m (Figures 4-7 b & c) and the valley wide cross section at 200 m (Figure 4-8 a) illustrate the stream erosion pattern and the high, steep hill slopes that surround the stream in this reach. Even though there is a broad valley floor here, the flood prone width (the width of the stream valley at two times bankfull depth) falls below the level of the current valley floor, suggesting that the valley is not an active floodplain of WHB. Remnant fluvial activity, groundwater sapping, and wetland development are likely responsible for much of the valley geomorphology in this area. Eroded sediments from the eastern and western hillslope (marine sand and reworked glacial outwash) contribute to the streambed sediment supply in this reach.

The meandering stream reach between 230 and 410 m transitions from a C to an F type stream. At 237 m (Figure 4-7 d), the stream cross section and plan form are more typical of a C stream but below the large log dam, the stream is deeply entrenched in an inactive floodplain and there is active stream bank undercutting and down cutting typical of an F stream. The inactive floodplain was probably formed when the stream base level was at a higher elevation. The topography suggests that the eastern valley wall was cut by past stream action. The 334 m cross section (Figure 4-7 e) exhibits the wide and squared off channel typical of

an F stream. The median streambed sediment grain size transitions from a medium to fine gravel along this reach. The streambed sediment in this area is likely carried from upstream sources and derived from bank failures along this reach.

Beyond the 410 m valley constriction, the stream has developed a broad floodplain. This is illustrated by valley cross-section 450 m (Figure 4-8 b). Here, the flood prone width of 34.5 m suggests that the flood flows extend beyond the upper stream bank, therefore the floodplain is active. The stream type of this reach is an E 5 due to the active floodplain, the lack of channel entrenchment, and the predominant fine to coarse sand sediment type. The classic E stream profile is illustrated by the 510 m cross section (Figure 4-7 f). Valley walls are more gradual in this reach and are likely a result of stream channel migration.

Table 4-1 – Stream characteristics and Rosgen stream classifications
 Wednesday Hill Brook in Lee, NH

FOD- DTS Cable Location (m)	Bankfull Width (ft)	Bankfull Depth (ft)	Width to Depth Ratio	Flood- prone Width (m)	Entrenchment Ratio	Reach Gradient	D50 (mm)	Alluvium Description	Rosgen Stream Classification
145	9.4	0.9	10.4	NM	NM	0.03	80	Medium cobble	B3
165	12.6	1.4	9.0	NM	NM	0.03	80	Medium cobble	B3
172	7.6	2.1	3.6	NM	NM	0.015	80	Very coarse gravel	G3
200	2.45	0.6	4.1	5.8	2.3	0.005	20	Coarse gravel	G4
237	9.9	0.8	12.4	NM	NM	0.003	10	Medium gravel	C4
334	8.7	0.7	12.4	12	1.4	0.001	7	Fine gravel	F4
453	3.4	0.6	5.7	34.5	10.1	0.005	0.8	Fine to coarse sand	E5
512	9.8	1.8	5.4	NM	NM	0.03	0.8	Fine to coarse sand	E5

NM- not measured

Stream flow

Measured stream flow

Figure 4-9 illustrates the stream flow measurements from the upstream and downstream limits of the study reach. Stream flow at the upper limit of the study reach averaged 0.29 cfs or 0.00812 cms (cubic m per second) during this time and increased to 0.0112 cms at the downstream limit of the study reach. The flume may have underestimated flow at the downstream limit of the study reach due to installation constraints especially during the first field campaign. The flow may be underestimated by 20% so that a total flow may be as high as 0.48 cfs (0.01344 cms).

Stream discharge decreased steadily during the first FC at both the upstream and downstream measurement points due to the lack of rainfall throughout the period. This period likely represents low flow conditions for the stream during 2007, which suggests that baseflow was the primary source of contribution to the stream at this time. Averaged over the length of the stream, the baseflow gain per meter of stream was estimated at 5×10^{-6} to $1.04 \times 10^{-5} \text{ m}^2 \text{ s}^{-1}$. This contribution represents not only groundwater discharge, but also flow from spring brooks and tributaries. Diurnal changes in stream flow measured at the downstream flume may be due to evapotranspiration demand. This daily fluctuation is most evident in late summer but

also continues in the early fall flume readings. The study reach contains a dense floodplain canopy and understory that actively transpires during the daytime.

During FC 07-2, in late September and early October, stream flow increased due to several rainfall events and a decrease in evapotranspiration. The average downstream discharge was 0.0126 cms. The upper stream flow measurement device was not working during FC 07-2, so no net flow value can be calculated between the upstream and downstream end of the study reach. Stream flow levels remained fairly constant at the downstream measuring point during FC 07-2.

Stream flow measurements made at the upstream stream flow gage in summer and early fall 2008 illustrate the significant discharge that occurs during heavy rain events on WHB (Figure 4-10). The average discharge during low flow after 2 weeks without a storm event was 0.0078 cms. A storm on August 8, 2008 and another on September 6, 2008 recorded rainfall of over 40 and 56 mm, respectively, over a 4-hour period (UNH, 2008). This resulted in stream flow of over 0.56 cms at the culvert measurement point. These were significantly more intense storms than those that occurred during the 2007 field season but are common for this area during the fall tropical storm season. The streamflow gage was not operating during the strong storms in Fall 2007, but the 2008 data provide a reasonable range of typical storm flows.

Digital elevation model flow stream flow analysis

Both filled and unfilled flow paths generated by ArcHydro were used to understand the hydrology of the WHB study reach. Figure 4-11 shows the drainage network calculated by ArcHydro after sinks were filled and using the 5,000 m² contributing area stream definition criteria. The tributaries identified by ArcHydro were also noted during field work. However, some drainages were often better defined or less well defined than ArcHydro results indicate.

As described in the methods section, the tributary flow was estimated by area weighting using the mean upstream gauged flow for FC-07-1 (0.00868 cms). Table 4-2 lists the streams identified, the contributing area, and the stream flow estimated for each stream. The contributing area and streamflow at the top and bottom of the study reach are also listed.

The difference in mean measured flow from upstream to downstream along the study reach is 0.00308 cms. The total ArcHydro tributary streamflow estimates are 0.002 cms along the reach. These tributaries appear to account for 2/3 of the streamflow pickup along the reach

The largest tributary discharge estimated is tributary 1W. This tributary is closest to Wednesday Hill Road and enters from the west at about 109 m. This stream receives runoff from the road and from the neighborhood that bounds

Wednesday Hill Road to the west. The next largest tributary, 6E, flows into the brook from the east in the floodplain area. This drainage flows from woods, behind the Lamprey Lane neighborhood and from the wetland floodplain area entering at 482 m. Tributary stream 2W has the third largest contributing area. This western tributary joins WHB at 185 m. Its flow into the stream is marked by a small delta formed from the deposition of sand and gravel at the outflow.

Tributary 5W enters the brook from the west near the 443 m piezometer. On the ground, this is a subtle drainage that flows largely under roots and vegetation in the floodplain. Tributary 7W drains a long and narrow area and enters the stream at about 540 m. This is also a subtle and largely buried feature. Tributary 4E drains the abandoned floodplain and enters the stream in two locations near the top of the active floodplain. The smallest delineated tributary, 3W, enters from the west at about 225 m. This and another small tributary, not delineated, just upstream of 225 m drain the lower box valley. Both originate from visible springs.

Table 4-2 Tributary delineation and stream flow estimates – ArchHydro analysis
Wednesday Hill Brook in Lee, NH

Location ID	FODTS Location (m)	Contributing Area (m ²)	Streamflow (cms)
WHB upstream reach	NA	921,870	0.00868 ¹
1W	109	30,836	0.00057
2W	185	16,108	0.00030
3W	225	5,842	0.00011
4E	400	6,044	0.00011
5W	443	14,856	0.00027
6E	481	24,652	0.00045
7W	540	10,541	0.00019
WHB downstream	640	1,064,109	0.01120
Western tributary total			0.00144
Eastern tributary total			0.00056
Total tributary streamflow			0.00200

¹Mean streamflow measured at culvert during FC-07-1

The flow accumulation data generated without filling sinks provide a different catchment discharge picture (Figure 4-12) . While some of the digital flowpath attenuation is due to data resolution, this map accurately portrays many hydrologic characteristics of the site. All drainage from the surrounding slopes does not enter tributaries in the catchment but instead flows to wetlands,

depressions or alluvial aquifers that surround the stream or travels under the multiple tributary streams. Thus the ArchHydro analysis likely overestimates the relative importance of the tributaries.

These flow accumulation data were evaluated in the area of the box valley and in the floodplain area to determine the possible contribution of shallow groundwater to stream flow. Figure 4-12 illustrates the truncated flow paths in these two areas. The discharge estimated for these areas was calculated by multiplying the total contributing area from all diffuse flow paths by the flow per unit area. Table 4-3 lists the total discharge estimated for these areas. The amount of contribution from the defined drainages, obtained from Table 4-2 supplemented by flow from smaller drainages was subtracted from these totals to approximate the diffuse contribution of flow to the stream. Based on these estimates there is approximately three times more tributary flow than diffuse flow in the box valley area. In the floodplain area diffuse flow makes up 57% and defined tributaries make up 43% of total flow.

Table 4-3 Estimate of diffuse discharge from box valley and floodplain by ArchHydro analysis, Wednesday Hill Brook in Lee, NH

Diffuse Drainage from Box Valley

Drainage type	Contributing Area (m ²)	Relative flow rate (cms) and % of total flow
Total	30,945	0.00057
Defined drainage contribution (2W, 3W and small adjacent tributary)	23,483	0.00043 (76%)
Net diffuse contribution	7,463	0.00014 (24%)
<u>Diffuse Drainage from Western Floodplain</u>		
Total	59,516	0.00110
Defined drainage contribution (5W and 7W)	25,397	0.000473 (43%)
Net diffuse contribution	34,119	0.000627 (57%)

Experimental results

Weather conditions

The dedicated weather station located at the downstream end of the study reach (Figure 4-3) monitored weather conditions from August 19 to October 8, 2008.

The air temperature (Figure 4-13a) during this time was between 2°C (nighttime) and 33°C (daytime). Temperatures were cool just before and during the first day of FC 07-1. High temperatures on August 21 were about 20°C and rose to 32°C by August 26. Daytime temperatures then stayed more or less steady until the end of FC 07-1. Diurnal temperature variations were pronounced on most days with the exception of August 24 and 25 when nighttime temperatures remained high as temperatures rose. During FC 07-2 daytime temperatures began at 32°C, dipped to 16°C on October 1, climbed back to 27°C, and then dropped to 12°C at the end of the FC 07-2.

No precipitation fell during FC 07-1 while 3 rain events occurred during FC 07-2. The first rainfall during the fall measurement period (Figure 4-13b) occurred on September 8 when a total of 9.2 mm of rainfall fell over three days. Another rainfall event (1.7 mm) occurred on September 14. Several short duration rainfall events occurred on September 27 (4.1 mm) and October 5 (10.8 mm) followed by a smaller rainfall on October 7 (2.2 mm). The relative humidity generally varied diurnally between 98% and 47%. Humidity (Figure 4-13 b) was low during

FC 07-1 and higher during FC 07-2. Between the two campaigns, several days of very high humidity coincided with the light but frequent rainfall from September 8 to September 11.

Wind speeds under the tree canopy (Figure 4-13c) were generally less than 1 m s^{-1} during the measurement period. During FC 07-1 there were light winds (less than 1 m s^{-1}) until August 24 when winds dropped to below 0.1 m s^{-1} . During FC 07-2 daily wind speeds were between 0.4 and 1 m/s . The highest wind speeds for both FC's were measured during the day and generally dropped to near 0 m s^{-1} at night.

Below-canopy solar radiation and net radiation were also measured during this time (Figure 4-13d). Daily maximum solar radiation was greatest between August 25 and September 7 (greater than 300 W m^{-2}). From September 8 to September 11 almost no solar radiation was measured for 3 days, during a prolonged rain event. Following this storm, solar radiation was generally lower but often rose to 100 W m^{-2} during the day. Net radiation was greatest between August 27 and September 5 when daily highs exceeded 700 W m^{-2} . The highest net radiation values were recorded between 11 am and 3 pm when the sun angle was highest. FC 07-1 included these higher solar and net radiation measurements but daytime maximums were quite variable. The FC 07-2 time period experienced much lower radiation levels than during the first field

campaign due to the changing season and shortened days, and daily maximum net and solar radiation were nearly equivalent from day to day.

Tree canopy density

Canopy density measurements were made on August 20, 2007 during the first field campaign (FC 07-1). The measured density is fairly uniform from upstream to downstream along the study reach. The mean canopy density is greatest to the west at 90.4% but is similar to the north, east and south at 88.4, 87.1 and 87.4% respectively. The sparsest canopy is at the upper end of the reach at the road crossing (82.8%-all directions) and at approximately 200 m downstream from the culvert (76.6%-all directions). A summary table showing densiometer measurements is included in Appendix A.4.

Hyporheic temperature amplitude analysis

The percent amplitude of diurnal streambed versus stream temperature fluctuations can be used to assess the degree of vertical hyporheic flow at the point of measurement. A percent amplitude greater than 10% suggests hyporheic exchange (Silliman, 1995). Table 4-4 summarizes the amplitude analysis conducted at fifteen locations along the study reach. At five locations (336, 370, 413, 486 and 491 m) amplitudes did not exceed 10% suggesting that little or no vertical hyporheic exchange occurs at these locations. Hyporheic exchange is greatest at 293 and 430 m. Both of these are riffle locations where

downward vertical gradients were observed. These analyses are furthered described by sub-reach.

Table 4-4 Amplitude of diurnal temperature variation in the stream and streambed, Wednesday Hill Brook in Lee, NH

Reach	Location (m)	Diurnal Stream Temperature Amplitude (°C)	Diurnal 20 cm bss Temperature Amplitude (°C)	Amplitude (%)
2	237	1.5	0.4	27
3	257	1.3	0.3	25
3	268	1.3	0.2	18
3	276	1.1	0.3	25
3	293	1.3	0.7	52
4	336	1.1	0.1	9
4	370	1.3	0.1	9
5	413	1.6	0.0	0
5	422	1.4	0.1	7
5	430	1.5	0.6	42
5	443	1.6	0.2	18
5	461	1.6	0.2	13
5	480	1.6	0.2	12
5	486	1.6	0.1	5
5	491	1.5	0.1	9

Streambed hydraulic potential

Mini-piezometers installed in the streambed were used to gather data on streambed hydraulic potential. Water rising within the piezometer indicates the vertical hydraulic potential of water within the alluvium as well as the potential travel direction to or from the stream to the streambed (downward potential) or from the streambed to the stream (upward potential). The convention is to consider downward flow positive potential and upward flow negative potential, but for illustrative purposes, this convention is reversed in Figures 4-14 (a) & (b) which show the magnitude of the vertical gradient on the measurement dates.

The complete vertical gradient data set is contained in Appendix A.5 and summarized in Table 4-4.

The majority of piezometers measure an upward flow gradient along the study reach. At piezometer pairs placed at adjacent riffles and pools, riffle vertical gradients were generally downward and pools upward in the stream section between 167 and 336 m. This pattern is expected where hyporheic upwelling and downwelling occur. Below this section vertical flow was slightly downward at riffles but the magnitude of the gradient was less than in the upper section. The strongest upward flows were measured between 370 and 480 m in the lower active floodplain area. More detail on vertical gradient patterns is provided in sub-reach specific discussions.

Groundwater temperatures

A monitoring well field is located in the western box valley area between 195 and 210 m. Continuous Hobo measurements in several of these wells documented the temperature of groundwater flowing from both the east and west hill slopes towards the brook. The well locations are listed in Appendix B and the well placement and construction details are summarized in Table 4-5. Water levels in the wells closest to the hillslope were above land surface, which suggests potential for groundwater discharge. This is supported by the abundance of seeps and springs at the base of the western valley slopes. Figure 4-15 shows groundwater temperatures between August 16 and September 16, 2007. Statistical data are summarized in Table 4-6.

Table 4-5 Average vertical hydraulic gradients at piezometers, August 17 to October 14, 2007, Wednesday Hill Brook in Lee, NH

FODTS Cable Station (m)	Streambed Feature	Mean Hydraulic Gradient (m m ⁻¹)
167	riffle	-0.075
171	pool	0.105
237	riffle (near logdam)	-0.056
257	riffle	-0.013
268	run	0.083
276	pool	-0.010
292	riffle	-0.026
294	pool	0.093
336	pool	0.031
370	riffle	0.021
372	pool	0.153
413	riffle	0.150
422	run	0.258
433	riffle (logdam)	-0.033
443	pool	0.133
461	riffle	0.070
480	riffle	0.091
486	pool	0.038
491	riffle	0.071
510	riffle	0.013
512	pool	0.026
525	run	0.038
634	pool	0.007

The warmest mean temperature for this late summer period, 15.5°C, was observed at L1A-11, which is close to the west bank of the stream at 199 m. The coldest mean temperature, 9.5°C was measured in L1A-42, which lies 15.6 m from the stream at the base of the steep western valley wall. Groundwater temperatures typically varied less than 1°C throughout the measurement period at all wells. The exception was Well L1A-11, which varied over 5°C during the

measurement period. Well L1A-42 varied less than 0.1°C over the measurement period.

Table 4-6 Monitoring well construction and location details
Wednesday Hill Brook Well in Lee, NH

Well	Subsurface Material Description	Location	Distance to Stream (m)	Well Depth (m)	Depth of Water Below Land Surface (m)
L1A-1	NA	East bank	0.5	0.61	0.47
L1A-2	NA	East bank	0.5	1.07	0.11
L1A-11	Coarse sand, near- stream alluvium	West bank	1.9	1.01	0.19
L1A-12	Fine sand, floodplain alluvium	West bank	3.1	1.16	0.15
L1A-21	Fine sand, floodplain alluvium	West bank	1.0	0.84	0.25
L1A-22	Sand, floodplain alluvium	West bank	3.2	1.91	-0.05
L1A-23	Sand, floodplain alluvium	West bank	4.5	0.73	0.43
L1A-42	Marine sand and clay	West bank	15.6	1.67	-0.28

This pattern of well temperature variation closely matches the longer record of well temperatures measured periodically at the wells between winter 2005 and summer 2007 by NHWRRC (Figure 4-16). All well temperatures varied seasonally with the lowest temperatures measured in late winter and the highest temperatures in late summer. Similar to the measurements taken in late summer 2007, L1A-42 show the least variation, less than 3°C over the

measurement period. Temperatures ranges at the other wells vary from 9°C (L1A-41) to 13°C at L1A-12 and L1A-23. The mean temperatures for this 2-year measurement period fall between 8.76°C at L1A-41 and 9.40°C at L1A-11. The well with the least variation, L1A-42, had a mean temperature of 9.19°C.

Table 4-7 Summary statistics for groundwater temperatures¹ – August 16 to September 16, 2007, Wednesday Hill Brook in Lee, NH

Well	L1A-1	L1A-2	L1A-11	L1A-12	L1A-21	L1A-22	L1A-23	L1A-42
Mean	11.366	10.995	15.503	13.778	12.181	13.172	13.361	9.453
Std Dev	0.159	0.151	1.319	0.164	0.239	0.214	0.172	0.039
Maximum	11.722	11.236	17.95	14.038	12.594	13.654	13.75	9.472
Minimum	11.041	10.651	12.883	13.365	11.722	12.883	13.076	9.373
Range	0.681	0.585	5.067	0.673	0.872	0.771	0.674	0.099

¹ all temperature values in °C

In general, the groundwater temperatures at wells become cooler and temporal variability decreases with increasing distance from the stream. Based on the well temperature means, it appears that well L1A-11 is either inaccurate or completed within active stream channel alluvium and could be within the hyporheic zone as its temperature varies widely and is similar to nearby stream temperature variations observed over the same time period. Interestingly, the wide variation in the short-term measurements at this well is not suggested by the periodic

measurements taken over 2 years. This discrepancy could be due to the Hobo sitting above the bottom of the well in the part of the water column that was subject to surface warming. Each Hobo was weighted to prevent this, but it is possible that it was improperly weighted during set-up.

The cooler temperatures measured in Well L1A-42 lie within a temperature range of 9.0 and 9.2°C. They are indicative of more regional groundwater temperatures and suggest that deeper groundwater discharges to WHB from the western hill slope.

The groundwater temperatures in the other western wells appear to measure shallow alluvial groundwater temperatures. The west bank of the well field is a peaty wet area crossed by several seepage channels. The higher mean temperatures measured during late summer 2007 and the variation shown for the two-year measurement period suggests these wells measure riparian groundwater temperatures where short flow paths and shallower groundwater can be more readily affected by seasonal surface temperature changes.

Wells L1A-1 (shallow) and L1A-2 (deeper) installed on the east bank of WHB have mean temperatures (11.36 and 10.97°C respectively) that are lower than the western riparian zone wells but higher than the near-slope groundwater wells

on the western bank. These wells also have lower temperature variability than the riparian wells on the western bank.

Although groundwater temperatures were not measured in downstream locations, many of the western tributaries in the lower reaches were observed to have a cool and constant temperature, which suggests a direct groundwater source. This phenomena is discussed in the following section.

WHB stream water temperatures

Temperatures along the main channel of WHB were measured continuously at each meter using the FODTS system and at fixed locations in the stream using the Hobo™ thermistor data loggers.

FODTS measurements

Figure 4-17 shows the FODTS average stream temperature for the study reach during the first field mobilization FC 07-1. The temperature spikes occur where the cable was out of the stream at log dams, rocky cascades or other exposed locations. Data from sections where the cable was out of the water were removed from the data set for plotting and statistical analysis. Figure 4-18 shows the average temperature and the standard deviation (SD) by the FO cable locations for the edited dataset.

Stream temperature changes greatly from upstream to downstream and also within short stretches of stream. Average stream temperatures along the study reach range from a high of 15.6°C at the upstream cable station at 75 m to a low of 12.3°C at cable station 420 m. Two significant temperature steps are evident. The first occurs at 104 m where the temperature drops 0.5°C in 7 m. The second occurs at 180 m where the temperature drops 1.2°C to 13.6°C. While the stream temperature varies locally up to 1.2°C to the end of the study reach no other sustained decreases are observed.

The longitudinal SD pattern is very similar to that of average stream temperature. The SD is roughly 1.6°C and quite constant in the first 30 m of the study reach. It decreases to approximately 1.4°C at 75 m and gradually rises until station 180 m where another sharp drop occurs. The step decreases in both average temperature and SD suggest small source areas of persistently cool water are entering the stream. The higher temperatures in the upper stream reach coincide with higher standard deviations. This suggests that there are few moderating temperature influences in this reach.

In the lower reaches the changes in temperature are less dramatic, but the cool temperature attained over the first 140 m of the reach (13.5°C) is sustained with minor variations until the end of the reach. Several areas of temperature decline have no obvious point source such as the tributaries and seeps in the upper

reach. There are two such anomalies in the lower reaches between 255 and 265 m and between 415 and 430 m. Both occur at changes in stream direction and are at the head of a long straight reach. The causes for these anomalies are explored in a later section.

Other changes in temperature along the reach are local and do not persist for more than 5 m downstream. Several areas of steady temperature increases are later moderated downstream.

The average stream temperature and standard deviation patterns are similar for both field campaigns. The temperature average and SD are lower during FC 07-2 (Figure 4-18) in the upper reaches but the areas with low standard deviation are more pronounced. In the lower reaches, the temperature anomalies are subdued as are many of the other "point sources" of temperature compared to FC 07-1.

There is a minimal temperature drop at 360 m, a more subdued drop at 410 m and fewer variations between 410 and 560 m. The first field campaign coincided with near baseflow conditions where the groundwater signature was strong.

Some of these cooler signatures are likely dampened during the second field campaign due to the rainfall and runoff that likely warmed the stream.

Comparison of the SD signatures between the two field campaigns shows that the temperature variability at each meter location is typically lower to about 480 m in FC 07-2. However, means and standard deviations agree well between

campaigns in the lower 160 m of the study reach. This is likely due to the reduced groundwater influence in this section of the stream.

Stream data logger measurements

The mean and median lines on the box and whisker plots of the Hobo stream temperature measurements (Figure 4-19) illustrate a similar temperature trend when compared to the FODTS measurements. The plots represent the same time interval as the FC-07-1 FODTS survey – August 22 to August 29, 2007. The warmest mean temperature was 15.3°C at the step at 75 m and the coolest mean (12.0°C) was located at the 512 m pool. The largest SD was recorded at 75 m (1.82°C). The smallest standard deviation, 0.6°C, occurred at three locations within a 20 m stretch at 258, 268, and 276 m. Table 4-6 lists the basic statistics for the surface water Hobo data portrayed in the box plots. The Hobo measurement trends compare well to the FODTS. However, these measurements are unable to capture the subtle temperature variations measured by the FODTS survey.

Figure 4-21 compares average stream temperature and standard deviation of temperature measured with the Hobos and FODTS. A strong correlation is observed for both the FODTS measurements ($r^2=0.97$) and the Hobos ($r^2=0.96$). Cooler waters have lower variability. This suggests a strong groundwater influence for the coolest portions of the reach.

Table 4-8 Summary statistics for stream temperatures measured with Hobo dataloggers¹ – August 22 to 28, 2007
 Wednesday Hill Brook in Lee, NH

FODTS cable location (m)	75	171	237	258	268	276	295	336	370	372	413
Mean	15.35	14.93	13.30	13.75	13.41	13.43	13.01	12.86	13.01	13.14	13.53
Median	15.86	15.38	13.65	13.75	13.46	13.46	13.27	13.17	13.27	13.37	13.56
Std. Dev.	1.82	1.48	1.17	0.58	0.56	0.57	1.00	0.98	1.11	1.08	0.61
Minimum	11.24	12.79	10.65	12.40	12.11	12.11	11.53	10.65	10.26	10.65	12.11
Maximum	18.05	17.00	15.09	14.61	14.33	14.42	14.52	14.33	14.80	14.80	14.61
FODTS cable location (m)	416	422	430	443	461	480	486	491	510	512	525
Mean	12.91	13.62	13.39	12.94	12.85	12.94	12.71	12.76	12.71	11.97	12.81
Median	13.17	13.65	13.46	13.17	13.08	13.12	12.88	12.98	12.88	12.11	12.98
Std. Dev.	1.10	0.60	0.60	1.07	1.08	1.02	1.01	1.01	1.05	0.75	1.05
Minimum	10.36	12.21	12.01	10.46	10.36	10.55	10.36	10.36	10.26	10.26	10.36
Maximum	14.61	14.61	14.42	14.61	14.61	14.61	14.33	14.42	14.42	13.08	14.52

¹all temperature values in °C

Stream temperatures show both diurnal variation and short-term fluctuations due to changing weather conditions (Figures 4-23 to 4-27). In the upstream section (Figure 4-23), temperatures are warmest at 75 m and dramatically decrease downstream as previously observed on the FODTS survey. This stream section is characterized by similar day to day and diurnal variation among points but distinctly different average temperatures.

At downstream measurement points, both temperature averages and fluctuations are nearly equivalent with minor differences due to the point sources of cool water illustrated by FODTS measurements (Figures 4-24 to 4-26). Only at the end of the reach do obvious differences in stream temperatures once again become apparent. In Figure 4-26, the difference between the adjacent 510 m riffle and 512 m pool temperature is apparent. This points to the substantial local variations in temperature sensed by the FODTS. Generally, however, these spatial details are missing from the Hobo data due to the difference in data density.

Tributary Temperatures

The term tributary is used loosely to define any surface inflow to the stream. A complete tributary temperature survey was conducted on August 14, 2007 prior to installation of Hobos or piezometers. A total of 16 tributaries, springs or seeps were identified at that time and five locations were chosen for continuous measurements during the 2007 field season. The temperature measured at each

location is included in Table 4-8. Tributary and seep locations are shown in Figure 4-27.

Table 4-9 Initial tributary, seep and spring temperatures, August 14, 2007
Wednesday Hill Brook in Lee, NH

FODTS Station (m)	Type	Direction of Inflow	Temperature (°C)
89	Tributary	West	15.2
109	Tributary	West	15.5
133	Seep	West	13.1
185	Tributary	West	11.3
214	Tributary	West	11.7
224	Tributary	West	11.0
287	Spring	West	9.2
332	Seep	West	12.7
365	Seep	West	10.7
396	Seep	East	16.3
400	Tributary	East	15.8
444	Tributary	West	12.9
472	Tributary	West	10.6
481	Tributary	East	16.0
538	Tributary	West	11.9
617	Tributary	West	8.8

Thirteen of the features flow from the western hillslope toward the stream while three flow from the eastern valley. A time series of the five features measured

using Hobos during the 2007 field season is shown in Figure 4-28. Table 4-10 summarizes statistics for these and other major tributaries measured in 2008.

Table 4-10 Summary statistics for measured tributaries, August 22 to 29, 2007 (109, 185, 400 and 472 m corrected to 2007 from 2008 data)
Wednesday Hill Brook in Lee, NH

FODTS Station (m) and ArchHydro ID	Tributary (T) Seep (S) or Spring (Sp)	Mean Temperature (°C)	Standard Deviation (°C)
109 (1W)	T	12.7	0.23
185 (2W)	T	11.5	0.30
214	T	11.1	0.30
225 (3W)	T	11.4	0.34
287	Sp	9.6	0.03
368	S	11.6	0.77
400 (4E)	T	15.5	0.74
472	T	10.7	0.16
481 (6E)	T	15.5	1.83
617	T	9.1	0.07

The 109, 185, 214 and 225 m tributaries flow from springs formed at the western valley wall. The upper tributary 109 m drains Wednesday Hill Road and an upstream neighborhood. It has a slightly higher temperature due to surface warming from the roads (12.7°C). The 185, 214 and 224 m tributaries travel at or below the surface beneath tree roots and sandy alluvium before discharging to the main stem of WHB. The temperature mean and diurnal variation at these streams are similar and average from 11.1 to 11.5 °C. Figure 4-19 illustrates that

these two streams may affect temperatures at the confluence and up to 10 m downstream.

Other western tributaries 472 and 617 m have even lower average temperatures and little diurnal variation. The steady temperature pattern for 617 m is shown in Figure 4-28. This can be attributed to their spring fed origin and their protection from surface warming by overlying roots. Permeable sands and gravel also surround these tributaries and represent areas of coincident preferential flow for groundwater.

The 365 m seep is located where the stream flows close to the western hillslope. A large seepage face extends 2 m vertically and 7 m horizontally. The average temperature of the seep is 11.6°C and has a 0.77 °C SD.

The eastern tributaries enter WHB at 400 and 481 m. These tributary temperatures vary more widely than the brook and they have an average temperature of 15.5°C. The tributaries both flow from floodplain wetlands formed at the toe of the eastern hillslope. The water that drains to the tributaries likely warms in the shallow wetland. The effect of the 481 m tributary on stream temperature (Figure 4-19) suggests a cooling influence, which is not expected from the high measured temperature. A cooler subsurface groundwater component of this tributary feature may account for this incongruous impact.

Also, the observed flow rate at the 400 m tributary was small during both August 2007 and 2008. The ArchHydro estimate of streamflow appears to be much higher than the observed flow amount would suggest for this and several of the other tributary locations.

In summary, western tributaries, springs and seeps are 2 to 6°C cooler than eastern tributaries and have one-third to one-tenth the range of variability of the eastern tributaries. The western valley clearly provides a significant water source for the stream and much cooler temperature discharge than the eastern tributaries.

Wednesday Hill Brook sub-reach descriptions

Designation of sub-reaches

The study reach contains several distinct regions based on fluvial and catchment geomorphologic characteristics. The catchment hydrology, stream flow and heat flow contributions to the stream are closely linked to these sub reach characteristics.

This section describes streambed and surface water/hyporheic zone temperatures and their relationship to stream and catchment geology and hydrology by sub-reach. Figures 4-1, 4-2 and 4-3 show each reach and sub-reach designations are labeled. Additional time series plots of stream temperatures and 20 cm bss Hobo streambed temperatures are located in Appendix B.

Reach 1

Reach 1 is a 105 m long section from 75 to 180 m (Figure 4-1). It begins at the culvert and ends just above tributary 2W. Table 4-10 summarizes morphologic, stream and tributary temperature characteristics for the reach. It is referred to as the armored reach because the streambed is composed of boulders, cobbles and large gravel and fines have been largely removed from the surface due to the energy at the culvert and the relatively steep gradient in the subreach. The stream gradient is 0.05 to 0.03 and is dominated by step-pool morphology. The reach contains tributary 1W at 109 m with an average temperature of 12.6°C during FC-07-1.

Tributary 1W enters the reach at 109 m and cools the reach significantly.

Multiple rock steps in WHB occur above and below the confluence of this tributary. This tributary is partially spring fed, but its temperature is also impacted by warmer runoff from Wednesday Hill Road. Large areas on the western stream bank are saturated by seepage even in late summer, indicating groundwater discharge from this side of the valley.

Table 4-11 Summary of sub-reach 1 stream characteristics
Wednesday Hill Brook in Lee, NH

Characteristic	Value
Reach boundaries (FODTS stations in m)	75 – 180
Reach length (m)	105
Morphologic description	Armored Reach
Stream type	B3
Streambed surface grain size (D50) (mm)	80
Stream gradient (m m ⁻¹)	0.03
Streambed vertical hydraulic gradient	Upward at 167 Downward at 171
Average reach temperature(°C)	15.0
Average upstream temperature (°C)	15.5
Average downstream temperature (°C)	14.8
Downstream temperature trend (°C)	-0.7
Hyporheic zone temperature at 20 cm bss (°C)	13.7
Tributary temperature (°C)	12.9
Streambed alluvium depth (m)	0.02 – 0.4, 0.8 at log dams
Electrical conductance range (umhos/cm)	5 - 40
Tree canopy density (%)	83 – 91

Diurnal variations in the spring-fed brook are much lower (<1°C) than WHB (2.7 to 3 °C), and help to provide a consistently cool temperature for stream temperature moderation. Diurnal variations in WHB stream water temperature the top of the reach are greater than 3°C. Diurnal variations at 171 m are more moderate at 2.7°C. Canopy cover varies between 83 and 91% across the reach with the least cover near the beginning of the reach at the road crossing. This could partially account for the higher variability and temperature at the top of the

reach. Temperature moderation in the lower portion of reach 1 is likely a result of hyporheic exchange.

Adjacent mini-piezometers at 167 m (riffle) and 171 m (pool) (Figure 4-29) provide information about streambed heat flow in this upper watershed area.

Recall that stream gradients are fairly steep and the streambed alluvium is fairly shallow (less than 40 cm). Although both piezometers have the same pattern of temperature decline from the surface to 0.40 m below the streambed, the average temperature at 171 m pool is 0.2°C cooler than the upstream riffle at 167 m. The vertical hydraulic gradients are downward at 167 m and upward at 171 m (Figure 4-14 a) as expected for a riffle-pool sequence where downwelling occurs at the riffle and upwelling at the pool. The longitudinal temperature drop in the hyporheic zone is also indicative of hyporheic cooling. While the bed materials in the upper portion of this reach may prevent some hyporheic exchange, the steeper gradient, step-pool morphology, several log dams, and increasing depth of streambed alluvium may promote hyporheic exchange in this reach.

In summary, stream temperatures are moderated in this reach by spring fed brooks, groundwater and hyporheic exchange. The heavy canopy provides shading along most of the reach except just downstream of the road crossing which prevents warming by direct solar radiation. Steep gradients and coarse streambed materials

promote hyporheic exchange as the armoring in the uppermost portion of the reach diminishes.

Reach 2

The dominant morphologic features in reach 2, 180 to 245 m, are the steep sided valley walls and box valley that drains the upland to the west of WHB (Figure 4-1).

There may have been floodplain development here in the past, but the stream is now somewhat entrenched and the floodplain is no longer active. The stream gradient is more moderate than reach 1, so the dominant streambed material is gravel and sand rather than gravel and cobbles. Table 4-11 summarizes morphologic and temperature characteristics of this reach.

Table 4-12 Summary of sub-reach 2 stream characteristics
Wednesday Hill Brook in Lee, NH

Characteristic	Value
Reach boundaries (FODTS stations in m)	180-245
Reach length (m)	65
Morphologic description	Box Valley Reach
Stream type	C4
Streambed surface grain size (D50) (mm)	20
Stream gradient (m m ⁻¹)	0.003
Streambed vertical hydraulic gradient (m m ⁻¹)	Downward at 237
Average reach temperature (°C)	13.6
Average upstream temperature (°C)	14.8
Average downstream temperature (°C)	13.5
Downstream temperature trend (°C)	-1.3
Hyporheic zone temperature at 20 cm bss (°C)	13.0
Tributary temperature (°C)	11.4
Streambed alluvium depth (m)	0.2 – 0.9
Electrical conductance range (umhos/cm)	1.3 - 30
Tree canopy density (%)	85 to 95

The increase in streambed alluvium provides a deeper hyporheic zone for substream cooling and a streambed more conducive to groundwater discharge. Coarse grained sediments from the toe of the western hillslopes are being carried to WHB by constant spring discharge from the marine sand and deltaic gravel deposit.

A small box valley is beginning to form on the western slope where springs flow from the toe of the valley wall. This formation provides a collection area for groundwater

that feed seeps and provides water for the spring that feeds tributary 2W. This tributary enters at the top of the reach and has formed a small delta at its outfall, evidence of the sediment transport occurring from the hillslope to WHB. Several log dams are located on WHB just upstream of the 2W confluence. Sediment has collected behind these dams to a depth of 0.5 m. A large deep pool has formed at the confluence and the stream bends sharply at this intersection.

Two smaller tributaries including 3W enter at 215 and 225 m, respectively, from the large box valley. Both brooks travel in and out of the subsurface beneath tree roots and in coarse gravels and sands before entering WHB. These streams channel both surface water and shallow groundwater discharge to the stream and temperatures remain cool as much of the flow is spring fed and the reach is well shaded. The percent canopy cover for this reach is 85 to 95%.

Downstream of 2W and 3W considerable sediment has accumulated in the streambed. Tributary sediment transport and sediment accumulation behind a 1 m high log dam just below the bottom of the reach are largely responsible for the streambed depth increase. This log dam occurs at a point where the valley narrows considerably and valley walls are steep on both sides of the stream. The dam increases the stream base level by a full meter.

The FODTS measurements indicate that the average stream temperature drops from 14.8 to 13.5°C from the beginning to end of the reach (Figure 4-19). The average stream Hobo value at 237 m was 13.3°C with a standard deviation of 1.2°C. The temperature of 2W and 3W tributaries is cooler than 1W with an average temperature of 11.4°C. The FODTS temperature profile illustrates the impact these tributaries have on WHB stream temperature. Tributary 2W has a sustained impact and there is over a 1°C decline in average temperature after the confluence.

One mini-piezometer was placed in this reach at 237 m at the lower end of a long riffle and just above the log dam. The measured hydraulic gradient in this location was strongly downward indicating downwelling of stream water into the streambed (Figure 4-14a). Streambed temperatures were measured continuously at 20, 40, 50 and 60 cm bss at this location. Figure 4-30 includes the stream temperature data and the streambed temperature data. The shallow subsurface temperatures are damped compared to the stream. An apparent reactivity to air temperature changes was evident in late August 2007. During a transition from cool to warm and back to cool air temperatures from August 21 to September 1 (Figure 4-13 a), the stream temperature drops below the streambed temperature then rapidly rebounds. This suggests that there is strong downwelling, which quickly transfers surface heat to the streambed.

A 27% hyporheic temperature amplitude was measured at 237 m (Table 4-12 and Figure 4-31). Lower amplitudes differences were recorded below the 20 cm depth at this location (9% at 40, 17% at 50 cm, 7% at 60 cm). This suggests that some hyporheic exchange does penetrate to 0.5 m at this location. Some streambed flow stratification is suggested as well.

In summary, significant tributary and groundwater discharge from the western valley and hyporheic exchange provide the greatest stream cooling influence in the study reach. The local gradient increases from log dams and the large accumulation of streambed alluvium provides an ample hyporheic zone and local longitudinal gradient changes promote hyporheic exchange. The box valley geomorphology focuses subsurface flow, providing the cooling influence of groundwater. The bedrock high beneath the downstream end of the subreach and the large log dam may also focus the groundwater discharge.

Reach 3

Reach 3 begins at a large log dam and continues downstream 75 m to the beginning of an entrenched meander reach (Table 4-13, Figure 4-2). The characteristic morphology of the reach is the succession of log dams that span the reach. The stream gradient is slightly steeper compared to surrounding reaches because of the log dams. The log dam cascade reach is bounded by a narrow and steep stream valley that opens to an abandoned floodplain at 280 m. This stream segment is entrenched into the former floodplain by several meters.

Stream erosion is undercutting the banks leading to tree fall, which maintains the accumulation of woody debris in the reach. Streambed sediment is up to 0.9 m above log dams and less than 0.2 cm at the toe of the dams.

The large log dam at about 250 m is co-located with distinct geophysical and geomorphologic features. The lowest earth conductivity measurements in the study reach were observed at the beginning of reach 3 (2 umhos/cm). The dominant stream flow direction also changes at this location from a southwestern trend, which dominates from the headwaters of WHB, to a southerly trend after the narrows. This constriction and stream direction change combined with the low conductivity values suggest shallow bedrock beneath the stream valley. This distinct stream morphology may be the result of the stream breaching its bedrock control. This underlying structure may impact stream temperature and local groundwater and hyporheic flow.

The FODTS survey shows a cool stream temperature anomaly between 255 and 275 m (Figure 4-19). There is no apparent source of cold water that enters the stream at this point, e.g., a tributary or seep. The temperature cools steadily at the log dam and decreases 0.5°C to the nadir of the anomaly. The average stream temperature returns to the upstream value within 15 m of the anomaly.

Table 4-13 Summary of sub-reach 3 stream characteristics
Wednesday Hill Brook in Lee, NH

<i>Characteristic</i>	<i>Value</i>
Reach boundaries (FODTS stations in m)	245-310
Reach length (m)	65
Morphologic description	Logdam Cascade Reach
Stream type	F4
Streambed surface grain size (D50) (mm)	10 – medium gravel
Stream gradient (m m ⁻¹)	0.005
Streambed alluvium depth (m)	.02-.95
Streambed vertical hydraulic gradient (m m ⁻¹)	Upward at 257 and 268 neutral at 276 downward at 292
Average reach temperature (°C)	13.2
Average upstream temperature (°C)	13.5
Average downstream temperature (°C)	13.3
Downstream temperature trend (°C)	-0.2
Hyporheic zone temperature at 20 cm bss (°C)	11.8
Tributary temperature (°C)	NA
Electrical conductance range (umhos/cm)	0.1-75
Tree canopy density (%)	77-89

Streambed temperatures measured at 257, 268 and 276 m (Figure 4-32) illustrate the substream manifestation of the anomaly. The 268 m temperatures are nearly constant from 20 cm to the streambed bottom at 72 cm. The deepest piezometer has a slightly larger range in temperature than the shallower depths suggesting some stratification in flow in the streambed. The absence of

maximum and minimum temperatures outliers exhibit the near-constant temperature at 257 and 268 m. At 276 m, the streambed bottom temperature is cool and comparable to 257 m. Shallower temperatures suggest that hyporheic flow is active above 75 m.

The 258 to 276 m temperature time series (Figure 4-33 to 4-35) shows that even during periods with cooler air temperatures, stream temperature never declines to the 20 cm streambed temperature. The relatively small stream temperature range at 276 m compared to 258 and 268 m suggests that cool water upwells locally to the stream. The amplitude analysis suggests that hyporheic exchange is occurring to 20 cm in this reach (Table 4-4) even though there is also strong streambed cooling. The streambed topography caused by the log dams likely induces hyporheic exchange in this reach.

The stream cooling effects decrease at 293 and 295 m. Stream and 20 cm streambed temperatures are nearly equivalent (Figure 4-36). The deepest temperature measurement at 0.4 m is not significantly cooler than the 0.2 m temperature. The amplitude analysis suggests that hyporheic exchange is greatest at 293 m (48%) in reach three and the entire study reach.

Interestingly, the vertical gradients at 257 to 276 m (Figure 4-14 a) do not suggest a strong upward streambed flow. The cool temperature suggests

groundwater discharge or upwelling. The gradients are minimal and change from positive to negative throughout the study period. At the bottom of the reach, where the 293 and 295 m piezometers are located, a typical downwelling and upwelling pattern in both gradient and temperature at these adjacent riffle and pool features is apparent.

A combination of groundwater discharge and hyporheic flow from reach 2, is the likely source of the cooler water. The bedrock and topographic restriction at the top of the reach may force cool streambed water through the logdam cascade at the bedrock high. The observed moderate vertical gradients may result from the variable streambed topography and converging vertical gradient influences created by the long log dam cascade. The cascade ends at 295 m where the stream bends sharply and the stream gradient once again begins to decrease. The amplitude analysis also suggests hyporheic exchange is induced by the log dams. A canopy gap at the bottom of the log dam cascade centered at 295 m may also contribute to increased stream and hyporheic zone temperatures at reach end. At this location the percent canopy cover is estimated at 77%, the lowest value in the watershed.

Reach 4

The meander reach, reach 4, flows from 310 to 410 m through an abandoned floodplain (Figure 4-2). This entrenched stream segment closely follows the

steep western valley wall. Long groundwater seepage faces border this side of the western stream bank. The seeps emanate from the boundary between the marine sand and the finer silt and clay unit. The earth conductivity increases along the reach, suggesting increasing silt and clay content near the streambed. Streambed sediment size decreases as the stream gradient decreases. Reach physical and temperature characteristics are summarized in Table 4-13. The stream temperature in this reach increases modestly until 360 m where the temperature begins to fluctuate from 0.1 to 0.4 °C to 365 m then returns to the moderate reach increase.

The 334 and 336 m piezometer pair, located in a riffle and pool, respectively, is in the moderately increasing section. Streambed temperatures are generally lower than the stream. The amplitude analysis does not suggest a strong temperature influence from hyporheic exchange (Table 4-4 and Figure 4-31). A time series at 336 m (Figure 4-38) illustrates that the streambed holds a steady temperature compared to the stream, which varies widely over the period of measurement.

Table 4-14 Summary of sub-reach 4 stream characteristics
Wednesday Hill Brook in Lee, NH

<i>Characteristic</i>	<i>Value</i>
Reach boundaries (FODTS stations in m)	310-410
Reach length (m)	100
Morphologic description	Meander Reach
Stream type	F5
Streambed surface grain size (D50) (mm)	7 – Fine gravel
Stream gradient (m m ⁻¹)	0.001
Streambed alluvium depth (m)	.8 to 1.3
Electrical conductance range (umhos/cm)	50-85
Streambed vertical hydraulic gradient (m m ⁻¹)	Upward to strongly upward
Average reach temperature(°C)	13.2
Average upstream temperature (°C)	13.2
Average downstream temperature (°C)	13.3
Downstream temperature trend (°C)	0
Hyporheic zone temperature at 20 cm bss (°C)	11.5
Tributary temperature (°C)	15.4 at 4E
Tree canopy density (%)	85-88

The amplitude analysis also shows little or no hyporheic exchange at 370 m (Table 4-4). The time series of continuous streambed temperature measurements (Figures 4-39 and 4-40) suggests a steady groundwater influence. The 20 cm bss temperatures are steady at both 370 and 372 m.

Vertical hydraulic gradient data for both piezometer pairs in the reach support the groundwater finding. The typical riffle /pool hydraulic gradient reversal is not apparent at either piezometer pair. The streambed vertical gradients are slightly upward at 334 and 336 m and strongly upward at both 370 and 372 m.

This reach flows through an abandoned floodplain. In the upper portion of the reach, the stream may be below the influence of permeable floodplain alluvium and be carved into the less permeable silt and clay, preventing shallow groundwater inflow. In the lower reach, entrenchment decreases and some remnant stream channels composed of coarser materials than the floodplain alluvium, may cross the existing channel and provide cooler groundwater discharge to the stream. This interpretation is also suggested by the lack of temperature variation along the profile in the upper segment and increased variation downstream (Figure 4-19).

The eastern tributary (4E), entering the stream at 400 m, had an average temperature of 15.4°C during August 2007 and exhibited strong diurnal variation. A small increase in mean temperature and variability was observed on the FODTS profile near the tributary discharge to WHB. However, the cable was out of the water at a small log dam just upstream of this point, which may also influence this temperature increase. Direct groundwater discharge probably does

not control the tributary temperature. Rather, the shallow wetlands likely warm the water as it drains to 4E.

In summary, only modest changes in water temperature were noted over reach 4. There was a small steady increase in temperature at the beginning of the reach, but overall there is no net change in stream temperature. The temperature variability, especially where the standard deviations suggest the persistence of cool temperatures, is likely due to the multiple seeps along the western valley wall, sub-stream discharge points and inflow from abandoned channels. Hyporheic exchange seems to be largely lacking in this reach. Tributary 4E contributed only minor streamflow during the study period and is 4°C warmer than the western tributaries.

Reach 5

Reach 5 occupies an active floodplain (Figure 4-3). There are multiple riffle pool sequences in the reach. Small log and debris dams are common. A temperature anomaly occurs at the beginning of this reach, then temperatures vary locally up to 0.5°C. Overall, stream temperatures do not increase in this reach but the average temperature is 0.1°C cooler than the upstream and downstream temperature. Table 4-15 lists the reach characteristics.

Table 4-15 Summary of sub-reach 5 stream characteristics
Wednesday Hill Brook in Lee, NH

<i>Characteristic</i>	<i>Value</i>
Reach boundaries (FODTS stations in m)	410-495 m
Reach length (m)	85
Morphologic description	Floodplain Reach
Stream type	E5
Streambed surface grain size (D50) (mm)	7 – fine gravel
Stream gradient (m m ⁻¹)	0.005
Streambed alluvium depth (m)	0.1 to 1.6
Streambed vertical hydraulic gradient (m m ⁻¹)	Upward Flat at 433 m
Average reach temperature (°C)	13.2
Average upstream temperature (°C)	13.3
Average downstream temperature (°C)	13.3
Downstream temperature trend (°C)	0.0
Hyporheic zone temperature at 20 cm bss (°C)	10.0 at 413 and 422 m 13.2 at 433 m 11.8 at 443 m
Tributary temperature (°C)	11.0 at 5 W 15.5 at 6 E
Electrical conductance range (mhos/cm)	45-100
Tree canopy density (%)	87-93

The reach begins at 410 m just beyond the confluence of tributary 4E at a bend in the stream. It extends to 495 m just below another eastern tributary, 6E, also at a significant stream bend. The gradient is moderate (0.005) and streambed materials are fine gravel and sand.

The ArchHydro analysis identified only 2 major drainage features in this reach, 5W and 6E, (Figure 4-3, 4-11). However, field observations revealed multiple small drainage features entering the stream from the west. Like the box valley tributaries, many of these drainage features are buried beneath tree roots and include a sandy streambed. These western tributaries are cool with small diurnal temperature variations (Figure 4-28). The eastern tributary, 6E, has a warmer mean temperature (15.5°C) and stronger diurnal variations than WHB. Like 4E, this stream passes through a shallow wetland within the floodplain and may be warmed in this shallow seepage zone.

At approximately 415 m there is a local 1°C temperature decrease. Five piezometers are located along a riffle that starts at 410 m and extends downstream to a log dam at 435 m (Figure 4-41). Piezometer 443 is in the pool below the log dam. These piezometers capture the streambed temperature dynamics associated with this anomaly and the log dam feature. The shallow streambed at 413 m is 3°C cooler than WHB and has virtually no variation over the 2-month measurement period. Just 7 m downstream, the cooling influence is still strong, but reduced to 2°C. This cool influence is evident to 443 m. The 413 and 422 m streambed Hobo temperatures show that groundwater not only decreases streambed temperatures but can also eliminate temporal variation. The 413 and 422 m streambed hobo temperatures show little influence from surface warming and vary less than 0.4°C.

The vertical hydraulic gradient is upward to strongly upward at the first three piezometers in this stretch. At 433 m, just upstream of a small logdam, downwelling is apparent from both the hydraulic gradient and the fluctuations in temperature in the streambed (Figures 4-31 and Figure 4-14b). The upward gradient downstream of the log dam at 443 m is caused by hyporheic upwelling. The temperatures at this location are generally cool in the subsurface compared to 433 m but also respond to surface warming (Appendix B.4).

An amplitude analysis for the piezometers in this area shows that no hyporheic exchange is occurring at 413 or 422 m, but hyporheic downwelling is occurring at 430 m as suggested by the 42% amplitude of the 20 cm streambed temperature compared to the stream at that location. This effect is moderated at 443 m.

A second series of streambed measurements were made along a riffle and pool feature that follows a stream bend. Piezometer 461 m is located just upstream of the bend. Piezometers at 480, 486 and 491 m fall within the run and pool along the bend. The hydraulic gradient at 461, 480 and 491 m is upward (Figure 4-14b).

The subsurface temperatures exhibit nearly identical subsurface behavior at all but 486 m. The streambed bottom temperature at these three piezometers is between 10 and 11°C and varies little. The average temperature at 20 cm bss is

typically below 12°C with more variability. The 20 cm streambed amplitude percentages at 461, 480 and 491 m are 13, 12 and 9% respectively (Table 4-4). The time series plots also illustrate this phenomenon (Appendix B.4). Hyporheic exchange is taking place in the shallow streambed but not at depth and there is less exchange occurring here than in the upstream section of this sub reach.

In contrast to the upward gradients measured at 461, 480 and 491 m, several downward gradients were measured at 486 m in late September and early October, 2007. Additionally at 486 there is no hyporheic exchange as suggested by its 5% amplitude and the time series plots (Table 4-4, Appendix B.4). The tributary at 481 m could be influencing both temperature and hydraulic gradients at the 486 m piezometer.

Tributary 5W enters WHB at about 445 m. The average stream temperature drops about 0.3 °C just downstream of this confluence. This pattern is repeated at several other small tributaries that enter from the west in this reach.

Tributary 6E at 481 m had a mean surface temperature greater than 5°C above the western tributaries. While it does not have a significant influence on temperature based on the FODTS temperature survey data (Figure 4-19), a local drop in temperature occurs just below the tributary outfall. It is possible that the streambed zone beneath the tributary delivers cooler water to the stream than the surface water in the tributary.

In summary, multiple local temperature variations suggest influence from localized groundwater inflow. Small drainages, which are not strongly expressed as surface features, appear to act as small point sources of groundwater flow. These may in part be due to remnant stream channels or sand bars with coarser sediments that preferentially carry the cooler groundwater to the stream and may also provide lateral hyporheic exchange flow. The cool temperatures and minor diurnal variations measured at these inflow points support this observation. Shallow hyporheic exchange is active in this reach especially in the upper portion between 410 and 450 m. The eastern tributary 6E is quite warm, but does not increase stream and streambed temperatures.

Reach 6

The final sub reach begins at 495 m and ends at the 635 m downstream flume. The dominating reach morphologic characteristic is the loss of the sand and gravel streambed and the increasing marine clay exposure in the streambed (Figure 4-3 and Table 4-16). This transition is captured by the dramatic EM increases and streambed sediment depth decreases (Figure 4-6) beginning at 540 m. Log and debris dams trap sand and gravel in the upper portion of the reach. While the temperatures at the upstream and downstream ends are similar, 13.3 and 13.4°C respectively, the average reach temperature is 13.5°C. A slow but steady rise in temperature is apparent over most of the reach as the stream becomes disconnected from the floodplain and loses its hyporheic zone.

Table 4-16 Summary of sub-reach 6 stream characteristics
Wednesday Hill Brook in Lee, NH

<i>Characteristic</i>	<i>Value</i>
Reach boundaries (FODTS stations in m)	495-635 m
Reach length (m)	140
Morphologic description	Shallow clay reach
Stream type	E6
Streambed surface grain size (D50) (mm)	3 - fine sand
Stream gradient (m m ⁻¹)	0.005
Streambed alluvium depth (m)	0.02-0.95
Streambed vertical hydraulic gradient (m m ⁻¹)	Slightly upward
Average reach temperature(°C)	13.5
Average upstream temperature (°C)	13.3
Average downstream temperature (°C)	13.4
Downstream temperature trend (°C)	0.1
Hyporheic zone temperature at 20 cm bss (°C)	12.0
Tributary temperature (°C)	11.2 at 548 m 9.2 at 617 m
Electrical conductance range (umhos/cm)	20-75
Tree canopy density (%)	88-92

Tributaries at 548 and 617 m cause local and sustained stream temperature decreases. A significant localized drop in temperature (0.5 °C) at 548 m corresponds to the confluence of tributary 7W with WHB. Like the previous reach, this tributary's surface expression is very subtle and it is more of a subsurface than a surface feature. It was only measured once in August 2007 at 11.2 °C. Based on this temperature and its western valley origins, it likely has

minor diurnal fluctuations and has a spring as its major source of flow. The 617 m temperature decrease coincides with the confluence of a western spring tributary. Continuous tributary measurements have a nearly constant temperature of 9.1°C.

The amount of hyporheic exchange in this reach corresponds well to the presence of alluvium in the streambed. Piezometers at 510 and 512 m, an adjacent riffle and pool, exhibit typical temperature (Figure 4-43) and hydraulic gradient patterns (Figure 4-14b) consistent with downwelling and upwelling. Hyporheic exchange appears to be active to 0.4 m bss. Below 0.4 m temperatures are stable at 10.5°C. This is the deepest pool in the study reach. The pool temperature, 12.0°C, is the coldest of all the temperatures measured by the stream hobs. Both the deep water and the cool hyporheic discharge keep this pool cool.

Other measured subsurface temperatures in the reach are much warmer. Just downstream at 525 m, located in a long run, subsurface temperatures have a larger diurnal fluctuation and are 0.5°C warmer than at 512 m. (Figure 4-43). At 634 m, which is completed in the clay streambed, there is almost no difference in mean temperature between the stream and streambed to 0.4 m. The temperature also varies similarly with depth suggesting strong surface warming

influence. The 20 cm streambed temperature is over 1.0°C warmer than at 525 m.

In summary, this reach exhibits warming due to the minimal streambed depths and reduced cooling influence provided by groundwater and hyporheic exchange compared to the upper reaches. Two tributaries do provide cooling but these influences appear to be local to their outfall.

Study reach summary

When viewed as a whole, the study reach at WHB displays temperature moderation dynamics on multiple scales. The 2°C temperature drop over the first 170 m of stream is due to the steady and stable inflow of cool water from the western tributaries and from directional and diffuse groundwater emanating from the western catchment area. The source of this groundwater is the deltaic sand and gravel deposit located in the western uplands beneath Lee center. The WHB valley is a local discharge zone for the groundwater moving through this deposit. Hyporheic exchange of water from the warm stream through the cool subsurface also plays a role in the temperature moderation process in this upper catchment area. The higher stream gradients imposed by instream steps and log dams also increase vertical hyporheic exchange and stream cooling.

Downcutting of the stream into the valley and groundwater sapping by springs has cut a hillslope, which, at its toe, provides the cool spring water discharge and coarse sediment supply that feeds the western tributaries. If bedrock structure controls the upper WHB watershed, this may help to explain the magnitude of groundwater discharge to this upper reach as less permeable bedrock is encountered by subsurface flow systems.

While tributaries are important to downstream temperature as well, the major tributary influences are in reach 1 and 2. Downstream, groundwater and lateral hyporheic exchange take on a greater role in temperature moderation and maintenance. Below reach 2, the temperature changes only locally and warms slightly in the downstream reach. Temperature maintenance rather than reduction dominates the lower reaches. Groundwater seeps and “subsurface” tributaries and possibly lateral hyporheic exchange provide cool water to the stream. The heavy canopy prevents large influences from solar radiation. Any temperature changes from radiation appear to be balanced by cool discharges from groundwater and tributaries.

Piezometer data interpreted through time series, amplitude analysis, and box plots, consistently suggest a typical hyporheic exchange depth of 0.2 m.

Notable exceptions include the riffle at 237 m just upstream of a logdam at the stream constriction and the 510-512 m riffle-pool where hyporheic exchange may

penetrate below 0.4 m. Little or no exchange occurs in reach 4 and in other areas of considerable groundwater discharge (e.g. the 413 and 420 m piezometers).

Time stability analysis

The characteristic temperature signal along the study reach suggests that there are persistent influences on temperature within the catchment area. If the stream does indeed exhibit time stable characteristics, then there is the potential to devise efficient future sampling strategies. These strategies are best informed by potentially relevant stream characteristics including streambed sediment characteristics, catchment geomorphology, and streambed morphology.

Time stability analysis was conducted on data collected during FC-07-1. Figure 4-44 shows the rank-ordered mean relative difference (MRD) values with corresponding reach designations. Locations having positive MRD values have warmer temperatures than the reach mean. Cooler locations have negative MRD values.

The sub reaches with temperatures closest to the entire study reach mean are reach 2 (orange boxes) and reach 6 (yellow triangles). The reaches farthest from the mean are reaches 1 and 5. In the armored reach (reach 1, blue diamonds) there is greater temperature fluctuation and less cooling has occurred in the upper reach

compared to the other areas. In contrast, reach 5 (floodplain, green circles) and to some extent, reach 4 (meanders, purple x's) is relatively cool.

The reach 1 measurement points clearly dominated the reach scale TSA during FC 07-1. To examine the more subtle differences in the remaining subreach these values were removed from the data set and the TSA was re-calculated (Figure 4-45). In this analysis, there is much more variability in the MRD by area. Reach 2 and many reach 6 points are generally warmer than the remaining reach mean temperature. Reaches 3, 4 and 5 are distributed along the rank spectrum, but reach 3 is closest to the mean while reaches 4 and 5 are generally lower than the mean.

Potentially relevant physical features were investigated to identify factors that cause time-invariant stability features. The stream temperature MRDs are classified by geomorphic reach classification, stream geomorphic feature, or D50 streambed surface grain size. Figures 4-46 to 4-48 represent the mean relative difference distributions of three stream characteristics for points below the armored reach. If streambed characteristics are time stable they will fall close to a 0.0 value of mean relative difference. The figures also show the 95% confidence interval (CI) for the MRD values for each characteristic. The CI further describes time invariance as a smaller CI suggests a greater central tendency.

Figure 4-46 illustrates mean relative difference of points classified by reach geomorphology – reach 2 (box valley), logdam cascade (reach 3), meander (reach 4), floodplain (reach 5), or shallow clay (reach 6) as described in the sub-reach description. These classifications broadly account for stream gradient, stream plan form, and catchment characteristics. As classified, none of the reaches are time stable; all are significantly different than zero. The box valley and shallow clay reaches are warmer than the reach mean and the meander, floodplain and log dam cascade sub-reaches are below the reach mean. The logdam cascade and shallow clay reaches have the smallest confidence interval.

This classification illustrates the amount of groundwater and hyporheic cooling that has occurred in the upper reaches and the ability of the middle reaches to maintain a steady temperature. It also illustrates that areas underlain by shallow clay are not able to effectively maintain the cool and constant temperature attained in the middle reach. In general, this analysis demonstrates that stream temperature sampling based on physical reach characteristics would result in a biased estimate of reach temperature. Colder bias is expected in the areas of temperature maintenance and warm biases in areas where groundwater and hyporheic exchange have not fully cooled the reach or where the alluvial streambed is absent.

Figure 4-47 shows stream temperature classified by D50 streambed sediment grain size. Since d50 sampling was done on 100 m stream segments the classification is somewhat artificial. Again, significant differences are identified based on dominant streambed grain size. All of the grain size classifications were significantly different from zero. Fine (0.25 mm) and coarse grained (8 mm) sediments had warmer temperatures than predominately sand and gravel (7 mm and 0.8 mm) streambed segments. In this heterogeneous stream, no unique D50 classification yields time stable characteristics. The most fine grained and largest grain size streambeds are warmest and sand and gravel reaches are the coolest in the study reach. Streambed sediment size cannot be used to characterize temperature stability in this heterogeneous stream.

Streambed morphologic features were also used to assess time stability (Figure 4-48). During the field campaign and as the cable was being removed from the stream, predominant stream features (riffle, pool, step) were noted by cable station where possible. If the notes did not indicate a feature, it was classified as undesignated. Only steps were found to be significantly different from zero. They were the only features with significantly cooler temperatures, but the small number of points and the range of variability make it difficult to assess their true impact.

Pools, undesignated reaches and riffles were found to be the most time stable, while steps and areas near tributaries were the least stable. Pool and undesignated feature temperatures had the smallest confidence interval, which suggests that they are most time stable.

In summary, it appears that the lowest sampling bias is in riffles, pools, or undesignated areas, but steps and tributary areas would give biased temperature results. If a representative temperature sample was required in the study reach, sampling in reach 2 away from tributaries or in the shallow clay reach would be the most representative temperature for the reach and pools would be the most time stable areas to sample. From a biological perspective, stream dwellers will find the most stable temperatures in pools but both pools and undesignated areas (glides, runs) remain relatively stable and close to the mean in WHB. The coolest and most stable locations are in areas of sand and gravel in reach 4 and 5 away from tributaries and steps.

Heat budget model

Figure 4-49 shows the potential heat sources and sinks in the WHB study reach. The heat budget was calculated to quantify the relative contributions of each heat source or sink to the longitudinal temperature change. This section first

describes the non-advective energy terms, then presents the model results by reach.

The non-advective heat flux components were analyzed at three locations, 75, 336 and 468 m. These locations were chosen to capture the reach's spatial variability and because there was little or no vertical hydraulic gradient measured at these locations, advection probably plays a minimal role in heat exchange. The same measured net radiation was applied to all locations. Evaporation, convection and conduction differ by location due to variations in stream and streambed temperatures. Table A.4 in Appendix A.6 summarizes the mean, minimum and maximum values of the non-advective heat flux components.

Figure 4-50 shows the net energy fluxes due to radiation, evaporation, convection and conduction at 336 m in reach 4, the meander reach during FC 07-1. Net radiation, which adds heat to the stream, peaked between 11:00 and 14:00 and fell below 0 W m^{-2} over night. Heat conduction from the stream to the streambed provided the greatest cooling during the late afternoon and modest warming during the early morning hours. Convection and evaporation usually added heat to the stream.

These fluxes show the relative importance of streambed conduction to stream cooling. Table 4-17 lists the streambed conduction by piezometer location for the

20 cm depth and for the total streambed depth. Since conduction is largely driven by the temperature gradient between the stream and streambed, the largest temperature gradient provides the most streambed conduction. Conduction over the full streambed depth ranges from -3.2 to -35.2 W m⁻². Conduction in the top 20 cm of the streambed was consistently higher than that measured over the entire streambed depth (-2.4 to -64.5 W m⁻²). An exception occurs at 634 m where it is minimally lower. This may be due to its completion in the clay streambed rather than in sand and gravel.

The greatest streambed conduction occurs at the 268 and 413 m riffles. Overall, the meander and floodplain reach (reach 4 and 5) have the greatest streambed conduction. The least conductive areas are 167, 237 and 292 m. At 167 m, the warmer stream temperature and the armored streambed likely influence the streambed. At 237 m, the streambed has cooled but the gradient is still small overall. At 292 m, the solar radiation that enters through the local canopy opening may warm the streambed.

Table 4-17 Summary of streambed conduction at piezometers
Wednesday Hill Brook in Lee, NH

Piezometer FODTS Location (m)	Reach	Mean Stream Temperature (°C)		Mean Streambed Temperature at 20 cm bss (°C)	Depth of Streambed (m)	Streambed Thermal Conductivity (J/m/s/C)	Total Streambed Conduction (W m ⁻²)	Streambed Conduction at 20 cm bss (W m ⁻²)
		Mean Stream Temperature (°C)	Mean Streambed Temperature at 20 cm bss (°C)					
167	1	15.5	13.8	13.8	0.40	2.8	-11.8	-9.1
171	1	15.5	13.6	13.6	0.38	2.8	-14.3	-20.0
237	2	13.5	12.5	12.5	0.60	2.6	-4.3	-6.5
257	3	13.2	11.7	11.7	0.40	2.6	-9.8	-10.4
268	3	13.3	9.5	9.5	0.72	2.6	-13.7	-44.2
276	3	13.9	10.7	10.7	0.75	2.6	-11.3	-5.5
292	3	13.6	12.7	12.7	0.32	2.6	-7.3	-2.6
295	3	13.7	12.4	12.4	0.38	2.6	-8.9	-18.2
334	4	13.7	12.1	12.1	0.33	2.6	-12.8	-19.5
336	4	13.7	12.1	12.1	0.33	2.6	-12.8	-18.2
360	4	13.5	10.5	10.5	0.60	2.6	-13.0	-32.5
362	4	13.5	11.0	11.0	0.60	2.6	-10.8	-26.0
413	5	13.8	9.0	9.0	0.30	2.2	-35.2	-64.5
422	5	13.8	10.6	10.6	0.40	2.2	-17.6	-24.2
430	5	13.9	10.9	10.9	0.65	2.2	-10.2	-18.7
433	5	13.6	12.1	12.1	0.60	2.2	-5.5	-14.3
443	5	13.5	10.3	10.3	0.55	2.2	-12.8	-24.2
461	5	13.6	9.9	9.9	0.53	2.2	-15.4	-34.1
480	5	13.4	11.0	11.0	0.73	2.0	-6.6	-23.1
486	5	13.5	11.0	11.0	0.62	2.0	-8.1	-25.3
491	5	13.5	11.5	11.5	0.33	2.0	-12.3	-18.7
510	6	13.0	10.0	10.0	0.60	2.0	-10.0	-11.0
512	6	12.8	10.5	10.5	0.60	2.0	-7.7	-19.8
525	6	13.9	12.3	12.3	0.40	2.0	-8.0	-14.3
634	6	13.7	13.0	13.0	0.40	1.8	-3.2	-2.4

Heat budget simulation

Reaches 1, 2, 4 and 5 were modeled according to the methods described in Chapter 3. Appendix A.7 lists the starting parameters used for each reach analysis. Table 4-18 presents the model results. Results are presented for non-advective and advective heat flow combinations. This section described the results at two scales, subreach and immediately surrounding major tributary confluences.

Reach 1 is 105 m long. It includes tributary 1 W at 109 m and ends immediately above tributary 2W. The upstream temperature, 15.5°C, cooled by 0.7°C over the reach to 14.8°C. Using the non-advective heat flux data alone, net radiation, evaporative, conductive, friction and convective flux with no tributary, groundwater or hyporheic discharge, the stream water would warm to 15.7°C. Thus the advective terms effectively cool this reach by 1.0°C.

In order to cool the stream to the observed 14.8°C with a tributary temperature of 12.6°C, the required tributary flow is 0.034 cms. This is 12 times the 0.000272 cms estimated tributary 1W discharge. Using groundwater alone to cool the stream water to the observed downstream value, the groundwater flux would be 0.0016 cms or twice the predicted reach discharge. For the water balance, groundwater flow three times that of the tributaries was required and

Table 4-18 a Results of heat budget modeling – Reach 1

Reach 1 - Armored Reach			
Run 1 - No tributaries, groundwater or hyporheic flux	Resulting temperature	°C	15.7
Run 2 - Tributary 1W only	Tributary flow	m ³ s ⁻¹	0.003400
	Resulting streamflow	m ³ s ⁻¹	0.015200
	ArcHydro estimated WHB flow	m ³ s ⁻¹	0.009050
	Resulting temperature	°C	14.8
Run 3 - GW only	Resulting GW flow	m ³ s ⁻¹	0.001575
	Resulting streamflow	m ³ s ⁻¹	0.009695
	Resulting temperature	°C	14.8
Run 4 - HZ flux only	Resulting HZ flux	m ² s ⁻¹	0.000044
	Hyporheic exchange coefficient	s ⁻¹	0.000295
	Resulting temperature	°C	14.8
Run 5 - Tributary and GW	Resulting Tributary Flow	m ³ s ⁻¹	0.000272
	Resulting GW flow	m ³ s ⁻¹	0.000658
	Resulting temperature	°C	15.2
Run 6 - Tributary 1W, GW and HZ	Resulting Tributary flow	m ³ s ⁻¹	0.000272
	Resulting GW flow	m ³ s ⁻¹	0.000660
	Resulting HZ flux	m ² s ⁻¹	0.000020
	Hyporheic exchange coefficient	s ⁻¹	0.000312
	Resulting temperature	°C	14.8
Observed temperature and flow conditions			
Upstream temperature		°C	15.5
Downstream temperature		°C	14.8
Change in temperature		°C	- 0.7
Upstream flow		cms	0.00812
Downstream flow		cms	0.00905
Change in upstream to downstream flow		cms	0.00093

only half of the required cooling occurs. For the final heat budget for the reach, the tributary and groundwater discharge estimated in the water balance and a hyporheic flux of 0.00002 m²/s achieve the observed downstream cooling.

Table 4-18 b Results of heat budget modeling – Reach 2

<i>Reach 2 - Box Valley Reach</i>			
Run 1 - No tributaries, groundwater or hyporheic flux	Resulting temperature	°C	15.0
Run 2 - Tributaries only	Tributary flow	m ³ s ⁻¹	0.007900
	Resulting streamflow	m ³ s ⁻¹	0.016950
	ArchHydro estimated flow	m ³ s ⁻¹	0.009670
	Resulting temperature	°C	13.5
Run 3 - GW only	Resulting GW flow	m ³ s ⁻¹	0.003640
	Resulting streamflow	m ³ s ⁻¹	0.012700
	ArchHydro estimated flow	m ³ s ⁻¹	0.009670
	Resulting temperature	°C	13.5
Run 4 - HZ flux only	Resulting HZ flux	m ² s ⁻¹	0.000004
	Hyporheic exchange coefficient	s ⁻¹	0.000006
	Resulting temperature	°C	13.5
Run 5 - Tributary 1W and GW	Resulting tributary flow	m ³ s ⁻¹	0.000193
	Resulting GW flow	m ³ s ⁻¹	0.000423
	Resulting streamflow	m ³ s ⁻¹	0.000967
	Resulting temperature	°C	14.7
Run 6 - Tributary 1W, GW and HZ	Resulting tributary flow	m ³ s ⁻¹	0.000193
	Resulting GW flow	m ³ s ⁻¹	0.000423
	Resulting HZ flux	m ² s ⁻¹	0.000095
	Hyporheic exchange coefficient	s ⁻¹	0.000160
	Resulting temperature	°C	13.5
Temperature and flow conditions			
Upstream temperature		°C	14.8
Downstream temperature		°C	13.5
Change in temperature		°C	-1.1
Upstream flow		cms	0.00905
Downstream flow		cms	0.00967
Change in upstream to downstream flow		cms	0.00062

Reach 2 cools from 14.8 to 13.5°C over the reach and gains 0.00062 cms in streamflow. It begins at the tributary at 190 m (2 W) and continues to the large log dam just downstream of measurement point 237 m. Two small western

tributaries enter at 214 and 225 m (3 W). Non-advective heat flow alone would warm the stream by 0.2°C. Using tributary flow alone at 11.9°C, discharge would be over 10 times that estimated previously. Using groundwater discharge alone at 10°C, the required discharge is six times the estimated value. A combination of hyporheic exchange, groundwater discharge and tributary discharge (at the ArchHydro estimate) achieve the downstream temperature and water balance. The water balance requires 0.00043 cms groundwater and a tributary discharge of 0.000193 cms but cools the stream water only 0.1°C. The final energy and water balance relies strongly on hyporheic exchange to cool the reach to 13.5°C with a final hyporheic flux of 0.000095 m²/s.

Reach 4, the meander reach, is 100 m long. It includes one major tributary from the east (4E) with an average temperature of 15.5°C and several seeps. It warms from 13.2 to 13.3°C and picks up 0.00020 cms. The addition of non-advective heat flux alone resulted in a downstream temperature of 13.34°C, slightly warmer than the starting and ending temperature. Tributary discharge was not added to achieve the downstream temperature because it is warmer than the stream. The addition of tributary water would only further warm the stream. With groundwater alone added to the reach, the flow rate needed to achieve the observed temperature was 0.0003 cms. The final simulation predicted a groundwater flow value of 0.00015 cms and a tributary flow of

0.000053 cms. No hyporheic flux was necessary to achieve the downstream temperature. It appears that hyporheic exchange is insignificant in reach 4.

Table 4-18 c Results of heat budget modeling – Reach 4

<i>Reach 4 - Meander Reach</i>			
Run 1 - No tributaries, GW or HZ	Resulting Temperature	°C	13.34
Run 2- Tributary only ⁽¹⁾	Not Applicable		
Run 3 - GW only	Resulting GW flow	m ³ s ⁻¹	0.000300
	Resulting WHB flow	m ³ s ⁻¹	0.010000
	Resulting temperature	°C	13.3
Run 4 - Tributary and HZ flux only	Resulting HZ flux	m ² s ⁻¹	0.000020
	Hyporheic exchange coefficient	s ⁻¹	0.000040
	Resulting tributary Flow	m ³ s ⁻¹	0.000053
	Resulting temperature	°C	13.3
Run 5 - Tributary and GW	Resulting tributary Flow	m ³ s ⁻¹	0.000053
	Resulting GW flow	m ³ s ⁻¹	0.000150
	Resulting streamflow	m ³ s ⁻¹	0.009920
	Resulting temperature	°C	13.31
Run 6 - Tributary, GW and HZ	Resulting tributary flow	m ³ s ⁻¹	0.000053
	Resulting GW flow	m ³ s ⁻¹	0.000150
	Resulting HZ flux	m ² s ⁻¹	0.000000
	Hyporheic exchange coefficient	s ⁻¹	na
	Resulting temperature	°C	13.3
Temperature and flow conditions			
	Upstream temperature	°C	13.2
	Downstream temperature	°C	13.3
	Change in temperature	°C	0.1
	Upstream flow	cms	0.00972
	Downstream flow	cms	0.00992
	Change in upstream to downstream flow	cms	0.00020

⁽¹⁾ Not completed as reach 4 tributary adds warm water to WHB

Table 4-18 d Results of heat budget modeling – Reach 5

<i>Reach 5 - Floodplain Reach</i>			
Run 1 - No tributaries, GW or HZ	Resulting Temperature	°C	13.50
Run 2 - HZ flux only	Hyporheic exchange coefficient	s ⁻¹	0.0000350
	Resulting HZ flux	m ² s ⁻¹	0.0000175
	Resulting Temperature	°C	13.30
Run 4 - Tributary and HZ flux only	Resulting HZ flux	m ² s ⁻¹	0.000020
	Hyporheic exchange coefficient	s ⁻¹	0.000040
	Resulting Tributary Flow	m ³ s ⁻¹	0.000303
	Resulting Temperature	°C	13.30
Run 5 - Tributary and GW	Resulting Tributary Flow	m ³ s ⁻¹	0.000303
	Resulting GW flow	m ³ s ⁻¹	0.000150
	Resulting streamflow	m ³ s ⁻¹	0.010680
	Resulting Temperature	°C	13.35
Run 6 - Tributary, GW and HZ	Resulting Tributary flow	m ³ s ⁻¹	0.000303
	Resulting GW flow	m ³ s ⁻¹	0.000510
	Resulting HZ flux	m ² s ⁻¹	0.000002
	Hyporheic exchange coefficient	s ⁻¹	0.000004
Temperature and flow conditions			
Upstream temperature		°C	13.3
Downstream temperature		°C	13.3
Change in temperature		°C	0.0
Upstream flow		cms	0.00992
Downstream flow		cms	0.01079
Change in upstream to downstream flow		cms	0.00087

In reach 5, the floodplain reach, the beginning and ending temperatures are the same (13.3°C) with multiple fluctuations along its length. With non-advective heat flux alone added to the model, the temperature would rise to 13.5°C. The reach 5 tributaries modeled were 5W, a cool stream, and 6E, a warm stream. The water balance suggests that tributaries contribute twice as much flow as

groundwater. The overall effect of these inflows and non-advective sources is an increase of 0.05°C. A modest hyporheic flux of 0.000002 m²/s provides the additional 0.05°C cooling.

Figures 4-51 and Table 4-19 present the final modeled energy fluxes as changes in stream temperature. The most significant source of heat to the reach is net radiation. Evaporation and convection combined equal the heat added by net radiation. The heat due to friction is negligible, but is highest in Reach 1 where the gradient is greatest. In Reach 4, tributary discharge adds a small amount of heat as well.

The mechanisms that reduce stream water temperature in the study reach are streambed conduction, tributary discharge, groundwater discharge and hyporheic exchange. The most significant influences vary by reach. Hyporheic exchange is very important in reaches 1 and 2 but is not a factor in reach 4. It is modestly important in reach 5. Groundwater is important as a cooling mechanism in all reaches but especially in reach 1 as modeled. The streambed conduction influence is greatest in reaches 4 and 5 and nearly offsets net radiation. Tributary discharge cools the stream slightly in reaches 1, 2 and 5.

Figure 4-52 and Table 4-19 illustrates the tributary and groundwater discharge values calculated in the modeling effort. Because water temperature plays a

Table 4-19 Summary of temperature changes (°C) and discharges (cms) calculated by heat budget model
 Wednesday Hill Brook in Lee, NH

	Net Radiation	Evaporation	Convection	Friction	Streambed Conduction	Groundwater Inflow	Hyporheic exchange	Tributary Discharge
Reach 1	0.154	0.077	0.070	0.008	-0.067	-0.412	-0.461	-0.101
Reach 2	0.114	0.057	0.052	0.001	-0.046	-0.214	-1.215	-0.061
Reach 4	0.204	0.107	0.095	0.000	-0.147	-0.185	0.000	0.012
Reach 5	0.170	0.089	0.079	0.001	-0.138	-0.210	-0.022	0.027

	Groundwater Discharge	Tributary Discharge
Reach 1	0.000658	0.000272
Reach 2	0.000422	0.000193
Reach 4	0.000150	0.000060
Reach 5	0.000255	0.000567

large role in its ability to cool a stream, groundwater plays a larger role than tributaries. In reaches 1 and 2 groundwater temperatures are significantly cooler than the tributaries, even though the tributaries are spring fed they are influenced by surface warming. In reach 4, the tributary was a warm stream. This added discharge but increased the reach temperature. Groundwater balanced this warming influence and also added streamflow. In this reach, temperatures increased in the upstream segment, then cooled for the remainder of the reach. This suggests that groundwater discharge cools the lower portion of reach 4.

Streambed conduction and groundwater appear equally important in keeping the stream cool in reach 4 and 5. As illustrated by the FODTS survey, there is a great deal of local temperature change in these reaches. Groundwater discharge to the stream creates cool zones, which also enhance streambed conduction. This feedback appears to be the major driver of temperature moderation in the lower study reach. Hyporheic exchange is active in reach 5, but not extremely important to temperature moderation as modeled.

Small scale heat budgets – Reach 1a and 2a

The greatest temperature changes occurred in reaches 1 and 2 at the confluence of tributaries 1W and 2W. These features are very apparent in the FODTS temperature profile. However, on the ground, they appear to be only modest features with relatively low, but steady flow. The heat budget model was used to

understand the heat flow dynamics along a short distance in the stream immediately adjacent to these confluences.

Reach 1a is 20 m long. The upstream temperature is 15.5°C and the downstream temperature is 14.7°C. In this area, WHB flows over boulders and cobbles in a step-pool morphology with a 5% gradient. Several steps occur just upstream and downstream of the confluence of 1W. A large permeable zone surrounds 1W, which likely carries spring water beneath the surface towards the stream. Field observation suggests that this feature may carry the majority of groundwater to the stream because small seeps are the only other apparent discharge zone.

Overall, reach 1 has 0.000272 cms tributary and 0.000660 cms groundwater flow. The groundwater inflow value was increased compared to the tributary by reducing streamflow by an order of magnitude and putting the reach streamflow gain in reach 1a as groundwater discharge. This coarse to fine analysis allows for refinement of groundwater discharge amounts where assumptions of tributary streamflow were estimated, not measured. To check the validity of this approach, calculation of potential groundwater flow from this feature resulted in estimating a groundwater discharge zone around the tributary with an area of 1 m² with an hydraulic conductivity of $2.2 \times 10^{-3} \text{ m s}^{-1}$, a porosity of 0.3, and a resulting discharge totaling $6.6 \times 10^{-4} \text{ m}^3 \text{ s}^{-1}$. The values of hydraulic conductivity

and porosity fall well within the expected range for coarse sand and gravel that make up the tributary streambed (Freeze and Cherry, 1987).

The tributary water temperature (12.9 °C) is lower than the average streambed temperature (13.7 °C measured at piezometer 93 m) and the groundwater temperature is 10°C based on well and spring temperatures. The streambed temperature, locally, where this cool discharge feature enters the stream, therefore, should also be much cooler than the surrounding streambed. For this short reach, the streambed temperature used to calculate streambed conduction and the hyporheic temperature used to calculate hyporheic temperature exchange were reduced to 10 °C. The resulting streambed conduction value for Reach 1a was 98 W m².

Table 4-20 Results of small-scale heat budget modeling – Reach 1a and 2a

Reach 1a – Tributary 1W			
Resulting Tributary flow	m ³ s ⁻¹		0.000027
Resulting GW flow	m ³ s ⁻¹		0.000660
Resulting HZ flux	m ² s ⁻¹		0.000032
Hyporheic exchange coefficient	s ⁻¹		0.00021
Resulting Temperature	°C		14.7
Reach 2a – Tributary 2W			
Resulting Tributary flow	m ³ s ⁻¹		0.000014
Resulting GW flow	m ³ s ⁻¹		0.000600
Resulting HZ flux	m ² s ⁻¹		0.000084
Hyporheic exchange coefficient	s ⁻¹		0.00021
Resulting Temperature	°C		13.7

The resulting analysis (Table 4-20 and Figure 4- 53) suggests that hyporheic exchange and groundwater each drop the stream temperature 0.4 °C. The

tributary flow had almost no effect on temperature while streambed conduction reduced the stream temperature by 0.08 °C. The very strong hyporheic exchange is likely driven by the streambed steps that surround this confluence and the enhanced cooling by tributary and groundwater inflow. Hyporheic exchange is more influential over this short distance as compared to the remainder of reach 1.

The reach 2a analysis is similar in many respects to reach 1a. The reach is 20 m long and the temperature drop is 1.1 °C. The tributary has a large subsurface component and is assumed to transmit groundwater. Just upstream of the confluence several logdams locally increase the gradient and allow for enhanced hyporheic exchange. The cool tributary water influences streambed temperature and hyporheic temperatures. The simulation for this reach also reduced the tributary discharge by a factor of 10 from that estimated by ArchHydro. The groundwater discharge value was slightly lower than 1a at 0.006 m³ s⁻¹. The alluvium is somewhat finer which would accordingly reduce the hydraulic conductivity of the substream sediments, so this reduction in discharge is in line with field observations. The hyporheic exchange accounted for 3 times the temperature reduction of groundwater even though the hyporheic exchange coefficient was modeled to be equivalent to reach 1a. This is due to the wider and deeper stream in this reach, which increases the hyporheic surface area over which exchange occurs. The hyporheic exchange coefficient is the value

that is adjusted in the final run in order to match observed temperature. This adjustment resulted in the same hyporheic coefficient for both reach 1a and 2a.

In summary, a unique combination of physical features and temperature characteristics allow for strong stream temperature moderation over a very short distance. The cool, groundwater-fed inflow below the tributary streambed is a primary influence. The water and sediment carried by the tributary itself and the presence of logdams and steps adjacent to the tributaries, creates a deep streambed and localized cooling zone for stream water. Based on this analysis, a similar confluence of physical features may influence stream temperature at other locations. This is most apparent in the upper reaches where the beginning stream temperature is elevated in contrast to groundwater temperatures.

Summary of heat budget modeling

In summary, hyporheic exchange and groundwater discharge are major factors in the temperature moderation in reaches 1 and 2. Groundwater and streambed conduction are the primary contributors to temperature moderation in reach 4. Hyporheic exchange is virtually absent in reach 4 and only plays a minor role in reach 5. Undoubtedly, without the contribution of groundwater from the deltaic sand and gravel deposit located west of WHB, less significant cooling and temperature moderation would occur along the brook. While the groundwater discharge drives the cooling in Wednesday Hill Brook, the streambed topography

and local gradient variations create a positive feedback through additional heat loss from hyporheic exchange and streambed conduction.

Sensitivity analysis

The heat budget model's sensitivity to hyporheic zone temperature gradient, hyporheic exchange coefficient, and thermal conductivity was analyzed. The hyporheic exchange coefficient and the hyporheic temperature gradient were varied by a factor of two above and below the final modeled value for each reach. The exchange coefficient was varied from 0.0 to 0.00027 s^{-1} , 0.0 to 0.0005 s^{-1} , and 0.0 to 0.00002 s^{-1} for reaches 1, 2, 4 and 5. The hyporheic zone temperature was varied from 0.0 to 3.6°C for reaches 1 and 2, respectively, and from 0 to 2.6°C for reach 5. Reach 4 was not subjected to sensitivity analysis for hyporheic temperature, as no hyporheic exchange appears to occur in this reach. Based on literature-derived values for sediment thermal conductivity, the values for WHB were varied between 1.8 and $3.2 \text{ J m}^{-1}\text{s}^{-1}\text{C}^{-1}$.

The hyporheic exchange terms both had similar sensitivities by reach (Figure 4-54). Reach 2 was highly sensitive to changes in parameter values. Reach 5 was insensitive to changes in hyporheic zone temperature and hyporheic exchange coefficient values. Because the upper reaches had a relatively high exchange coefficient, small changes may disproportionately modify temperatures. However, the temperature gradients, which were fairly similar showed the same high sensitivity in the upper reach and low sensitivity in the lower reach.

The overall error for thermal conductivity was lower than the hyporheic zone parameter error by over an order of magnitude. The sensitivity results were reversed for streambed thermal conductivity. Reaches 4 and 5 were more sensitive to conductivity than reaches 1 and 2. Streambed conduction plays a stronger role in the heat budget in lower reaches. The streambed temperature gradient is larger in the lower reaches as well (Table 4-17). Reach 2 was more sensitive to conductivity than reach 1. While the sensitivity varies among reaches, the absolute change in stream temperature due to thermal conductivity is small.

Section 4 – Results

Figures

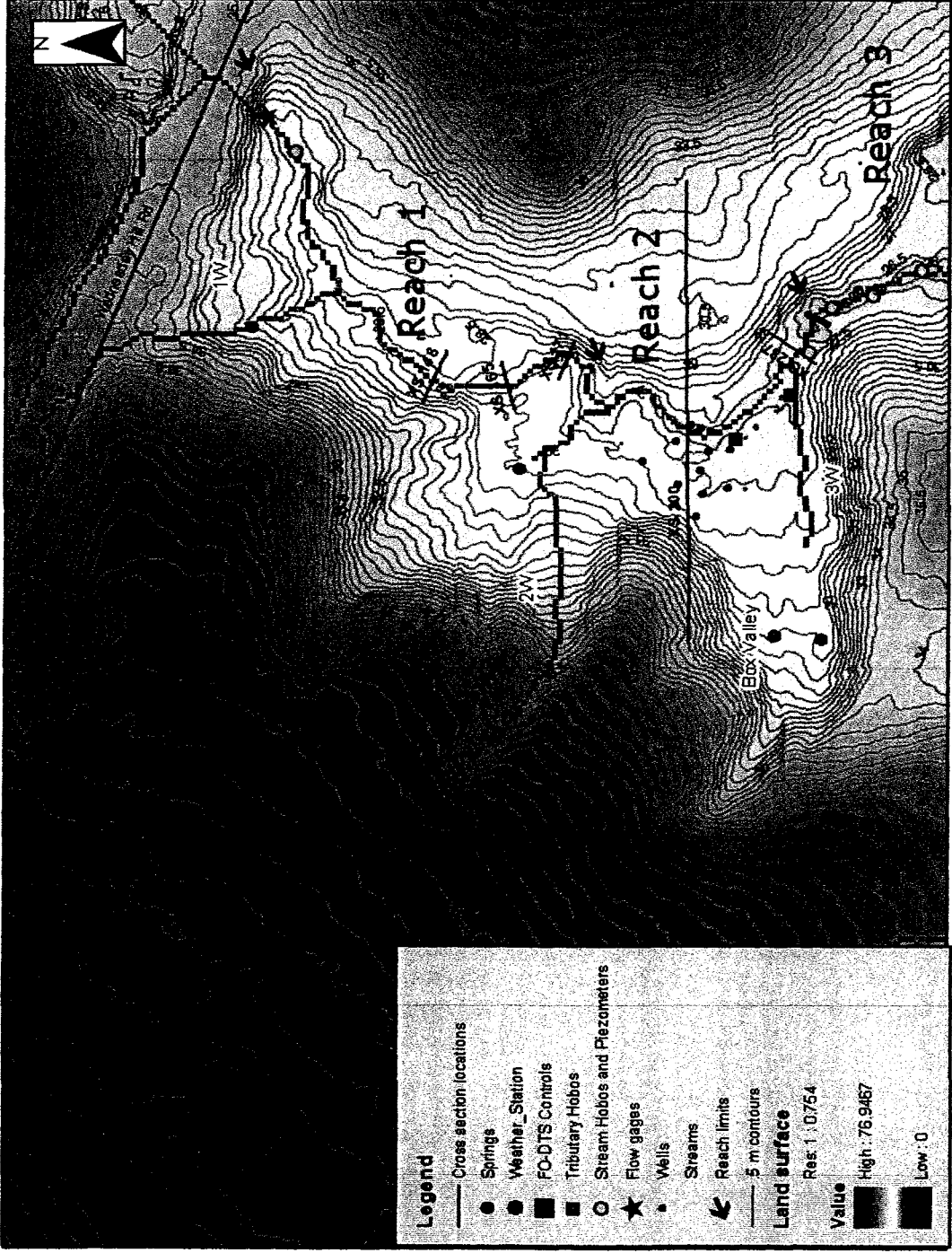


Figure 4-1 Upper study reaches Wednesday Hill Brook in Lee, NH Topography developed from LiDAR imagery – National Center for Aerial Laser Mapping

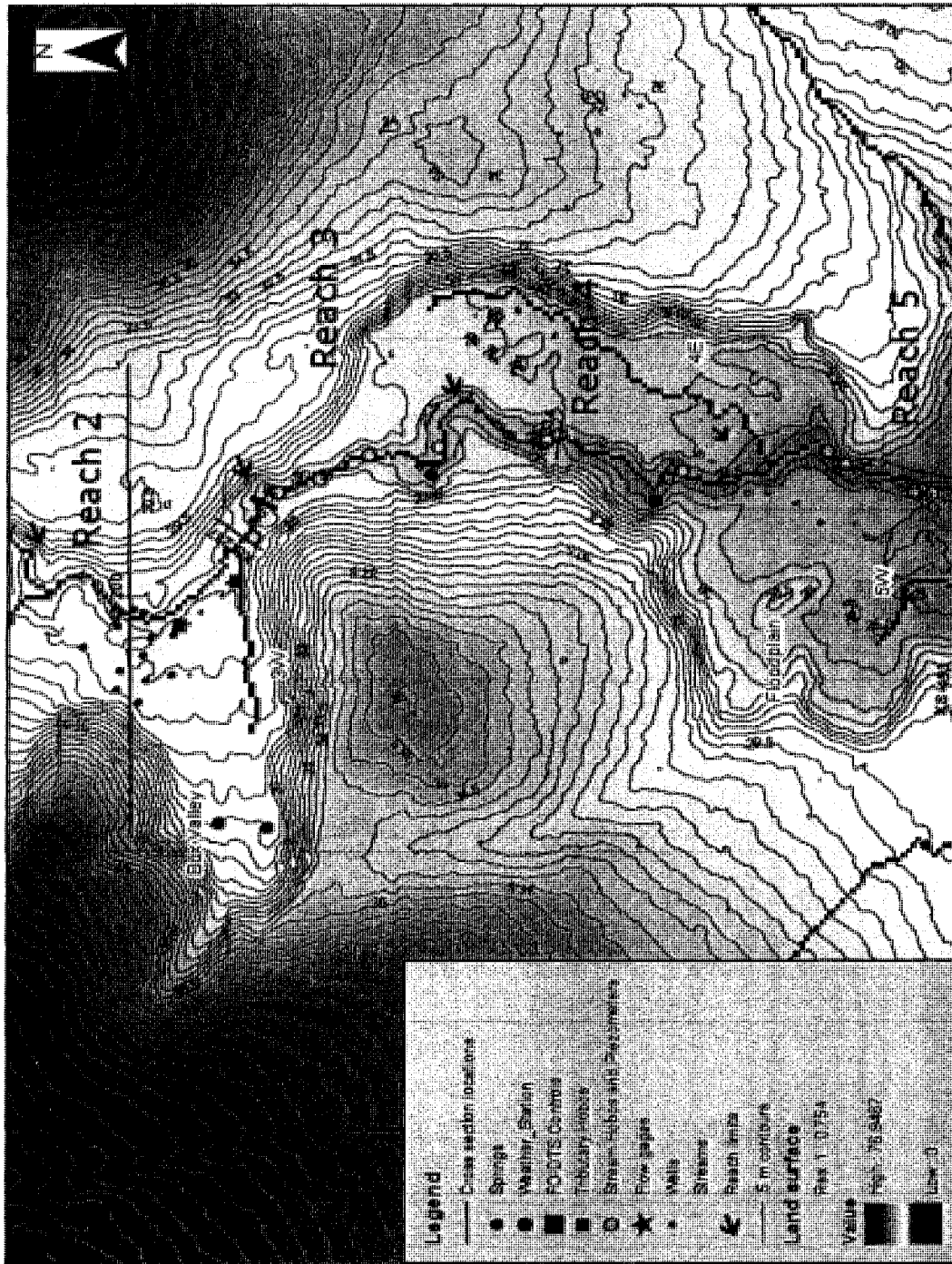


Figure 4-2 Middle study reaches in Lee, NH
 Wednesday Hill Brook in Lee, NH
 Topography developed from LiDAR imagery – National Center for Aerial Laser Mapping

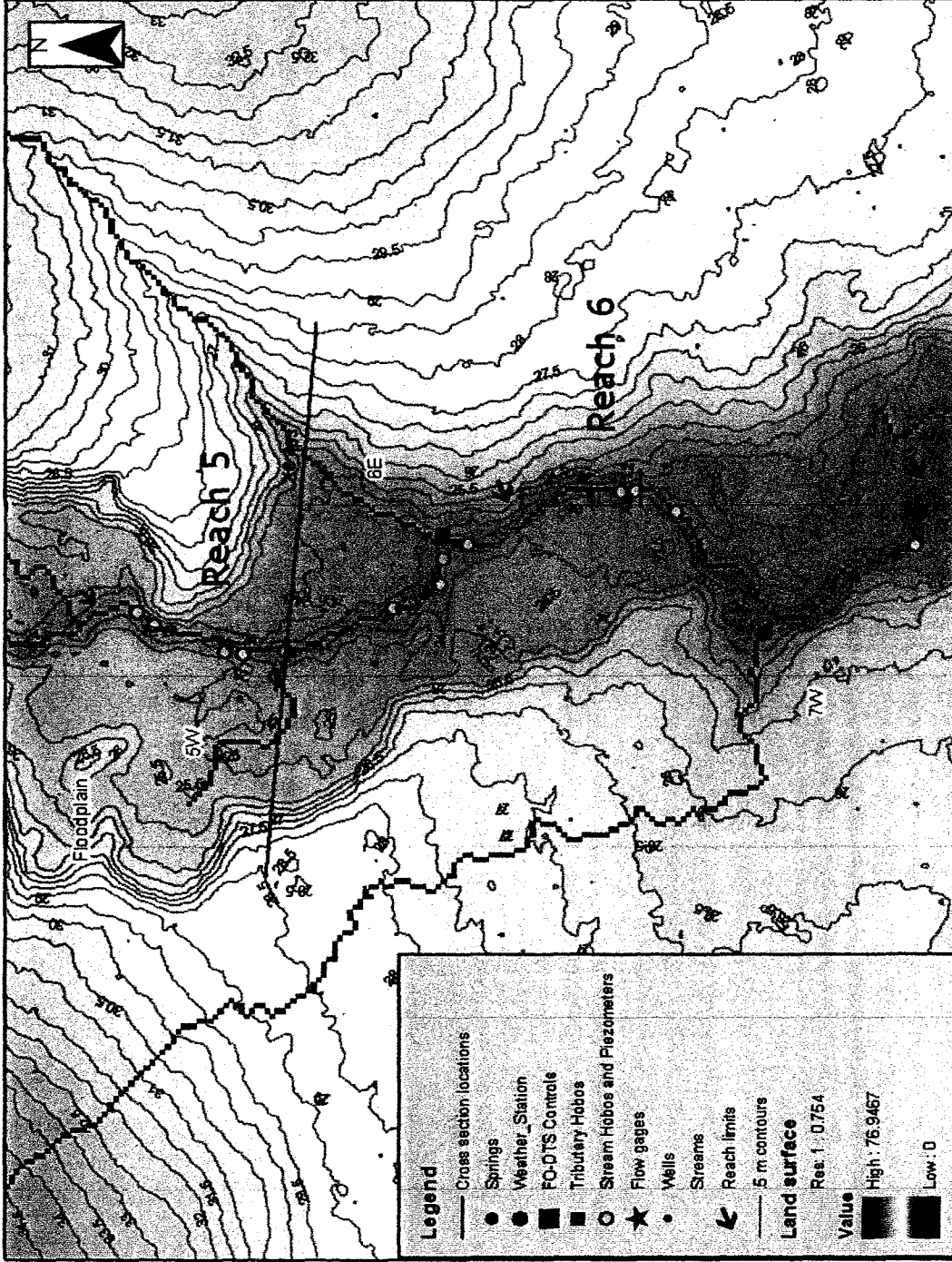
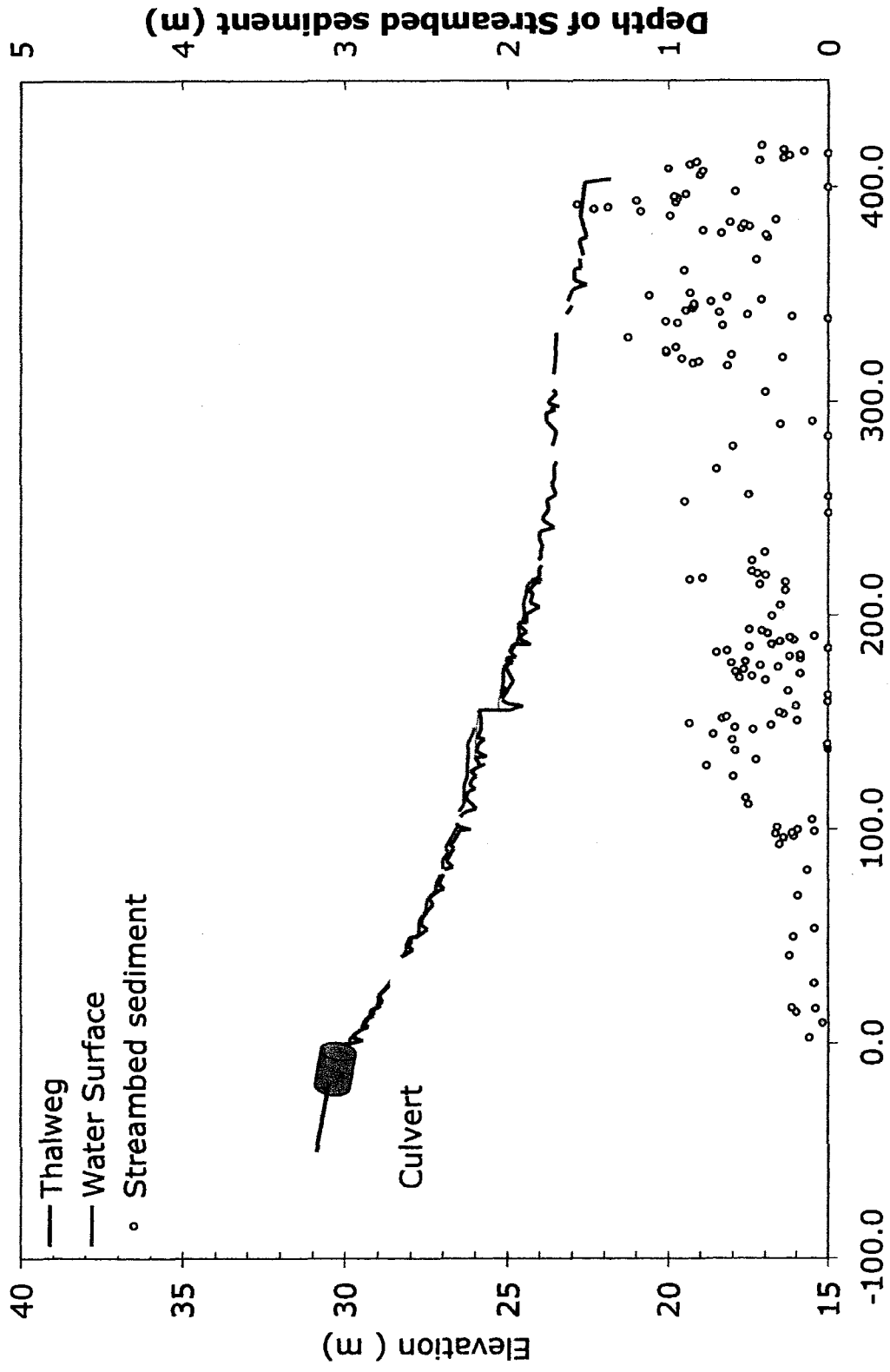


Figure 4-3 Lower study reaches Wednesday Hill Brook in Lee, NH Topography developed from LiDAR imagery – National Center for Aerial Laser Mapping



Distance downstream from Culvert (m)

Figure 4-4 Longitudinal profile and sediment depths on study reach
Wednesday Hill Brook in Lee, NH

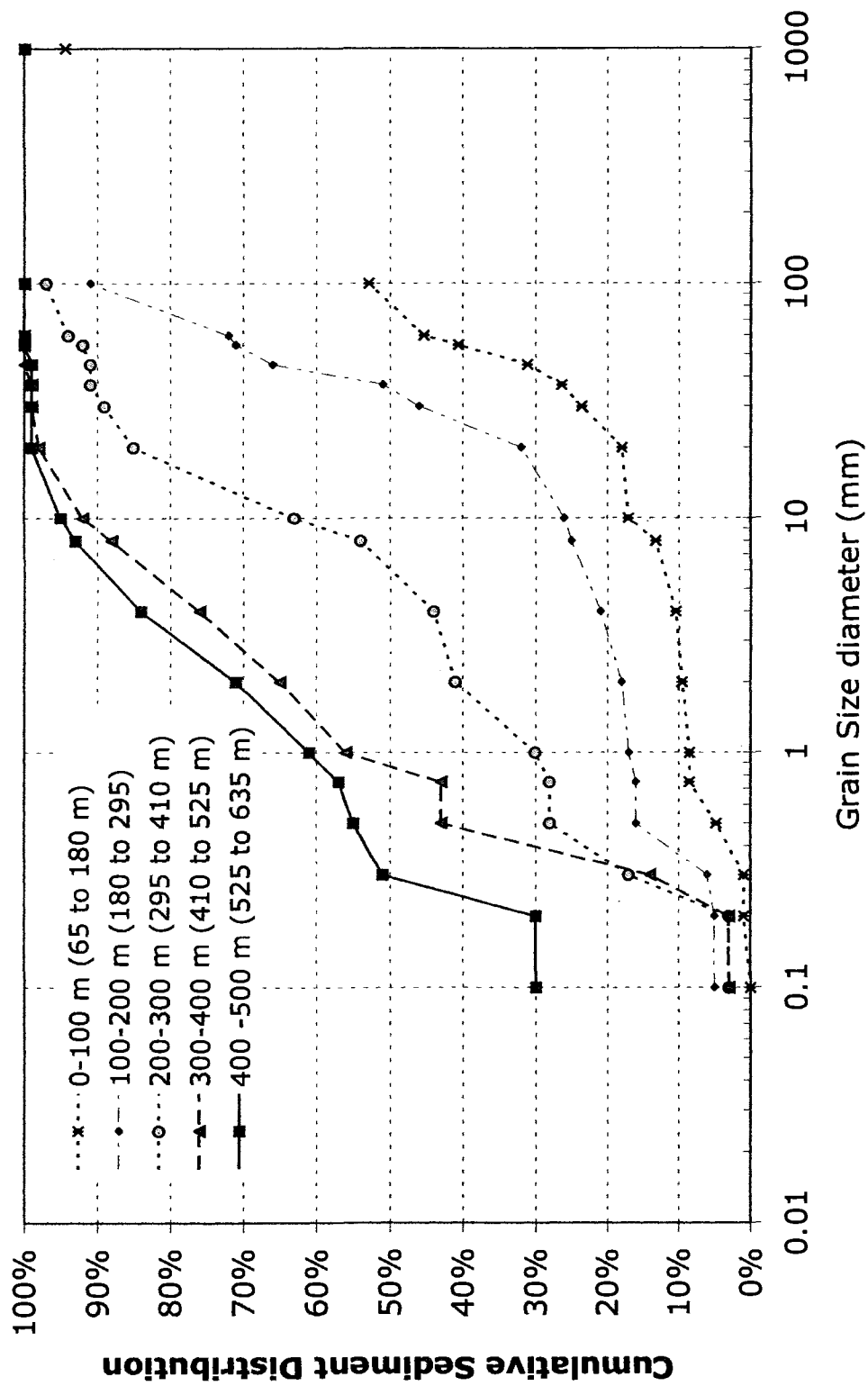


Figure 4-5 Pebble counts of streambed sediment along the study reach, Wednesday Hill Brook in Lee, NH

Numbers in parentheses are approximate FODTS cable station locations

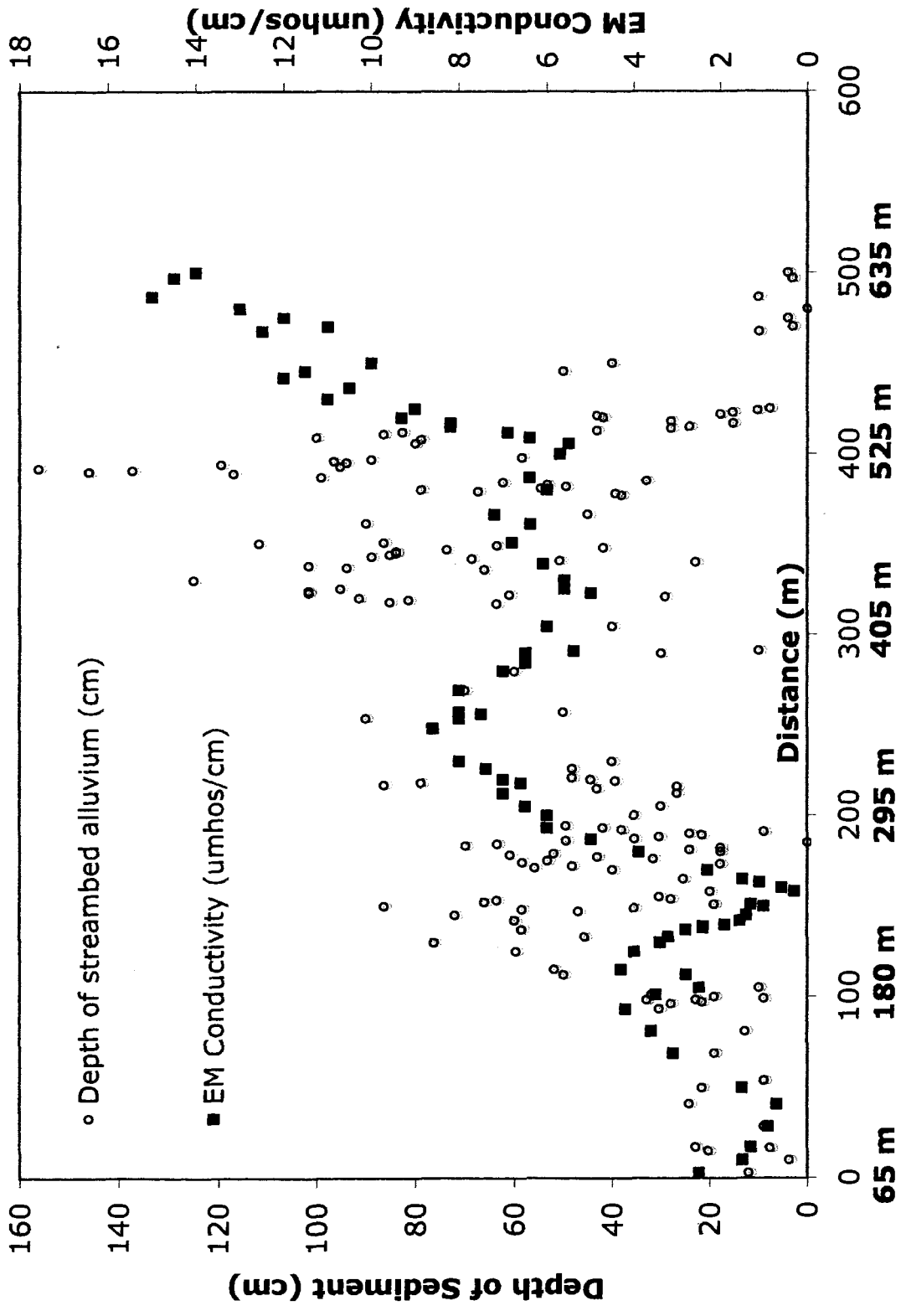
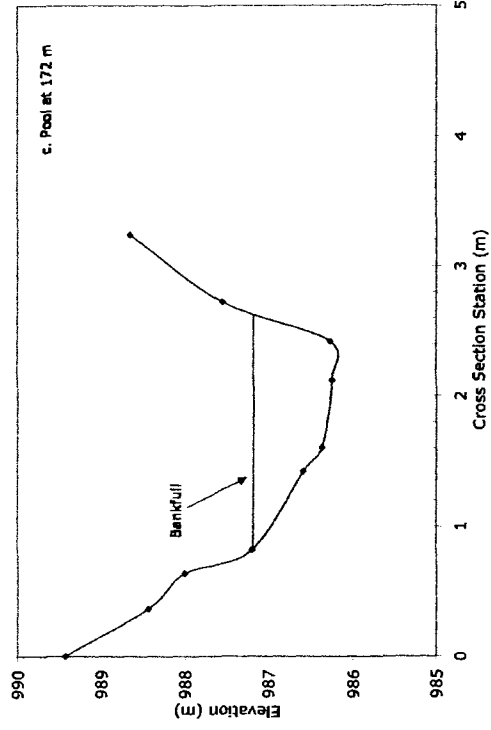
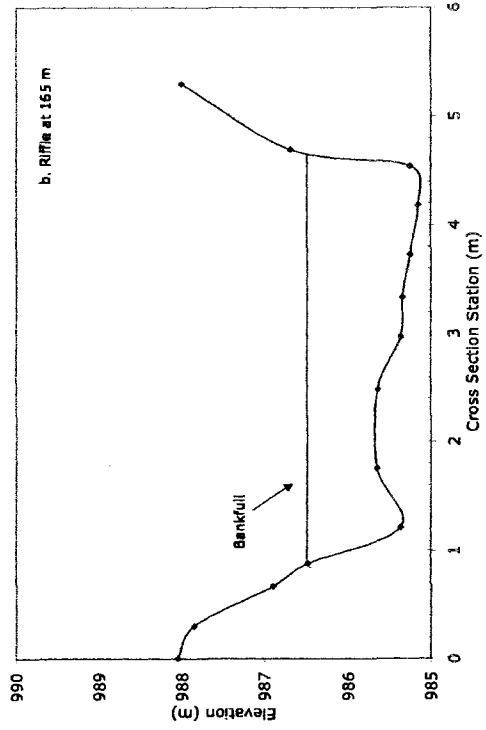
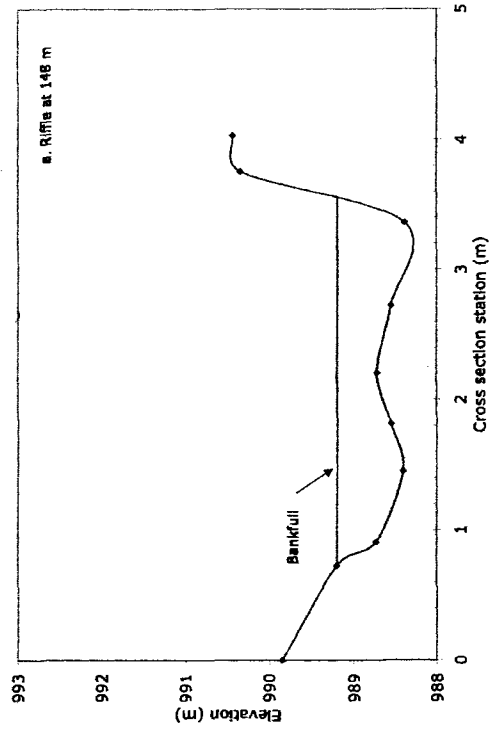


Figure 4-5 -Streambed electrical conductance and stream bed sediment depths, Wednesday Hill Brook in Lee, NH, numbers in bold on X axis are FODTS cable locations



Figures 4-7 a, b, c
Riffle and pool cross sections at 145, 165 and 172 m
Wednesday Hill Brook in Lee, NH

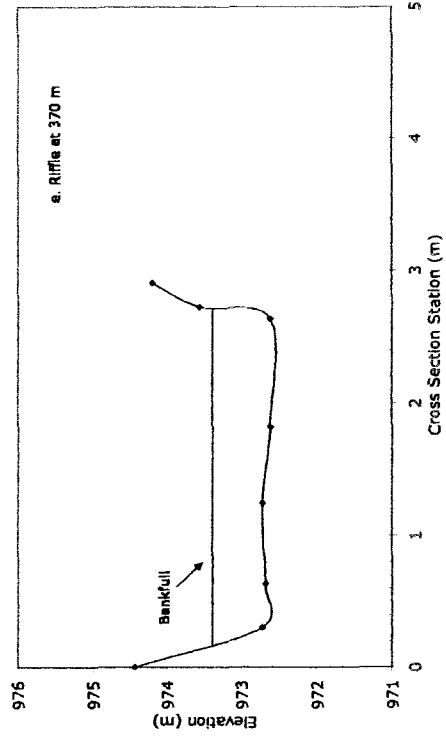
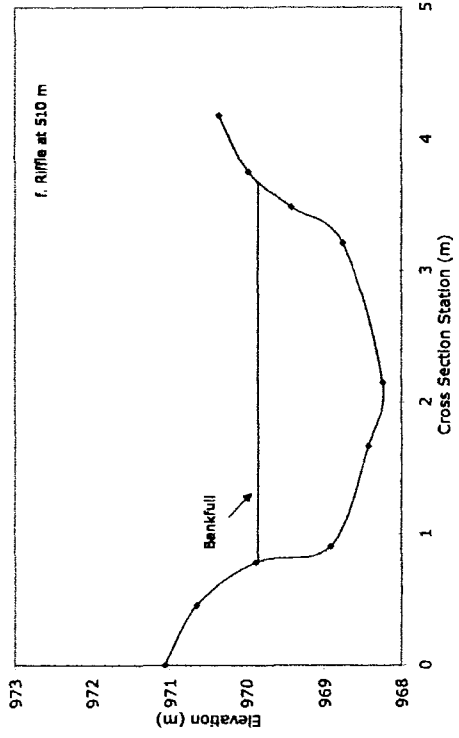
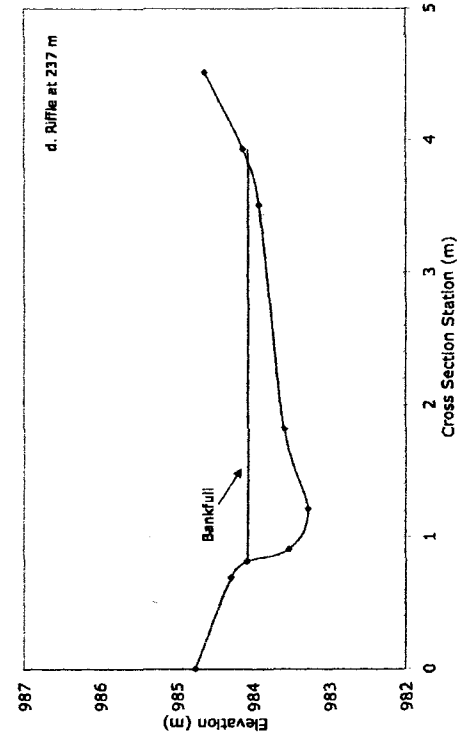


Figure 4-7 d, e & f
 Riffle cross sections at 237, 334 and 510 m
 Wednesday Hill Brook in Lee, NH

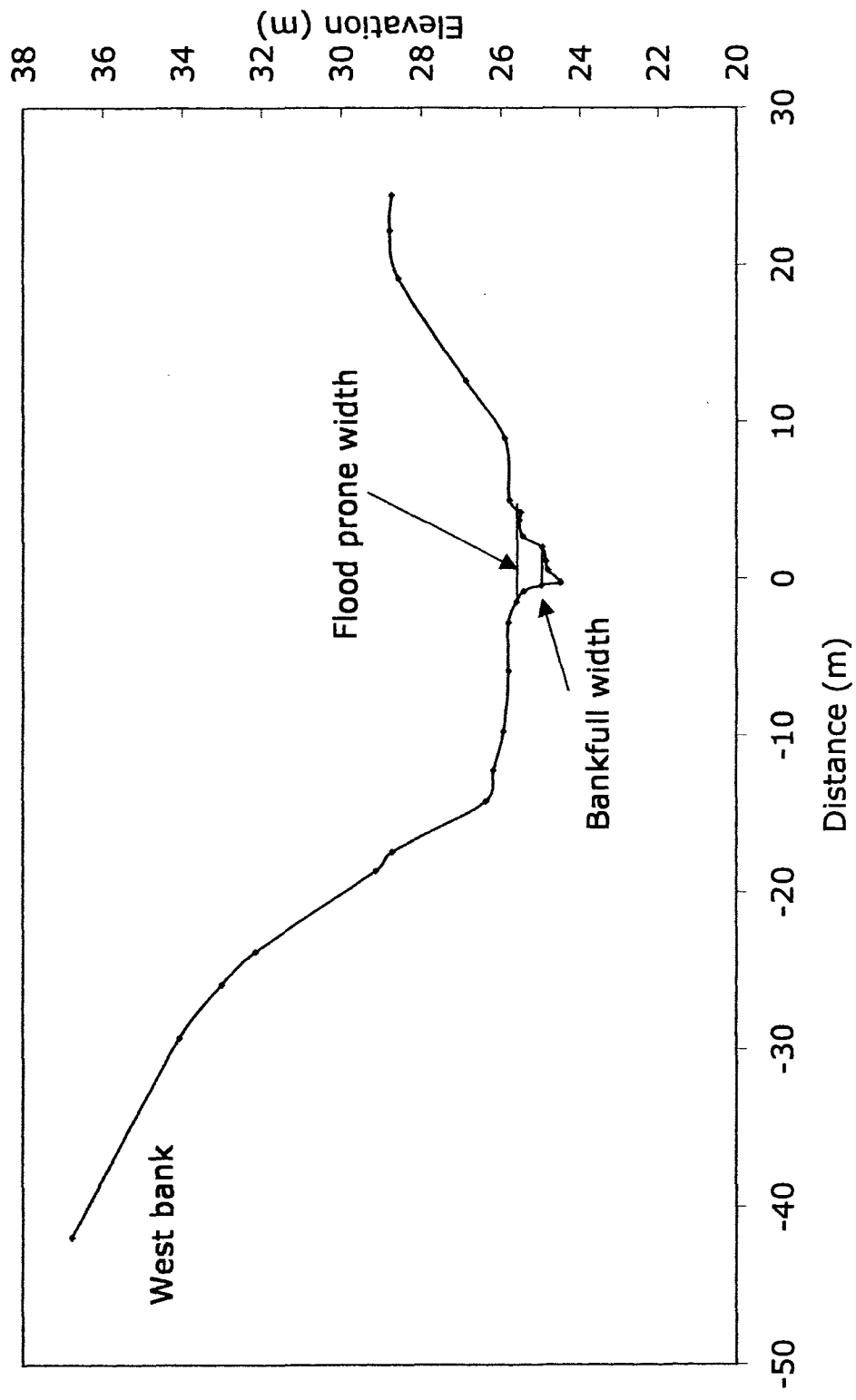


Figure 4-8 a Valley wide cross section at 200 m
 Wednesday Hill Brook in Lee, NH

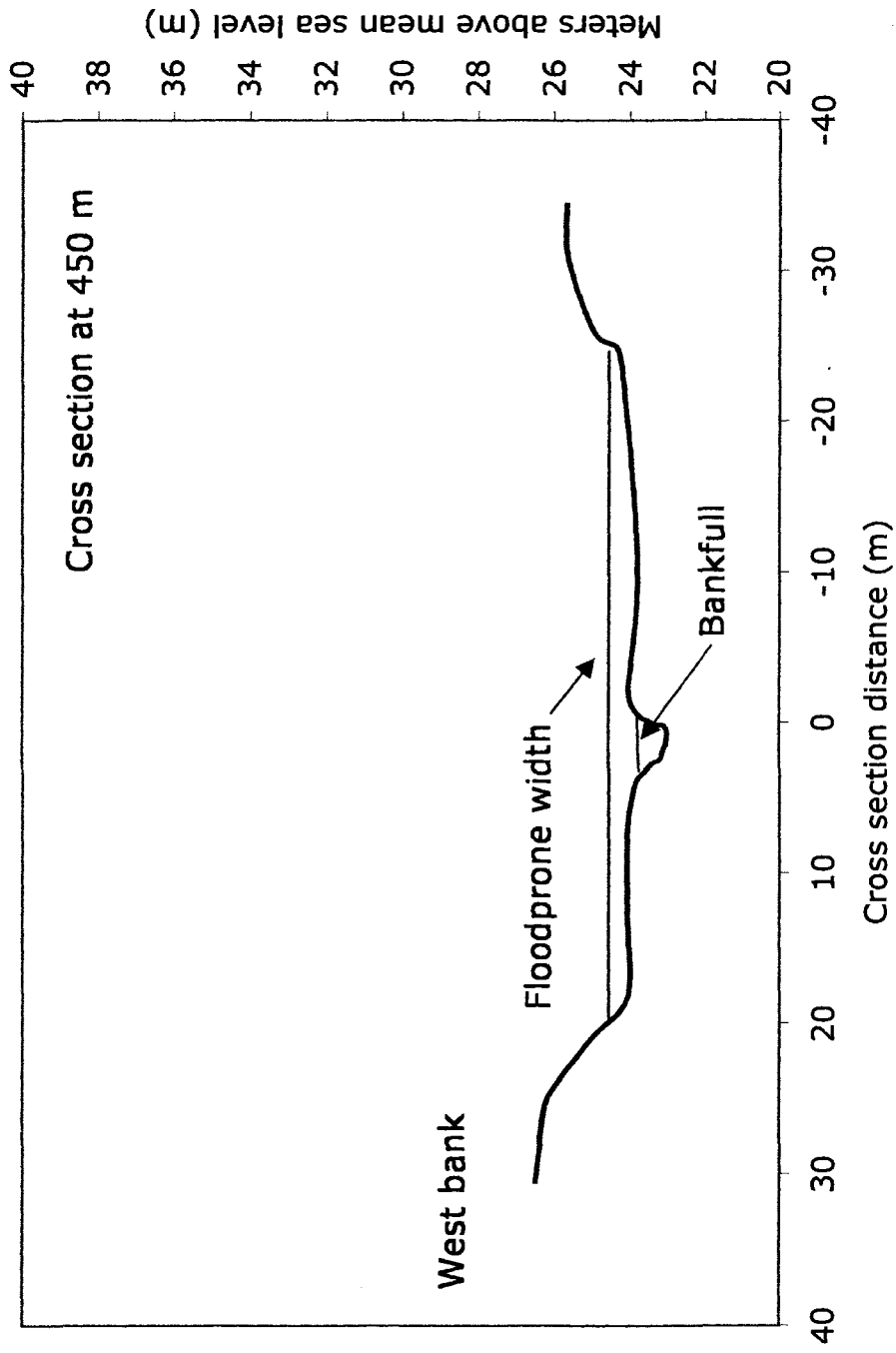


Figure 4-8 b Valley wide cross section at 450 m
 Wednesday Hill Brook in Lee, NH

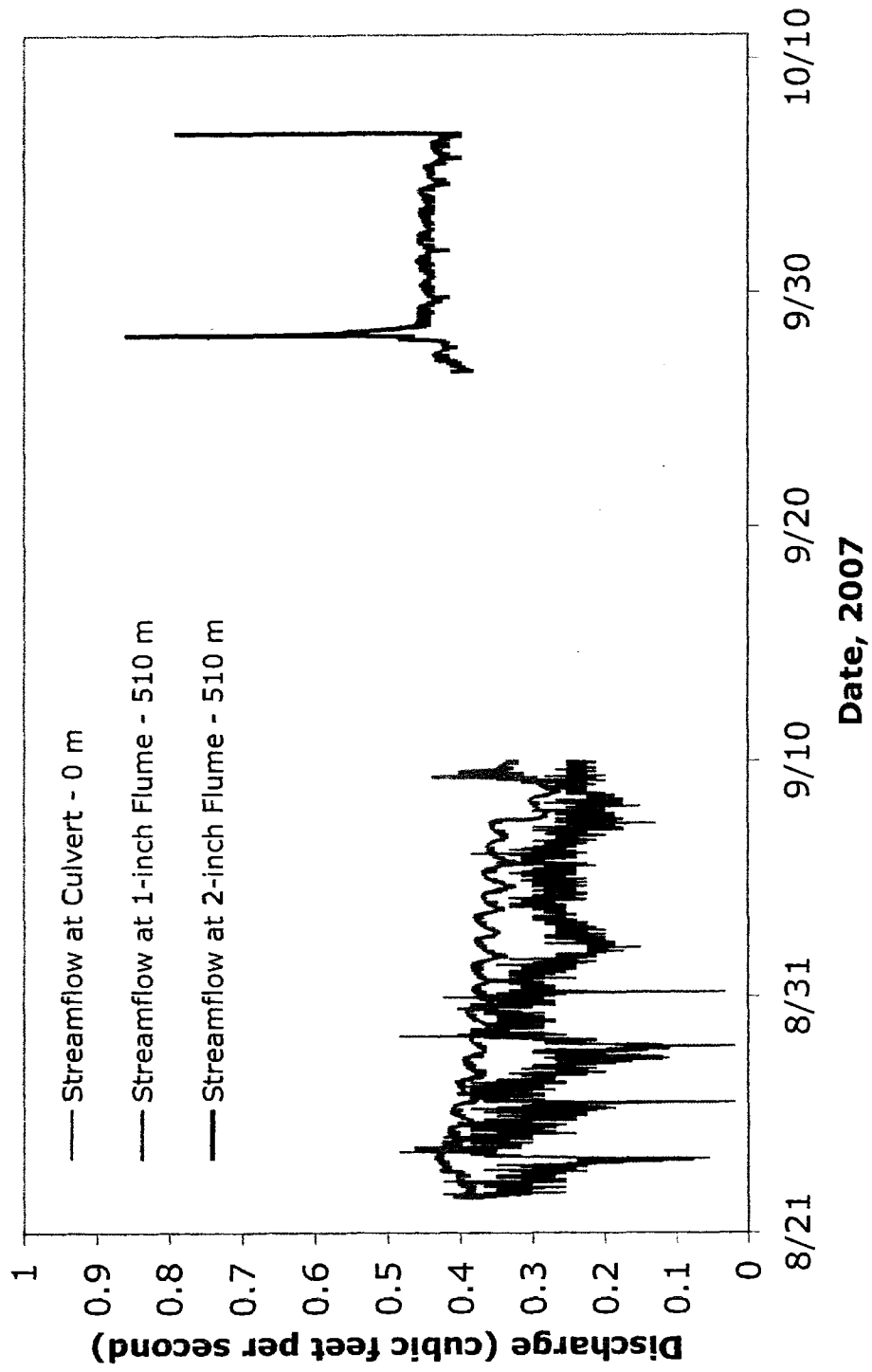


Figure 4-9 Stream flow measurements on study reach August to October 2007
 Wednesday Hill Brook in Lee, NH

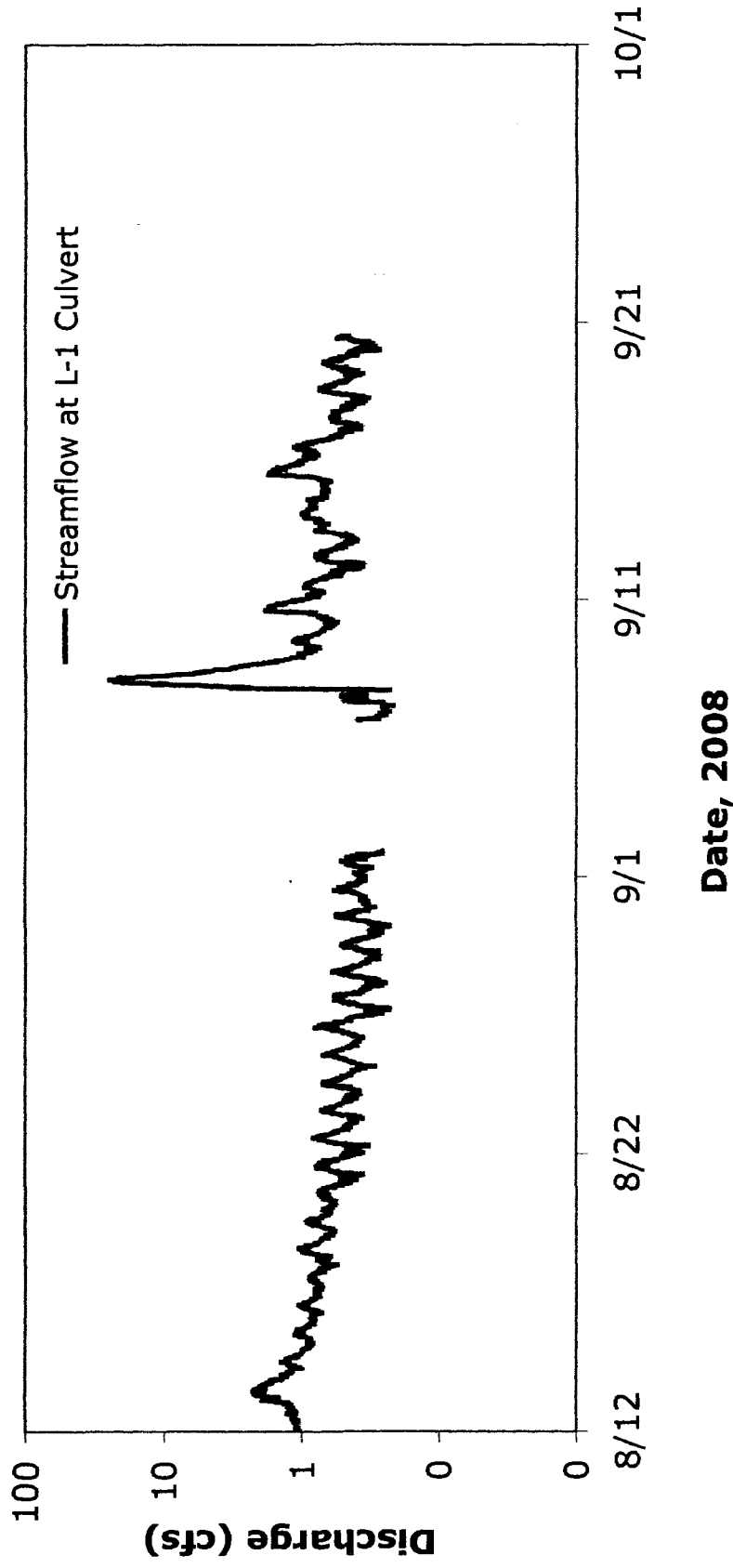


Figure 4-10 Stream flow measurements on study reach August to October 2008
 Wednesday Hill Brook in Lee, NH

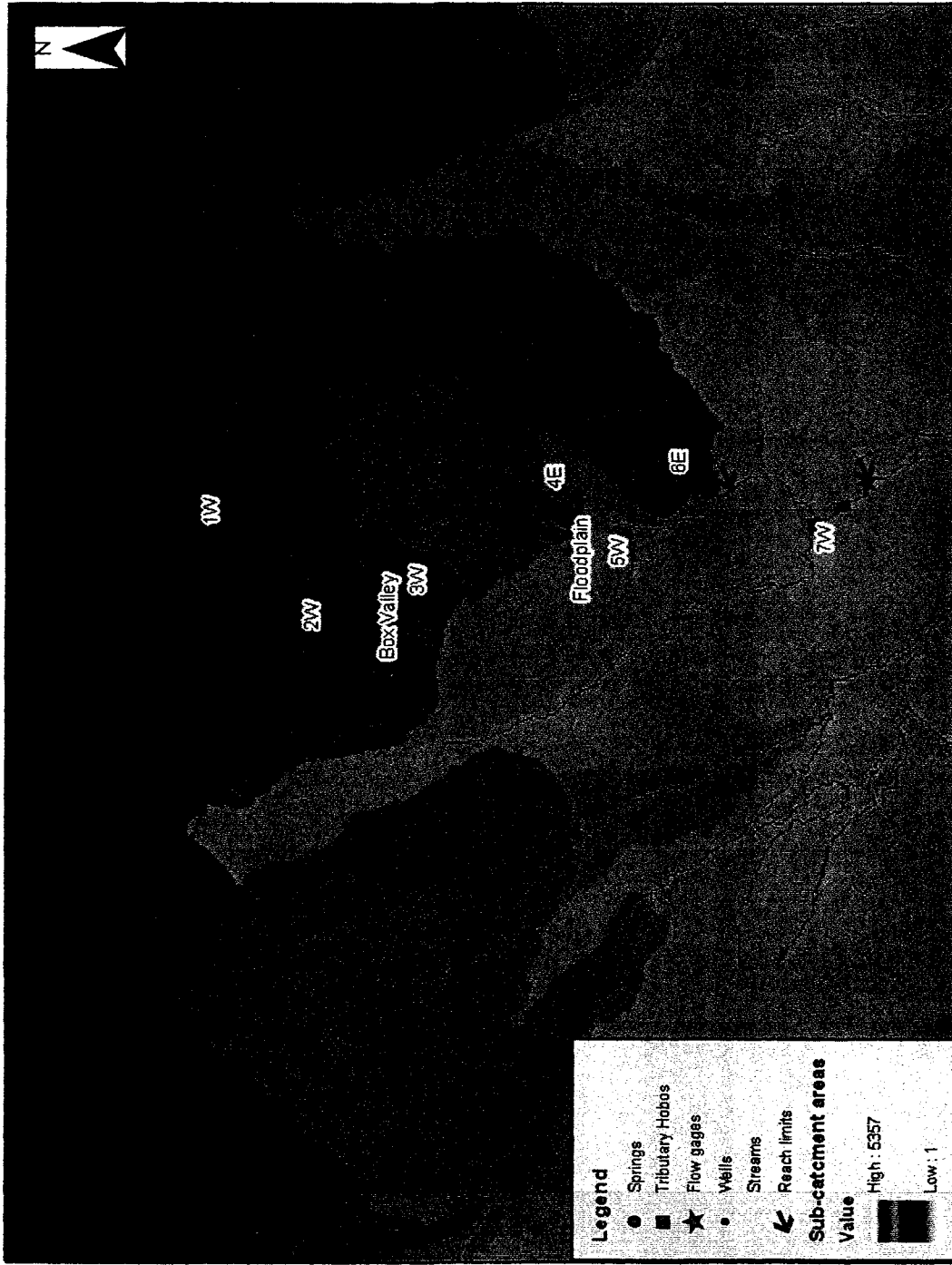


Figure 4-11 Sub catchments and streams Wednesday Hill Brook in Lee, NH Topography, catchments and drainage developed from LiDAR imagery – National Center for Aerial Laser Mapping

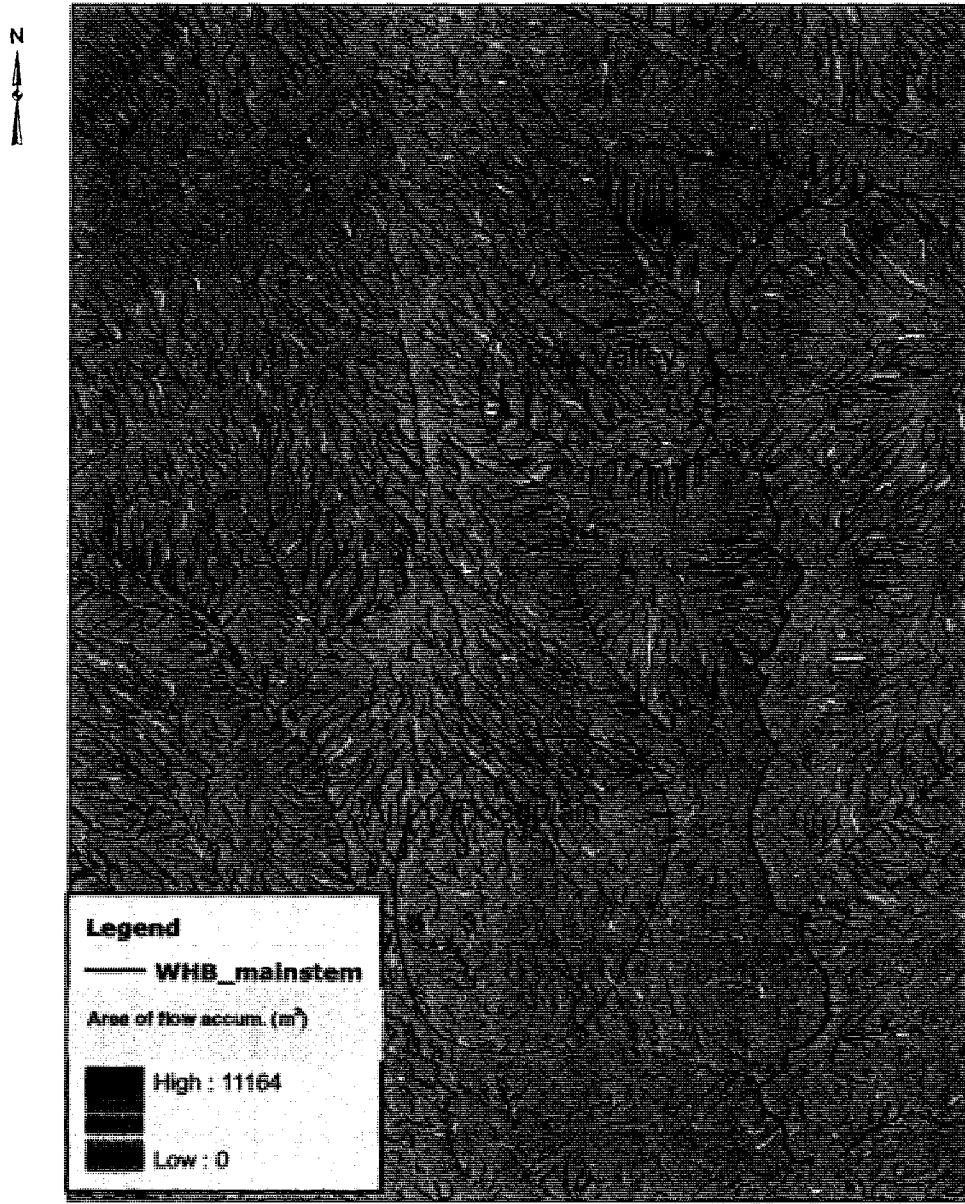


Figure 4-12 Streamflow accumulation - unfilled DEM
Wednesday Hill Brook in Lee, NH
Drainage developed from LiDAR imagery – National Center for Aerial Laser Mapping

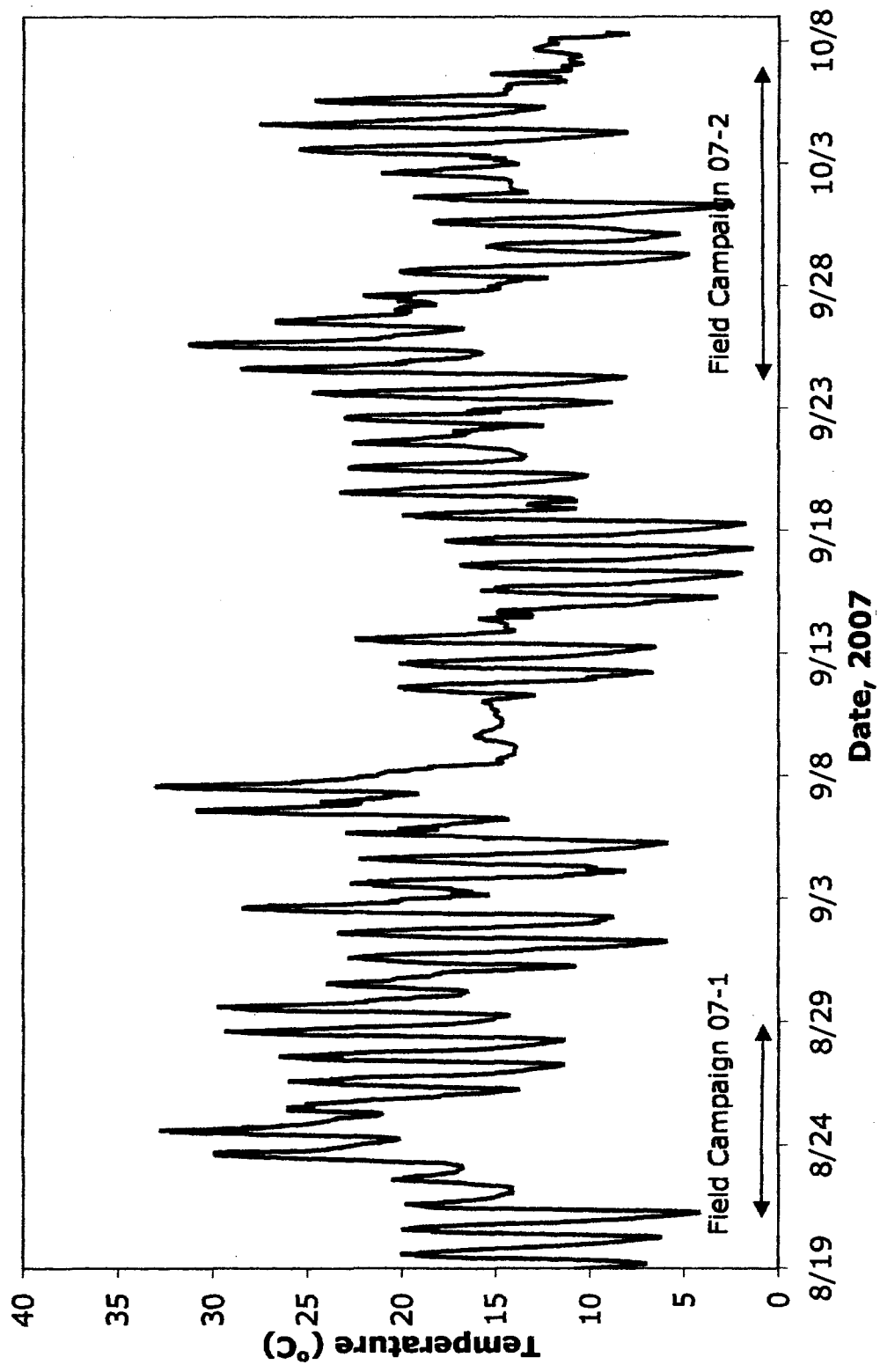


Figure 4-13 a Air Temperature during field campaigns -- August to October 2007
 Wednesday Hill Brook in Lee, NH

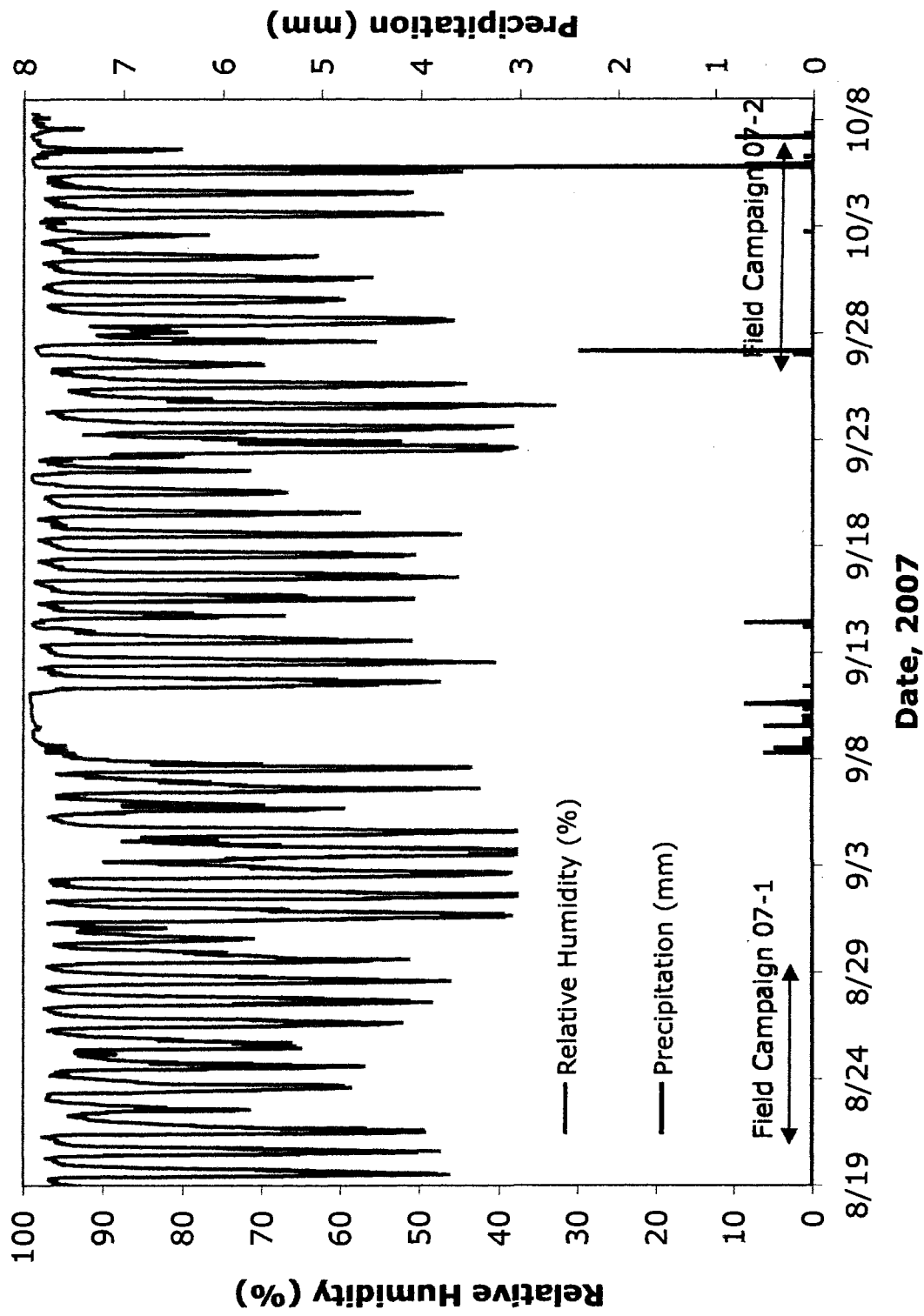


Figure 4-13 b Precipitation and relative humidity during field campaigns – August to October 2007
 Wednesday Hill Brook in Lee, NH

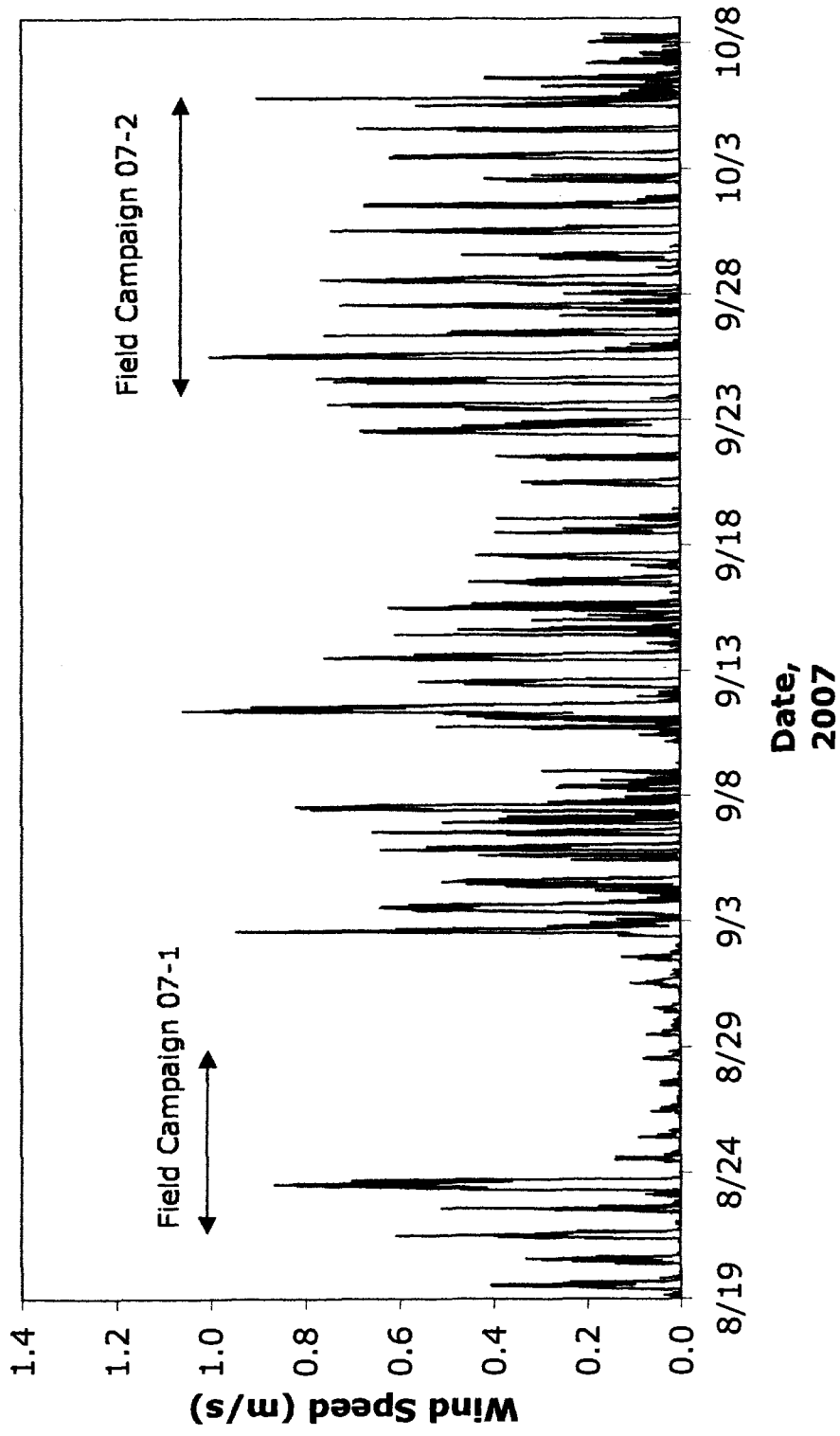


Figure 4-13c Wind speeds during field campaigns – August to October 2007
 Wednesday Hill Brook in Lee, NH

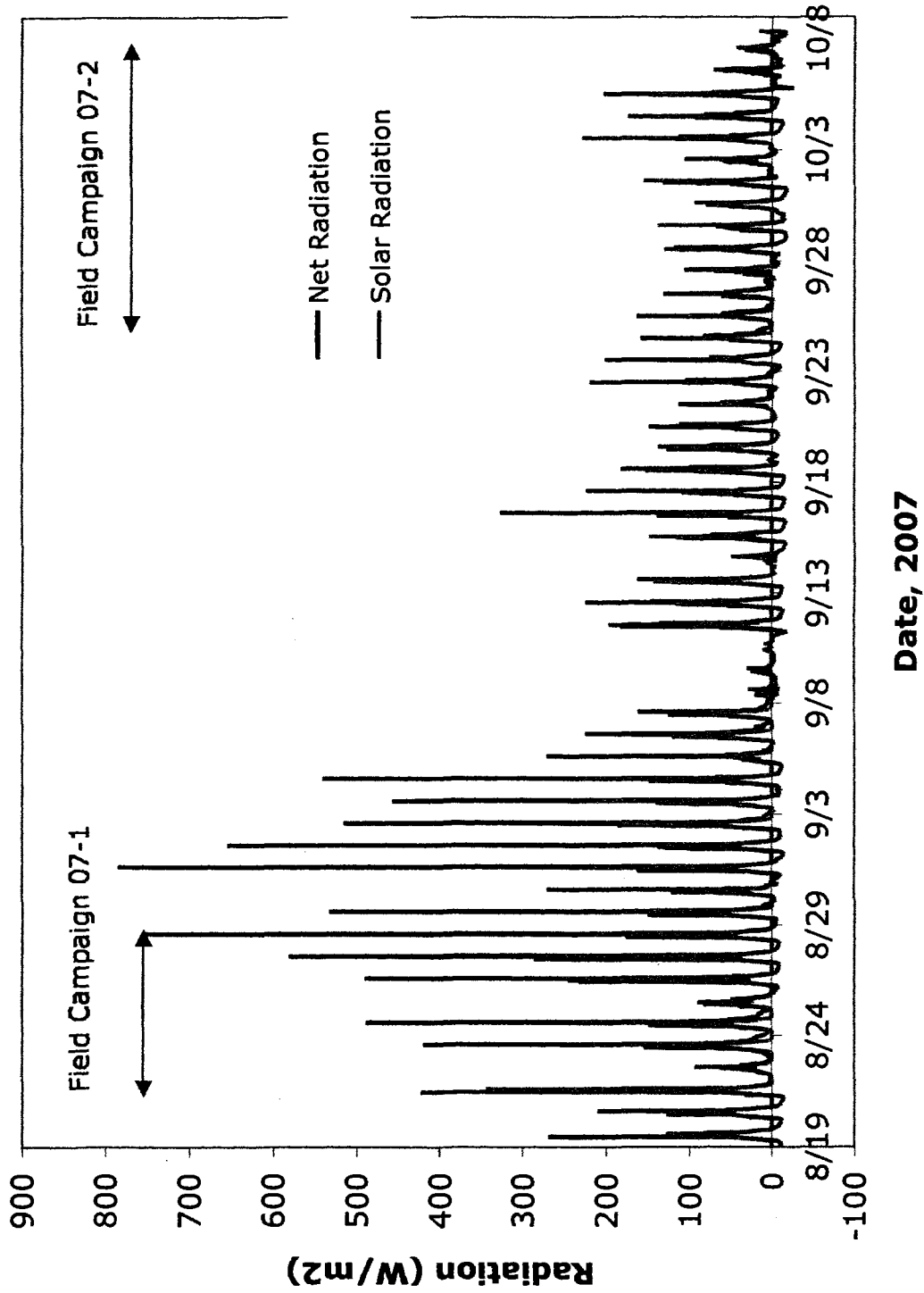


Figure 4-13 d Solar radiation and net radiation during field campaigns – August to October 2007
 Wednesday Hill Brook in Lee, NH

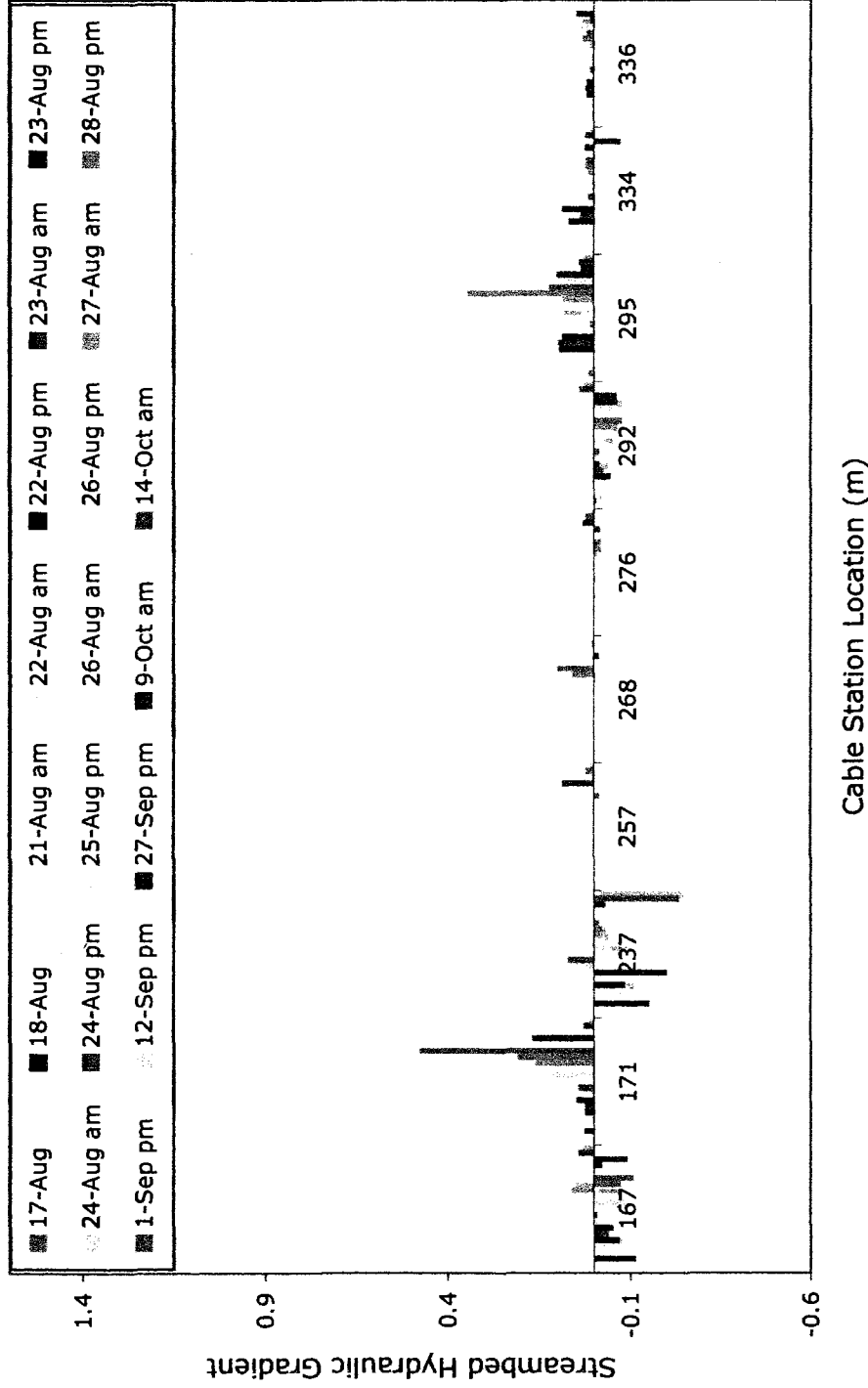


Figure 4-14 a Vertical hydraulic gradients at mini-piezometers 167 to 336 m, August to October 2007 Wednesday Hill Brook in Lee, NH

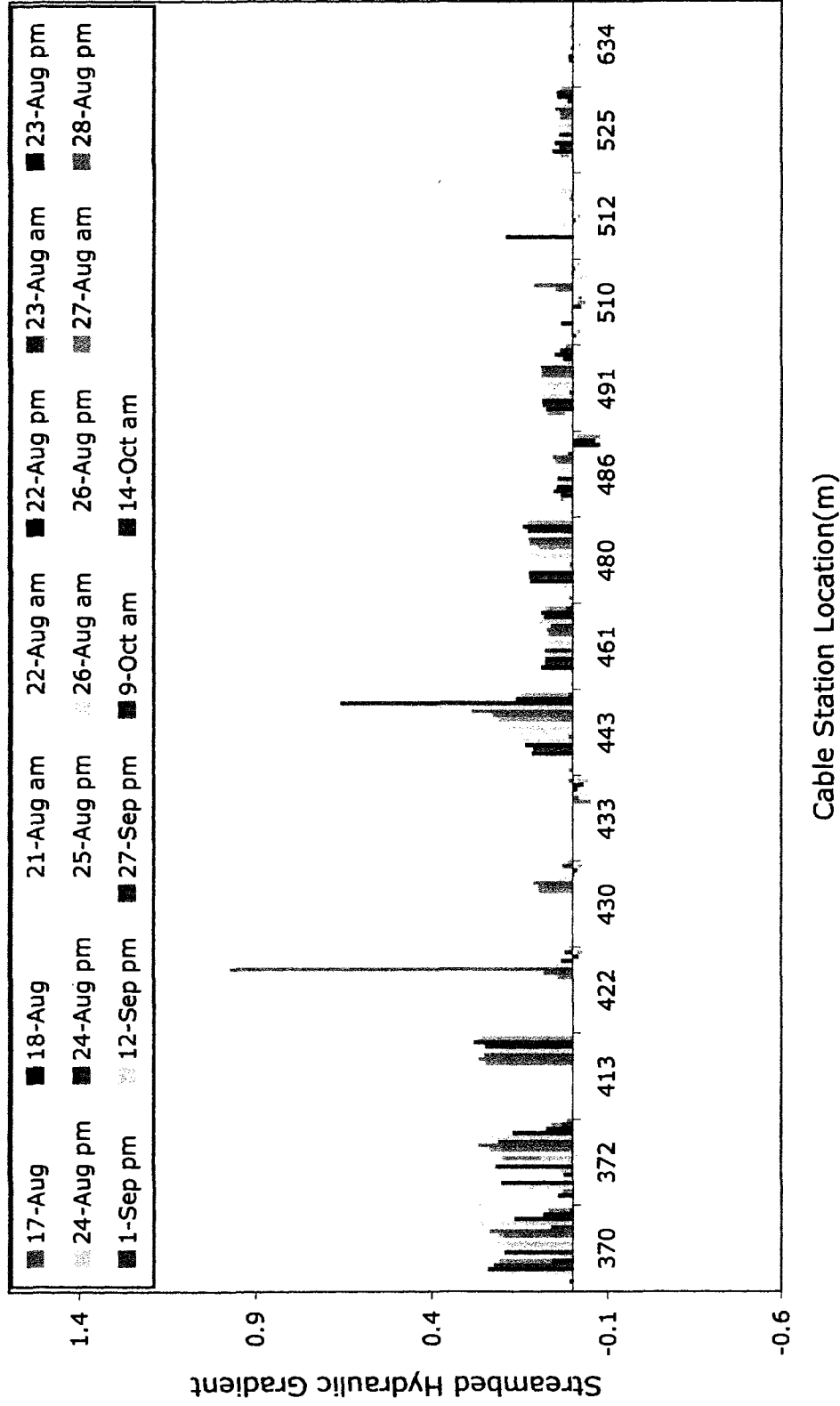


Figure 4-14 b Vertical hydraulic gradients at mini-piezometers 167 to 336 m, August to October 2007
 Wednesday Hill Brook in Lee, NH

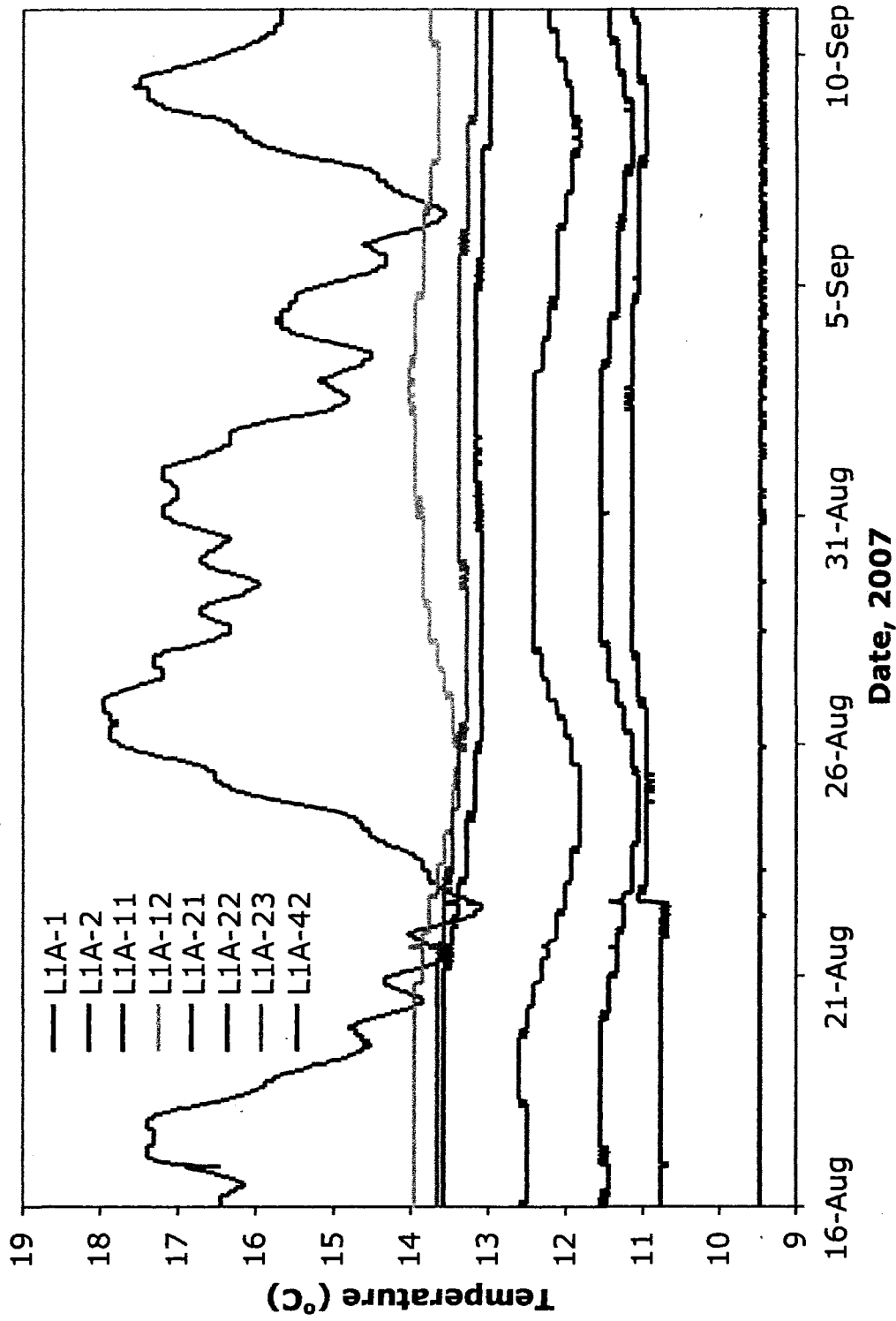


Figure 4-15 Monitoring well field temperatures – August and September 2007
 Wednesday Hill Brook in Lee, NH

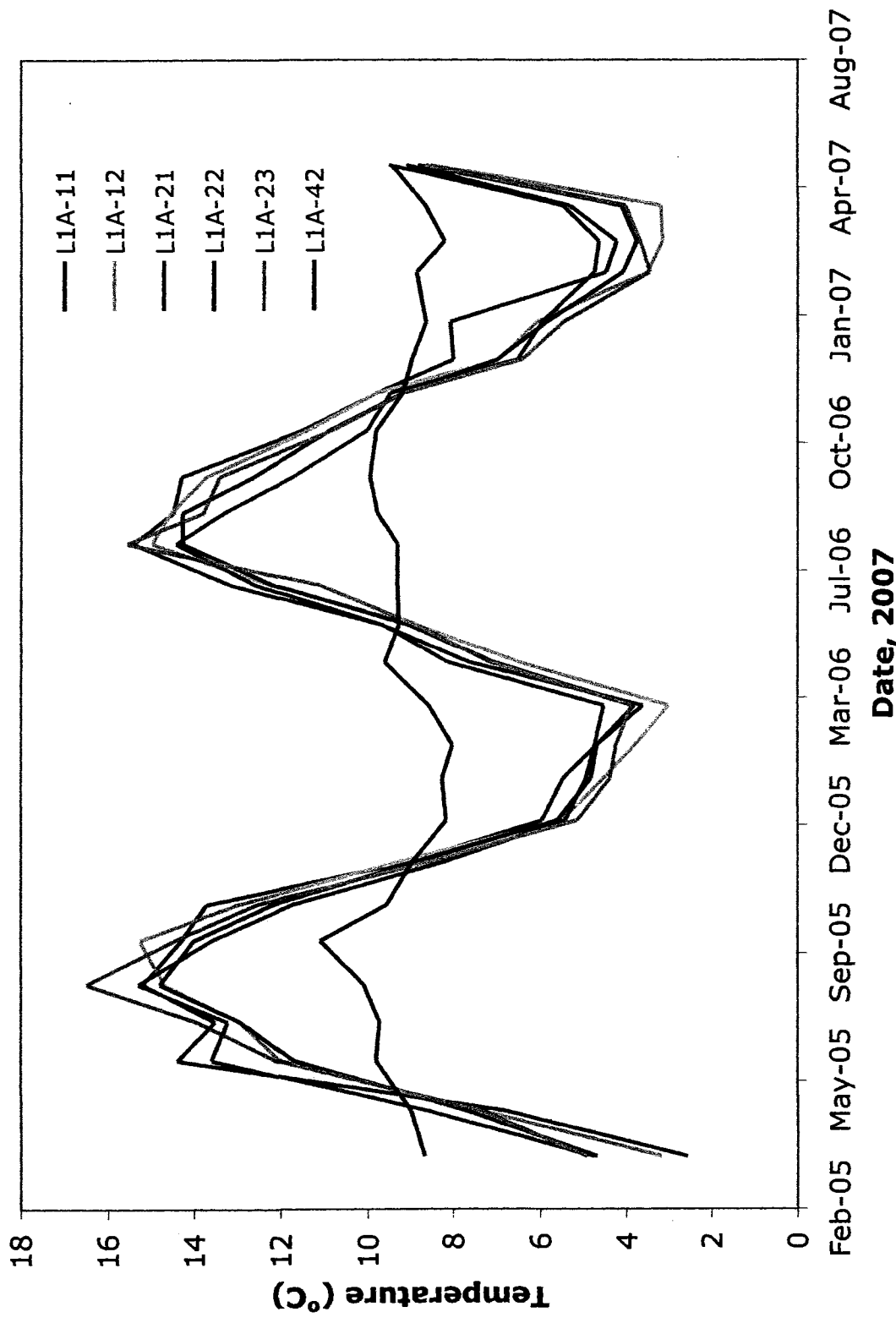


Figure 4-16 Monitoring well field temperatures – 2005 to 2007
 Wednesday Hill Brook in Lee, NH

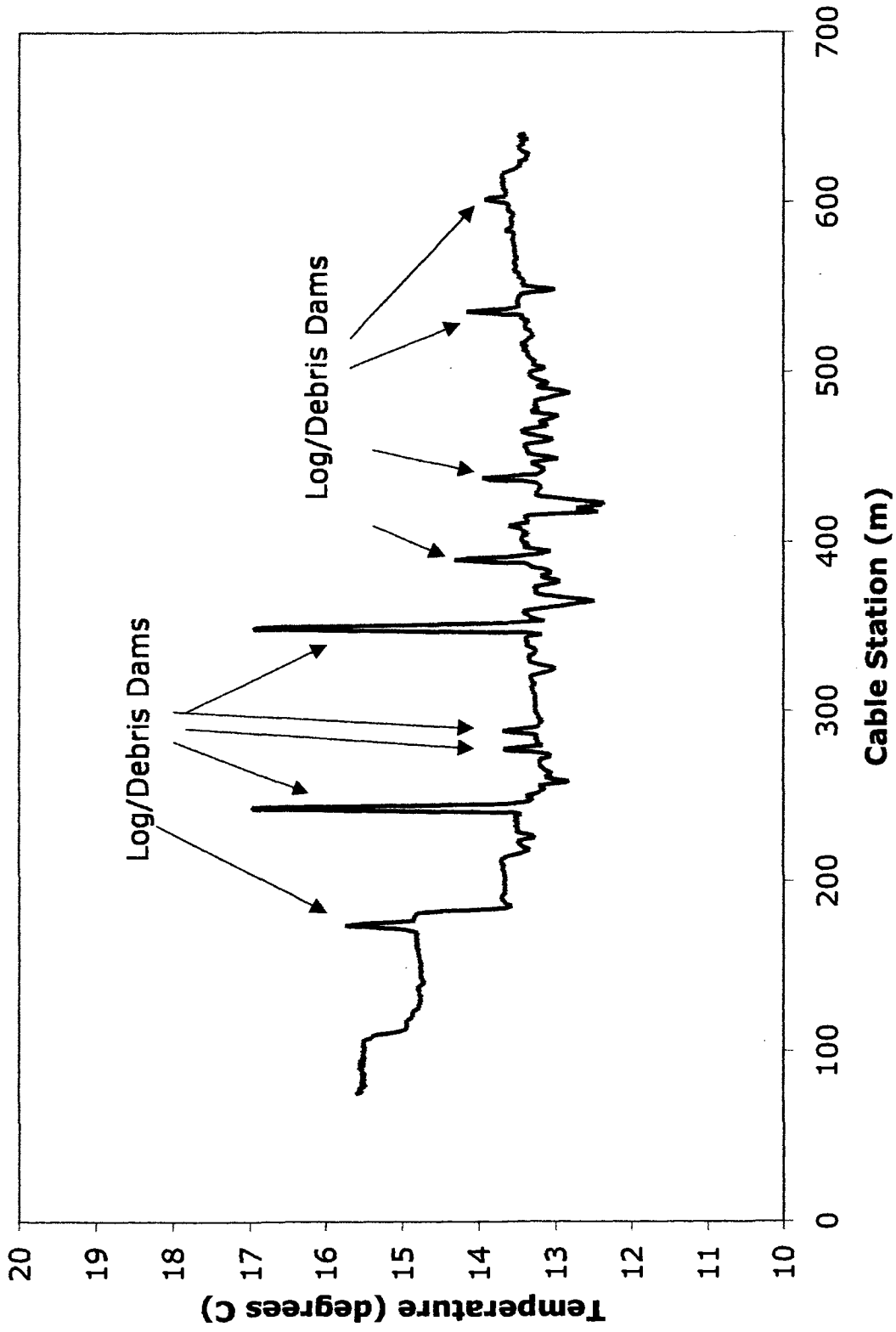


Figure 4-17 Average FODTS temperature measurements along the study reach showing log dam temperature spikes, August 22 to August 29, 2007 Wednesday Hill Brook in Lee, NH

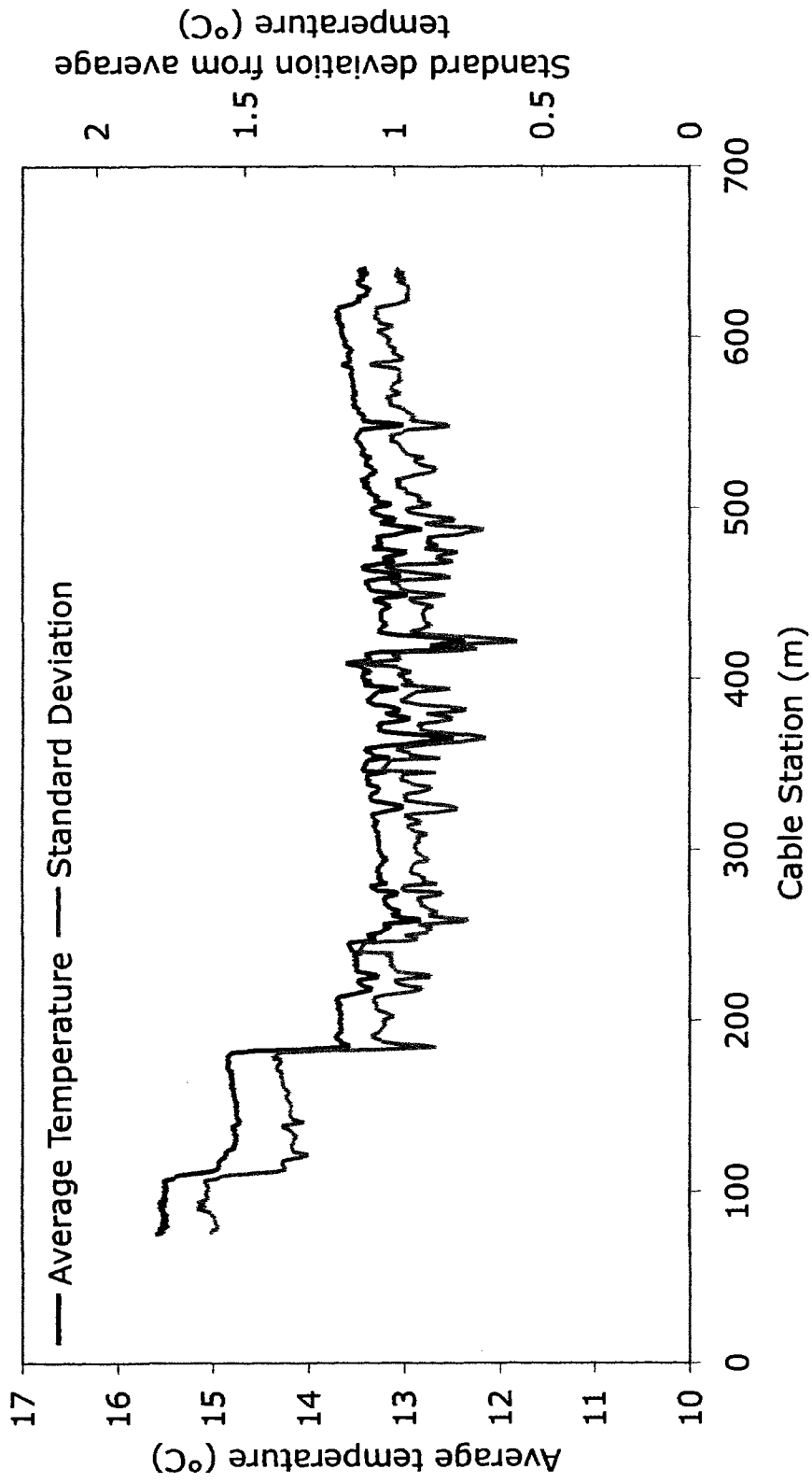


Figure 4-18 Average FODTS temperature measurements and standard deviations along study reach -- edited August 22 to August 29, 2007 Wednesday Hill Brook in Lee, NH

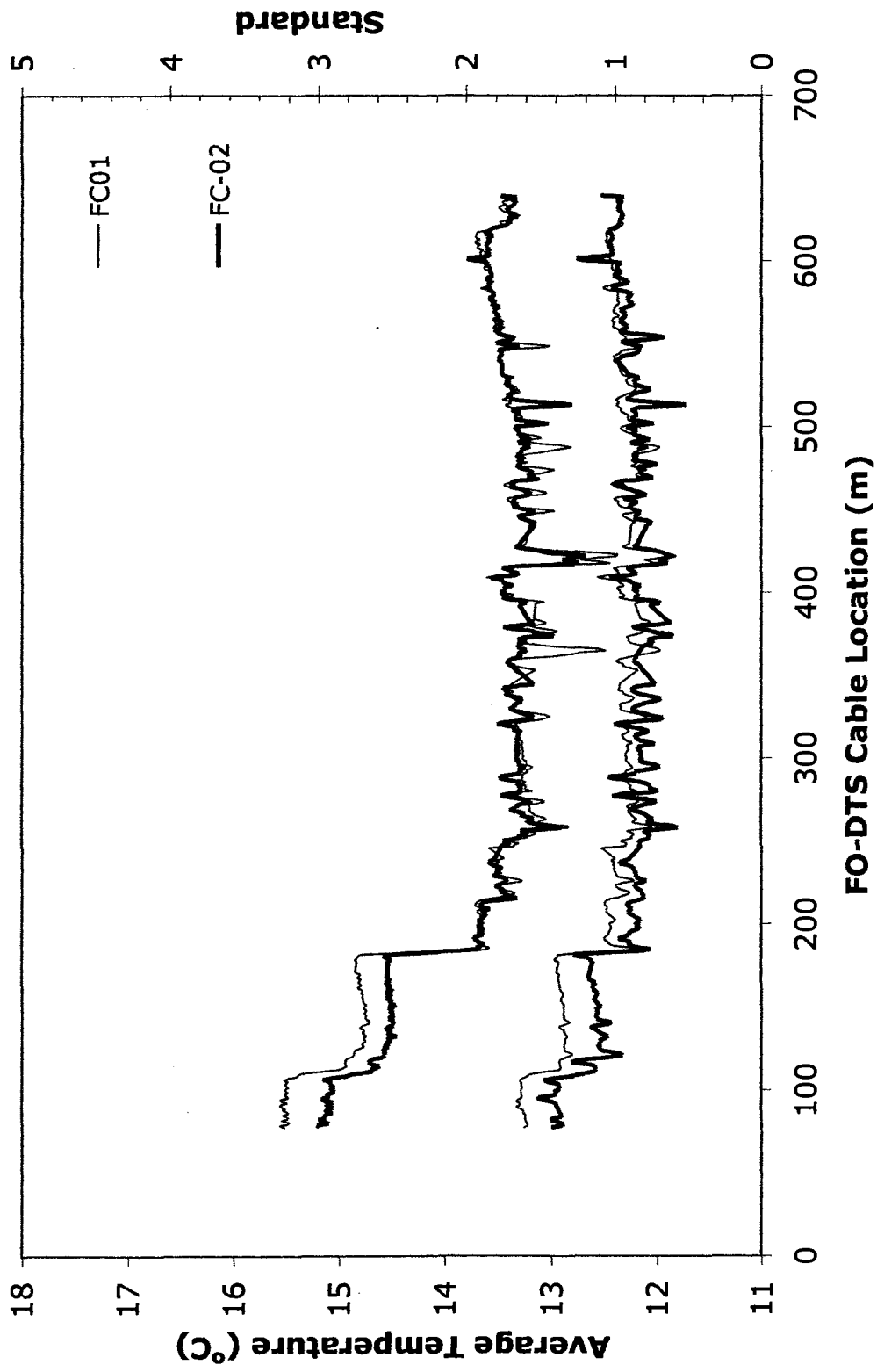


Figure 4-19 Average FODTS temperature measurements (top) and standard deviations (bottom) from both field campaigns along study reach – edited, August to October 2007, Wednesday Hill Brook in Lee, NH

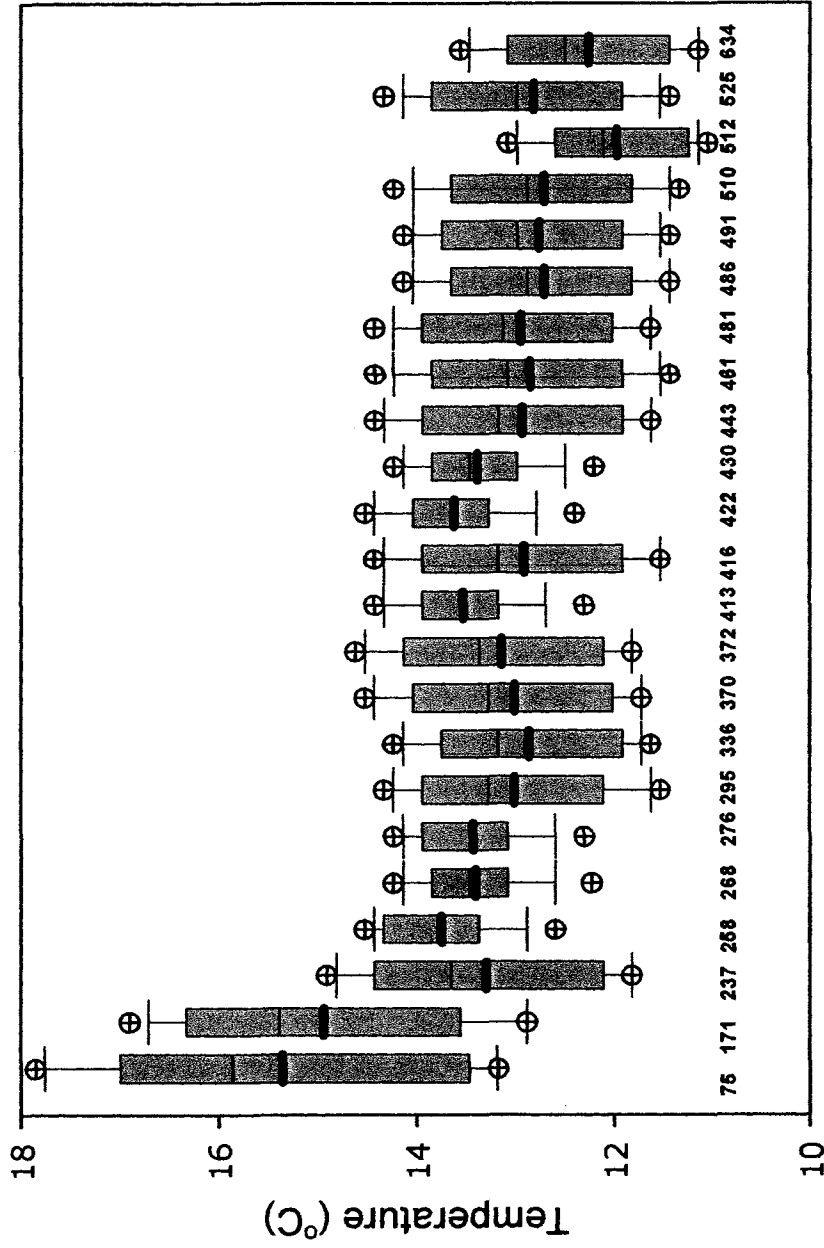


Figure 4-20 Box and whisker plots of stream temperature measurements 75 m to 634 m August to September 2007, Wednesday Hill Brook in Lee, NH

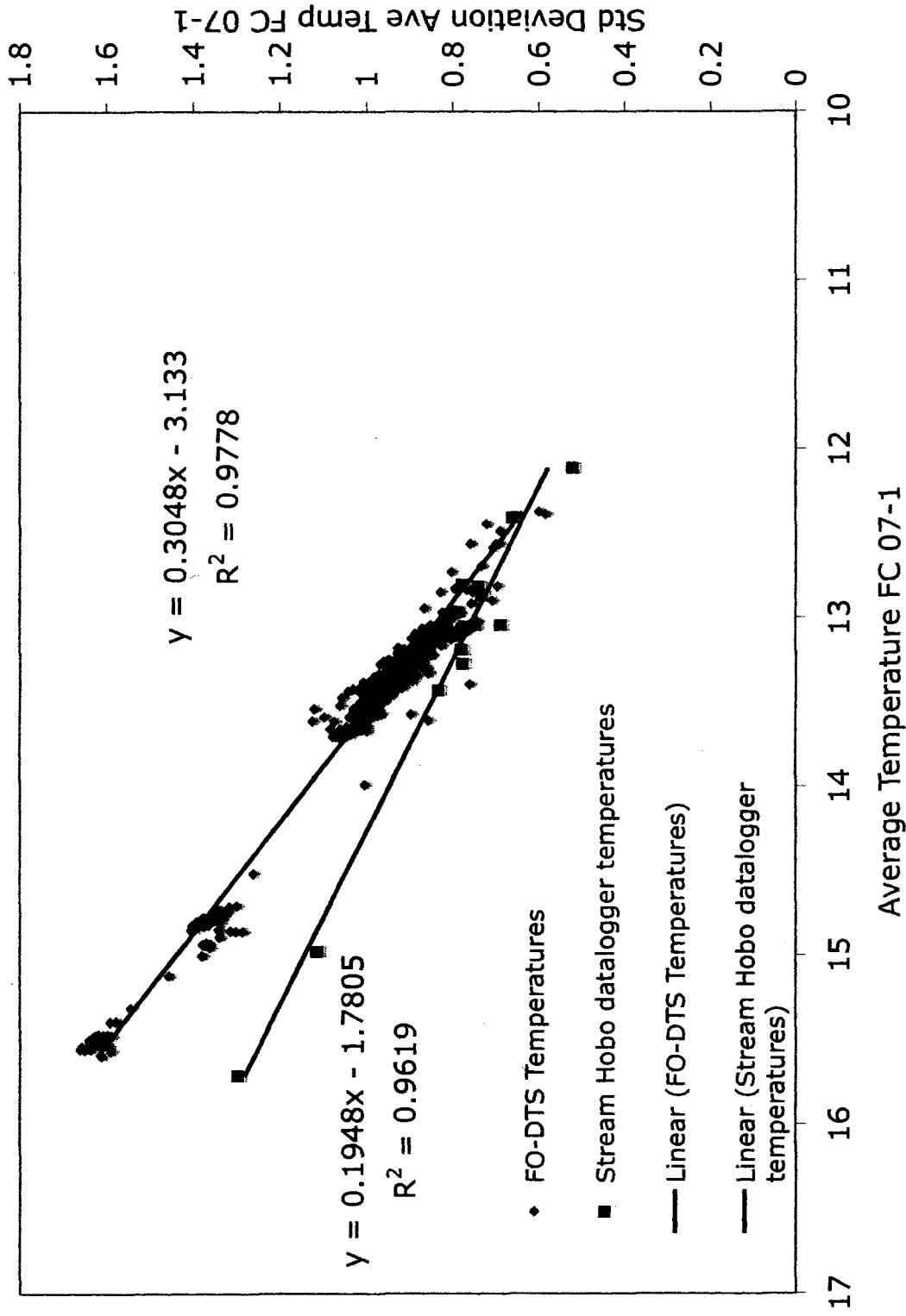


Figure 4-21 Average temperature and standard deviation for FODTS mean temperatures and stream Hobo mean temperatures, August 22 to 29, 2007, Wednesday Hill Brook in Lee, NH

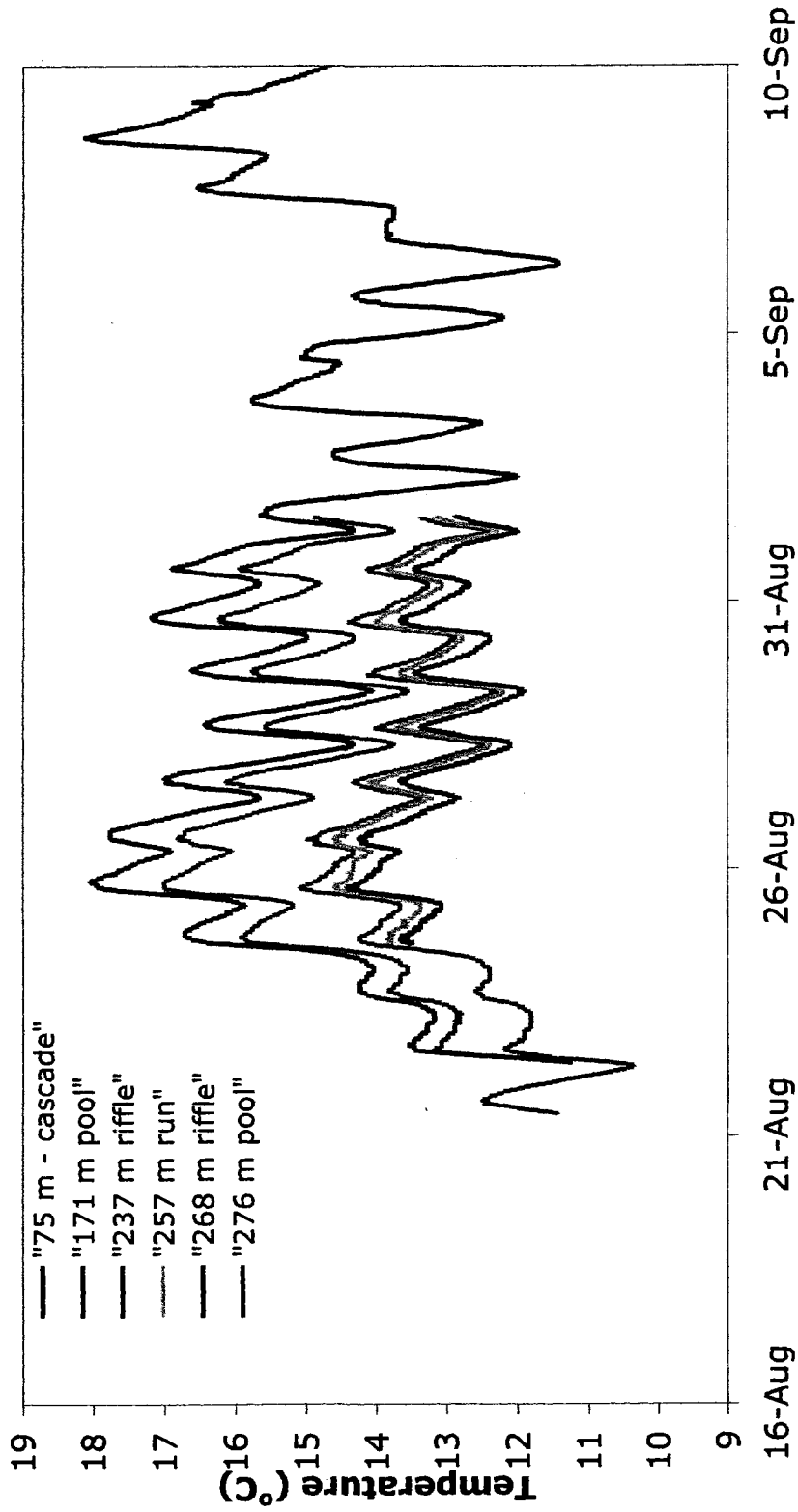


Figure 4-22 Stream temperatures in the Upper study reach 75 to 276 m. August to September 2007, Wednesday Hill Brook in Lee, NH

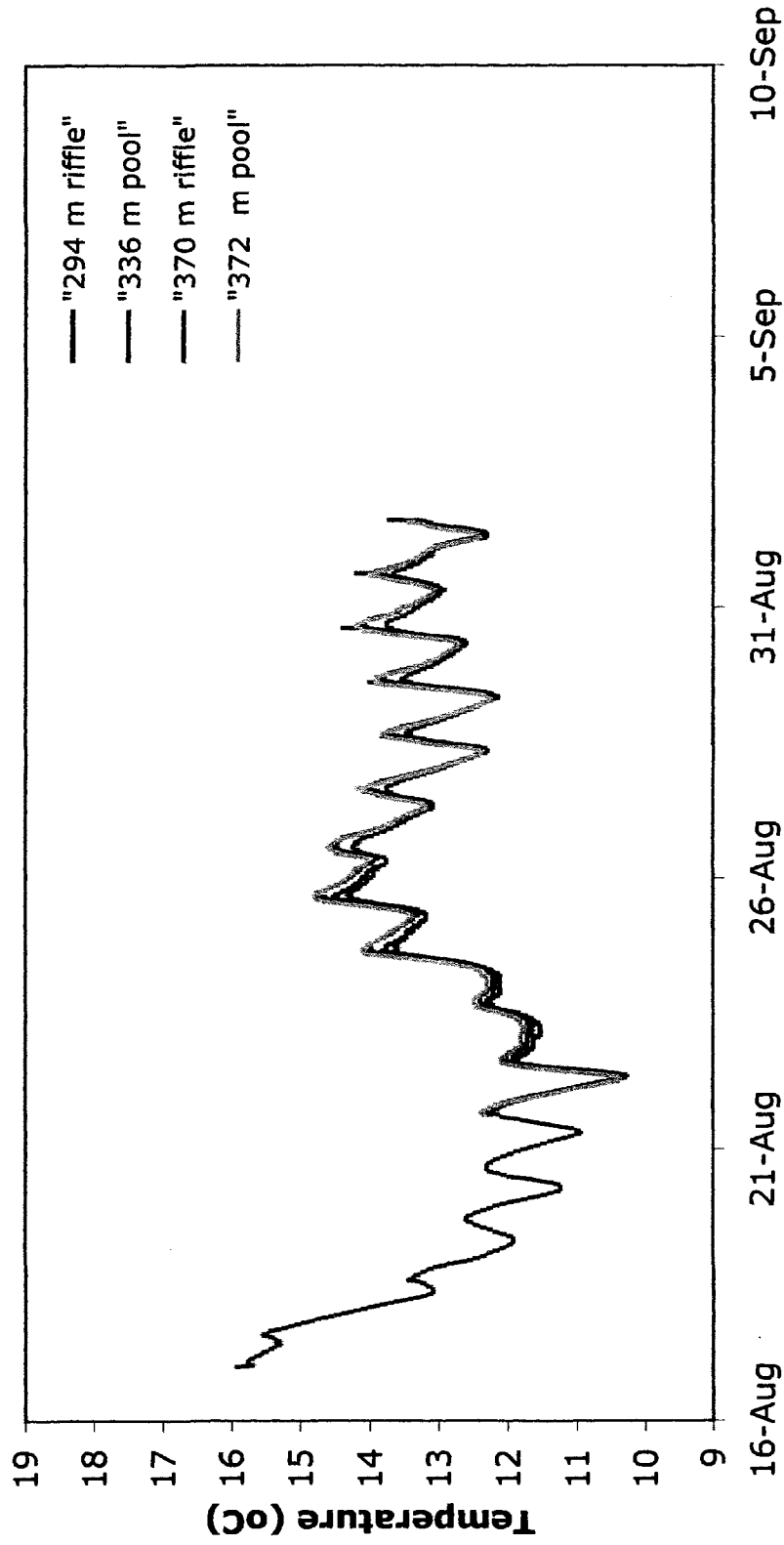


Figure 4-23 Stream temperatures in the middle study reach 293 to 372 m August to September 2007, Wednesday Hill Brook in Lee, NH

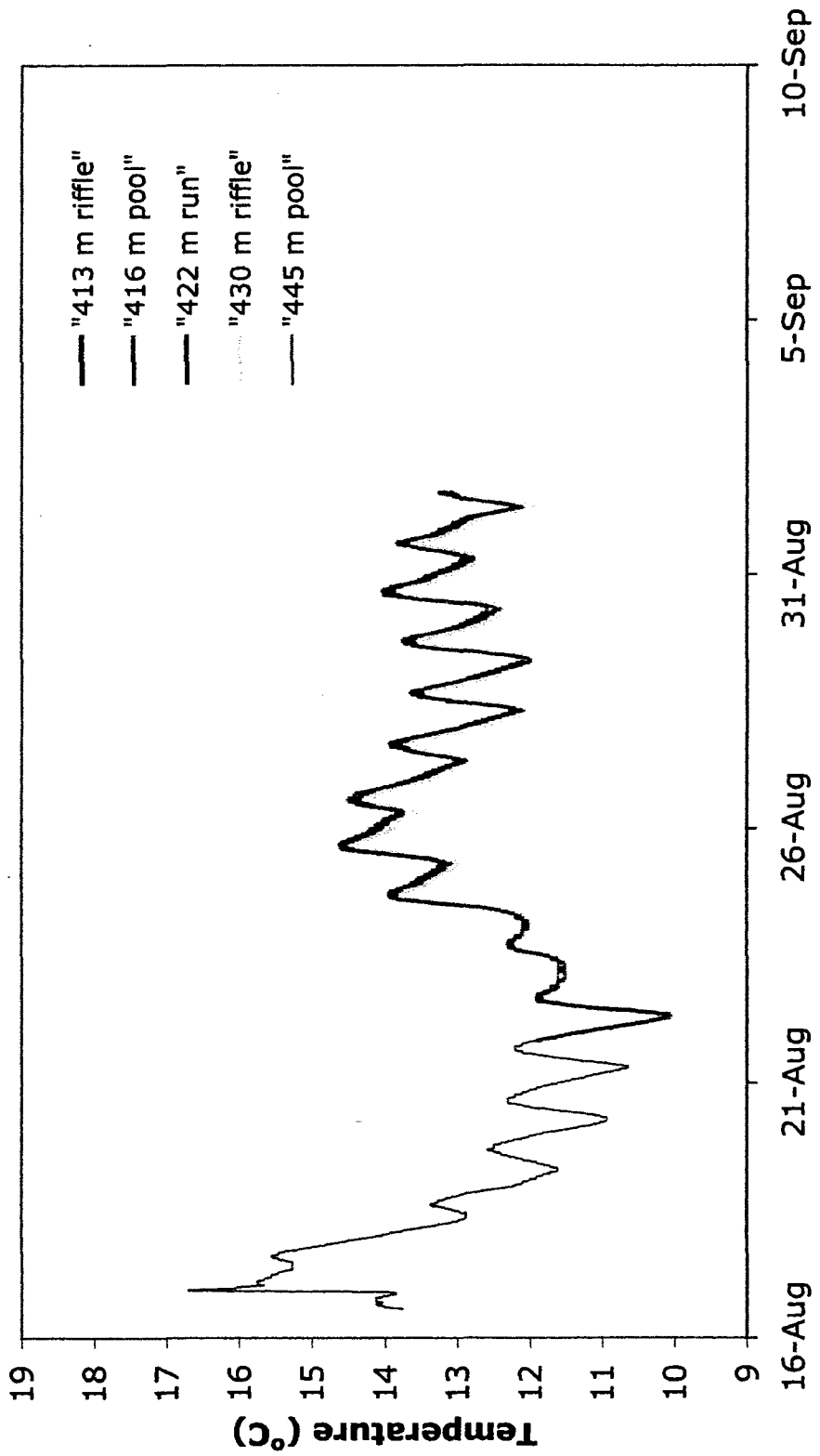


Figure 4-24 Stream temperature measurements from the middle study reach 413 to 445 m August to September 2007, Wednesday Hill Brook in Lee, NH

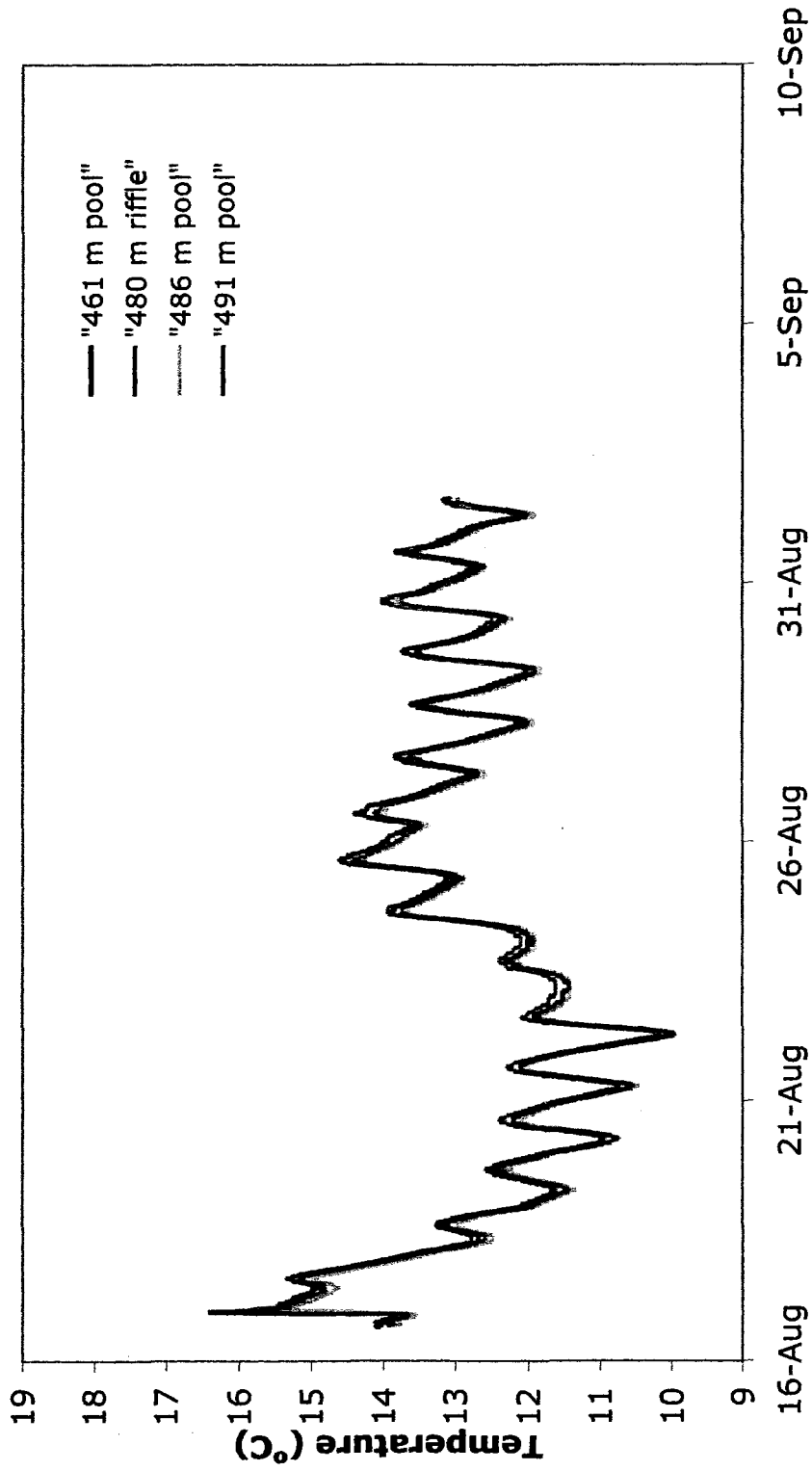


Figure 4-25 Stream temperature measurements in the lower study reach 461 to 491 m August to September 2007, Wednesday Hill Brook in Lee, NH

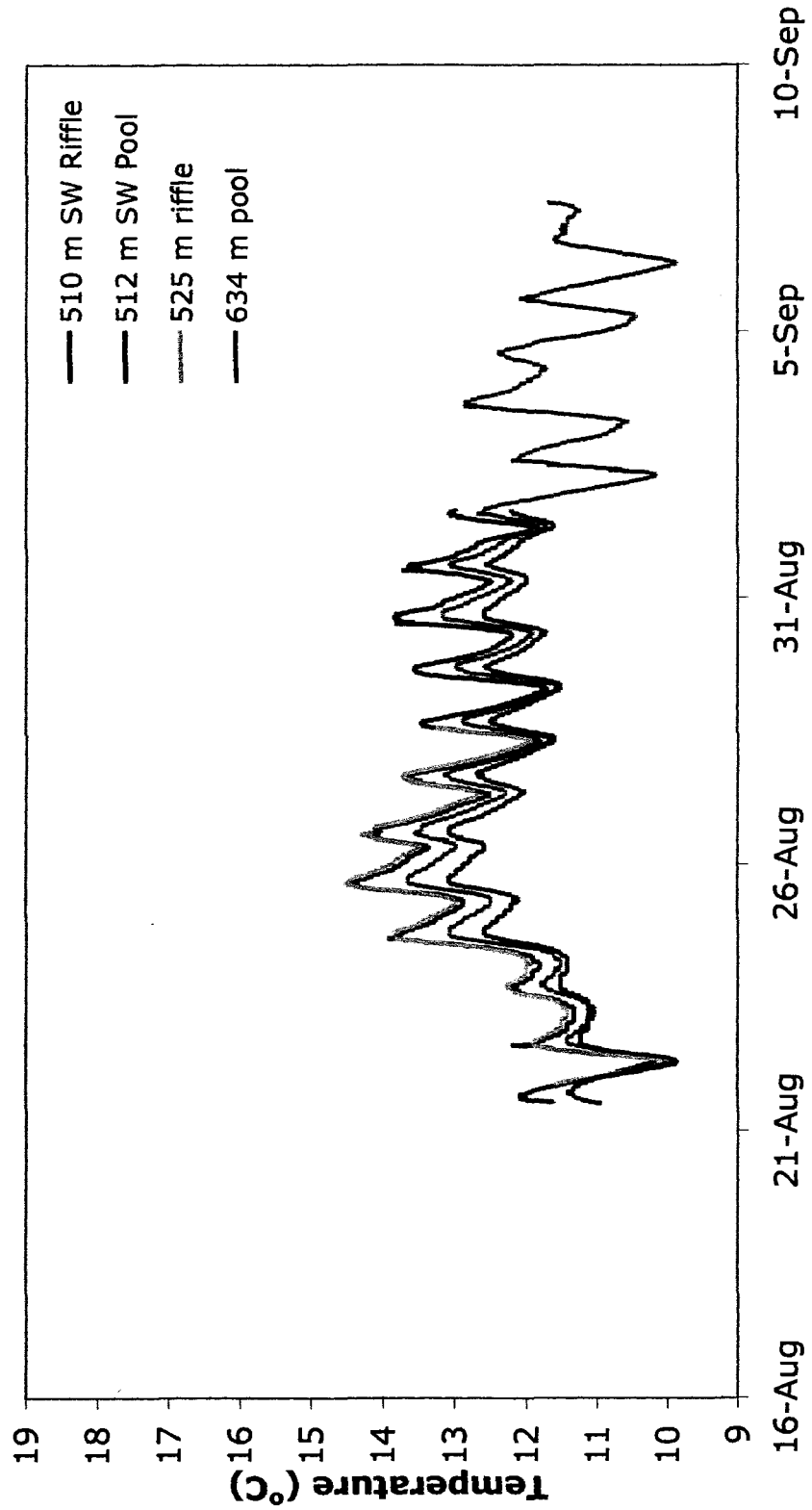


Figure 4-26 Stream temperature measurements from the lower study reach 510 to 634 m August to September 2007, Wednesday Hill Brook in Lee, NH

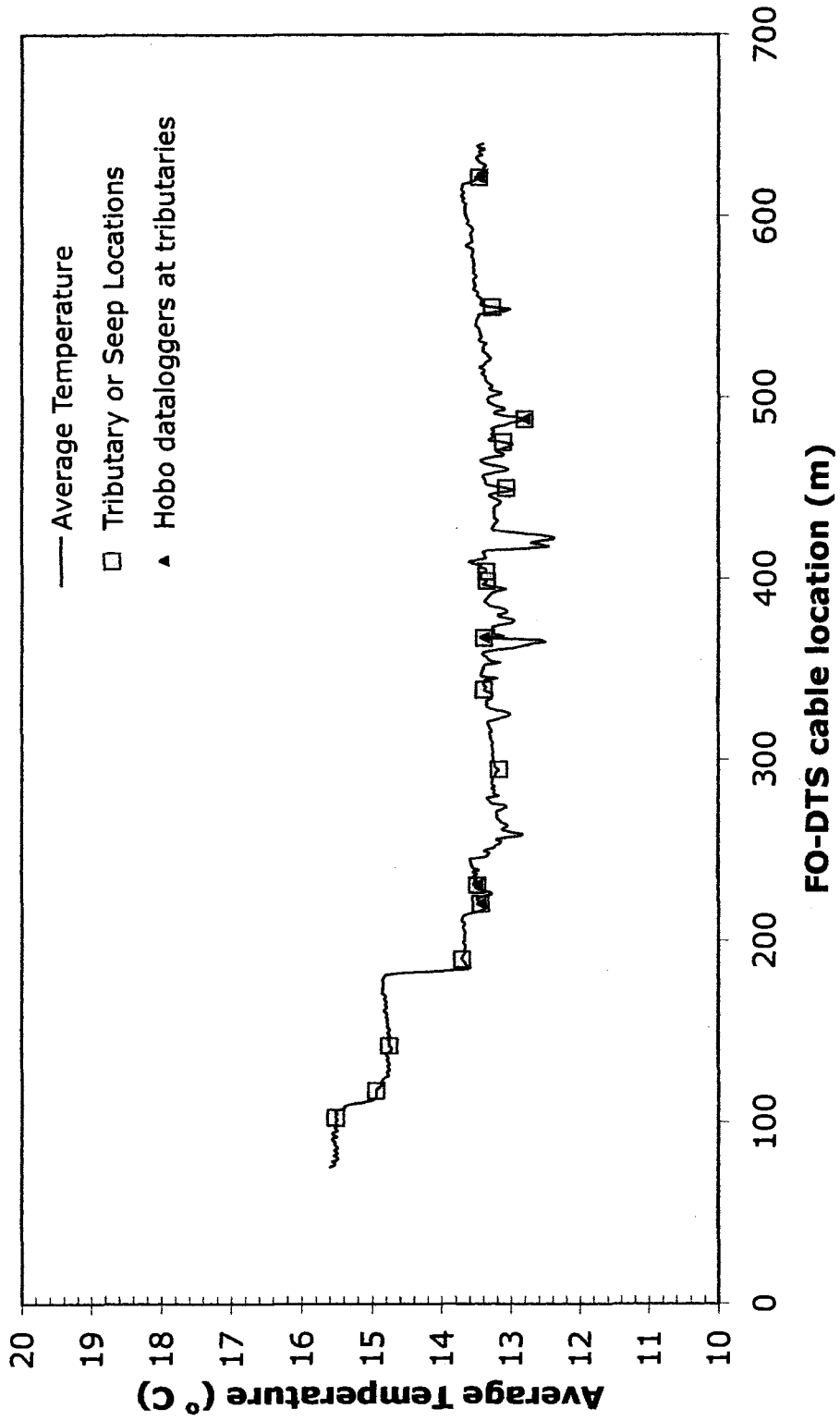


Figure 4-27 Tributaries and data logger locations plotted on FC-07-1 FODTS trend line Wednesday Hill Brook in Lee, NH

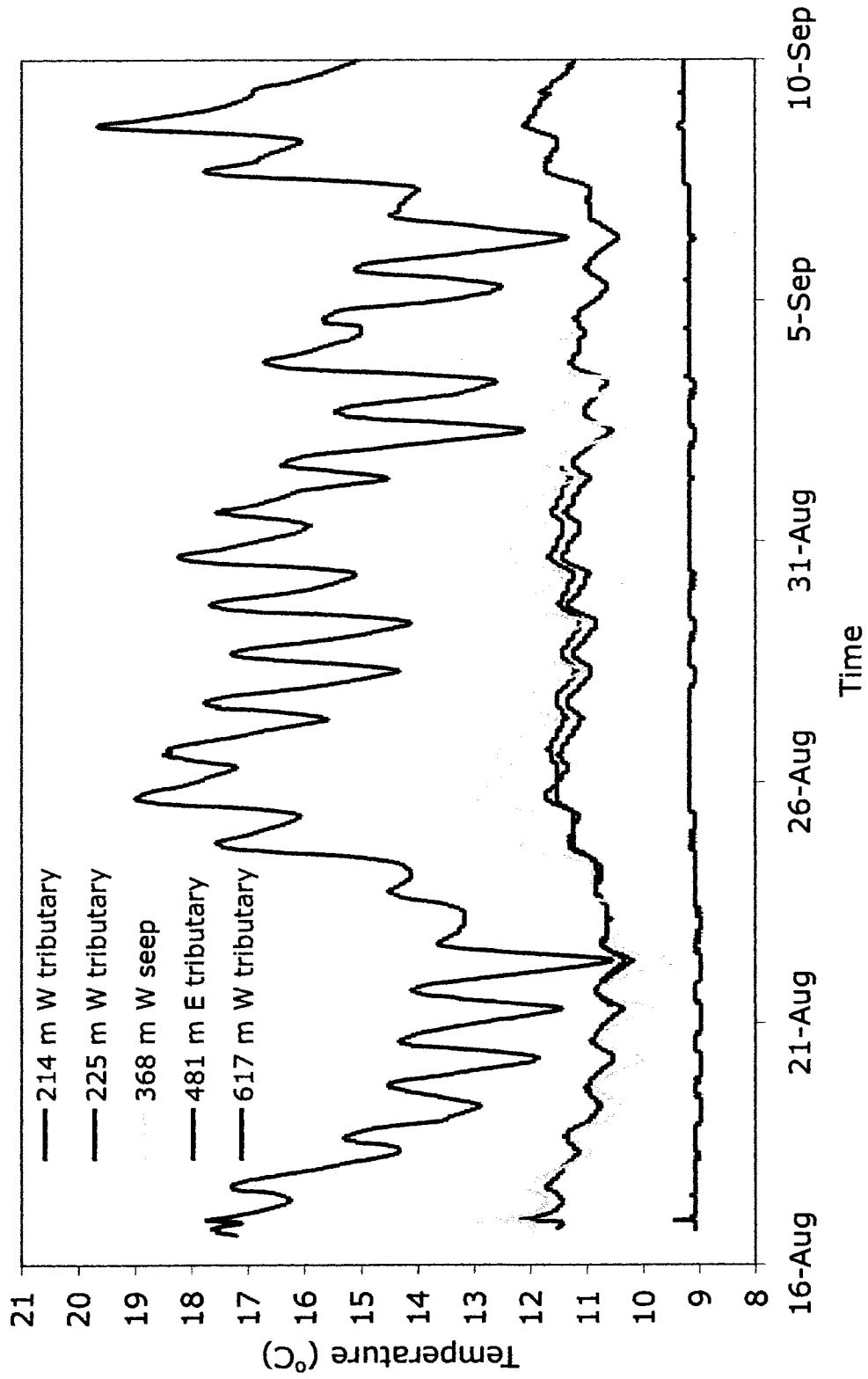


Figure 4-28 Tributaries temperatures -- August to September 2007, Wednesday Hill Brook in Lee, NH

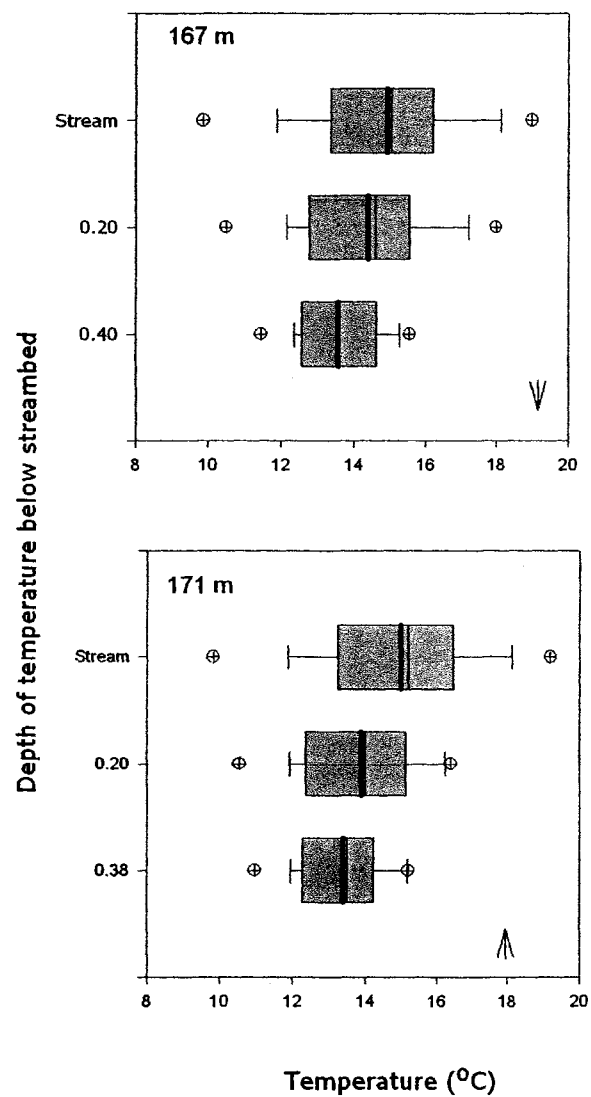


Figure 4-29 Reach 1 mini-piezometer streambed temperature box and whisker plots, Wednesday Hill Brook in Lee, NH

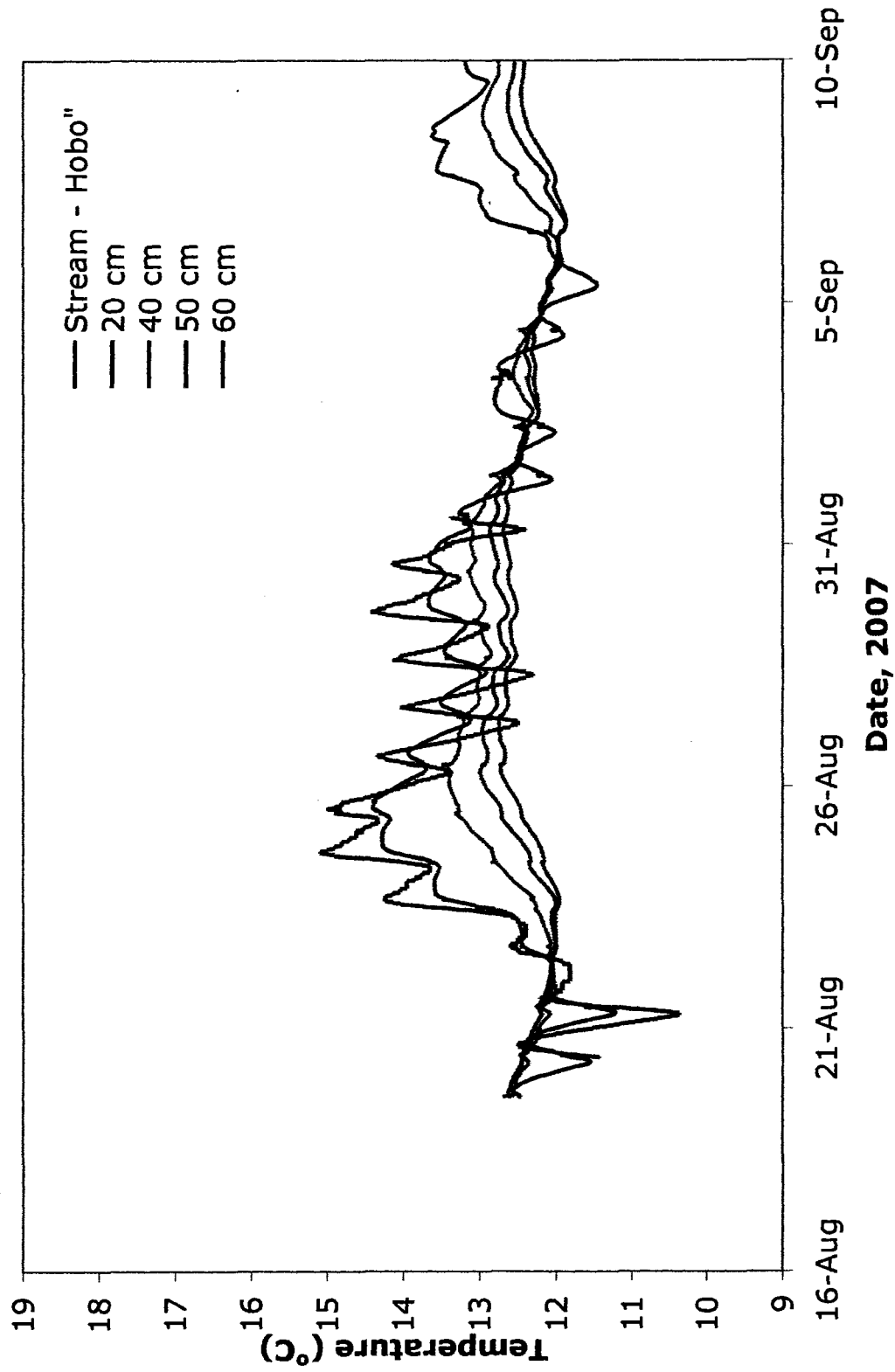


Figure 4-30 Stream and hyporheic zone temperatures at 237 m, August to September 2007
 Wednesday Hill Brook in Lee, NH

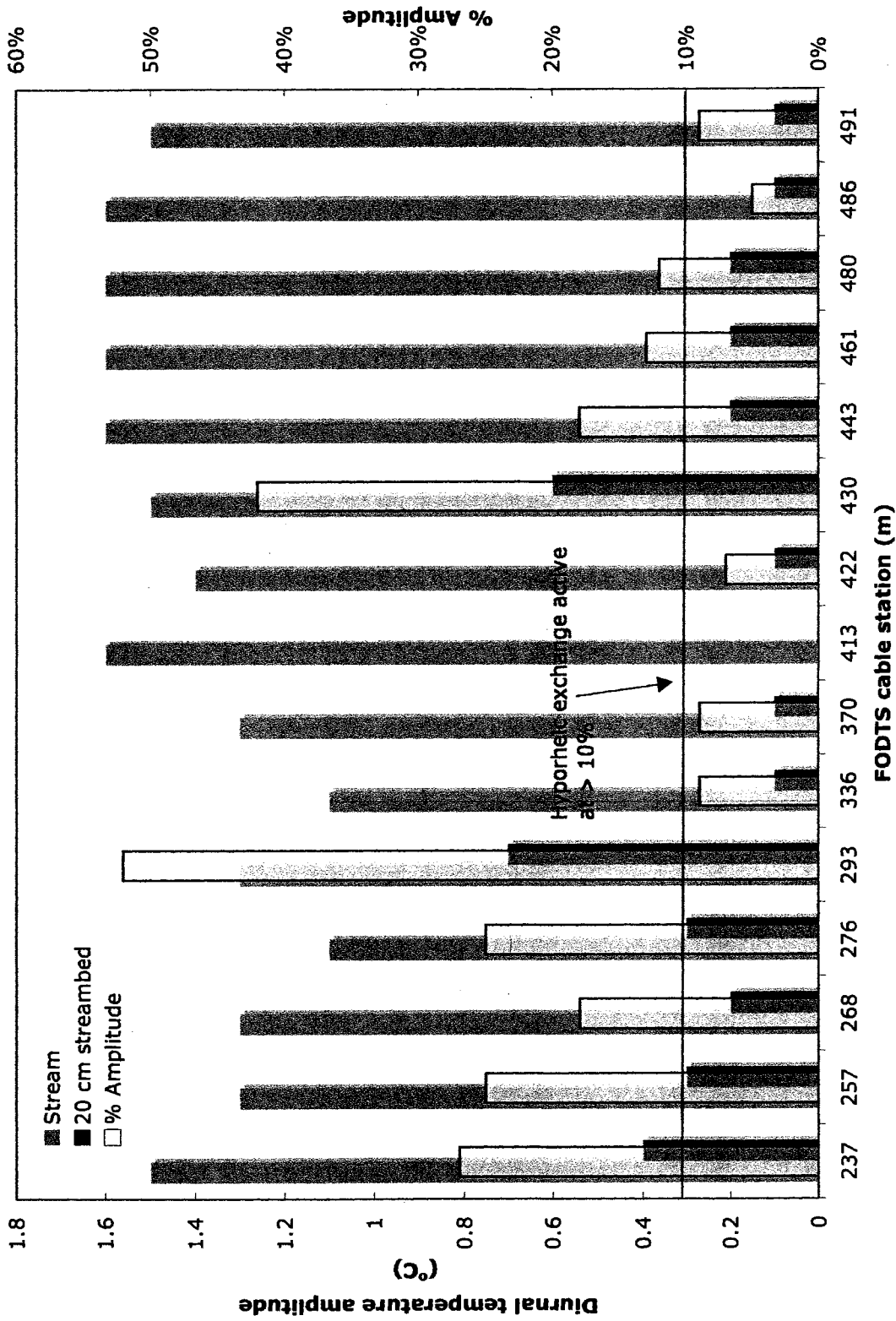


Figure 4-31 Percent Amplitude Analysis – Hyporheic zone temperatures at 20 cm bss and stream temperature. Wednesday Hill Brook in Lee, NH. Percent amplitude is 20 cm/stream temperature x 100

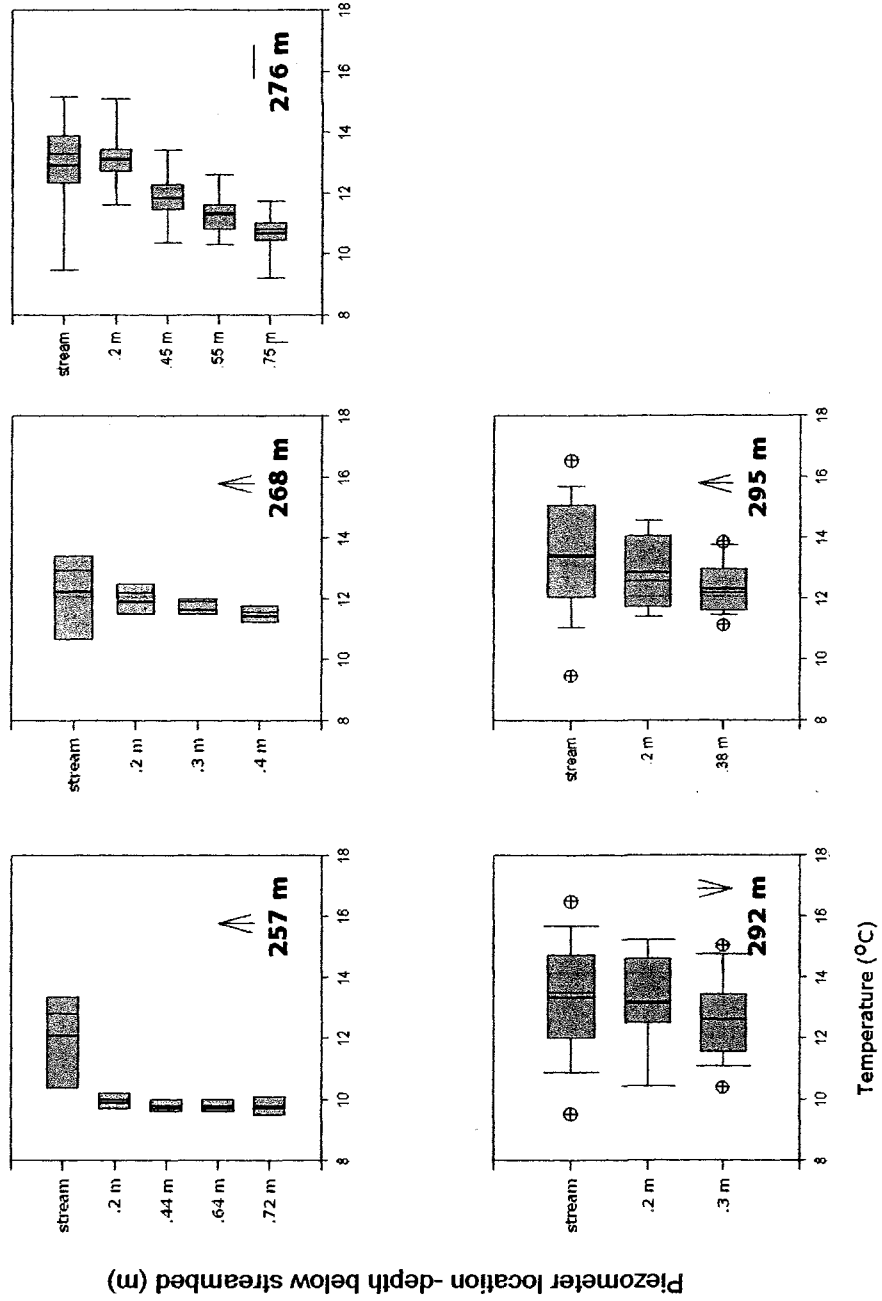


Figure 4-32 Reach 3 mini piezometer streambed temperature box plots, Wednesday Hill Brook in Lee, NH

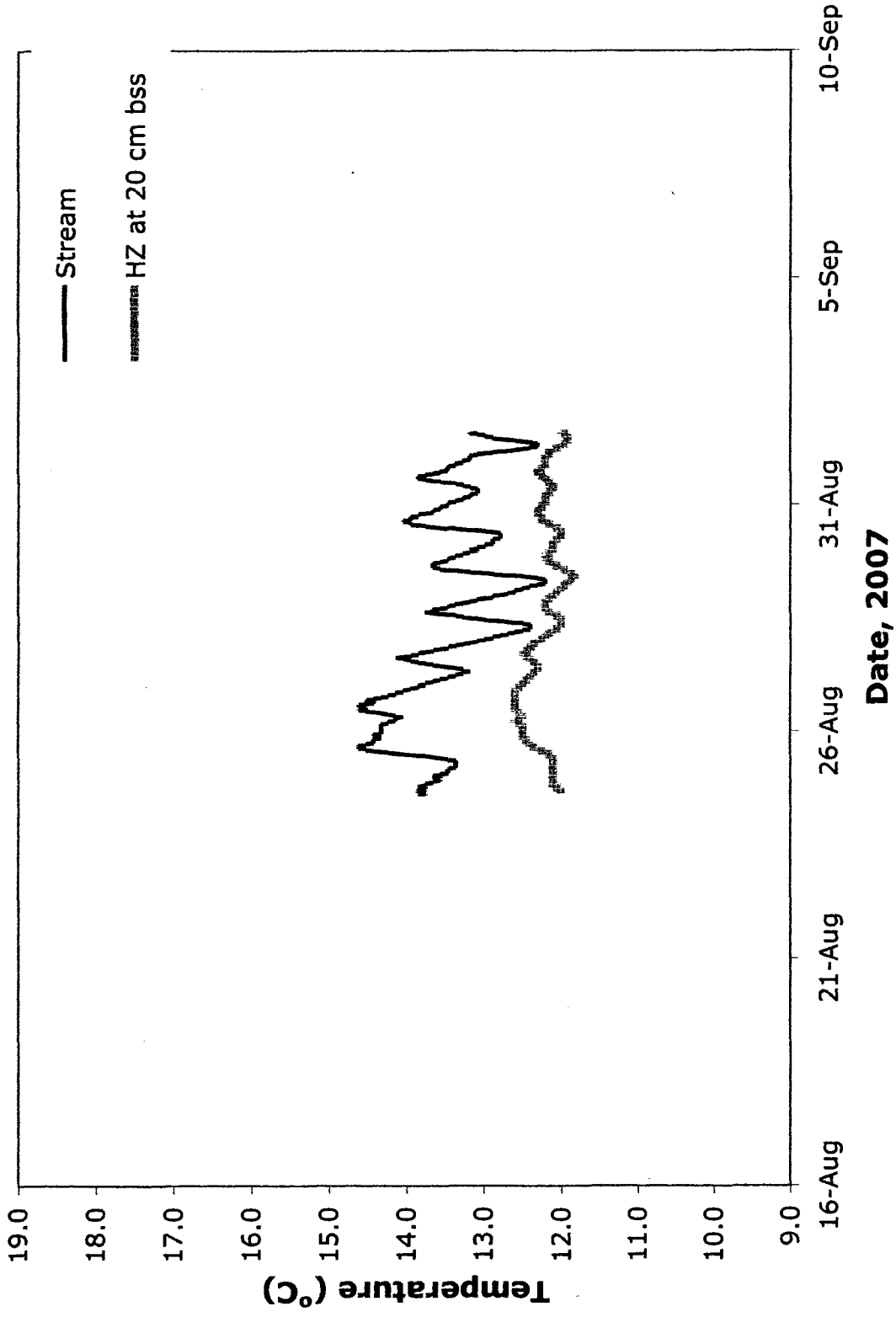


Figure 4-33 Stream and hyporheic zone temperatures at 257 m, August to September 2007
 Wednesday Hill Brook in Lee, NH

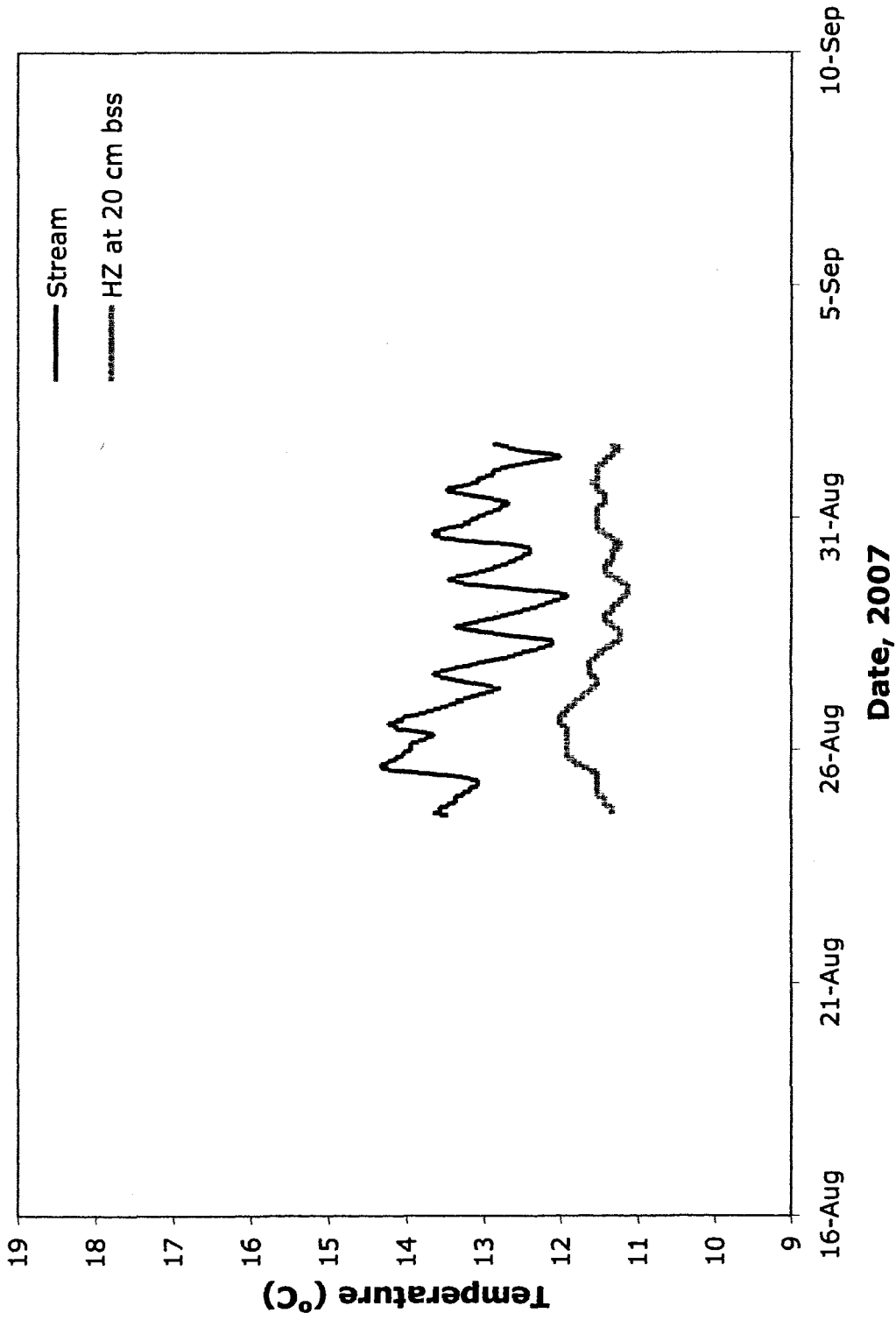


Figure 4-34 Stream and hyporheic zone temperatures at 268 m, August to September 2007
 Wednesday Hill Brook in Lee, NH

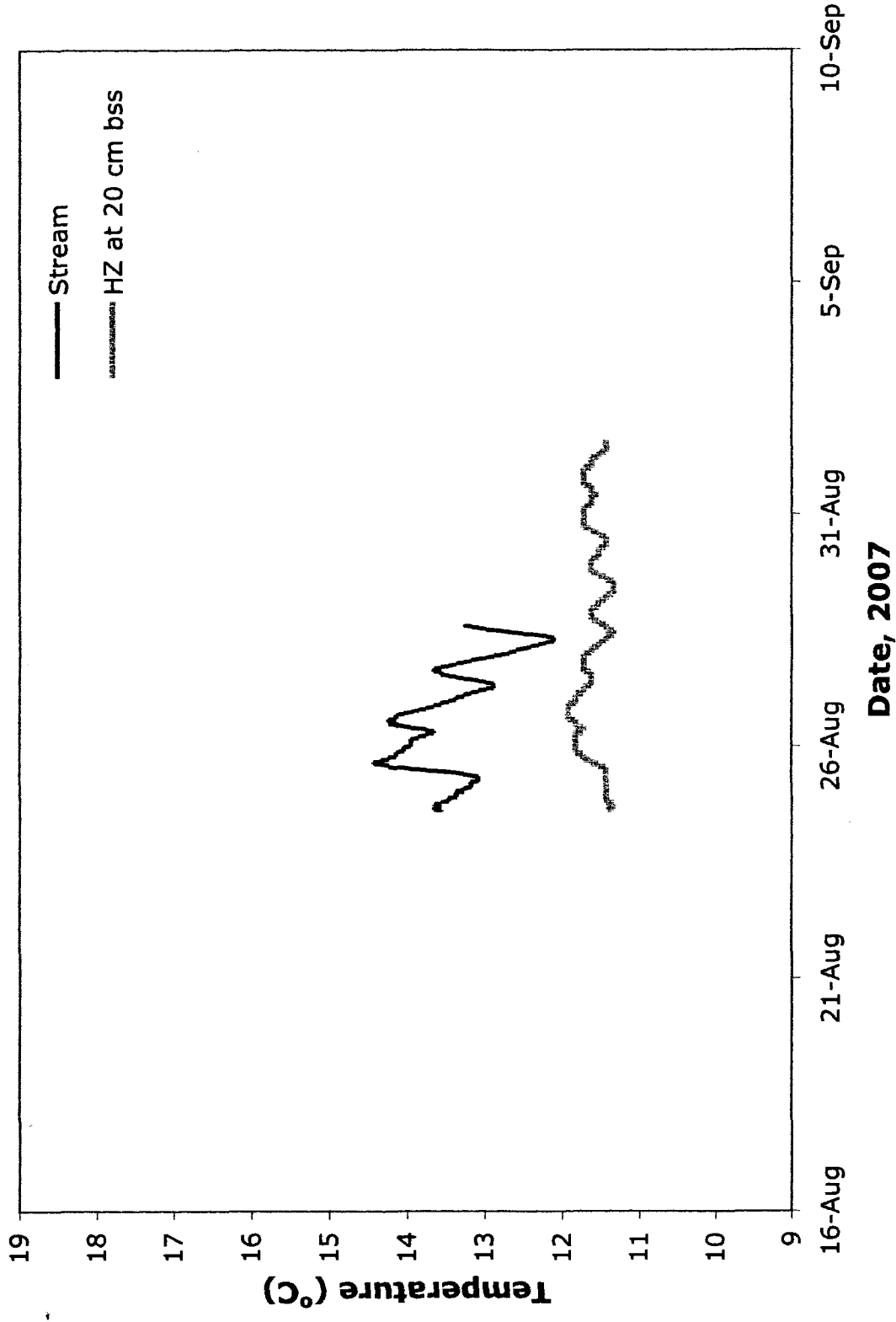


Figure 4-35 Stream and hyporheic zone temperatures at 276 m, August to September 2007
 Wednesday Hill Brook in Lee, NH

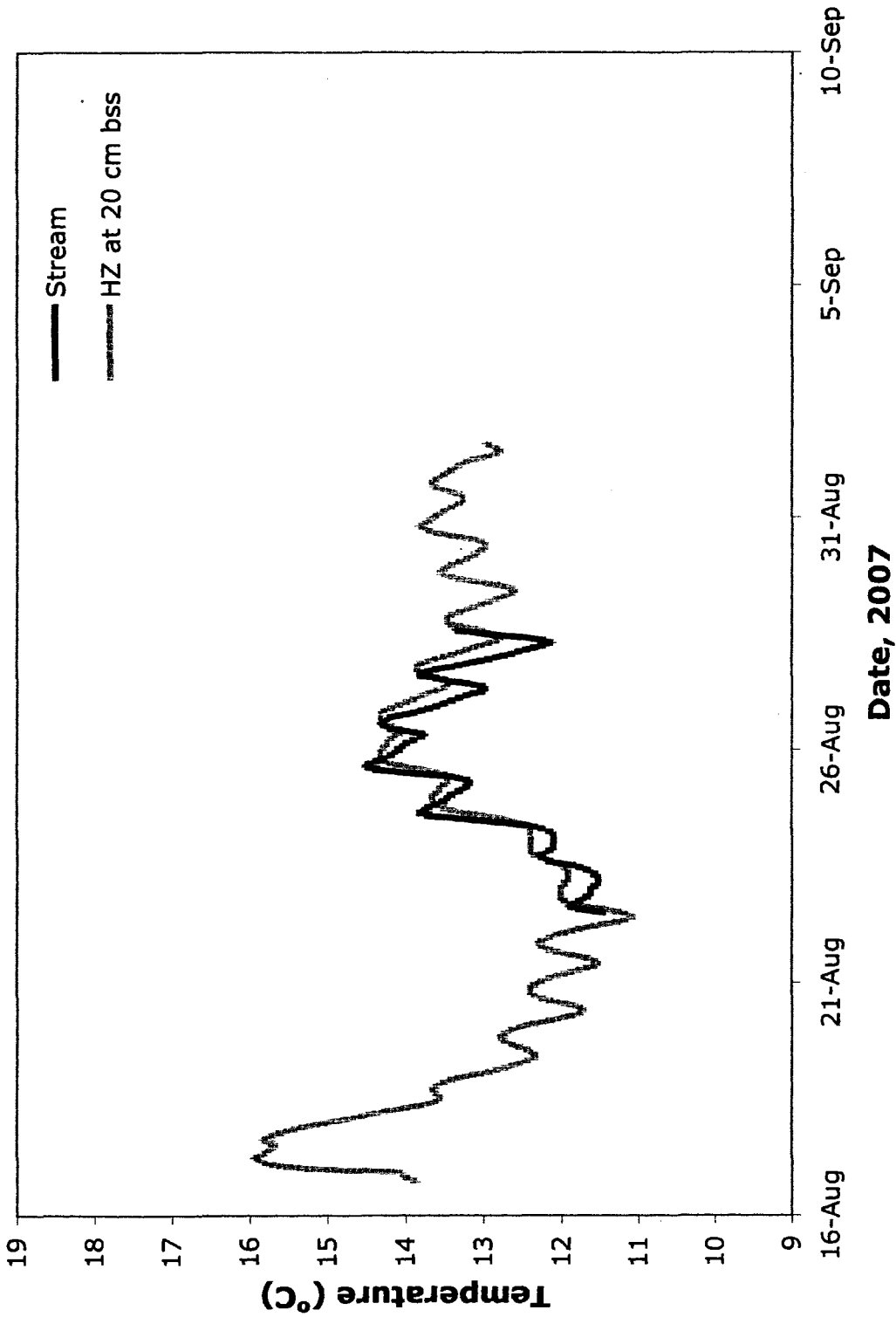


Figure 4-36 Stream and hyporheic zone temperatures at 293 m, August to September 2007
Wednesday Hill Brook in Lee, NH

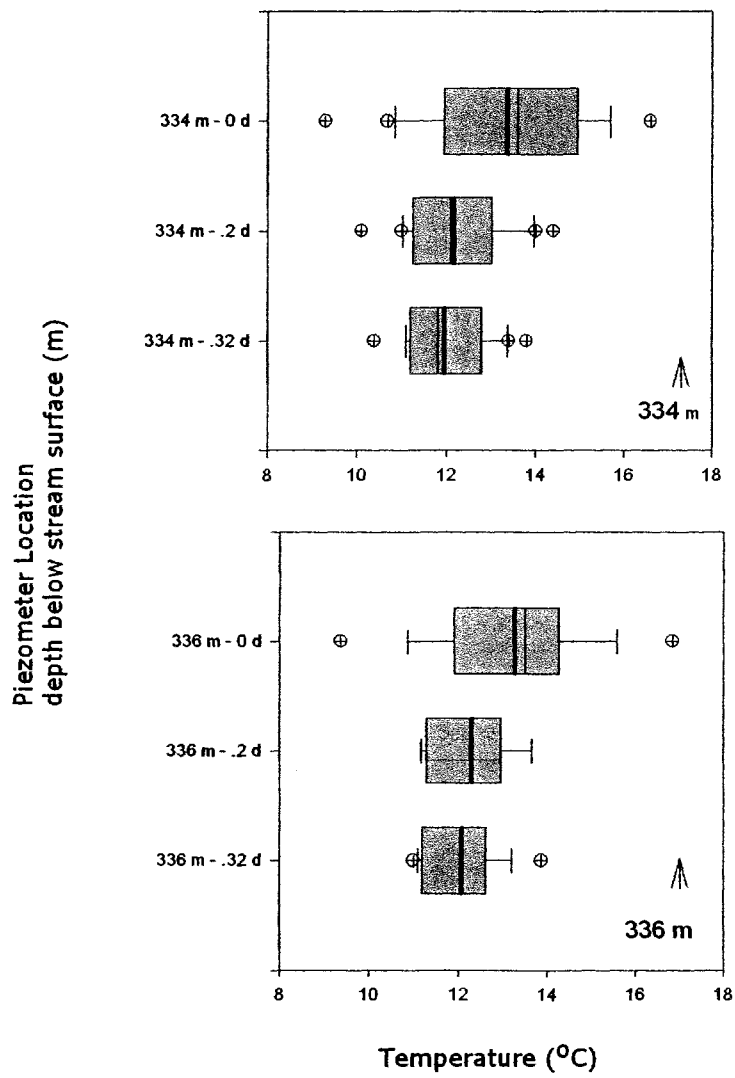


Figure 4-37 Reach 4 mini piezometer streambed temperature box and whisker plot, Wednesday Hill Brook in Lee, NH

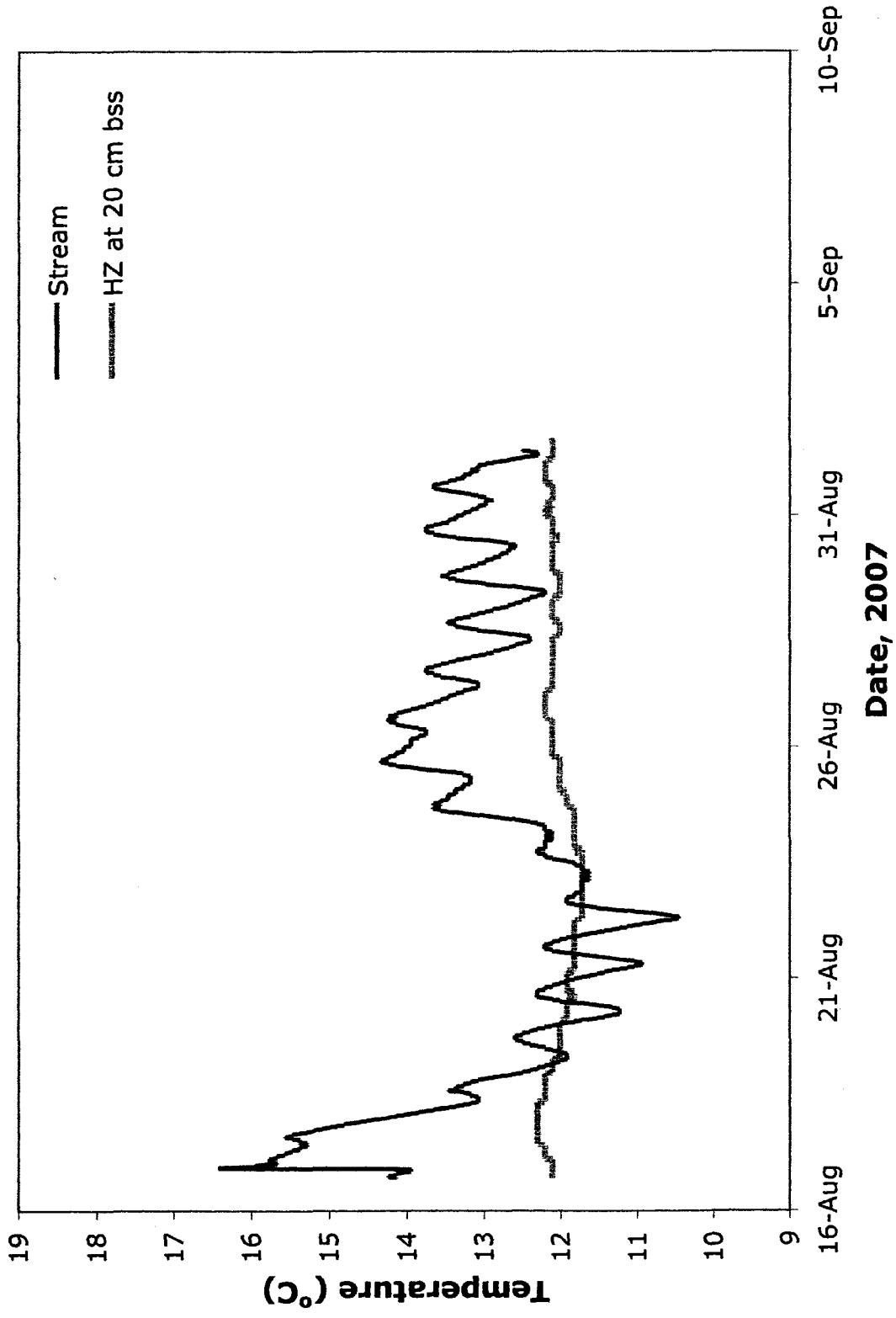


Figure 4-38 Stream and hyporheic zone temperatures at 336 m, August to September 2007
 Wednesday Hill Brook in Lee, NH

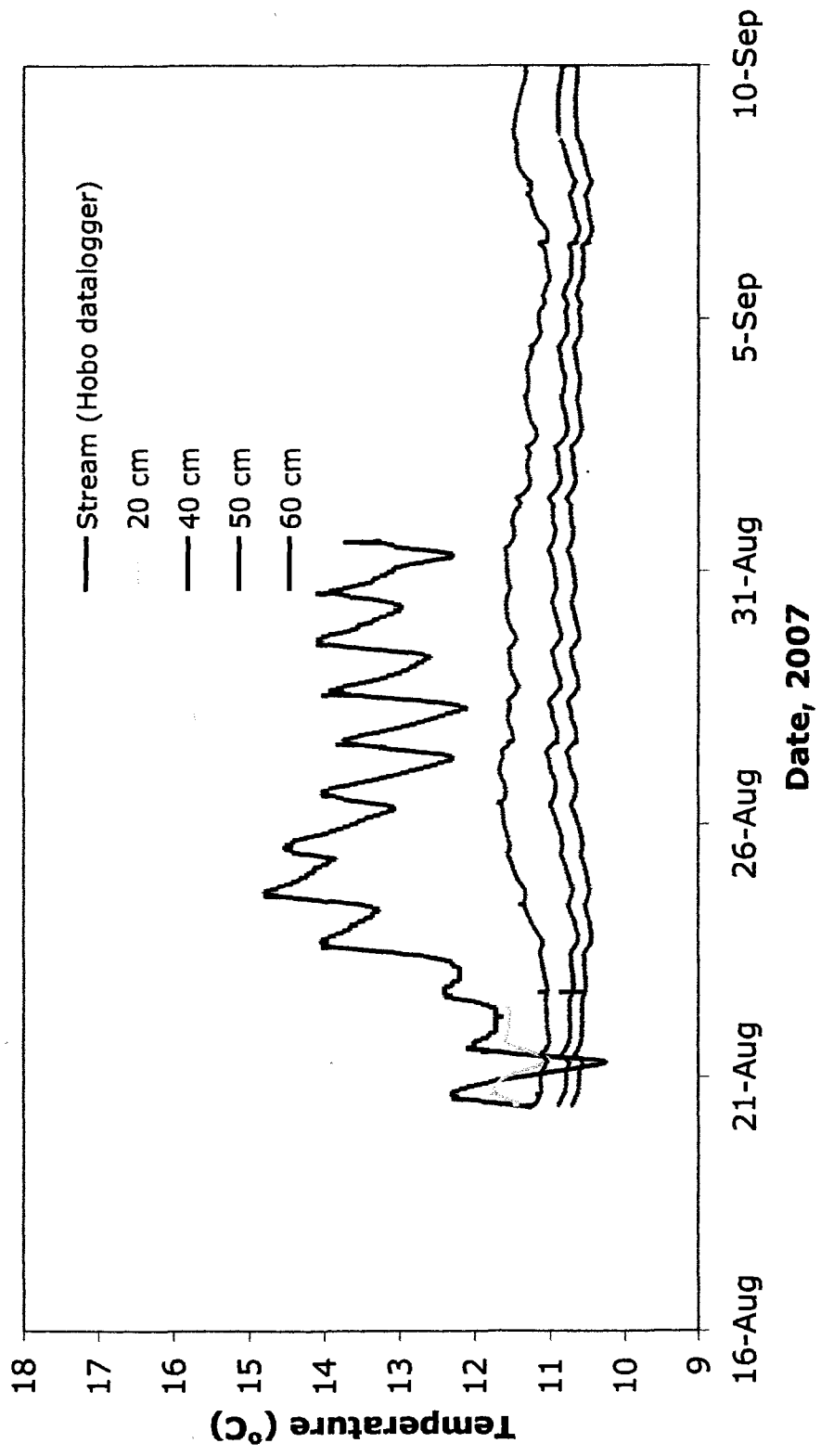


Figure 4-39 Stream and hyporheic zone temperatures at 370 m, August to September 2007
Wednesday Hill Brook in Lee, NH

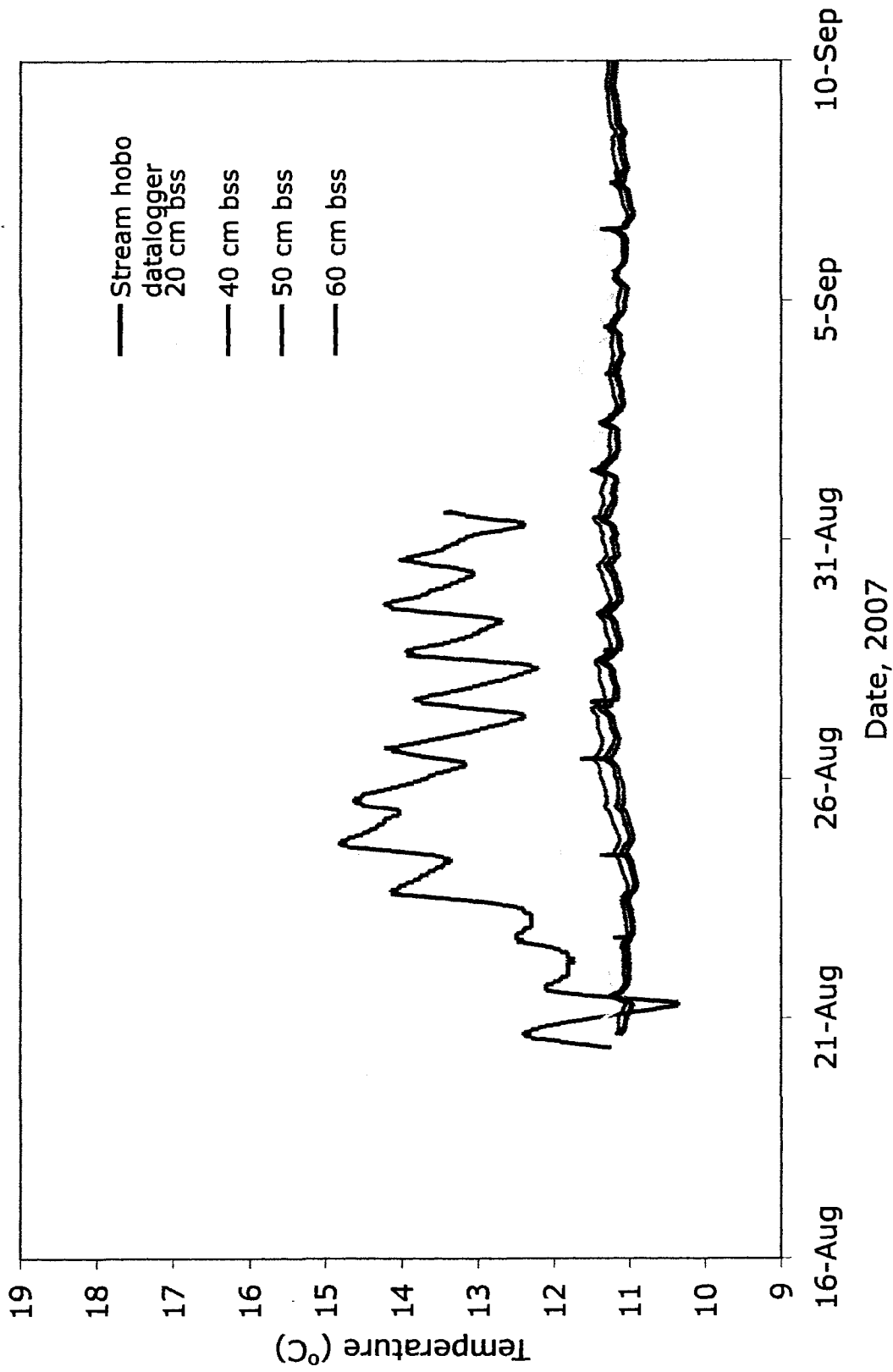


Figure 4-39 Stream and hyporheic zone temperatures at 372 m, August to September 2007
 Wednesday Hill Brook in Lee, N

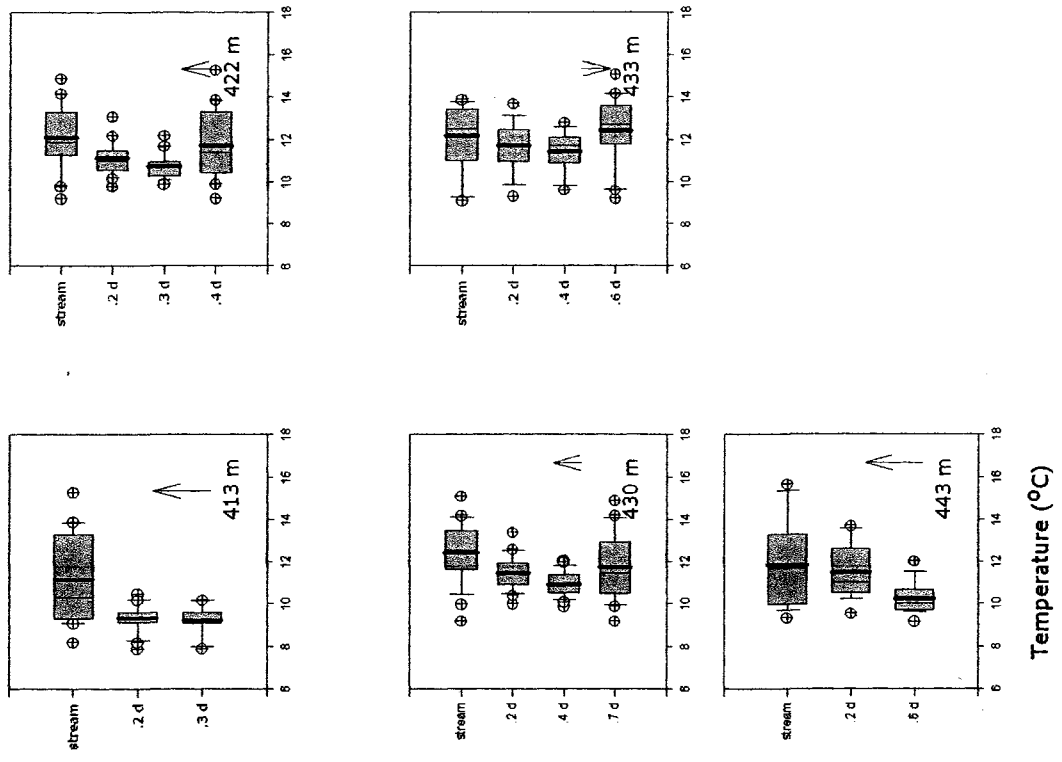


Figure 4-40 Reach 5 413 to 443 m mini piezometer streambed temperature box and whisker plots, Wednesday Hill Brook in Lee, NH

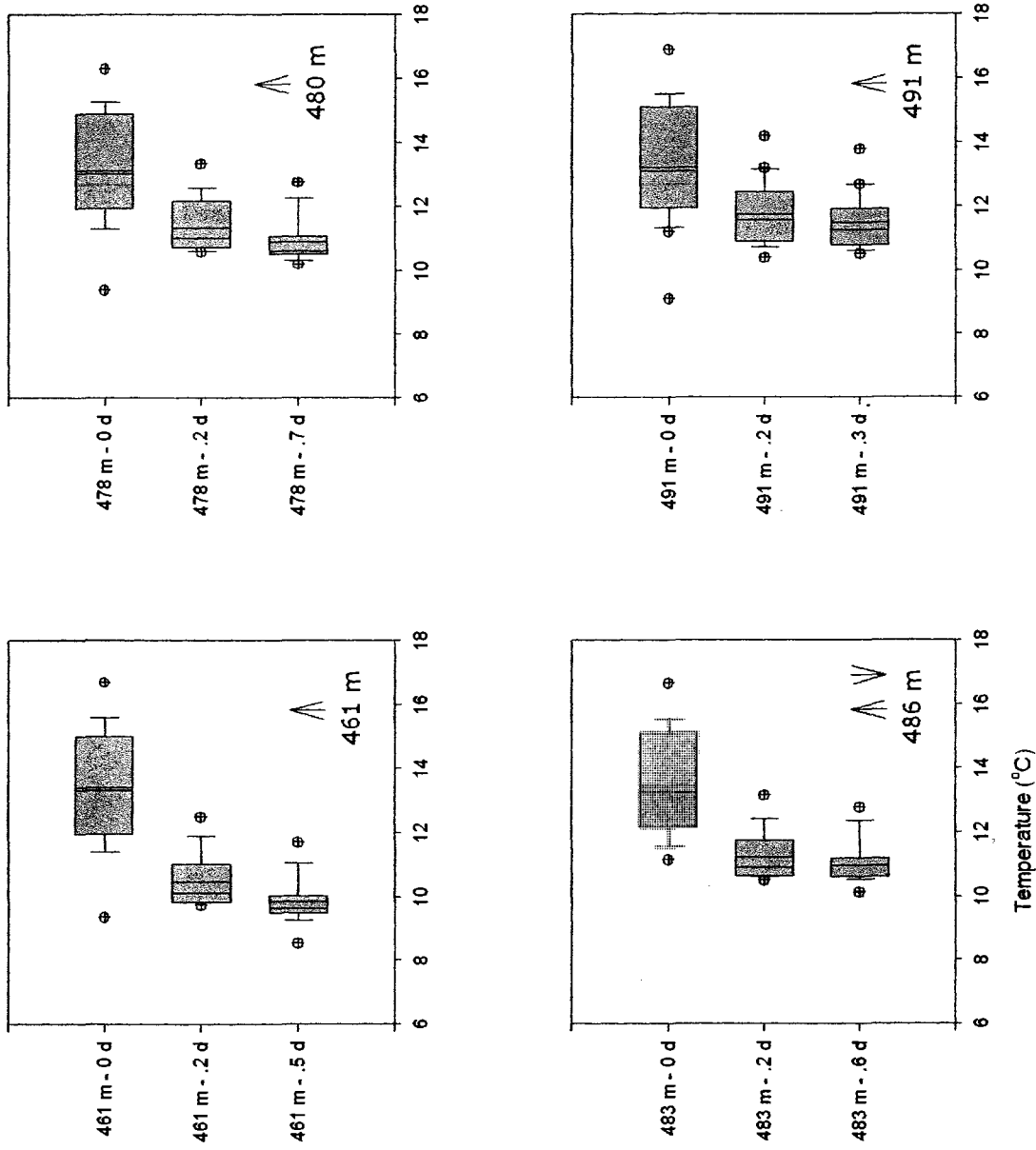


Figure 4-42 Reach 5 - 461 to 491 m mini piezometer streambed temperature box plots, Wednesday Hill Brook in Lee, NH

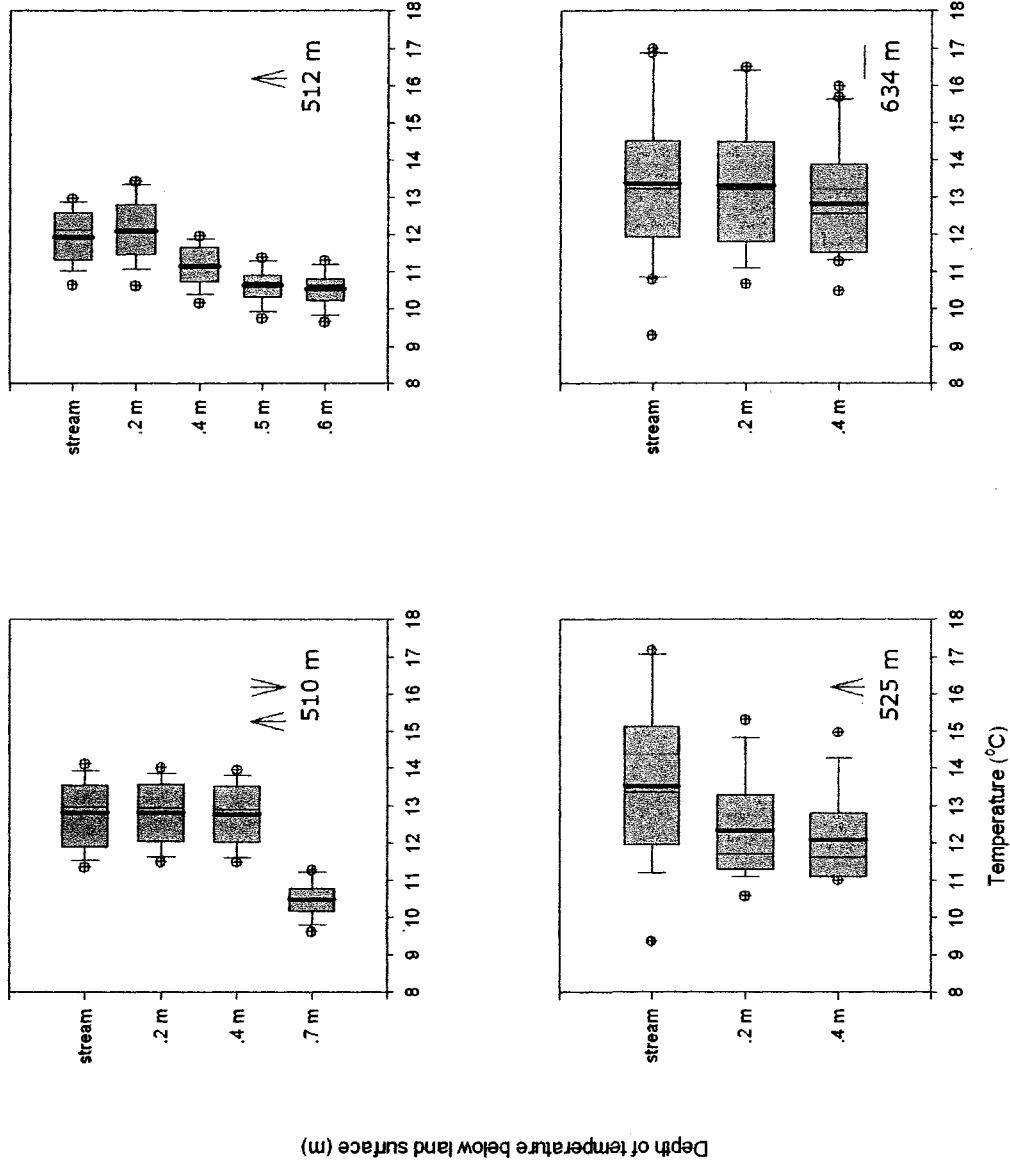


Figure 4-43 Reach 6 - 510 to 634 m mini piezometer streambed temperature box plots, Wednesday Hill Brook in Lee, NH

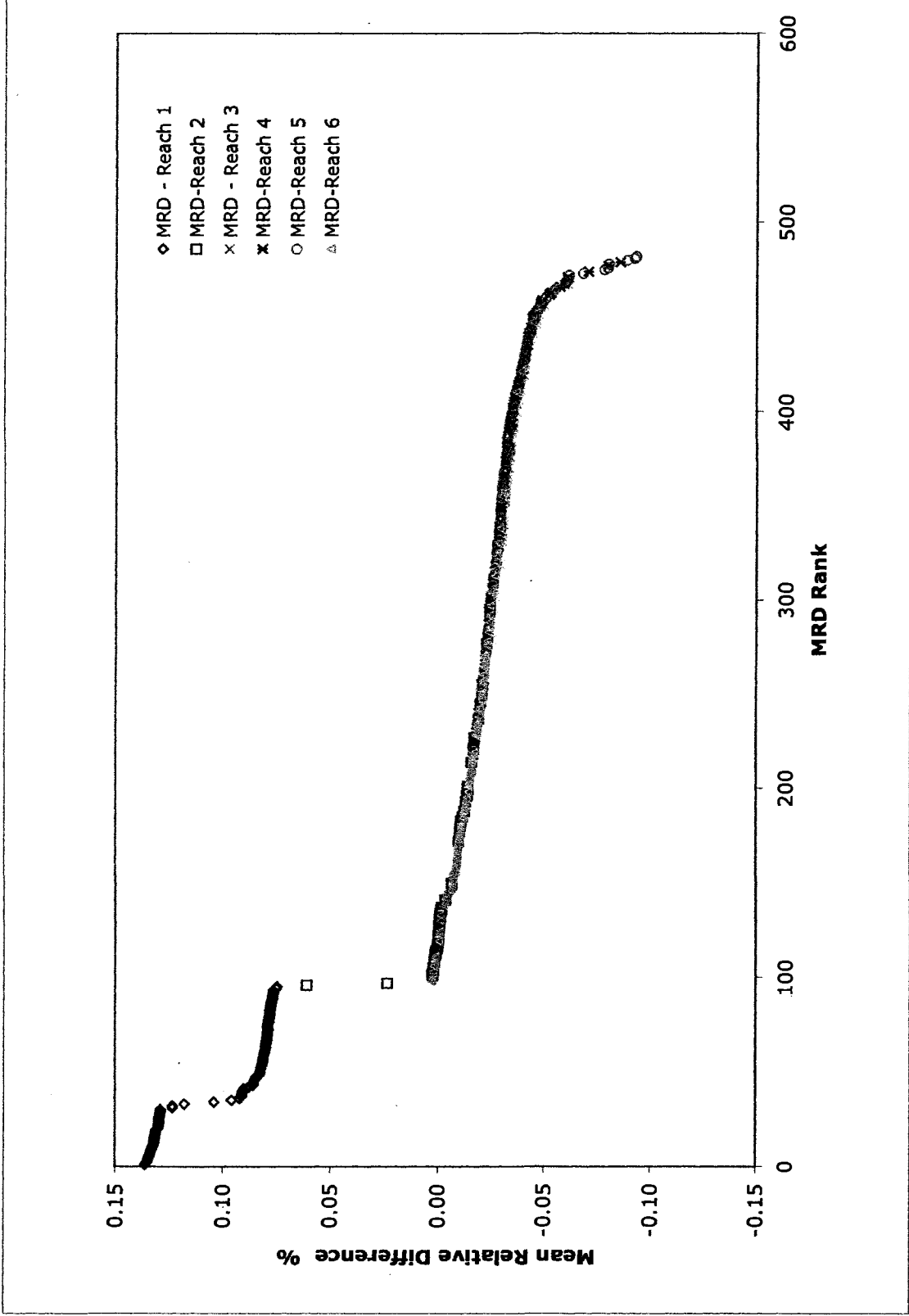


Figure 4-44 Mean relative difference in FODTS stream temperatures – FC-07-1
 Wednesday Hill Brook in Lee, NH

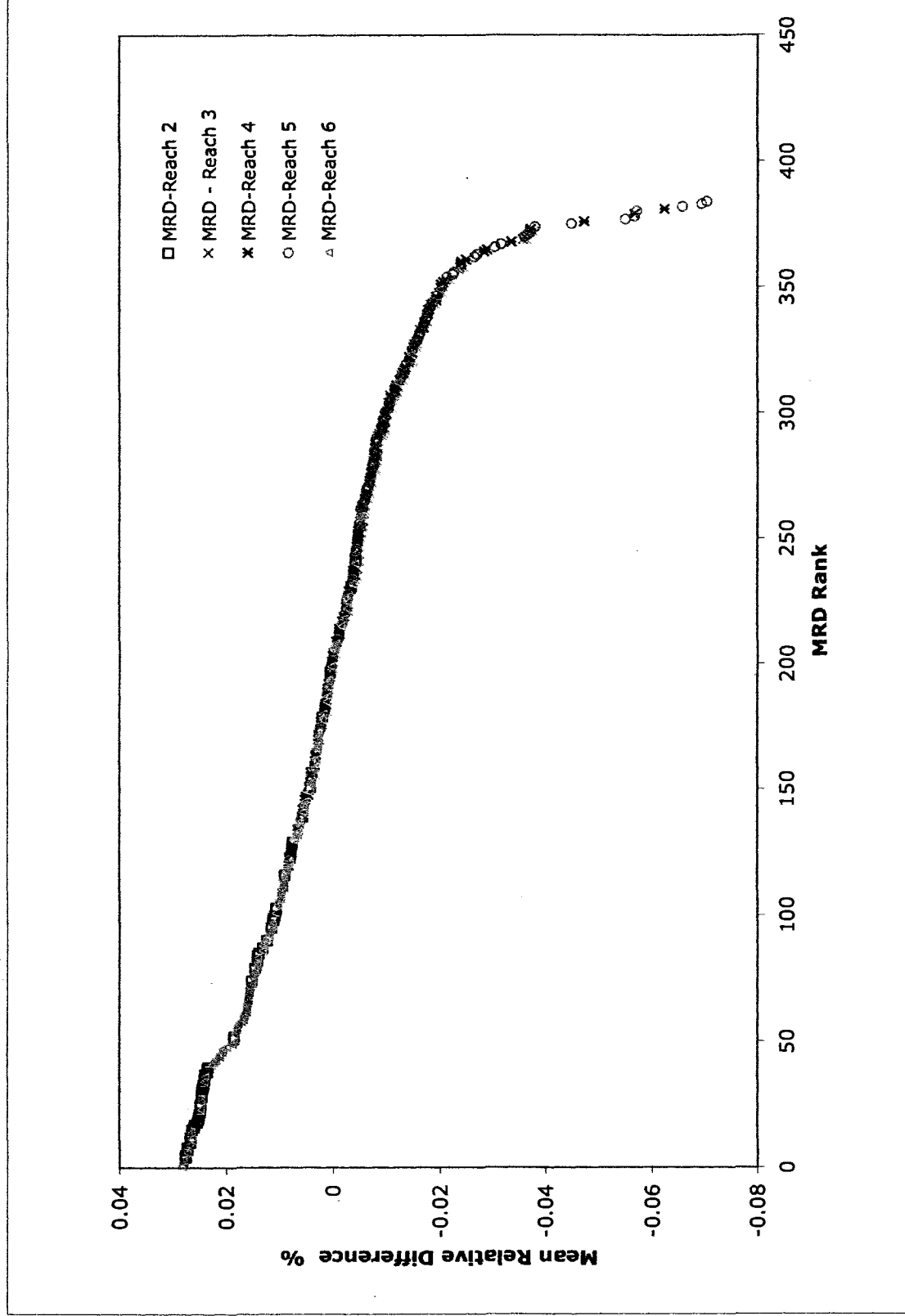


Figure 4-45 Mean relative difference in FODTS stream temperature without armored reach data
 Wednesday Hill Brook in Lee, NH

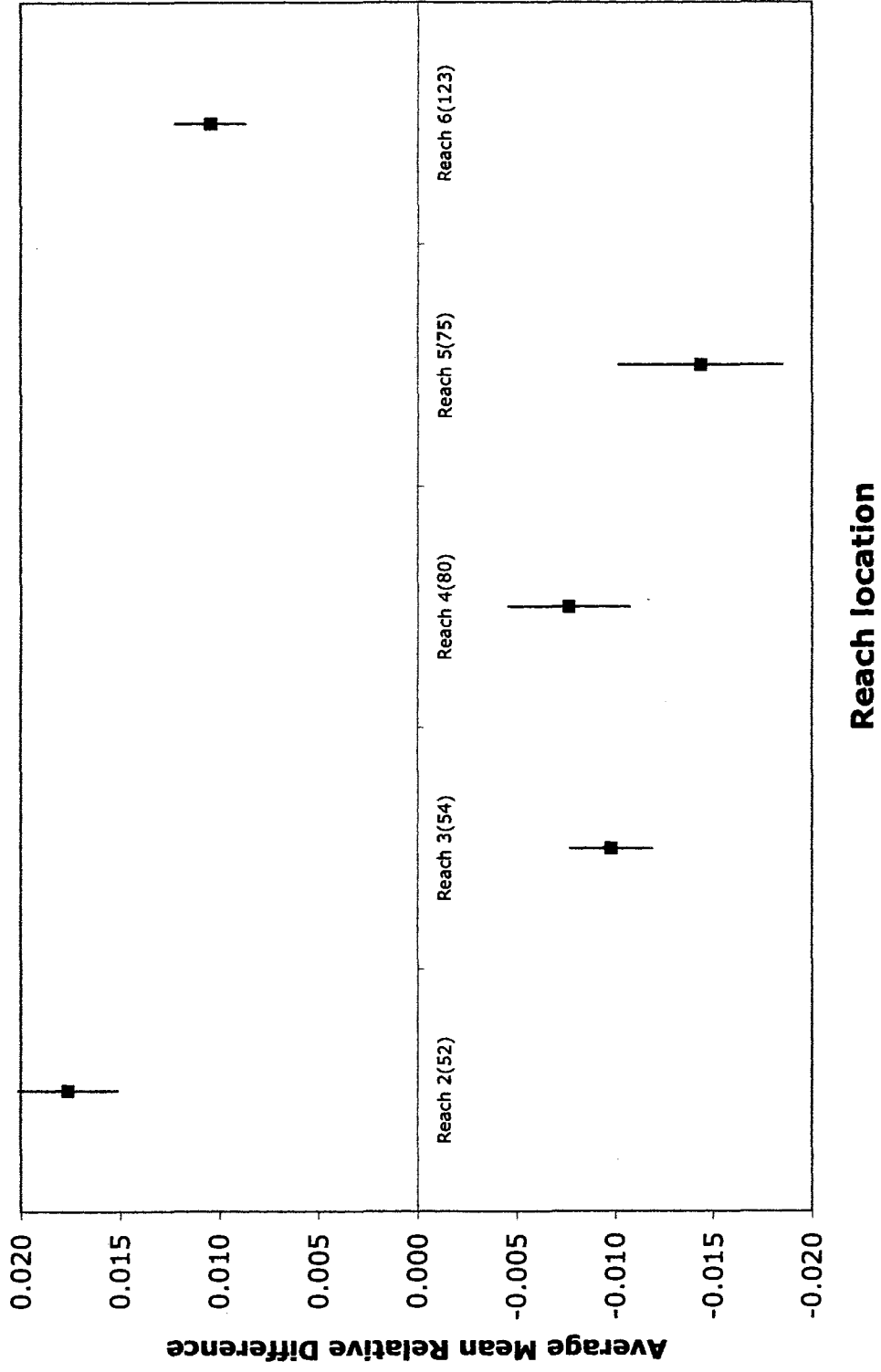
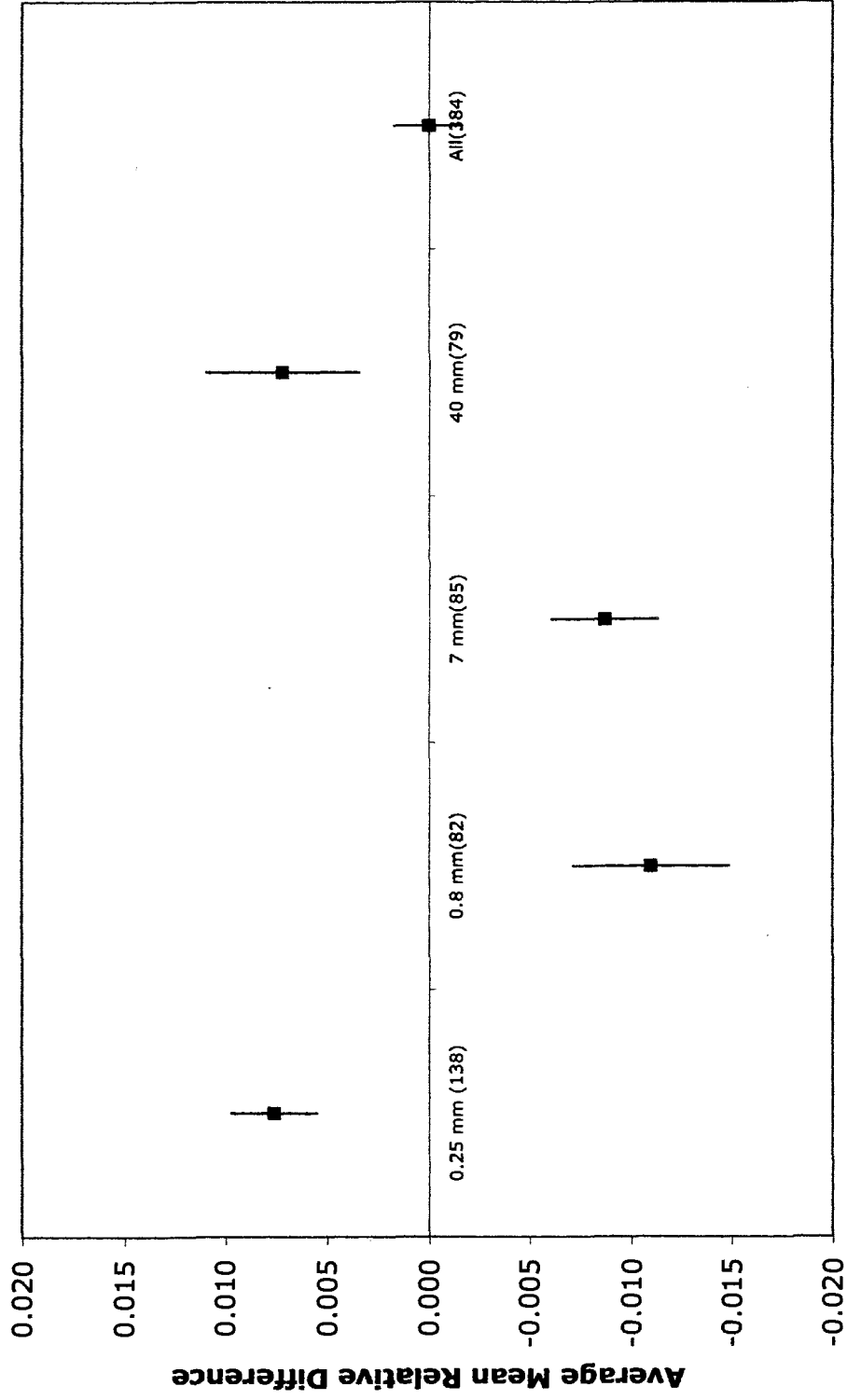


Figure 4-46 Average mean relative difference by sub-reach classification and 95% confidence interval, Wednesday Hill Brook in Lee, NH



D50 grain size

Figure 4-47 Mean relative difference by D50 streambed sediment size and 95% confidence interval, Wednesday Hill Brook in Lee, NH

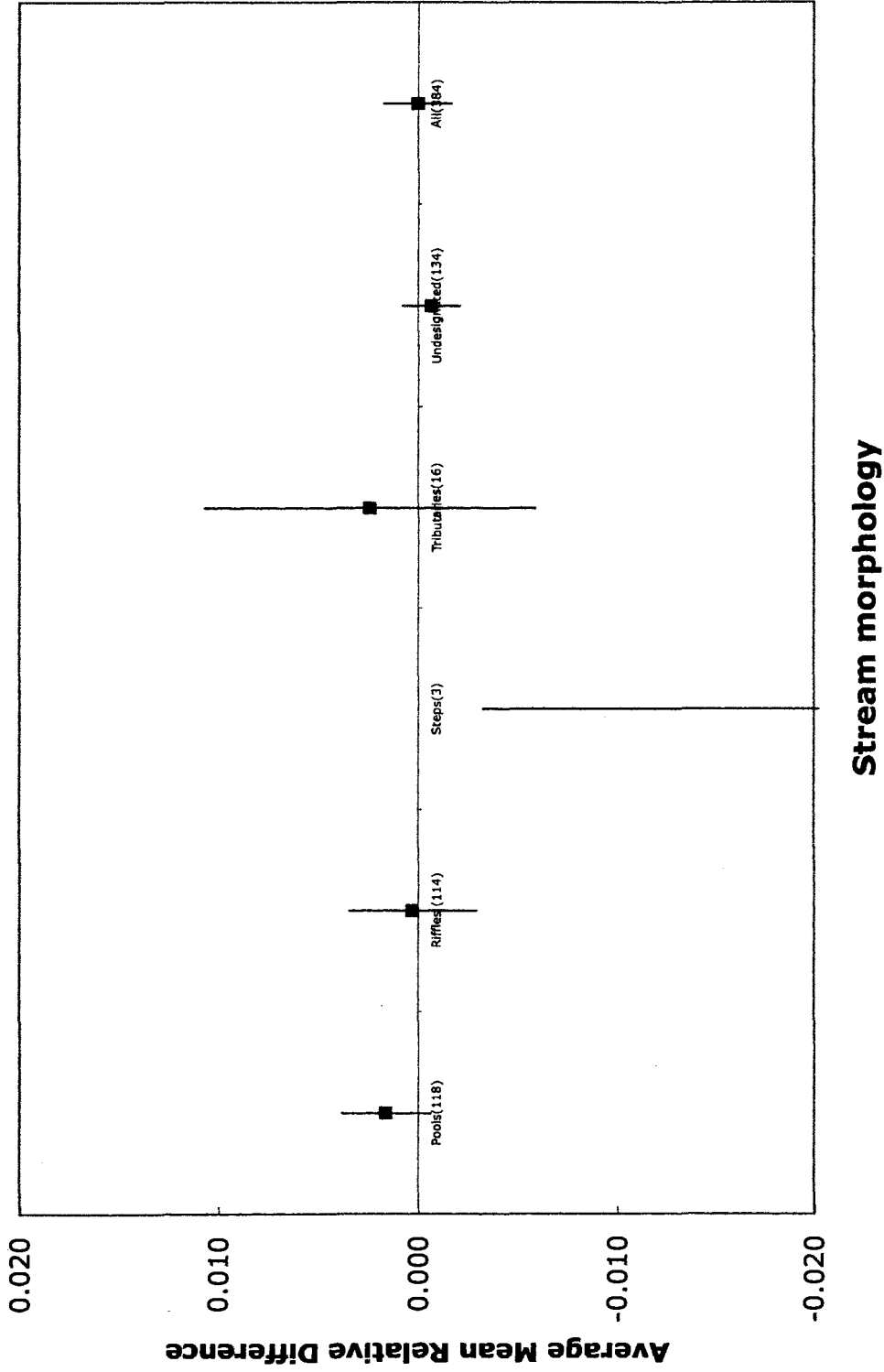


Figure 4-48 Mean relative difference by stream morphology with 95% confidence intervals, Wednesday Hill Brook in Lee, NH

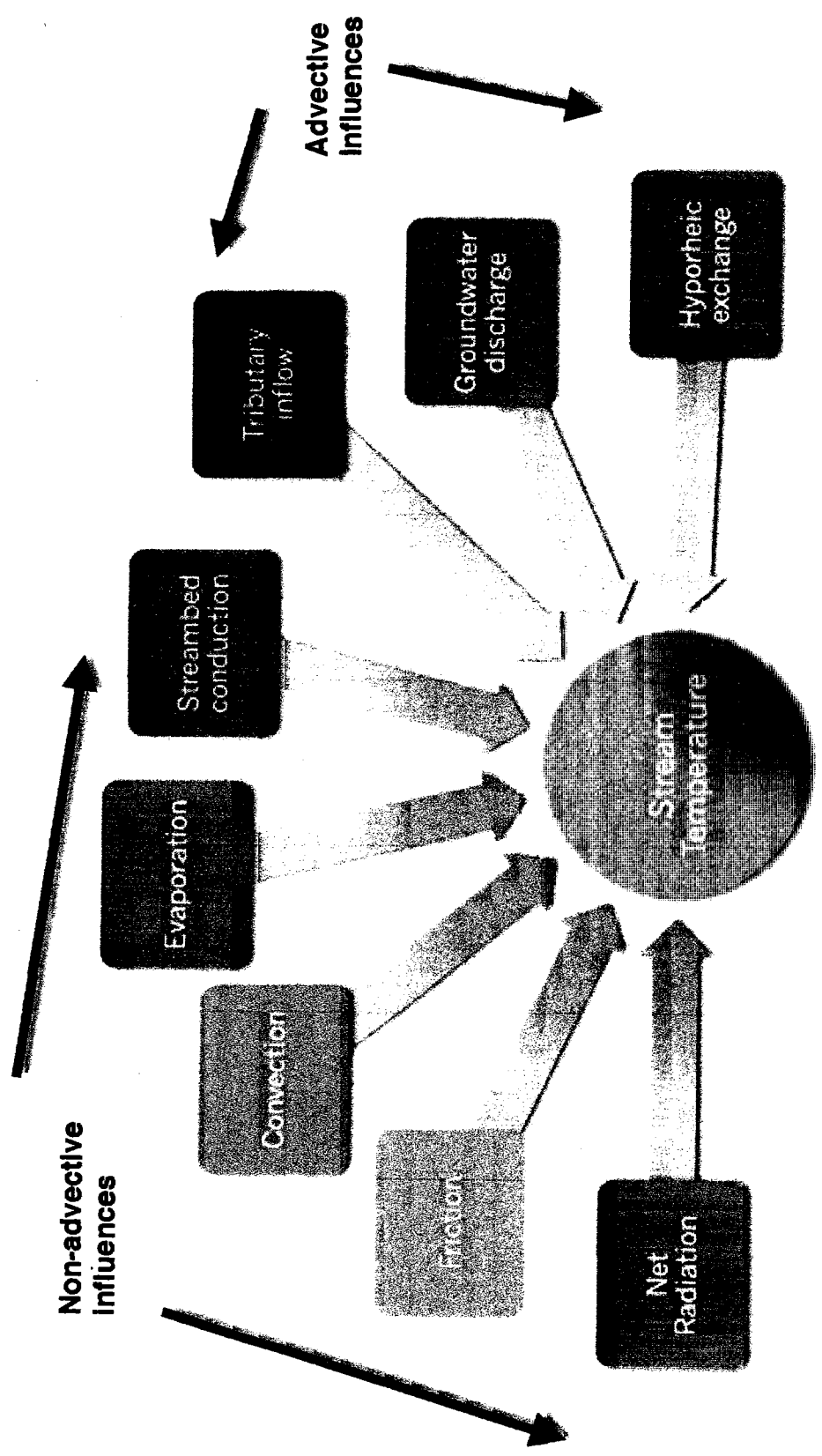


Figure 4-49 Non-advective and advective components of stream temperature heat budget for Wednesday Hill Brook in Lee, NH

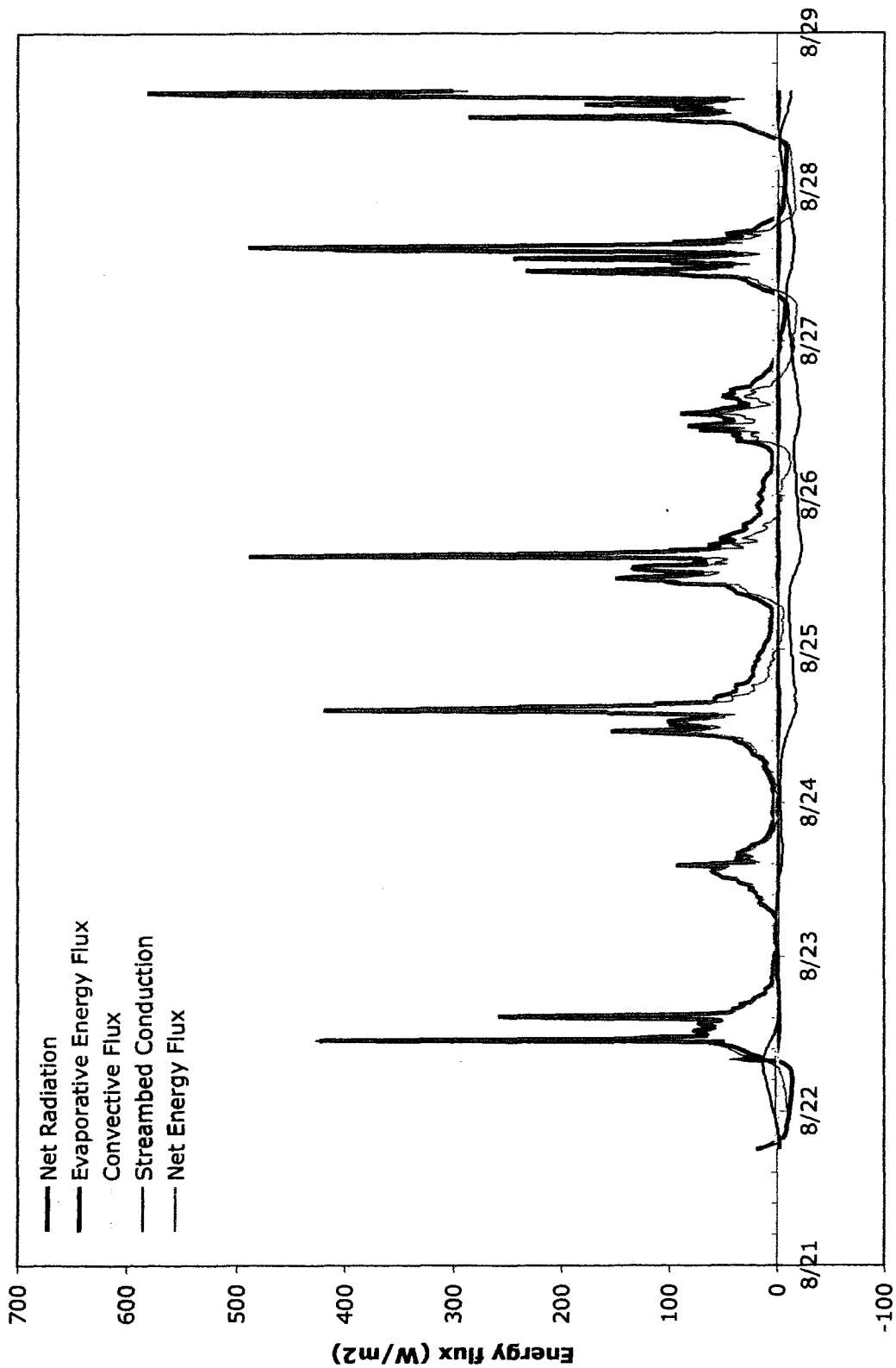


Figure 4-50 Non advective heat flux to and from Wednesday Hill Brook at 336 m, Wednesday Hill Brook in Lee, NH

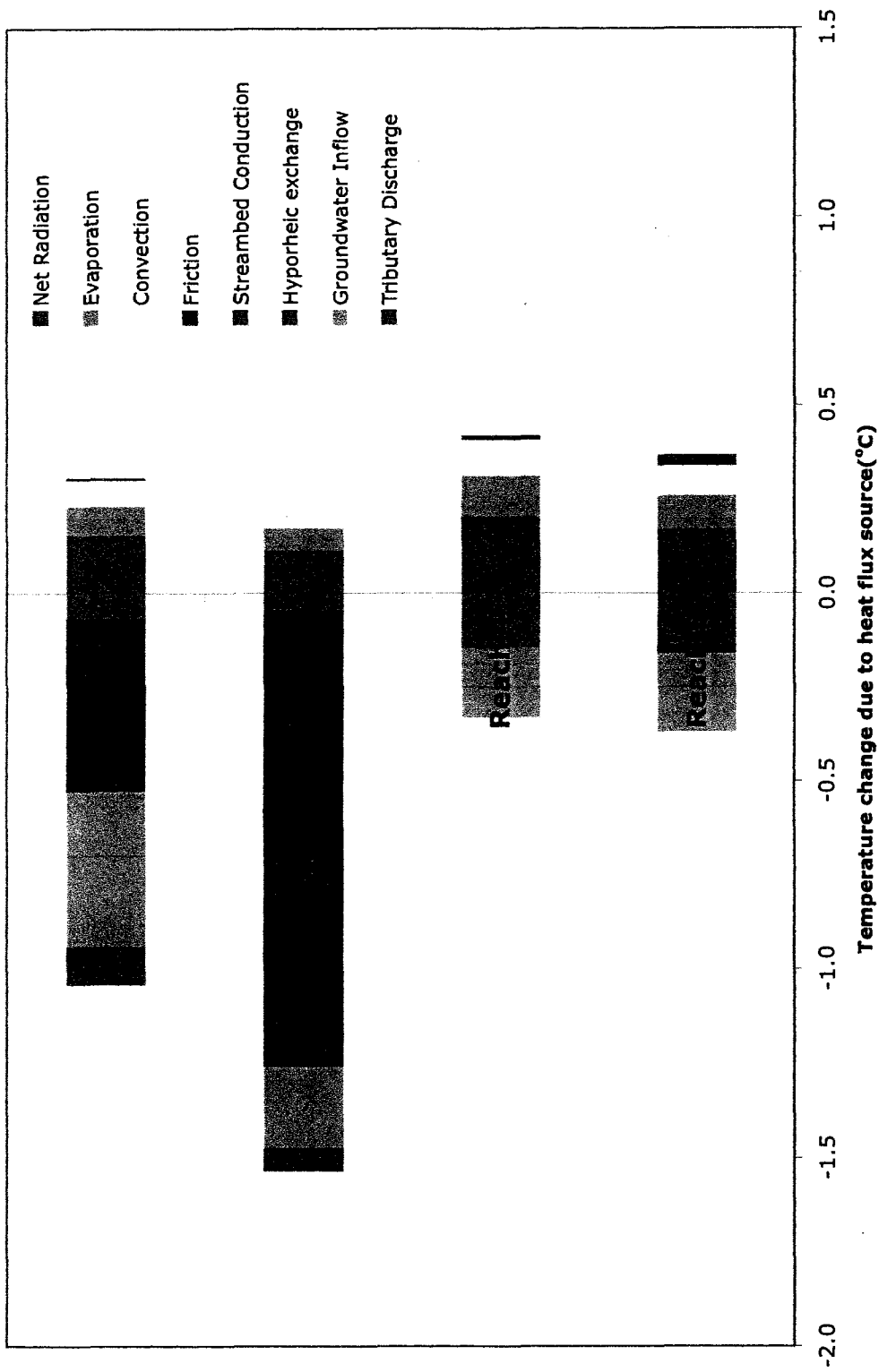


Figure 4-51 Temperature change by mechanism and reach, Wednesday Hill Brook in Lee, NH

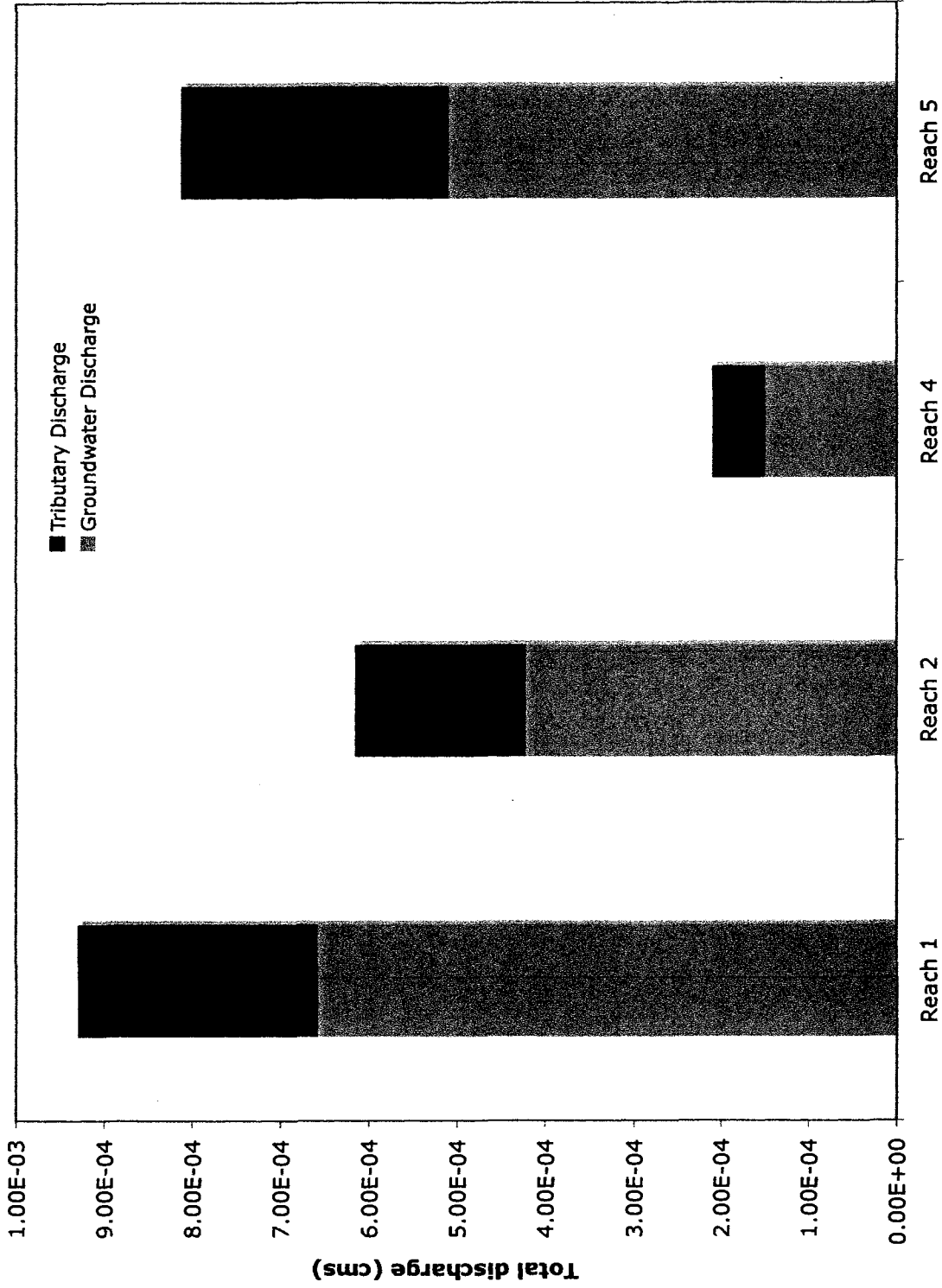


Figure 4-52 Groundwater and tributary discharge estimates – heat budget water balance Wednesday Hill Brook in Lee, NH

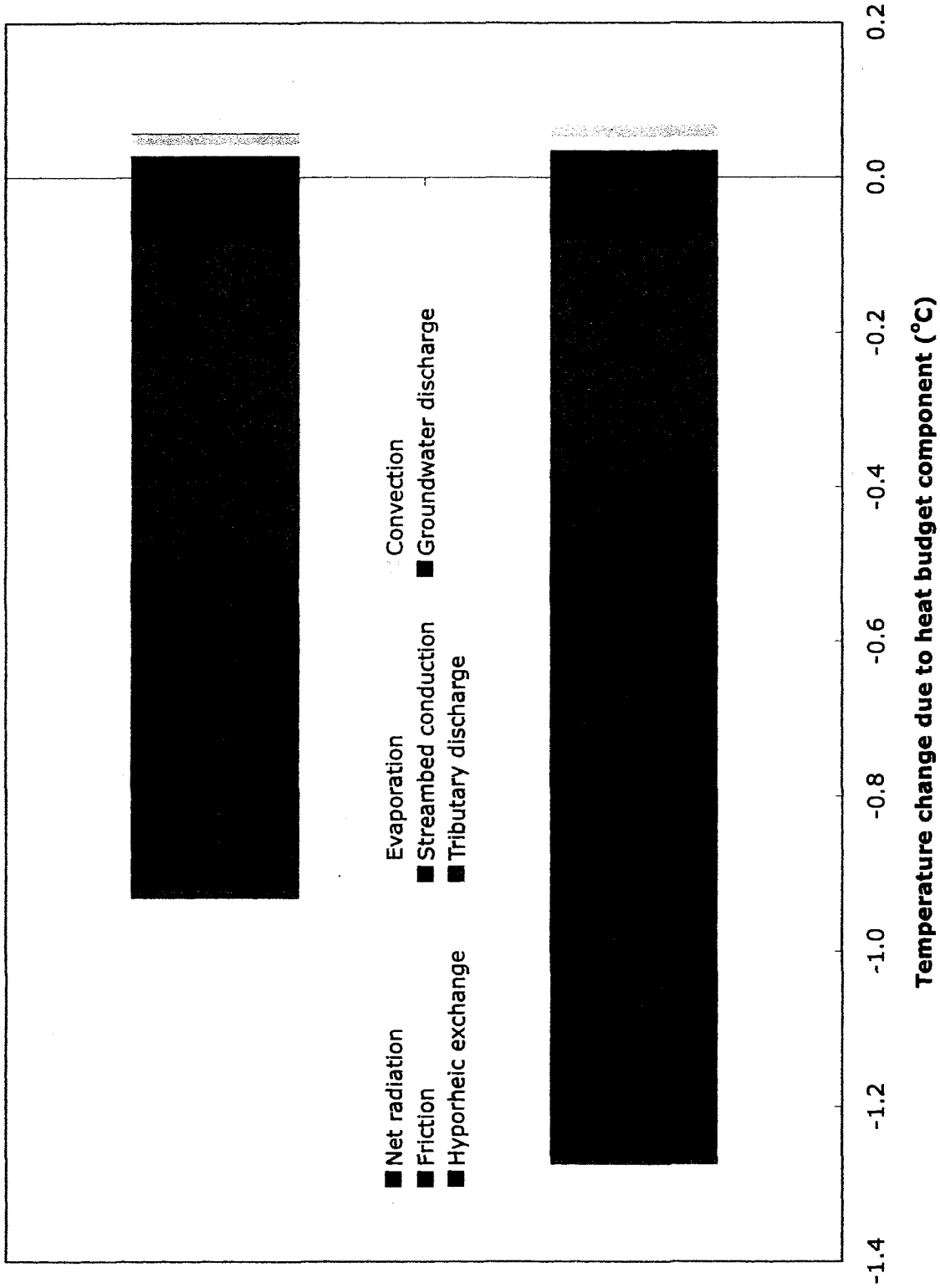


Figure 4-53 Modeled temperature change by mechanism and reach – Reach 1a and 2a Wednesday Hill Brook in Lee, NH

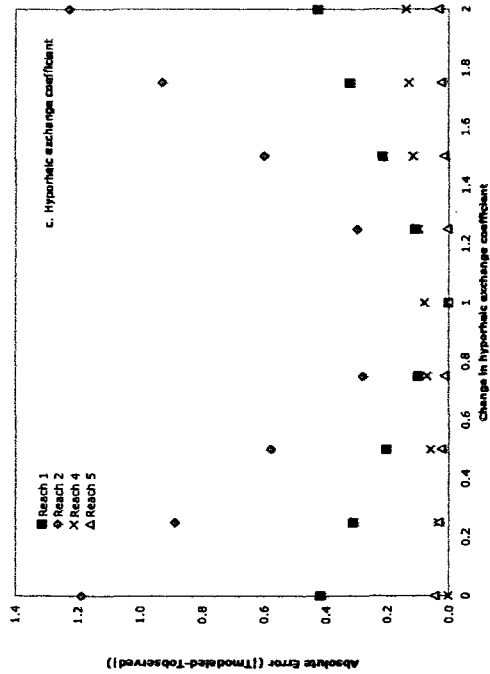
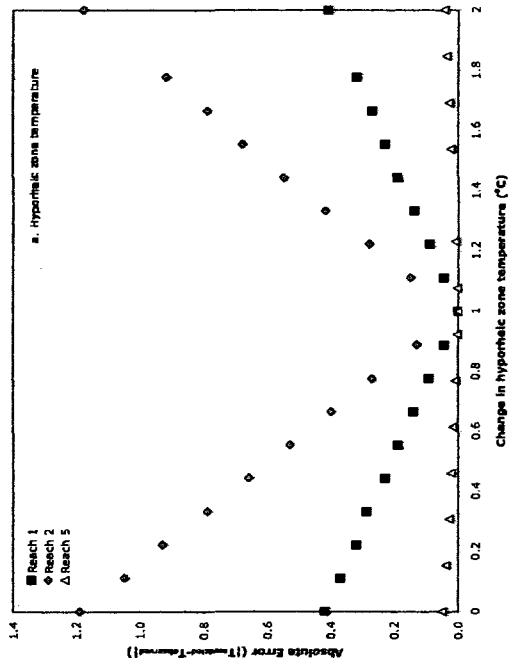
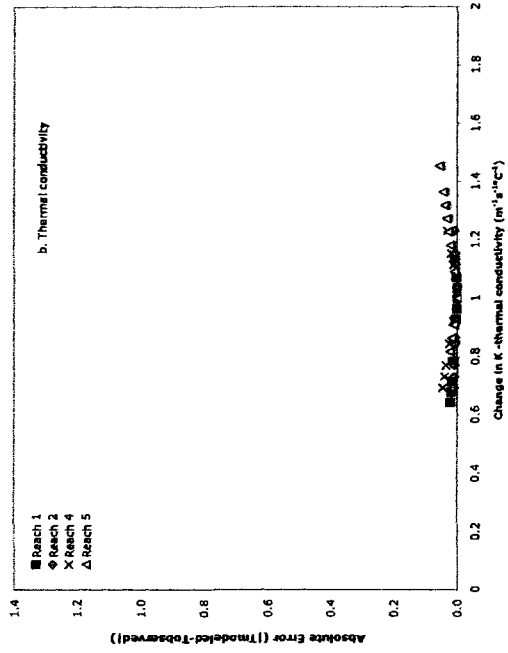


Figure 4-54 Heat budget model sensitivity analysis –
 a. hyporheic zone temperature, b. thermal
 conductivity, and c. hyporheic exchange coefficient
 Wednesday Hill Brook in Lee, NH

CHAPTER 5

DISCUSSION

Introduction

The research on Wednesday Hill Brook helped to answer many of research questions, refuted several hypotheses, and raised new questions about the role of groundwater and hyporheic exchange on Wednesday Hill Brook and other coastal streams. Detailed temperature measurements, geomorphic characterization and statistical and heat budget analysis reveal that the WHB watershed is a complicated hydrologic system. Stream and catchment *geomorphology, groundwater and tributary discharge, and instream structures* and bedforms are all important components of stream temperature reduction and maintenance.

Data analysis and heat budget modeling identified coupled groundwater and tributary discharge, hyporheic exchange, and streambed conduction processes significantly moderating WHB stream temperature. Groundwater discharge and hyporheic exchange are the most important summer cooling mechanisms in reach 1 and 2. In the lower reaches, groundwater discharge and streambed conduction are the most significant influences. Net radiation had the largest influence on stream warming. The study reach has a dense canopy cover of

88% so the radiation influence is small compared to the cooling influence of groundwater and hyporheic exchange.

This section describes and places the research questions in context. Important linkages among geomorphology, hyporheic exchange and stream temperature moderation as well as heat budget results are compared to similar research. A short review of possible errors and data gaps is also presented. Future application of FODTS for stream hydrology is explored. Finally, the potential contribution of these findings to understanding coldwater stream habitat and biogeochemistry is summarized.

Spatial and temporal distribution of temperature

A clear pattern of temperature change occurs along the study reach during the late summer and early fall period in 2007. A mean stream temperature reduction from 15.5 to 13.5°C is achieved over the first 150 m (reduction zone). Below, only moderate temperature change occurs. Cool temperatures are maintained with only minor warm ups in the lower two-thirds of the reach (maintenance zone).

The longitudinal temperature pattern in the reduction zone contains two major and two minor areas of temperature reduction. The major areas correspond to the confluence of western spring fed tributaries to the brook (1W and 2W) and

the minor areas correspond to the confluence of an undesignated tributary and 3W, also small spring fed features.

Below the reduction zone, multiple local temperature declines coincide with log dams and steps as well as zones of preferential groundwater flow. A cool temperature anomaly occurs at the head of reach 3 and at the head of reach 5. Stretches of gradual temperature increase are moderated by cooling influences. The final mean stream temperature at the end of WHB, 13.5°C, equals that at the end of reach 2.

Groundwater is the foundation for temperature reduction and moderation from upstream to downstream. FODTS mean temperature profiles for FC 07-1 and FC 07-2 show that longitudinal temperature changes persist over time. The strong correlation between temperature standard deviation and average temperature substantiates that a strong and constant summer cooling influence is provided by groundwater. This temperature change pattern is expected to be reversed in winter when the stream is colder than groundwater. Temperature declines would become temperature increases and vice versa.

Stream temperature is generally expected to increase downstream in rivers and streams as streams widen, canopy cover is reduced and heat is added to the stream through radiation (Vanotte et al., 1980, Bechsta et al., 1987). Small scale

studies have shown, however, that temperature can decrease downstream from increased canopy cover, groundwater discharge and hyporheic exchange (Story et al., 2003; Johnson, 2004; Selker et al., 2006).

Pools and unclassified features (largely runs and glides) were found to be the most time stable features. Riffles, steps, and areas near tributaries were less time stable. This follows the expected pattern of upwelling and downwelling defined and reinforced by Hendricks and White (1988), Storey et al. (2003), and Kashahara and Wondsell (2003) as shallow riffles and steps respond more quickly to radiation influences and pools and runs are influenced by upwelling of cooled water. More importantly areas defined by unique geomorphology, as illustrated in the comparison of reach time stability characteristics, had unique temperature patterns and time stability characteristics.

Vertical hyporheic extent and hyporheic exchange coefficients

There is significant cooling with depth in most locations on WHB. Diurnal variations in stream and streambed temperature suggest hyporheic flow is largely limited to the upper 20 cm in most locations. At many riffle-pool or step-pool features, a pattern of upwelling and downwelling was documented by vertical hydraulic gradients and dampening of diurnal temperature fluctuations with depth. At WHB, the piezometers and pairs that have the most significant vertical hydraulic gradients and temperature penetration are adjacent log dams that

create significant local changes in topographic gradient (237, 292, 295, 430 and 443 m). In several studies, large local variations in topography from features such as steps and beaver dams have been found to induce hyporheic exchange (Lautz and Siegel, 2006; Fanelli and Lautz, 2008; Kashahara and Hill, 2006).

The heat budget model identified hyporheic exchange as a major mechanism in temperature moderation in reach 1 and 2, but hyporheic exchange was absent in reach 3 and only moderately important in reach 5. Furthermore, small-scale heat budget modeling at reach 1a and 2a showed local enhancements in hyporheic exchange in zones having strong lateral groundwater inflows. Unfortunately, no piezometers were located in the zones and hydraulic gradients or detailed temperature patterns around these features were not documented. Temperatures at the nearby piezometer, 237 m, support hyporheic exchange to a 40 cm depth. Downstream of reach 2, another area of locally enhanced hyporheic zone exchange was documented at the log dam cascade. Hyporheic exchange is nearly absent in the meander reach and penetrates to roughly 20 cm in reach 5. It is locally strong only at the step created by the logdam between 430 and 445 m. This is consistent with Story et al.'s, (2003) finding that in groundwater discharge areas only local stream gradient increases can induce hyporheic exchange.

No tracer tests were conducted for this study so hyporheic exchange rates were not independently tested. Hyporheic exchange rates estimated using the heat budget model were in a range from 0.000004 s^{-1} in reach 5 to 0.00023 s^{-1} in reach 2. Cozzetto et al. (2006) arrived at an exchange coefficient of 0.0000023 s^{-1} through tracer tests in an Antarctic stream. Story et al. (2003) calculated an exchange coefficient between 0.0006 and 0.0027 s^{-1} through tracer tests in a small stream setting in Canada. Lautz and Siegel (2006) estimated exchange coefficients between 0.0003 and 0.0006 s^{-1} in the Red Canyon Creek, which is a slightly larger stream and has several beaver and logdams. The values derived for WHB agree well with previous observations and suggest that FODTS and energy budget analysis can provide reasonable values at a range of scales.

Geomorphology and stream temperature

Both catchment and instream geomorphology are important to the reduction and maintenance of summer cool temperatures at WHB. The catchment morphology controls both the delivery and temperature of groundwater and surface water that enters WHB. The streambed morphology influences temperature moderation with instream structures, streambed topography and streambed alluvial deposits.

The vertical hydraulic gradient data were essential to understanding the localized hyporheic exchange patterns and areas of groundwater discharge. Some of the

measurements did not always correspond with the expected downward gradients at riffles and upward gradients at pools.

Gradients observed at the pools within the stream are upward as generally expected. Only one pool suggests a downward gradient. The piezometer at this location (276 m) is within a reach where multiple log dams create a cascade. These bed forms may work to alter subsurface hydraulic gradients downward even though a pool is observed at the surface.

The upward hydraulic potential observed at 7 of the 14 riffles or runs was not expected, based on published observations and modeling that suggests that downwelling predominates at riffles and convex bed forms (Vaux, 1968; White et al., 1988). Several factors may contribute to these anomalous observations. Riffles in this stream can be long and the distance between riffle head and riffle tail was observed vary from less than 1 to 10 m depending on location.

Bedform irregularities created by multiple log dams often form cascades. In areas of groundwater discharge to a stream, the upward potential of discharging groundwater, may overprint the otherwise downward potential at riffles due to hyporheic exchange. The potential due to upward migration of groundwater into the streambed may impose a hydraulic head great enough to moderate or negate the downward potential due to downwelling at riffles (Storey et al., 2003).

Catchment influences on stream temperature

Groundwater discharge provides stream baseflow and is an important source of cool water for the stream and streambed. WHB is a gaining stream throughout most of the study reach and catchment hydrology controls the delivery of groundwater to the stream. The upper catchment, that contains reach 1 and 2, is a discharge zone for groundwater from the deltaic sand and gravel deposit to the west of WHB. The contact of this permeable sand with the marine silt and clay creates springs near the base of the hillslope. These springs coalesce to form small tributaries that flow even during low flow in late summer. The springs also carry the coarse sand and gravel away from the hillslope and form a large permeable groundwater discharge zone beneath the tributaries. These conduits enter WHB as surface water and focused groundwater discharge zones. Seepage occurs along the stream, which also provides some groundwater discharge. In reach 1 and 2, spring brooks are the primary points of discharge.

Bedrock beneath the upper catchment area also influences groundwater discharge. The EM survey suggests that bedrock is shallow at the top of the reach and the end of reach 2 where the valley constricts and changes course. This bedrock high may also focus groundwater discharge to the stream in reach 2 and at the beginning of reach 3.

In reaches 3 and 4, the catchment provides less groundwater because the stream is entrenched below the floodplain into the less permeable silt and clay

deposit. Near the end of reach 4 however, catchment influences increase as the stream approaches an active floodplain. In the lower portion of reach 4, reach 5 and upper reach 6, preferential flow pathways and small tributaries carry groundwater primarily from the western hillslope to the stream. The stream is slightly entrenched and largely disconnected from the floodplain again at the end of the study reach. Where the stream is entrenched in reach 4 and reach 6, the temperature increases suggest that there is no groundwater gain in these segments.

The focused groundwater discharge zones identified by Selker et al. (2006) and Lowry et al. (2007) were also identified at WHB. In the upper reaches, these zones were few but significant. More, less significant zones were evident in the lower meander reach and many were observed in the floodplain reach. FODTS and remotely sensed studies of groundwater discharge to streams and estuaries also show that groundwater discharge occurs in focused zones, rather than as consistent, diffuse groundwater discharge (Roseen, 2002; Loheide and Gorelick, 2006, Henderson et al., 2009). Though discrete areas of groundwater discharge to streams and rivers have been identified in many hydrologic studies, evenly distributed diffuse groundwater discharge is the typical conceptual model of groundwater influence to a stream or river. As detailed measurements become more routinely available through FODTS surveys, a new model with zones of discrete groundwater discharge should be considered.

Stream channel morphology and stream temperature

Step pool morphology gives way to riffle pool morphology within the first 80 m of the study reach. Multiple log dams downstream of the step pool sections create locally steeper gradients. Log dams were clustered in several areas. The transition between reach 1 and 2, the upper portions of reach 3, and upper reach 5 and 6 all contain clusters of log or debris dams.

As suggested in the previous section on vertical hyporheic extent, stream steps and logdams at WHB create enhanced hyporheic flow zones. Several step-pool units were observed upstream and downstream of the major temperature decline near 1W in reach 1. At 2W in reach 2, two log dams were observed upstream of the confluence. There is also a deep pool at the 2W outlet coincident with the local temperature decline. These stream features locally increase the longitudinal gradient.

At 3W and the smaller western tributary adjacent to it, only a small and localized temperature decline occurs even though tributary temperatures are significantly lower than WHB. Unlike 1W and 2W, the confluence of 3W does not coincide with a significant instream feature but joins WHB at a long riffle section with a mildly sloping and deep streambed. The lack of streambed topography prevents strong hyporheic exchange and translates to a small temperature impact.

The influence of instream structures and bedforms on hyporheic flow is well documented. Step-pool units, log dams, both natural and manmade, and riffle-pool units all increase hyporheic exchange and flux (Hendricks and White, 1991; Harvey and Bencala, 1993; Kashahara and Wondzell, 2003; Storey et al., 2003; Kashahara and Hill, 2006; Lautz and Siegel, 2006; Gooseff et al., 2007; Fanelli and Lautz, 2008; Hester and Doyle, 2008). Hendricks and White (1988), Lautz and Siegel (2006) and Fanelli and Lautz (2008) documented log dams or beaver dams as important drivers of hyporheic exchange. Step-pool units were also found to promote significant hyporheic exchange flow (Harvey and Bencala, 1993; Kashahara and Wondzell, 2003; Gooseff et al., 2005). These bedforms also promote local downwelling and upwelling patterns in streambed flow.

Increased local longitudinal gradient and coarse substrate in constructed riffles and steps was found to increase the vertical gradient and hyporheic zone penetration depth (Kashahara and Hill, 2006). In the case of WHB, steps, log dams and riffles and pools retain or are composed of permeable sand, gravel and cobbles that are regularly flushed by streamflow and stormflow. Their high hydraulic conductivity likely further enhances hyporheic exchange.

Prior to heat budget modeling, it was assumed that groundwater inflow beneath small tributaries was the primary cause of the observed temperature reduction zones. The modeling shows that hyporheic exchange has an equal or greater

role in temperature reduction at both large and small scales. The combination of steps and log dams and these discharge features promote sustained cooling. Strong downwelling through a very cool streambed enhances hyporheic cooling and streambed conduction. The WHB results are similar to other gaining streams in which instream structures played a major or singular role in driving hyporheic flow (Harvey and Bencala, 1993; Hester and Doyle, 2008).

Kashahara and Wondsell (2003) measured and modeled hyporheic exchange in second order and fifth order streams and compared hyporheic exchange mechanisms through sensitivity analysis. Local gradient changes and channel morphology were major morphologic differences between the second and fifth order streams. They found that hyporheic exchange was most heavily influenced by stream morphology, step-pool and riffle-pool sequences, in the second order stream whereas secondary channels in the anastomosing stream were most sensitive to hyporheic flux in the fifth order streams. Even though WHB is a first order stream along the entire study reach, the progression of stream and channel morphology from a step-pool to riffle-pool and stream gradient changes from 0.5 to 0.001 could emulate these differences. Vertical hyporheic exchange is dominant in the upper reaches where local gradient changes are imposed by step-pool units and log dams. In the lower reaches, preferential flow pathways in floodplain materials deliver cool water and promote enhanced streambed conduction. Vertical hyporheic flow is minimal here compared to reaches 1, 2

and 3, but lateral hyporheic flow may be at work especially in the floodplain-influenced areas of reaches 4 and 5. Not enough data are available on lateral flow to and from the floodplain to document this process.

In summary, at WHB the steps, logdams and riffle pool sequences seem to be most important to hyporheic exchange and temperature moderation in the upper reaches. Small tributaries and subsurface preferential flow pathways (which could be compared to secondary channels) were most important to temperature moderation below reach 2.

Heat budget modeling

Poole and Berman (2001) state that riparian shade and groundwater have the greatest influence on stream temperature. Hyporheic groundwater (exchange) and tributaries are only moderately important in first and second order streams. Heat budget modeling at WHB confirms that the limited radiation afforded by the heavy riparian canopy and groundwater discharge are the underlying keys to temperature moderation at WHB. But, at WHB, it is the focused groundwater discharge associated with tributaries, in combination with hyporheic exchange that is critically important to temperature reduction and moderation.

The heat budget developed for this study was based on previous work by Webb and Zhang (1999), Storey et al. (2003); Johnson (2004); Webb and Zhang (2004)

and Cozzetto et al. (2006). Non-advective heat fluxes were primarily modeled in some studies (Webb and Zhang, 1999, 2004; Johnson, 2004) but they acknowledged the importance of advective processes. Other studies specifically targeted the advective components of the heat budget (Storey et al., 2003; Cozzetto et al., 2006; Loheide and Gorelick, 2006).

The rivers studied by Webb and Zhang (1999) are in Dorset, UK. They are strongly influenced by springs and groundwater discharge but are somewhat larger than WHB with average channel widths of 3 to 10 m. During the summer monitoring period, net radiation accounted for 89 to 94% of the heat gain followed by convection. At WHB, net radiation added approximately 50% of the heat to the stream followed by equal parts of convection and evaporation in most reaches. Heat gain from friction was less than 1% for the UK water courses and was much less than 1% at WHB. The major heat losses in the UK rivers were from bed conduction for the smaller stream (70%) and evaporation for the larger stream (57%). Bed conduction was of minor importance in the upper reaches of WHB, but accounted for nearly 50% of the heat loss in the lower reaches. Because the stream temperatures were significantly lower than the air and humidity and wind speed were low, condensation added heat to WHB rather than providing heat loss through evaporation.

The advective heat gains studied in the UK were groundwater and precipitation. Summer precipitation heat gain was found to be minimal while groundwater accounted for as much as 15% of the summer heat gain in the smaller river. In contrast, at WHB, groundwater and hyporheic exchange are the major components of heat loss in the upper reaches and groundwater inflow in combination with streambed conduction dominates heat loss in the lower reaches. No discussion of hyporheic exchange was included in the Webb and Zhang (1999) study.

Johnson (2004) studied a steep mountain stream in Oregon that was dominated by bedrock in one reach and had an alluvial streambed in another reach. She artificially shaded portions of the stream to determine the impact of radiation on stream temperature. The artificially shaded reaches of the study stream had the greatest heat gains from convection. Heat losses from evaporation and bed conduction were the most important non-advective temperature influences. Advective influences were not quantified, but the decrease in temperature downstream in this study was attributed to changes in substrate, bedrock to gravel and sand, and hyporheic exchange.

The heat budget analysis of a wide Antarctic stream that drains an alpine glacier, (Cozzetto et al., 2006) determined that radiation accounted for 81% of reach heat gain and groundwater discharge accounted for 19%. Convection and

evaporation were the major heat loss fluxes, 30 and 29%, respectively. Bed conduction and hyporheic exchange made up 24 and 17% of the heat loss, respectively. Direct comparison of this study to WHB is difficult due to the size of the stream, the more extreme temperature conditions, and the presence of permafrost beneath the streams. It does point out, however, the importance of multiple advective factors in stream temperature moderation.

Perhaps the most relevant studies to that of WHB were conducted in British Columbia (BC) along streams that had been recently clearcut (Story et al., 2003) and along restored and unrestored reaches of Cottonwood Creek in Northern California (Loheide and Gorelick, 2006). The BC streams were similar in width to WHB but had a steeper longitudinal gradient (7% and 25%). The length of the study reaches were approximately 160 and 225 m long. The temperature at one of Story et al.'s (2003) study streams decreased with distance downstream like WHB. Their observed downstream temperature decrease of 2.3°C was comparable to the 2.2°C decrease at WHB. Using data from one day in mid August, streambed conduction and hyporheic exchange were found to account for 35 and 25% of stream cooling, respectively, and groundwater accounted for the remaining 40% of heat loss. Daily temperature fluctuations were also found to be moderated by hyporheic exchange and streambed conduction.

Loheide and Gorelick (2006) modeled groundwater and hyporheic flux in restored and unrestored reaches of a 1.7 m stream and found that measured temperature moderation in the restored reach required both groundwater and hyporheic flux in order to match the observed temperature fluctuations. If hyporheic exchange was ignored, temperatures were over predicted by 2°C in the middle restored reaches and were over predicted by 4°C without groundwater and hyporheic flux. They concluded that hyporheic exchange was an important factor in stream temperature moderation where highly transmissive riffles were created during stream restoration. At WHB, heat budget modeling indicated that if hyporheic exchange was ignored, then temperatures were over-predicted by 0.4°C or nearly 50% of the total temperature change in reach 1. In reach 2, no hyporheic cooling results in an over-prediction of temperature by 1.2°C or 90% of the total temperature change. Both these reaches contained transmissive stream steps or log dams that are thought to promote hyporheic exchange.

A recent review of stream and river temperature dynamics articles shows that heat budget analyses make up less than 5% of these publications topics (Hannah, 2008). The application of the heat budget to WHB stream temperature was key to the understanding of the major controls on temperature changes along a reach. It was especially useful for looking at sub-reach processes. These models can be further refined as more detailed measurements are taken. A logical next step at WHB would be to use the continuous data collected with

the Hobos and FODTS to model both advective and non-advective influences and further define temporal changes in both non-advective and advective fluxes. This could lead to a better understanding of the dynamic influence of hyporheic exchange and streambed conduction.

FODTS surveys for stream hydrology and temperature research

Few stream temperature studies show the detail in stream temperature variation that is provided by the FODTS survey method. This is still an emerging tool in hydrology. Selker et al. (2006) used an FODTS survey to measure stream temperature along an 1,100 m reach of the Maisbich River in Luxembourg. Like WHB, groundwater discharge to the stream was discrete and was found to enter the stream in four locations. Selker used the magnitude of temperature change at inferred discharge points to estimate groundwater flow rates to the river. A wetland stream in Wisconsin was also characterized using FODTS (Lowry et al., 2007). Like WHB, they noted local decreases of several degrees at focused groundwater discharge points but there was no sustained temperature reduction over the length of the survey. The FODTS data were cross-referenced to seepage meter data, which allowed the definition of losing, transitional and gaining portions of the stream.

Other detailed temperature surveys on a larger scale were conducted using infrared imagery. Loheide and Gorelick (2006) used forward looking infrared (FLIR) imagery to analyze temperature along a restored and unrestored reach of

Cottonwood Creek in northern California. This method also provided spatially detailed information on stream and riparian temperatures over a 1.7 km reach. The FLIR data were cross referenced to temperatures measured at six Hobo temperature datalogger sites. Similar to WHB, they found that groundwater discharge was important to temperature moderation but that buffering of stream temperatures was significantly enhanced by hyporheic exchange at constructed riffles composed of sediments with high hydraulic conductivity. Thermal infrared imagery was also used to study temperature changes along the Clackamas River in Oregon (Burkholder et al., 2008). Multiple local temperature changes were interpreted from the data, and accuracy of interpreted temperature was found to be 0.5°C over a 15 km reach. These larger scale projects would be difficult logistically and economically with FODTS technology. FODTS advantages over remotely sensed temperature include higher instream detail and the ability to work in narrow headwater channels and streams with riparian canopy.

Other FODTS survey limitations include the need for a continuous power supply, as well as protection against weather and security for the computer and laser signal generator and processor. At WHB, a small and efficient generator and large steel box were used to provide these needs, but at remote sites this mobilization would be difficult. Installing and retrieving the cable was also very time consuming and strenuous, but once installed it stayed in place until large rain events began to erode the streambed and unearth the cable. Rodents chewed through the FODTS cable at multiple locations where the cable ran over the ground in the first field survey. Suspending the cable above the ground in the second survey prevented a repeat of this expensive encounter with nature.

Detailed notes and cross-referencing is also required in FODTS surveys in order to benchmark stream and catchment morphology to changes in temperature. The printed meter markings on the cable greatly assisted this process. Establishing FODTS stations prior the preliminary field data collections would have greatly assisted analysis.

Data deficiencies and additional data needs

Streamflow measurement and ArcHydro analysis

The tributaries to WHB have a significant streambed zone, which is important to stream temperature moderation. In future efforts, direct discharge measurements would better quantify the relationship between groundwater and surface water at these features. While ArcHydro streamflow analysis was found to be valuable in delineating major drainage areas and streamflow gains, it significantly over predicted actual surface water flow during this period of low flow in late summer. Intermediate streamflow measurements along WHB would also have been helpful to verify ArcHydro estimates of streamflow gain and to distinguish gaining and non-gaining segments of the stream. The LiDAR DEM made the ArcHydro streamflow estimates possible. With 30 m DEM that is more readily available, the analysis would have been much more error-prone or impossible at the fine scale required for WHB.

Vertical hydraulic gradient data

Hydraulic gradient data are questionable at some piezometers and additional gradient data would have provided much needed data on hyporheic exchange

near 1W and 2W. Occasional point measurements from piezometers offer limited spatial and temporal resolution. For example, in longer reaches where runs occur before pools, subsurface flow may turn upward prior to entering a pool as stream gradients moderate and bedforms change. Additionally, the stream flow discharge, and correspondingly, the depth of stream water was dropping over the course of FC 07-1 because there had not been rainfall for several weeks. This drop in stream levels could lead to an overestimate of the hydraulic potential at certain sites, especially at riffles where the anomalous results occurred. Pressure transducers in the stream and subsurface in reaches 1 to 3 would have been valuable to better define longitudinal changes in gradient and to detect diurnal changes in streambed gradients in long riffles and at instream structures and bedforms.

The upper reaches had few gradient or subsurface temperature measurements. The working hypothesis was that hyporheic exchange would predominantly occur in the deeper sand beds in the meander and floodplain reaches. Additional hydraulic gradient and streambed temperature data collection in the step-pool units around 1W and within the log dams and downstream pool at 2W would provide extremely valuable information to support or refute the heat budget model's hyporheic exchange and streambed conduction results.

Floodplain and valley geomorphology

The LiDAR survey provided crucial topographic detail in understanding surface flow patterns and controlling catchment structures. Detailed floodplain subsurface evaluations and additional geophysics could provide further clues into the shallow subsurface geology and hydrology in reaches 2, 4 and 5. In reach 2, soil pit excavations would lead to a better understanding of groundwater sapping as a geomorphic mechanism in valley formation and groundwater discharge. Seismic refraction would better characterize the bedrock surface in the stream valley and support or refute the hypothesis that groundwater discharge is enhanced by shallow bedrock. It might also define structure that influences the cold-water anomalies at valley constrictions in reaches 3 and 5.

Remnant stream channels could be identified in reaches 4 and 5 with additional subsurface probes, piezometers, sediment cores, and geophysics. Definition of these channels supplemented by water levels and temperature measurements would help to determine floodplain and streambed connectivity and define lateral hyporheic exchange.

Recommendations for stream temperature measurement

It is apparent from this study that one temperature measurement at Wednesday Hill Road would not have adequately characterized the temperature regime of this stream. But how much is enough? The FODTS provided excellent detail

and this foundation will greatly enhance future hydrologic and temperature research at WHB. However, a survey of this nature is not often possible or warranted. In this study, Hobos were also placed at points of interest and at regular intervals along the study reach. This information provided the general downstream temperature pattern but could not identify minor and major anomalies and temperature variations that are valuable to understanding temperature processes and structure.

This study has underscored the importance of understanding instream and catchment geomorphology and local geologic influences in hydrologic studies. After a site walk and review of surficial geology and hydrology, a basic first step to better understanding stream dynamics would be an initial survey of stream temperature with hand held temperature equipment to measure trends and significant temperature differences followed by a Hobo type data logger survey at regular intervals and at places of interest identified in the initial survey. The scale of the measurements would be dictated by the information sought. The temperature patterns detected could then lead to strategically collecting measurements in areas of interest.

If only a few measurements are needed for regular stream temperature monitoring, it appears that pool temperatures provide the most time stable locations. In this stream, where groundwater plays a large role in stream

temperature, both riffles and pools provide representative temperatures.

Measuring temperature at road crossings and just upstream and downstream will probably not provide sufficient detail if biological characterization is desired.

Coldwater stream habitat and groundwater

This study sheds light on the local and regional features that sustain cool headwater streams and could lead to identification of other low order streams with similar temperature dynamics. Coldwater streams are those that maintain an average monthly temperature of 18°C or less (NHDES, 2007). Brook trout require temperatures of less than 20°C (EBTJV, 2005). Clearly WHB qualifies as a coldwater stream within the limits of the study reach. These cool streams are thought to be uncommon in coastal New Hampshire. Currently coldwater streams are delineated in NH primarily using latitude and elevation (NHDES, 2007). Areas north of the Lakes region are the expected locale for these streams.

Because coldwater streams provide valuable habitat for species such as brook trout and anadromous fish, further identification of these stream and stream reaches is important to better understand cold stream distribution.

Understanding the important temperature drivers will help to protect and restore the habitats and landscape that sustain them. Areas with similar geologic

settings could be identified and mapped through GIS then followed up with reconnaissance temperature and biological surveys.

As reviewed in the introduction, several studies clearly link groundwater with coldwater habitat. Power et al. (1999) states that the moderating influence of groundwater contribution to a stream or river is important for redds, the gravelly area where fish lay eggs and fry develop. Thermal refugia in the summer (cool regions) and in the winter (warmer regions that do not freeze) are also important for the survival of many fish species. The presence and size of coldwater patches was found to be essential to salmonid species survival in an Oregon stream and supported additional data collection and stream restoration to maximize these areas (Ebersole et al., 2003).

Boulton and Hancock (2006) refer to rivers and streams fed by groundwater as groundwater dependent ecosystems and recommend that unique management strategies be employed to maintain their ecologic value. Chu et al. (2008) developed a GIS model for Ontario fisheries that links sustainable coldwater fish habitat and geology by assigning a stream baseflow index based on the properties of adjacent geologic materials. Streams that flowed within coarse sand and gravels deposited by Quaternary glacial processes and over bedrock were assigned the highest baseflow index values. Because baseflow represents groundwater discharge, the authors suggest that high baseflow areas will be

most effective in moderating stream temperature changes due to climatic change and canopy disruption.

Like eastern Canada and many formerly glaciated northern landscapes, New Hampshire rivers and streams are often coincident with or close to small to large pockets of sand and gravel deposits. The large deposits have been well mapped for groundwater resource extraction and protection. This study clearly points to the importance of even small deposits such as the delta in Lee to stream habitat and temperature moderation. Alluvial deposits that contain preferential flow paths should also be important to lateral hyporheic exchange in lower gradient and higher order streams.

Section 6

CONCLUSIONS

This research defined in detail the site specific geomorphologic and hydrologic characteristics that combine to sustain a coldwater stream setting in coastal New Hampshire. Underlying all other factors is the continuous discharge of groundwater to the catchment and catchment and instream structures that enhance and maintain the cooling influences.

Groundwater provides a constant source of coldwater to tributaries and focused groundwater discharge points. Groundwater also maintained low streambed temperatures, which provided a consistent streambed temperature gradient for streambed conduction and hyporheic cooling. Sources of large woody debris create and maintain log dams that also provide local stream gradient changes that enhance hyporheic exchange.

Where a series of steps or log dams occurs in conjunction with focused groundwater discharge, longitudinal and vertical streambed gradients combined with cold streambed temperatures create a stable, instream cooling zone. This combination of influences over a short distance has not been previously identified in hyporheic zone and stream temperature literature. Definition of this hydrologic setting could lead to identification of similar areas within the region and

elsewhere. It also suggests that stream restoration design could be modified where appropriate to incorporate structures that enhance hyporheic exchange near cool tributaries or groundwater discharge features.

This study also reinforces findings by others that vertical hyporheic exchange is most important in steeper stream reaches and lateral hydrologic discharge is more important as gradients decrease. Streambed conduction in areas of lateral groundwater inflow has also been shown to be an important cooling mechanism.

The temperature delineation made possible by the FODTS stream temperature survey and the detailed topographic definition of the catchment and stream afforded by the LiDAR survey provided the resolution needed to define the focused groundwater discharge zones, the morphology of the entrenched and active floodplain areas and to identify the unique geomorphic features that are developed by groundwater sapping. Groundwater discharge or recharge within streams and rivers is largely understood and defined by the amount of streamflow gain or loss along a reach. At WHB, groundwater discharge was determined to be focused in discrete areas along the reach and the characteristics of these focused areas changed from upstream to downstream. This detailed temperature survey tool may re-define our understanding groundwater discharge mechanisms.

Most importantly this work should provide further corroboration of the importance of small scale features and mechanisms in low order and headwater streams. As we urbanize and suburbanize our landscape, attention to the importance of small riparian features such as the apparently minor tributaries and seeps on WHB as well as limiting the impervious surfaces area that cover groundwater recharge areas will only become more important. The relative importance of these capillary systems to the stream and river arteries, in terms of ecological linkages, sources of primary production and areas of nutrient transformation cannot be overemphasized.

References Cited

- Alexander, M. D., and D. Caissie. 2003. Variability and comparison of hyporheic water temperatures and seepage fluxes in a small Atlantic salmon stream. *Ground Water* 41:72-82.
- Anderson, M. P. 2005. Heat as a ground water tracer. *Ground Water* 43:951-968.
- Anderson, J. K., S. M. Wondzell, M. N. Gooseff, and R. Haggerty. 2005. Patterns in stream longitudinal profiles and implications for hyporheic exchange flow at the H.J. Andrews Experimental Forest, Oregon, USA. *Hydrological Processes* 19:2931-2949.
- Bechsta, R.L., Bilby, R.E., Brown, G.W., Holtby, L.B., and Hofstra, T.D. 1987. Stream temperature and aquatic habitat: fisheries and forest interactions. In *Streamside management: forestry and fishery interactions*. Edited by E.O. Salo and T.W. Cundy. Institute of Forest Resources. University of Washington. Seattle, WA. pp. 191-232.
- Bencala, K. E., V. C. Kennedy, G. W. Zellweger, A. P. Jackman, and R. J. Avanzino. 1984. Interactions of Solutes and Streambed Sediment .1. An Experimental-Analysis of Cation and Anion Transport in a Mountain Stream. *Water Resources Research* 20:1797-1803.
- Bencala, K. E. 1984. Interactions of Solutes and Streambed Sediment .2. A Dynamic Analysis of Coupled Hydrologic and Chemical Processes That Determine Solute Transport. *Water Resources Research* 20:1804-1814.
- Bencala, K. E. 1993. A Perspective on Stream-Catchment Connections. *Journal of the North American Benthological Society* 12:44-47.
- Birch, F.S., 1980, Seismic refraction surveys of kame plains in southeastern New Hampshire. *Northeastern Geology*, 2: 81-88.
- Birch, F.S., 1989, A geophysical study of Quaternary sediments near the late Pleistocene marine limit in Epping, New Hampshire. *Northeastern Geology*, 11: 124-132.
- Blumberg, J.E., 2002, Instream nutrient dynamics in five first order tributaries in the Lamprey River Watershed, New Hampshire, University of New Hampshire, MS Thesis, December 2002.

- Boulton, A. J., S. Findlay, P. Marmonier, E. H. Stanley, and H. M. Valett. 1998. The functional significance of the hyporheic zone in streams and rivers. *Annual Review of Ecology and Systematics* 29:59-81.
- Boulton, A. J., and P. J. Hancock. 2006. Rivers as groundwater-dependent ecosystems: a review of degrees of dependency, riverine processes and management implications. *Australian Journal of Botany* 54:133-144.
- Boulton, A. J. 2007. Hyporheic rehabilitation in rivers: restoring vertical connectivity. *Freshwater Biology* 52:632-650.
- Bowen, I.S. 1926. The ratio of heat losses by conduction and by evaporation from any water surface. *Physics Review*, 27, 779-787.
- Brown, L. E., D. M. Hannah, and A. M. Milner. 2005. Spatial and temporal water column and streambed temperature dynamics within an alpine catchment: implications for benthic communities. *Hydrological Processes* 19:1585-1610.
- Brunke, M., and T. Gonser. 1997. The ecological significance of exchange processes between rivers and groundwater. *Freshwater Biology* 37:1-33.
- Brocca, I., F. Melone, T. Moramarco and R. Morbidelli. 2009. Soil moisture temporal stability over experimental areas in Central Italy, *Geoderma*. 148: 364-374.
- Burkholder, B. K., G. E. Grant, R. Haggerty, T. Khangaonkar, and P. J. Wampler. 2008. Influence of hyporheic flow and geomorphology on temperature of a large, gravel-bed river, Clackamas River, Oregon, USA. *Hydrological Processes* 22:941-953.
- Castro, N. M., and G. M. Hornberger. 1991. Surface-Subsurface Water Interactions in an Alluviated Mountain Stream Channel. *Water Resources Research* 27:1613-1621.
- Chestnut, T. J., and W. H. McDowell. 2000. C and N dynamics in the riparian and hyporheic zones of a tropical stream, Luquillo Mountains, Puerto Rico. *Journal of the North American Benthological Society* 19:199-214.
- Chu, C., N. E. Jones, N. E. Mandrak, A. R. Piggott, and C. K. Minns. 2008. The influence of air temperature, groundwater discharge, and climate change on the thermal diversity of stream fishes in southern Ontario watersheds. *Canadian Journal of Fisheries and Aquatic Sciences* 65:297-308.
- Chow, V.T. D. Maidment and L. Mays. 1988. *Applied Hydrology*, Columbus, McGraw Hill.

- Collins, B. M., W. V. Sobczak, and E. A. Colburn. 2007. Subsurface flowpaths in a forested headwater stream harbor a diverse macroinvertebrate community. *Wetlands* 27:319-325.
- Conant, B. 2004. Delineating and quantifying ground water discharge zones using streambed temperatures. *Ground Water* 42:243-257.
- Constantz, J., C. L. Thomas, and G. Zellweger. 1994. Influence of Diurnal-Variations in Stream Temperature on Streamflow Loss and Groundwater Recharge. *Water Resources Research* 30:3253-3264.
- Constantz, J. 2008. Heat as a tracer to determine streambed water exchanges. *Water Resources Research* 44.
- Cozzetto, K., D. McKnight, T. Nylen, and A. Fountain. 2006. Experimental investigations into processes controlling stream and hyporheic temperatures, Fryxell Basin, Antarctica. *Advances in Water Resources* 29:130-153.
- Delcore, M and C. Koteff, 1989, Surficial geologic map of the Newmarket quadrangle, Rockingham and Strafford Counties, New Hampshire. U.S. Geological Survey Open File Report 89-105.
- Dent, L., J. Schade, N. Grimm, and S. Fisher. 2000. Subsurface influences on surface biology. In J.P. Jones and P.J. Mulholland, eds. *Streams and Groundwater*, 1st Edition, Philadelphia, Elsevier, 2000.
- Eastern Brook Trout Joint Venture, 2005, *Conserving the Eastern Brook Trout: An Overview of Status, Threats, and Trends*. Prepared by the Conservation Strategy Work Group.
- Ebersole, J. L., W. J. Liss, and C. A. Frissell. 2003. Cold water patches in warm streams: Physicochemical characteristics and the influence of shading. *Journal of the American Water Resources Association* 39:355-368.
- Edwardson, K. J., W. B. Bowden, C. Dahm, and J. Morrice. 2003. The hydraulic characteristics and geochemistry of hyporheic and parafluvial zones in Arctic tundra streams, north slope, Alaska. *Advances in Water Resources* 26:907-923.
- Eller, Michael.P., Radar facies and structure of the late Pleistocene marine and deltaic outwash deposits near the glacial-marine limit in coastal New Hampshire. M.S. Thesis, University of New Hampshire.
- Evans, E. C., and G. E. Petts. 1997. Hyporheic temperature patterns within riffles. *Hydrological Sciences Journal-Journal Des Sciences Hydrologiques* 42:199-213.

- Fanelli, R. M., and L. K. Lautz. 2008. Patterns of water, heat, and solute flux through streambeds around small dams. *Ground Water* 46:671-687.
- Findlay, S. 1995. Importance of Surface-Subsurface Exchange in Stream Ecosystems - the Hyporheic Zone. *Limnology and Oceanography* 40:159-164.
- Fischer, H., F. Kloep, S. Wilzcek, and M. T. Pusch. 2005. A river's liver - microbial processes within the hyporheic zone of a large lowland river. *Biogeochemistry* 76:349-371.
- Fowler, R. T., and R. G. Death. 2001. The effect of environmental stability on hyporheic community structure. *Hydrobiologia* 445:85-95.
- Franken, R. J. M., R. G. Storey, and D. D. Williams. 2001. Biological, chemical and physical characteristics of downwelling and upwelling zones in the hyporheic zone of a north-temperate stream. *Hydrobiologia* 444:183-195.
- Freeze, R.A and J. Cherry, 1979, *Ground Water*, Englewood Cliffs, NJ. Prentice-Hall.
- Freeze, R. A., and P. A. Witherspoon, 1968, Theoretical analysis of regional groundwater flow, 3, Quantitative interpretations, *Water Resour. Res.*, 4, 581-590.
- Goldsmith, R. 1990. Surficial geologic map of the Barrington Quadrangle, Rockingham and Strafford Counties, New Hampshire, U.S. Geological Survey Open File Report NH-90-2
- Goldsmith, R. 1990. Surficial geologic map of the Epping Quadrangle, Rockingham and Strafford Counties, New Hampshire, U.S. Geological Survey Open File Report NH-90-1.
- Gooseff, M. N., J. K. Anderson, S. M. Wondzell, J. LaNier, and R. Haggerty. 2005. A modeling study of hyporheic exchange pattern and the sequence, size, and spacing of stream bedforms in mountain stream networks, Oregon, USA (Retracted article. See vol 20, pg 2441, 2006). *Hydrological Processes* 19:2915-2929.
- Gooseff, M. N., R. O. Hall, and J. L. Tank. 2007. Relating transient storage to channel complexity in streams of varying land use in Jackson Hole, Wyoming. *Water Resources Research* 43.

- Greig, S. M., D. A. Sear, and P. A. Carling. 2007. A review of factors influencing the availability of dissolved oxygen to incubating salmonid embryos. *Hydrological Processes* 21:323-334.
- Hakenkamp, C. C., H. M. Valett, and A. J. Boulton. 1993. Perspectives on the Hyporheic Zone - Integrating Hydrology and Biology - Concluding Remarks. *Journal of the North American Benthological Society* 12:94-99.
- Hall, R. O., E. S. Bernhardt, and G. E. Likens. 2002. Relating nutrient uptake with transient storage in forested mountain streams. *Limnology and Oceanography* 47:255-265.
- Hannah, D. M., I. A. Malcolm, C. Soulsby, and A. F. Youngson. 2004. Heat exchanges and temperatures within a salmon spawning stream in the Cairngorms, Scotland: Seasonal and sub-seasonal dynamics. *River Research and Applications* 20:635-652.
- Hannah, D. M., I. A. Malcolm, C. Soulsby, and A. F. Youngson. 2008. A comparison of forest and moorland stream microclimate, heat exchanges and thermal dynamics. *Hydrological Processes* 22:919-940.
- Hannah, D.M., Webb, B.W., and F. Nobilis, 2008, River and stream temperature: dynamics, processes, models and implications. *Hydrologic Processes*. 22: 899 – 901.
- Harvey, J.W. and K. Bencala. 1993. The effect of streambed topography on surface-subsurface water exchange in mountain catchments. *Water Resources Research*. 29: 89-98.
- Harvey, J. W., B. J. Wagner, and K. E. Bencala. 1996. Evaluating the reliability of the stream tracer approach to characterize stream-subsurface water exchange. *Water Resources Research* 32:2441-2451.
- Hatch, C. E., A. T. Fisher, J. S. Revenaugh, J. Constantz, and C. Ruehl. 2006. Quantifying surface water-groundwater interactions using time series analysis of streambed thermal records: Method development. *Water Resources Research* 42.
- Harvey, J.W. and B.J Wagner. Quantifying hydrologic interactions between streams and their subsurface hyporheic zones. In J.P. Jones and P.J. Mulholland, eds. *Streams and Groundwater*, 1st Edition, Philadelphia, Elsevier, 2000.
- Henderson, R.D., F.D. Day-Lewis and C. Harvey, 2009, Investigation of aquifer-estuary interaction using wavelet analysis of fiber-optic temperature data, *Geophysical*

Research Letters. 36: L06403.

Hendricks, S. P., and D. S. White. 1988. Hummocking by Lotic Chara - Observations on Alterations of Hyporheic Temperature Patterns. *Aquatic Botany* 31:13-22.

Hendricks, S. P., and D. S. White. 1991. Physicochemical Patterns within a Hyporheic Zone of a Northern Michigan River, with Comments on Surface-Water Patterns. *Canadian Journal of Fisheries and Aquatic Sciences* 48:1645-1654.

Hendricks, S. P. 1993. Microbial Ecology of the Hyporheic Zone - a Perspective Integrating Hydrology and Biology. *Journal of the North American Benthological Society* 12:70-78.

Hester, E. T., and M. W. Doyle. 2008. In-stream geomorphic structures as drivers of hyporheic exchange. *Water Resources Research* 44.

Isaak, D. J., R. F. Thurow, B. E. Rieman, and J. B. Dunham. 2007. Chinook salmon use of spawning patches: Relative roles of habitat quality, size, and connectivity. *Ecological Applications* 17:352-364.

Jacobs, J.M., B.P. Mohanty, E. Hsu, and D. Miller, 2004. SMEX02; Field scale variability, time stability and similarity of soil moisture, *Remote Sensing of Environment*. 92: 436-446.

Johnson, S. L. 2004. Factors influencing stream temperatures in small streams: substrate effects and a shading experiment. *Canadian Journal of Fisheries and Aquatic Sciences* 61:913-923.

Jones, J. B., and R. M. Holmes. 1996. Surface-subsurface interactions in stream ecosystems. *Trends in Ecology & Evolution* 11:239-242.

Jones, K. L., G. C. Poole, W. W. Woessner, M. V. Vitale, B. R. Boer, S. J. O'Daniel, S. A. Thomas, and B. A. Geffen. 2008. Geomorphology, hydrology, and aquatic vegetation drive seasonal hyporheic flow patterns across a gravel-dominated floodplain. *Hydrological Processes* 22:2105-2113.

Kasahara, T., and S. M. Wondzell. 2003. Geomorphic controls on hyporheic exchange flow in mountain streams. *Water Resources Research* 39.

Kasahara, T., and A. R. Hill. 2006. Hyporheic exchange flows induced by constructed riffles and steps in lowland streams in southern Ontario, Canada. *Hydrological Processes* 20:4287-4305.

- Keery, J., A. Binley, N. Crook, and J. W. N. Smith. 2007. Temporal and spatial variability of groundwater-surface water fluxes: Development and application of an analytical method using temperature time series. *Journal of Hydrology* 336:1-16.
- Koteff, C., R. Goldsmith, and G. Gephart, 1989. Surficial geologic map of the Dover West quadrangle, Strafford County, New Hampshire, U.S. Geological Survey Open File Report 89-166.
- Lapham, W. 1989. Use of temperature profiles beneath streams to determine rates of vertical groundwater flow and vertical hydraulic conductivity. U.S. Geological Survey Water Supply Paper 2337.
- Lautz, L. K., and D. I. Siegel. 2006. Modeling surface and ground water mixing in the hyporheic zone using MODFLOW and MT3D. *Advances in Water Resources* 29:1618-1633.
- Lautz, L., and R. Fanelli. 2008. Seasonal biogeochemical hotspots in the streambed around restoration structures. *Biogeochemistry* 91:85-104.
- Lemmon, P. E. 1956. A spherical densimeter for estimating forest overstorey density. *Forest Sci.* 2: 214-320.
- Leopold, L.B., M.G. Wolman, and J. Miller. *Fluvial Processes in Geomorphology*. Mineola, NY, Dover Publications. 1995.
- Loheide, S. P., and S. M. Gorelick. 2006. Quantifying stream-aquifer interactions through the analysis of remotely sensed thermographic profiles and in situ temperature histories. *Environmental Science & Technology* 40:3336-3341.
- Lowry, C.S., J.F. Walker, R.J. Hunt and M.P. Anderson, 2007, Identifying spatial variability of groundwater discharge in a wetland stream using a distributed temperature sensor. *Water Resources Research*, 43, W10408, doi:10.1029/2007WR006145.
- Lyons, J.B., W.A. Bothner, R. H. Moench and J.B. Thompson. 1997. *Bedrock Geologic Map of New Hampshire*. U.S. Geological Survey.
- Maidment, D., 2002, *Arc Hydro: GIS for Water Resources*, ESRI Press.
- Malard, F., M. Lafont, P. Burgherr, and J. V. Ward. 2001. A comparison of longitudinal patterns in hyporheic and benthic oligochaete assemblages in a glacial river. *Arctic Antarctic and Alpine Research* 33:457-466.

- Malcolm, I. A., C. Soulsby, D. M. Hannah, P. J. Bacon, A. F. Youngson, and D. Tetzlaff. 2008. The influence of riparian woodland on stream temperatures: implications for the performance of juvenile salmonids. *Hydrological Processes* 22:968-979.
- McDonald, M.G., and Harbaugh, A.W., 1988, A modular three-dimensional finite-difference ground-water flow model: U.S. Geological Survey Techniques of Water-Resources Investigations, book 6, chap. A1, 586 p.
- Moore, R.B., 1990, Geohydrology and water quality of stratified-drift aquifers in the Exeter, Lamprey, and Oyster River basins, southeastern New Hampshire. USGS WRIR 88-4128.
- Moore, R. D., and S. M. Wondzell. 2005. Physical hydrology and the effects of forest harvesting in the Pacific Northwest: A review. *Journal of the American Water Resources Association* 41:763-784.
- Moore, R. D., D. L. Spittlehouse, and A. Story. 2005. Riparian microclimate and stream temperature response to forest harvesting: A review. *Journal of the American Water Resources Association* 41:813-834.
- Moore, R. D., P. Sutherland, T. Gomi, and A. Dhakal. 2005. Thermal regime of a headwater stream within a clear-cut, coastal British Columbia, Canada. *Hydrological Processes* 19:2591-2608.
- Morrice, J. A., H. M. Valett, C. N. Dahm, and M. E. Campana. 1997. Alluvial characteristics, groundwater-surface water exchange and hydrological retention in headwater streams. *Hydrological Processes* 11:253-267.
- Nelitz, M. A., E. A. MacIsaac, and R. M. Peterman. 2007. A science-based approach for identifying temperature-sensitive streams for rainbow trout. *North American Journal of Fisheries Management* 27:405-424.
- National Geodetic Survey, 2008, CORS Network, <http://www.ngs.noaa.gov/CORS/>.
- NHDES, 2007, Predicated coldwater fish indicator species in New Hampshire, wadeable streams.
- NHDES, 2009, New Hampshire water resources primer.
- NHWRRRC, 2009, Lamprey River Hydrologic Observatory, <http://www.wrrc.unh.edu/lrho/index.htm>.
- NHWRRRC, 2009, Lamprey River Hydrologic Observatory Research, <http://www.wrrc.unh.edu/lrho/research.htm>.

- Olsen, D. A., and R. G. Young. 2009. Significance of river-aquifer interactions for reach-scale thermal patterns and trout growth potential in the Motueka River, New Zealand. *Hydrogeology Journal* 17:175-183.
- Onset Computer Corporation. 2009. Information on temperature data loggers. <http://www.onsetcomp.com/products/data-loggers/ua-002-64>.
- Peterson, B. J., W. M. Wollheim, P. J. Mulholland, J. R. Webster, J. L. Meyer, J. L. Tank, E. Marti, W. B. Bowden, H. M. Valett, A. E. Hershey, W. H. McDowell, W. K. Dodds, S. K. Hamilton, S. Gregory, and D. D. Morrall. 2001. Control of nitrogen export from watersheds by headwater streams. *Science* 292:86-90.
- Poole, G.C. and C. Berman. 2001. An ecological perspective on In-stream temperature: natural heat dynamics and mechanisms of human-caused thermal degradation. *Environmental Management*. 27: 787-802.
- Poole, G. C. 2002. Fluvial landscape ecology: addressing uniqueness within the river discontinuum. *Freshwater Biology* 47:641-660.
- Poole, G. C., J. A. Stanford, S. W. Running, and C. A. Frissell. 2006. Multiscale geomorphic drivers of groundwater flow paths: subsurface hydrologic dynamics and hyporheic habitat diversity. *Journal of the North American Benthological Society* 25:288-303.
- Power, G., R.S. Brown and J. Imhof. 1999. Groundwater and fish – insights from northern North America. *Hydrologic Processes*. 13: 401-422.
- Roberts, B. J., P. J. Mulholland, and A. N. Houser. 2007. Effects of upland disturbance and instream restoration on hydrodynamics and ammonium uptake in headwater streams. *Journal of the North American Benthological Society* 26:38-53.
- Roseen, R. 2002. Quantifying groundwater discharge using thermal imagery and conventional groundwater exploration techniques for estimating the nitrogen loading to a meso-scale inland estuary. Ph.D. dissertation, University of New Hampshire.
- Rosgen, D. 1996. Applied river morphology. Pagosa Springs, CO. Wildland Hydrology.
- Rosgen, D. and L. Silvey. 1998. Field guide for stream classification. Pagosa Springs, CO. Wildland Hydrology.
- Ryan, R. J., and M. C. Boufadel. 2006. Influence of streambed hydraulic conductivity on solute exchange with the hyporheic zone. *Environmental Geology* 51:203-210.

- Selker, J. S., L. Thevenaz, H. Huwald, A. Mallet, W. Luxemburg, N. V. de Giesen, M. Stejskal, J. Zeman, M. Westhoff, and M. B. Parlange. 2006. Distributed fiber-optic temperature sensing for hydrologic systems. *Water Resources Research* 42.
- Smith, J. W. N., M. Bonell, J. Gibert, W. H. McDowell, E. A. Sudicky, J. V. Turner, and R. C. Harris. 2008. Groundwater-surface water interactions, nutrient fluxes and ecological response in river corridors: Translating science into effective environmental management. *Hydrological Processes* 22:151-157.
- Sophocleous, M. 2002. Interactions between groundwater and surface water: the state of the science. *Hydrogeology Journal* 10:52-67.
- Stanford, J. A., and J. V. Ward. 1993. An Ecosystem Perspective of Alluvial Rivers - Connectivity and the Hyporheic Corridor. *Journal of the North American Benthological Society* 12:48-60.
- Stallman, R.W. 1965 . Steady one-dimensional fluid flow in a semi-infinite porous medium with sinusoidal surface temperature. *Journal of Geophysical Research* 70: 2821-2827.
- Stonestrom, D.A. and J. Constantz. 2003. Heat as a tool for studying the movement of groundwater near streams. *US Geological Survey Circular* 1260.
- Storey, R. G., K. W. F. Howard, and D. D. Williams. 2003. Factors controlling riffle-scale hyporheic exchange flows and their seasonal changes in a gaining stream: A three-dimensional groundwater flow model. *Water Resources Research* 39.
- Story, A. R.D. Moore and J. McDonald. 2003. Stream temperatures in two shaded reaches below cutblocks and logging roads: downstream cooling linked to subsurface hydrology. *Canadian Journal of Forest Resources*. 33: 1383-1396.
- Tetzlaff, D., C. Soulsby, C. Gibbins, P. J. Bacon, and A. F. Youngson. 2005. An approach to assessing hydrological influences on feeding opportunities of juvenile Atlantic salmon (*Salmo salar*): a case study of two contrasting years in a small, nursery stream. *Hydrobiologia* 549:65-77.
- Thouin, Joseph A., 2008, The biochemical influences of nitrate, dissolved oxygen, and dissolved organic carbon on stream nitrate uptake. University of New Hampshire Master's thesis.
- Theurer, F. D., Voos, K. A., and Miller, W. J., 1984. Instream water temperature model, US Fish Wildlife Serv. Instream Flow Information Pap., 16, 200 pp.

- Traer, K., 2007, Controls on denitrification in a northeastern coastal suburban riparian zone. University of New Hampshire Master's Thesis.
- Triska, F. J., V. C. Kennedy, R. J. Avanzino, G. W. Zellweger, and K. E. Bencala. 1989. Retention and Transport of Nutrients in a 3rd-Order Stream - Channel Processes. *Ecology* 70:1877-1892.
- Toth J. 1963. A theoretical analysis of groundwater flow in small drainage basins. *Journal of Geophysical Research* 68: 4795 – 4812.
- U.S. Geological Survey, 2008, Water Resources Data, National Water Information System. <http://waterdata.usgs.gov/usa/nwis/>.
- Valett, H. M., C. C. Hakenkamp, and A. J. Boulton. 1993. Perspectives on the Hyporheic Zone - Integrating Hydrology and Biology - Introduction. *Journal of the North American Benthological Society* 12:40-43.
- Valett, H. M. 1993. Surface-Hyporheic Interactions in a Sonoran Desert Stream - Hydrologic Exchange and Diel Periodicity. *Hydrobiologia* 259:133-144.
- Vanotte, R.L., G.W. Minshall and C. Cushing, 1980, The River Continuum Concept, *Canadian Journal of Fisheries and Aquatic Sciences*. 37: 130-137.
- Vaux, W.G. 1968. Intragravel flow and interchange of water in a streambed. USDI, US Fish and Wildlife Service, *Fishery Bulletin* 66: 479-489.
- Ward, J. V., K. Tockner, U. Uehlinger, and F. Malard. 2001. Understanding natural patterns and processes in river corridors as the basis for effective river restoration. *Regulated Rivers-Research & Management* 17:311.
- Webb, B. W. and Zhang, Y. 1997. Spatial and seasonal variability in the components of the river heat budget, *Hydrologic. Processes*.11: 79-101.
- Webb, B. W., and Y. Zhang. 1999. Water temperatures and heat budgets in Dorset chalk water courses. *Hydrological Processes* 13:309-321.
- Webb, B. W., and Y. Zhang. 2004. Intra-annual variability in the non-advective heat energy budget of Devon streams and rivers. *Hydrological Processes* 18:2117-2146.
- White, D. S. 1993. Perspectives on defining and delineating hyporheic zones. *Journal of the North American Benthological Society* 12:61-69.
- Winter, T. C., J. Harvey, O. Franke, and W. Alley. 1998. Groundwater and surface water, a single resource. US Geological Survey Circular 1139.

- Woessner, W. W. 2000. Stream and fluvial plain ground water interactions: Rescaling hydrogeologic thought. *Ground Water* 38:423-429.
- Wright, K.K., C.V. Baxter and J.L. Li, 2005, Restricted hyporheic exchange in an alluvial river system: implications for theory and management. *J. N. Am. Benthol. Soc.*, 2005, 24(3), p. 447–460.
- Wroblicky, G. J., M. E. Campana, H. M. Valett, and C. N. Dahm. 1998. Seasonal variation in surface-subsurface water exchange and lateral hyporheic area of two stream-aquifer systems. *Water Resources Research* 34:317-328.

Appendix A - Data Tables

Appendix A.1 Earth conductivity measurements (April 15, 2007) and streambed sediment depths (2007 and 2008), Wednesday Hill Brook in Lee, NH,

Cable Station (meters), approximate	Distance (meters)	Depth of gravel/sand (cm)	EMI Conductivity m-mhos/m
67	3	12	2.5
75	10	3.81	1.5
82	15	20.32	
83	16.5	7.62	
84	17	22.86	1.3
96	28.5	8.89	0.9
110	41	24.13	0.7
123	50	21.59	1.5
127	54	8.89	
143	69	19.05	3.1
161	81	12.7	3.6
171	93	30.48	4.2
174	96	27.94	
175	97	21.59	
176	98	33.02	
176.5	98.5	22.86	
177	99	8.89	
178	100	19.05	
179	101	32	3.5
192	105	10	2.5
199	112	50	2.8
202	115	52	4.3
214	125	59.69	4
219	130	76.2	3.4
222	133	45.72	3.2
226	137	58.42	2.8
227	138		2.4
228	139		2.4
229	140		1.9
232	142	60	1.55
236	145	72	1.4
237	147	46.99	
238	148	58.42	
239	149	35.56	
240	150	86.36	1
241	151	19.05	1.3
243	152	66.04	
245	153	63.5	
246	154	27.94	
247	155	30.48	
251	158	20	0.3
252	160		0.6
Cable Station (meters), approximate	Distance (meters)	Depth of gravel/sand (cm)	EMI Conductivity m-mhos/m

254	163		1.1
255	165	25.4	1.5
268	170	40	2.3
270	171	55.88	
271	172	48.26	
272	173	17.78	
273	174	58.42	
274	175	53.34	
275	176	31.75	
276	177	43.18	
277	178	60.96	
278	179	52.07	
279	180	17.78	3.9
280	181	24.13	
281	182	17.78	
282	183	69.85	
283	184	63.5	
284	185	0	
285	186	49.53	
287	187	35.56	5
288	188	30.48	
289	189	21.59	
290	190	24.13	
291	191	8.89	
292	192	38.1	
293	193	41.91	6
294	194	49.53	
297	200	35.56	6
299	205	30	6.5
312	212	26.67	7
315	215	43.18	
316	216	26.67	
317	217	86.36	
318	218	78.74	6.6
320	219	39.37	
323	220	44.45	7
327	221	48.26	
330	226	48.26	7.4
334	230	40	8
360	248		8.6
370	253.5	90	8
374	256		7.5
375	257	50	8
382	269	70	8
399	279.5	60	7
403	284		6.5
406	289.5	30	6.5
410	291	10	5.4
			EMI Cond-
	Distance		uctivity
Cable Station (meters), approximate	(meters)	Depth of gravel/sand (cm)	m-mhos/m
422	304.5	40	6
440	317	63.5	

441	318	85.09	
442	319	81.28	
443	320	91.44	
444	321	29.21	
445	322	60.96	
446	323	101.6	5
447	324	101.6	
448	325.5	95.25	5.6
450	330	125	5.6
456	336	66.04	
457	337	93.98	
458	338	101.6	
459	339		6.1
460	340	22.86	
461	341	50.8	
462	342	68.58	
463	343	88.9	
464	344	85.09	
465	345	83.82	
466	346	83.82	
467	347	73.66	
468	348	41.91	
469	349	63.5	
470	350	111.76	
472	351	86.36	6.8
480	361.5	90	6.4
485	366.5	45	7.2
495	377	38.1	
496	378	39.37	
497	379	67.31	
498	380	78.74	6
501	381	54.61	
503	382	49.53	
504	383	53.34	
506	384	62.23	
507	385	33.02	
509	387	99.06	6.4
511	389	116.84	
512	390	146.05	
513	391	137.16	
514	392	156.21	
515	393	95.25	
516	394	119.38	
517	395	93.98	
518	396	96.52	
519	397	88.9	
			EMI Conductivity
Cable Station (meters), approximate	Distance (meters)	Depth of gravel/sand (cm)	m-mhos/m
520	398	58.42	
525	400		5.7
531	406	80	5.5
533	408	78.74	

534	409	100	6.4
536	411	86.36	
538	412	82.55	6.9
540	413	43.18	
541	414	27.94	
543	415	24.13	8.2
545	416		
546	417	15.24	8.2
547	418	27.94	
548	420	41.91	9.3
549	421	43.18	
550	422	17.78	
551	423	15.24	
552	424	10.16	
553	425	7.62	9
558	430		11
562	436.5		10.5
567	442		12
573	445.5	50	11.5
578	450	40	10
594	467.5	10	12.5
597	470	3	11
602	475	4	12
607	480	0	13
613	486.5	10	15
623	497	3	14.5
625	500	4	14
626	501	0	15
635	510	30	13
638	513	20	13

Appendix A.2 Pebble count data

0-100 m Pebble count

Grain size	TOTAL	Grain size (mm)	Percent
Silt/Clay	1	0.1	1.00%
Very Fine Sand	0	0.2	1.00%
Fine Sand	4	0.3	5.00%
Medium Sand	4	0.5	9.00%
Coarse Sand	0	0.75	9.00%
Very Coarse Sand	1	1	10.00%
Very Fine Gravel	1	2	11.00%
Fine Gravel	3	4	14.00%
Fine Gravel	4	8	18.00%
Medium Gravel	1	10	19.00%
Medium Gravel	6	20	25.00%
Coarse Gravel	3	30	28.00%
Coarse Gravel	5	37	33.00%
Very Coarse Gravel	10	45	43.00%
Very Coarse Gravel	5	55	48.00%
Small Cobbles	8	60	56.00%
Small Cobbles	19	100	75.00%
Large Cobbles	12	200	87.00%
Large Cobbles	8	300	95.00%
Small Boulders	5	400	100.00%
Small Boulders	0	500	100.00%
Medium Boulders	0	700	100.00%
Large - Very Large Boulders	0	900	100.00%
Bedrock (hard Pan marine clays)	0	1000	100.00%

100-200 m Pebble count

Grain size	TOTAL	Grain size (mm)	Percent
Silt/Clay	5	0.1	5.00%
Very Fine Sand	0	0.2	5.00%
Fine Sand	1	0.3	6.00%
Medium Sand	10	0.5	16.00%
Coarse Sand	0	0.75	16.00%
Very Coarse Sand	1	1	17.00%
Very Fine Gravel	1	2	18.00%
Fine Gravel	3	4	21.00%
Fine Gravel	4	8	25.00%
Medium Gravel	1	10	26.00%
Medium Gravel	6	20	32.00%
Coarse Gravel	14	30	46.00%
Coarse Gravel	5	37	51.00%
Very Coarse Gravel	15	45	66.00%
Very Coarse Gravel	5	55	71.00%
Small Cobbles	1	60	72.00%
Small Cobbles	19	100	91.00%

Large Cobbles	4		95.00%
Large Cobbles	0		95.00%
Small Boulders	5		100.00%
Small Boulders	0		100.00%
Medium Boulders	0		100.00%
Large - Very Large Boulders	0		100.00%
Bedrock (hard Pan marine clays)	0	1000	100.00%

200- 300 m Pebble count

Grain size	TOTAL	Grain Size (mm)	
Silt/Clay	3	0.1	3%
Very Fine Sand	0	0.2	3%
Fine Sand	14	0.3	17%
Medium Sand	11	0.5	28%
Coarse Sand	0	0.75	28%
Very Coarse Sand	2	1	30%
Very Fine Gravel	11	2	41%
Fine Gravel	3	4	44%
Fine Gravel	10	8	54%
Medium Gravel	9	10	63%
Medium Gravel	22	20	85%
Coarse Gravel	4	30	89%
Coarse Gravel	2	37	91%
Very Coarse Gravel	0	45	91%
Very Coarse Gravel	1	55	92%
Small Cobbles	2	60	94%
Small Cobbles	3	100	97%
Large Cobbles	2		99%
Large Cobbles	1		100%
Small Boulders	0		100%
Small Boulders	0		100%
Medium Boulders	0		100%
Large - Very Large Boulders	0		100%
Bedrock (hard Pan marine clays)	0	1000	100%

300-400 m Pebble count

Grain size	Total	Grain size (mm)	Percent
Silt/Clay	3	0.1	3%
Very Fine Sand		0.2	3%
Fine Sand	11	0.3	14%
Medium Sand	29	0.5	43%
Coarse Sand		0.75	43%
Very Coarse Sand	13	1	56%
Very Fine Gravel	9	2	65%
Fine Gravel	11	4	76%
Fine Gravel	12	8	88%
Medium Gravel	4	10	92%
Medium Gravel	6	20	98%

Coarse Gravel	1	30	99%
Coarse Gravel		37	99%
Very Coarse Gravel	1	45	100%
Very Coarse Gravel		55	100%
Small Cobbles		60	100%
Small Cobbles		100	100%
Large Cobbles			100%
Large Cobbles			100%
Small Boulders			100%
Small Boulders			100%
Medium Boulders			100%
Large - Very Large Boulders			100%
Bedrock (hard Pan marine clays)		1000	100%

400 – 500 m Pebble count

Grain size	Reach	Grain size (mm)	Percent
Silt/Clay	30	0.1	30%
Very Fine Sand		0.2	30%
Fine Sand	21	0.3	51%
Medium Sand	4	0.5	55%
Coarse Sand	2	0.75	57%
Very Coarse Sand	4	1	61%
Very Fine Gravel	10	2	71%
Fine Gravel	13	4	84%
Fine Gravel	9	8	93%
Medium Gravel	2	10	95%
Medium Gravel	4	20	99%
Coarse Gravel		30	99%
Coarse Gravel		37	99%
Very Coarse Gravel		45	99%
Very Coarse Gravel	1	55	100%
Small Cobbles		60	100%
Small Cobbles		100	100%
Large Cobbles			100%
Large Cobbles			100%
Small Boulders			100%
Small Boulders			100%
Medium Boulders			100%
Large - Very Large Boulders			100%
Bedrock (hard Pan marine clays)		1000	100%

**Appendix A.3 Spherical Densimeter Readings – August 21, 2007
Wednesday Hill Brook in Lee, NH**

Stream Station(m)	Dot Count (Raw Data)				% Open				% Canopy				% Canopy Mean - All Directions
	N	E	S	W	N	E	S	W	N	E	S	W	
10													
40	14	16	20	16	14.6	16.6	20.8	16.6	85.4	83.4	79.2	83.4	82.8
93	6	12	10	8	6.2	12.5	10.4	8.3	93.8	87.5	89.6	91.7	90.6
112	13	2	14	18	13.5	2.1	14.6	18.7	86.5	97.9	85.4	81.3	87.8
124	4	4	8	4	4.2	4.2	8.3	4.2	95.8	95.8	91.7	95.8	94.8
132	14	10	16	17	14.6	10.4	16.6	17.7	85.4	89.6	83.4	82.3	85.2
150	12	13	12	6	12.5	13.5	12.5	6.2	87.5	86.5	87.5	93.8	88.8
155	12	6	12	10	12.5	6.2	12.5	10.4	87.5	93.8	87.5	89.6	89.6
180	16	8	20	10	16.6	8.3	20.8	10.4	83.4	91.7	79.2	89.6	86.0
190	16	12	24	8	16.6	12.5	25.0	8.3	83.4	87.5	75.0	91.7	84.4
200	30	24	20	16	31.2	25.0	20.8	16.6	68.8	75.0	79.2	83.4	76.6
230	12	16	8	12	12.5	16.6	8.3	12.5	87.5	83.4	91.7	87.5	87.5
250	14	16	16	10	14.6	16.6	16.6	10.4	85.4	83.4	83.4	89.6	85.4
253.5	18	14	16	8	18.7	14.6	16.6	8.3	81.3	85.4	83.4	91.7	85.4
255	14	8	12	10	14.6	8.3	12.5	10.4	85.4	91.7	87.5	89.6	88.6
258	12	12	20	8	12.5	12.5	20.8	8.3	87.5	87.5	79.2	91.7	86.5
300	12	12	16	12	12.5	12.5	16.6	12.5	87.5	87.5	83.4	87.5	86.5
325	8	9	9	12	8.3	9.4	9.4	12.5	91.7	90.6	90.6	87.5	90.1
340	9	10	17	10	9.4	10.4	17.7	10.4	90.6	89.6	82.3	89.6	88.0
360	8	8	12	8	8.3	8.3	12.5	8.3	91.7	91.7	87.5	91.7	90.6
365	10	16	15	9	10.4	16.6	15.6	9.4	89.6	83.4	84.4	90.6	87.0
366.5	7	15	12	5	7.3	15.6	12.5	5.2	92.7	84.4	87.5	94.8	89.9
370	11	10	8	5	11.4	10.4	8.3	5.2	88.6	89.6	91.7	94.8	91.2
386	6	9	5	9	6.2	9.4	5.2	9.4	93.8	90.6	94.8	90.6	92.5
390	9	7	8	12	9.4	7.3	8.3	12.5	90.6	92.7	91.7	87.5	90.6
400	5	7	5	9	5.2	7.3	5.2	9.4	94.8	92.7	94.8	90.6	93.2
417	8	12	11	11	8.3	12.5	11.4	11.4	91.7	87.5	88.6	88.6	89.1
425	7	16	7	5	7.3	16.6	7.3	5.2	92.7	83.4	92.7	94.8	90.9
430	7	8	10	8	7.3	8.3	10.4	8.3	92.7	91.7	89.6	91.7	91.4
436.5	9	15	5	3	9.4	15.6	5.2	3.1	90.6	84.4	94.8	96.9	91.7
467.5	9	19	7	8	9.4	19.8	7.3	8.3	90.6	80.2	92.7	91.7	88.8
486.5	16	18	20	5	16.6	18.7	20.8	5.2	83.4	81.3	79.2	94.8	84.7
497	10	17	13	6	10.4	17.7	13.5	6.2	89.6	82.3	86.5	93.8	88.0
500	12	16	11	6	12.5	16.6	11.4	6.2	87.5	83.4	88.6	93.8	88.3
510	11	16	8	11	11.4	16.6	8.3	11.4	88.6	83.4	91.7	88.6	88.0
Weather Station (~500m)	8	6	7	8	8.3	6.2	7.3	8.3	91.7	93.8	92.7	91.7	92.5
Mean					11.6	12.5	12.9	9.6	88.4	87.5	87.1	90.4	88.4
Median					11.4	12.5	12.5	9.4	88.6	87.5	87.5	90.6	
Std. Dev					4.9	4.9	5.3	3.8	4.9	4.9	5.3	3.8	

Stream Type	Dominate Bed Material							
	1 Bedrock	2 Boulder	3 Cobble	4 Gravel	5 Sand	6 Silt-Clay		
A								
B								
C								
D								
DA								
E								
F								
G								
Entrenchmt	< 1.4	1.4 - 2.2	> 2.2	n/a	> 4.0	> 2.2	< 1.4	< 1.4
W/D Ratio	< 12	> 12	> 12	> 40	variable	< 12	> 12	< 12
Sinuosity	1 - 1.2	> 1.2	> 1.2	n/a	variable	> 1.5	> 1.2	> 1.2
Slope	.04-.099	.02-.039	< .02	< .04	< .005	< .02	< .02	.02-.039

Appendix A.4 Primary delineative criteria for the major stream types (from Rosgen and Silvey, 1998)

**Appendix A.5 Streambed vertical hydraulic gradients at piezometers
Wednesday Hill Brook in Lee, NH August to October 2007**

Stream station (m)	Cable Station (m)	Depth (cm)	8/17/07		8/18/07		8/21/07		8/22/07		8/22/07		8/23/07		8/23/07		8/24/07		8/24/07		8/25/07		8/26/07		8/26/07			
					am	pm	am	pm	am	pm	am	pm	am	pm	am	pm	am	pm	am	pm	am	pm	am	pm	am	pm	am	pm
88.9	167	40																										
93	171	38																										
146	237	60																										
158	257	40																										
168	268	72																										
174	276	75																										
196.9	292	31																										
199.5	295	38																										
228	334	33																										
229.5	336	33																										
250	370	60																										
251.5	372	70																										
298	413	30																										
308	422	40																										
312	430	65																										
315	433	60																										
325	443	55																										
340	461	53																										
360	480	73																										
365	486	62																										
370	491	33																										
390.5	518	70																										
392	520	60																										
400	525	40																										
500	634	40																										

**Appendix A.6 Non advective heat flux summary 75, 336 and 468 m
August 21 to 29, 2007 Wednesday Hill Brook in Lee, NH**

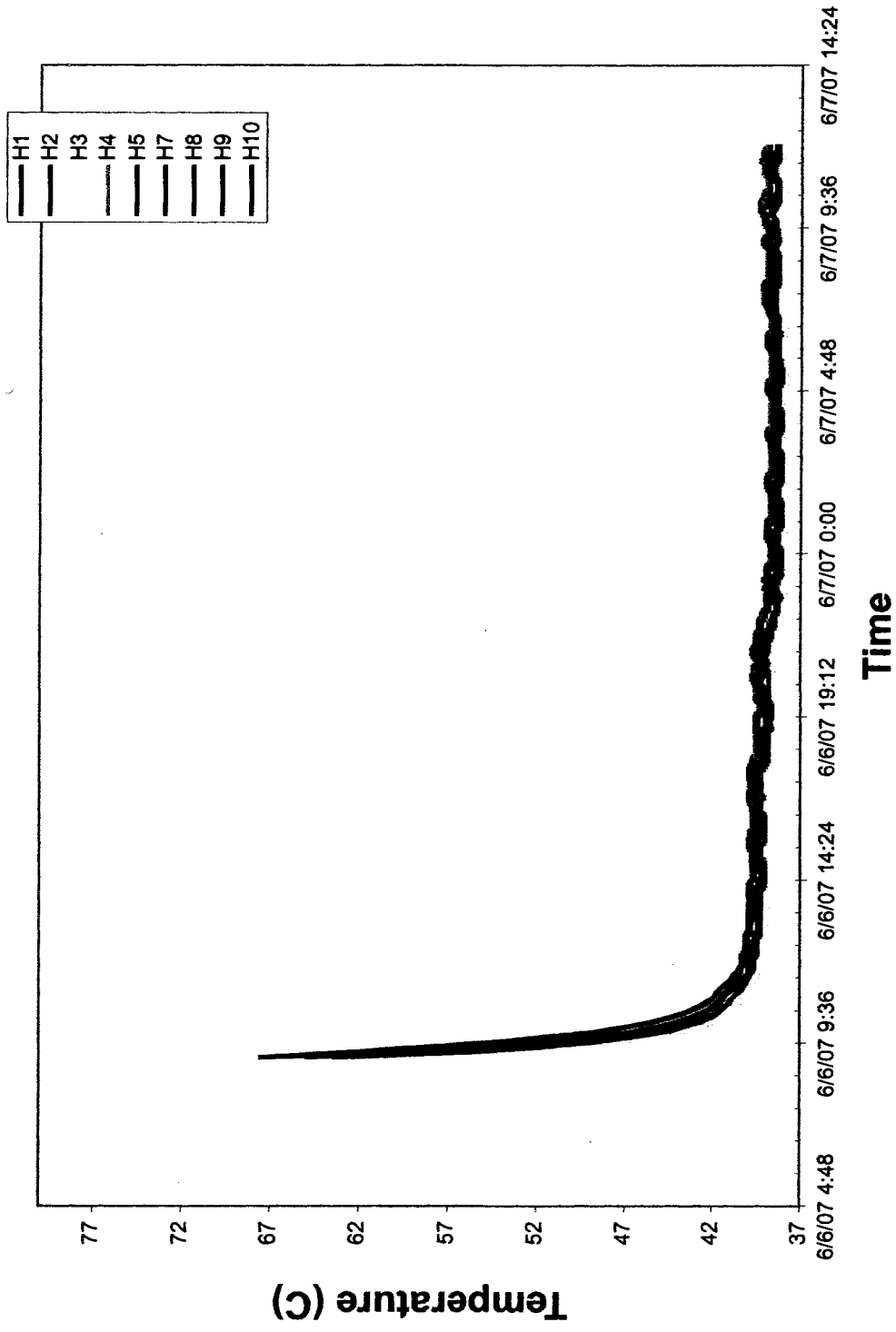
Statistic	Net Radiation (W/m²)	Evaporation (W/m²)	Convection (W/m²)	Conduction (W/m²)	Net Energy Flux (W/m²)
Location - 75 m (8-22-07 to 8-28-07)					
Mean	37.287	-9.070	-11.406	16.631	41.132
Maximum	580.900	23.252	6.448	39.105	580.076
Minimum	-9.420	-67.391	-50.709	-22.176	-39.695
Location 336 m (8-21-07 to 8-28-07)					
Mean	33.219	-16.613	-15.015	8.730	56.117
Maximum	580.900	17.569	13.763	23.120	526.448
Minimum	-14.510	-65.723	-61.880	-12.670	125.762
Location 468 m (8-21-07 to 8-28-07)					
Mean	33.219	-17.494	-15.510	12.796	53.427
Maximum	580.900	16.841	12.714	28.674	522.671
Minimum	-14.510	-67.391	-61.506	-9.684	124.071

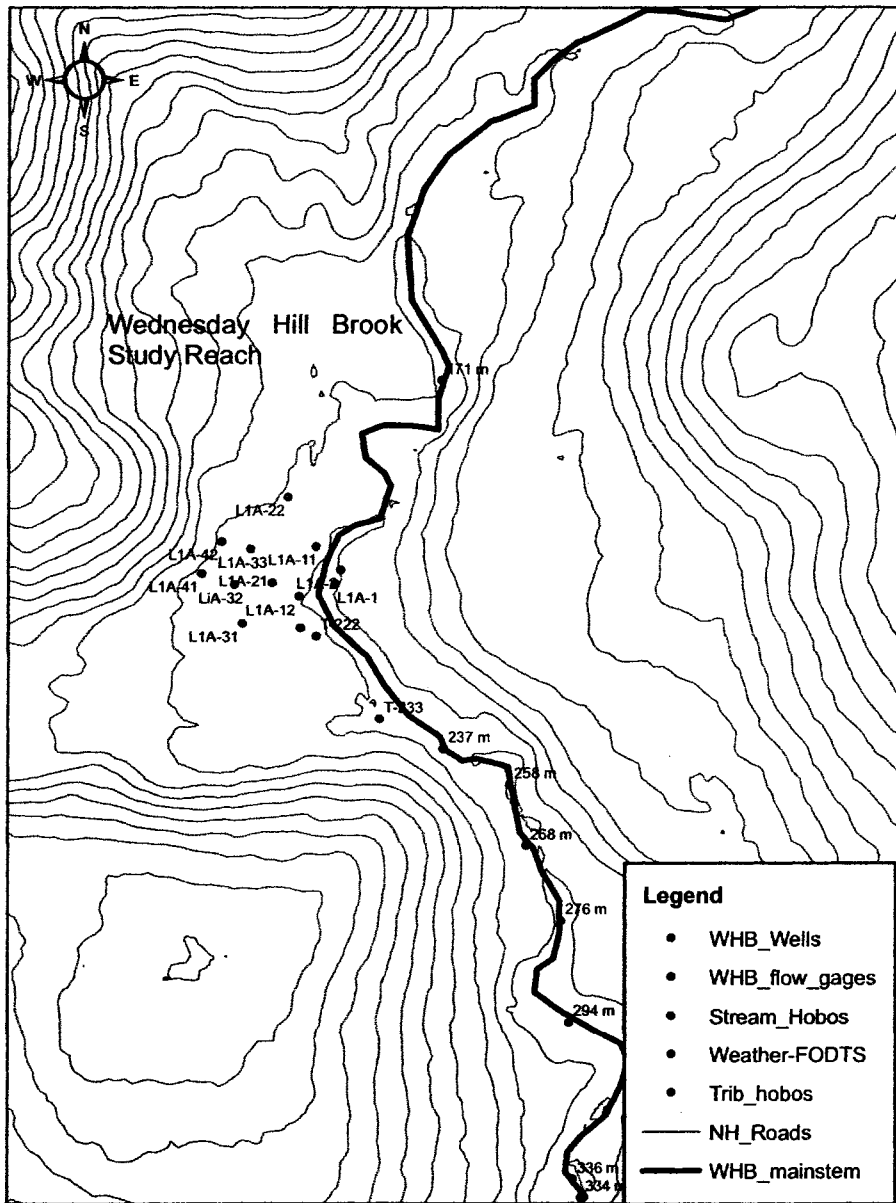
Appendix A.7 Input parameter – Heat budget modeling,
Wednesday Hill Brook in Lee, NH

Reach Characteristics	Reach 1	Reach 1a	Reach 2	Reach 2a	Reach 4	Reach 5
Length (m)	105	20	65	20	100	80
Average stream width (m)	1.5	1.5	2	2	2.5	2.5
Average depth (m)	0.1	0.1	0.2	0.2	0.2	0.2
Upstream temperature(oC)	15.5	15.5	14.8	14.8	13.2	13.3
Downstream temperature(oC)	14.8	14.7	13.5	13.7	13.3	13.3
Non-advective heat flux						
Net radiation (Wm ⁻²)	33.2	33.2	33.2	33.2	33.2	33.2
Evaporative flux (Wm-2)	-16.6	16.6	-16.6	-16.6	-17.5	-17.5
Convective flux (Wm-2)	-15.0	15.0	-15.0	-15.0	-15.5	-15.5
Friction (Wm-2)	1.6	1.7	0.2	0.2	0.1	0.2
Streambed conduction (Wm-2)						
	167	171				
	m	m				
	171	98.0	-20	77.0	413	-27.0
	m	237	-13.3	334	-24.0	-64.5
		m	-6.5	336	-64.5	-64.5
				360	-24.2	-24.2
				362	-18.7	-18.7
					-14.3	-14.3
					443	-24.0
					461	-34.0
					480	-23.0
					491	18.0

Appendix B – Additional graphics

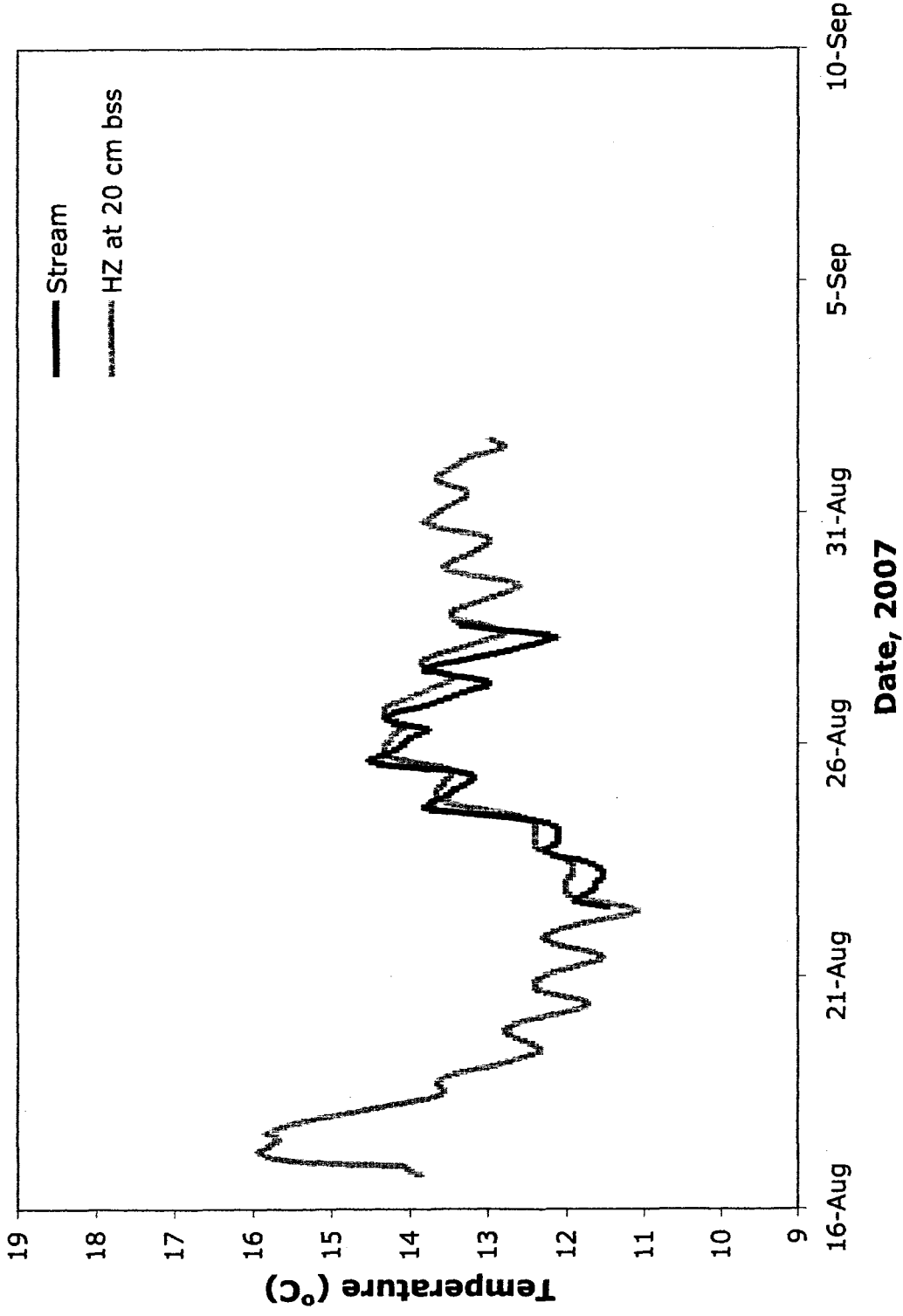
Calibration Test - Hobo dataloggers



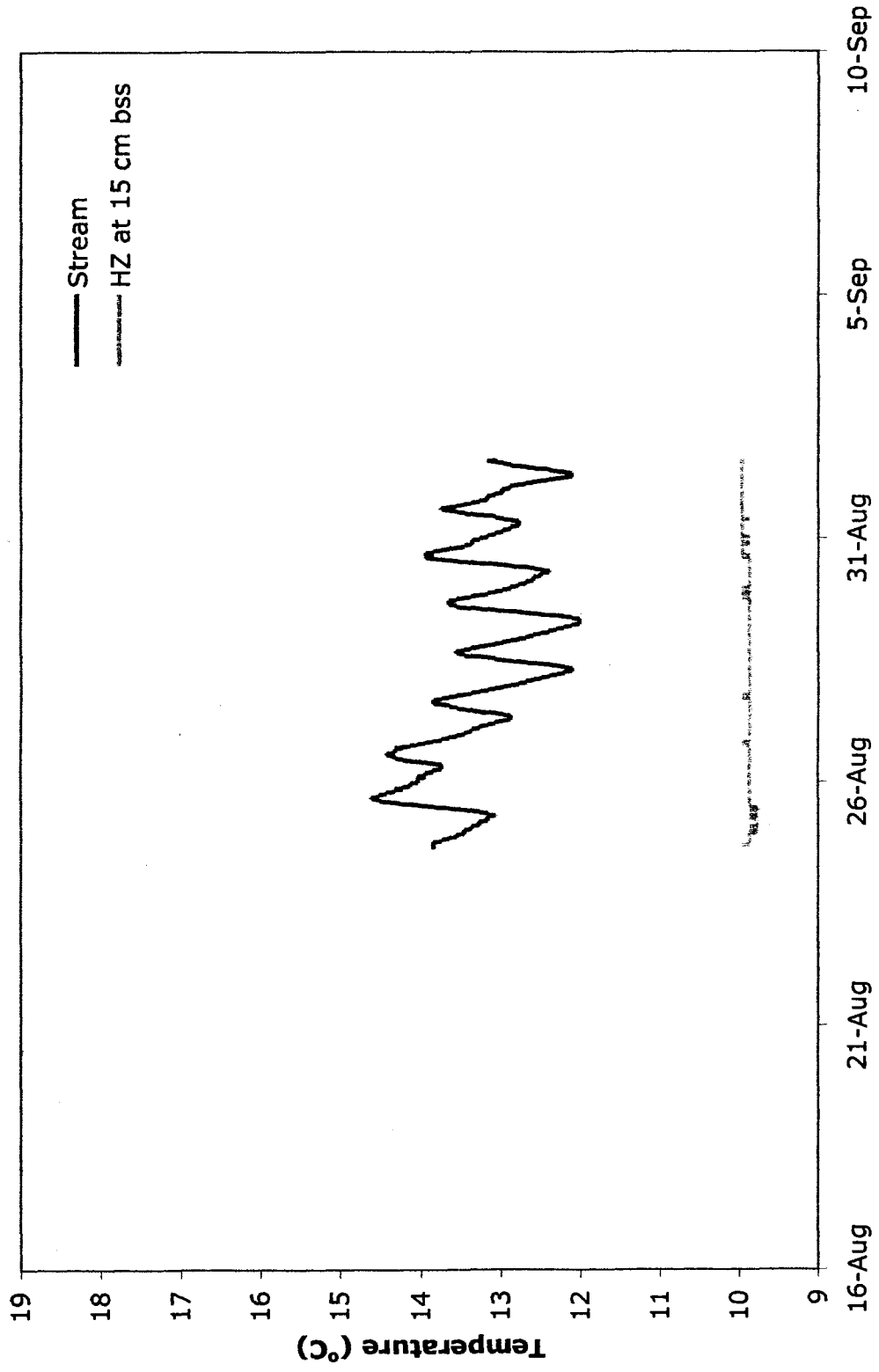


0 3.57 14 21 28
 Meters

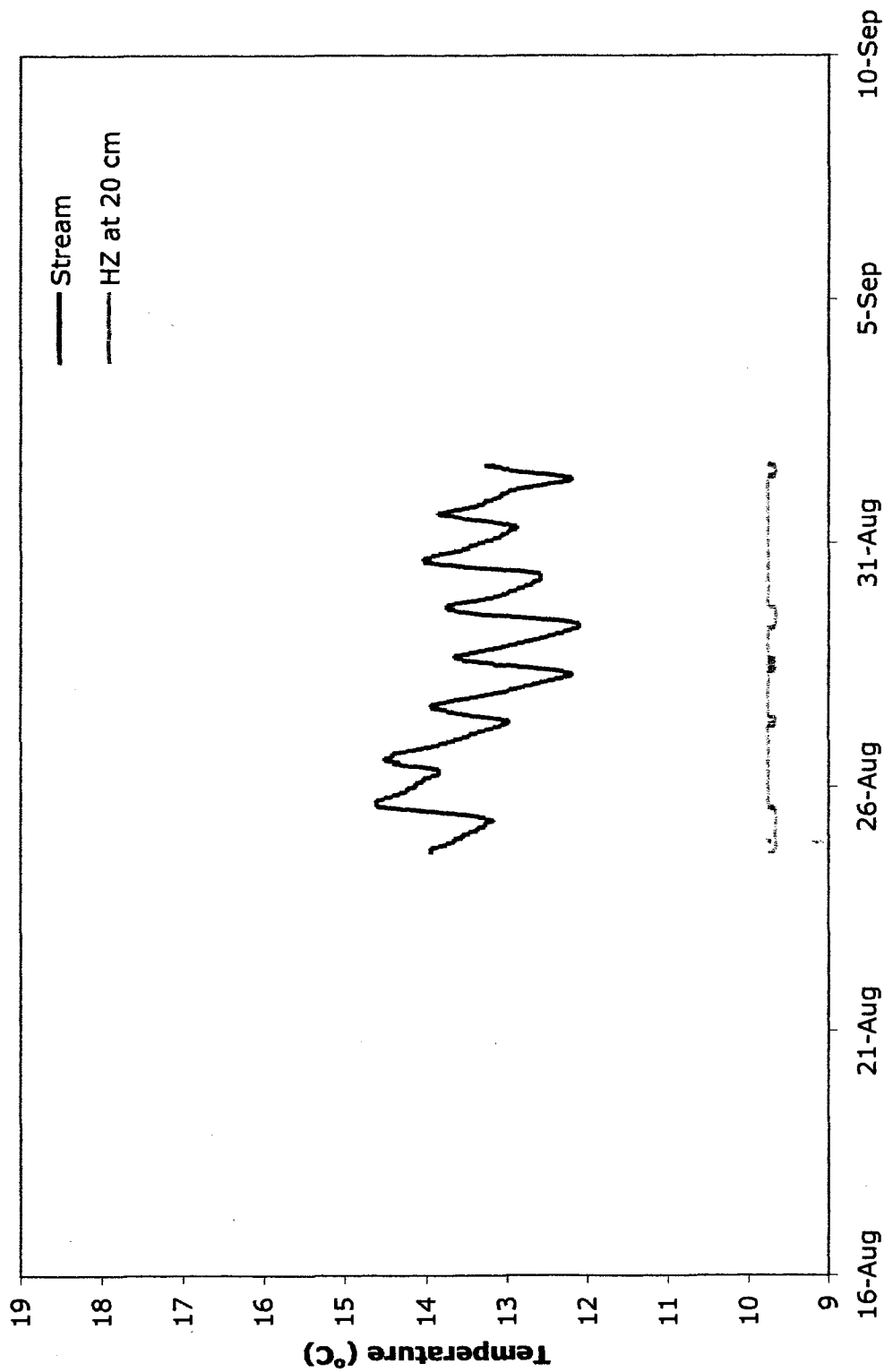
Topographic data from NCALM flight - November 2008
 1 centimeter = 7 meters



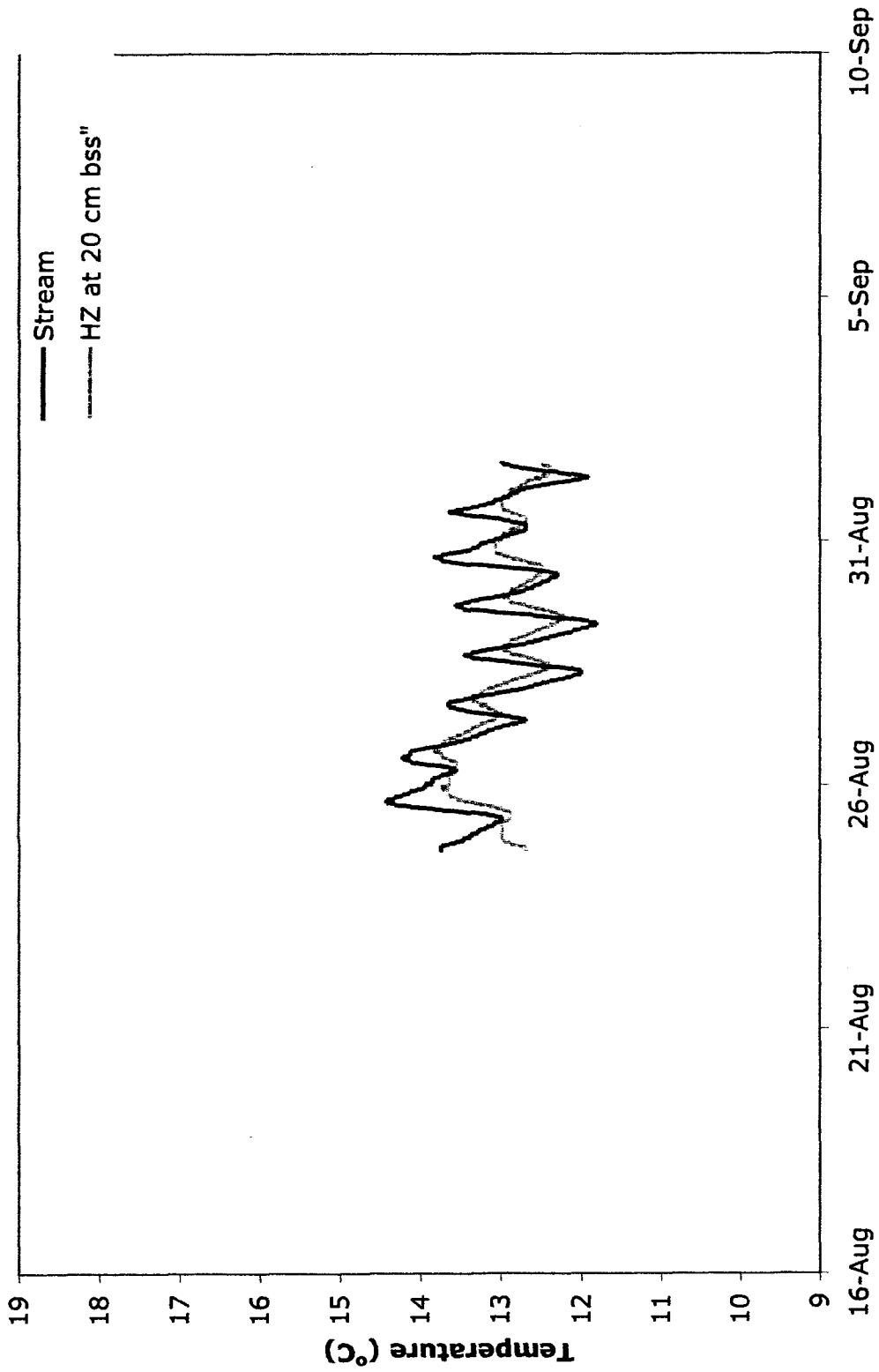
Stream and hyporheic zone temperatures at 293 m, August to September 2007
 Wednesday Hill Brook in Lee, NH



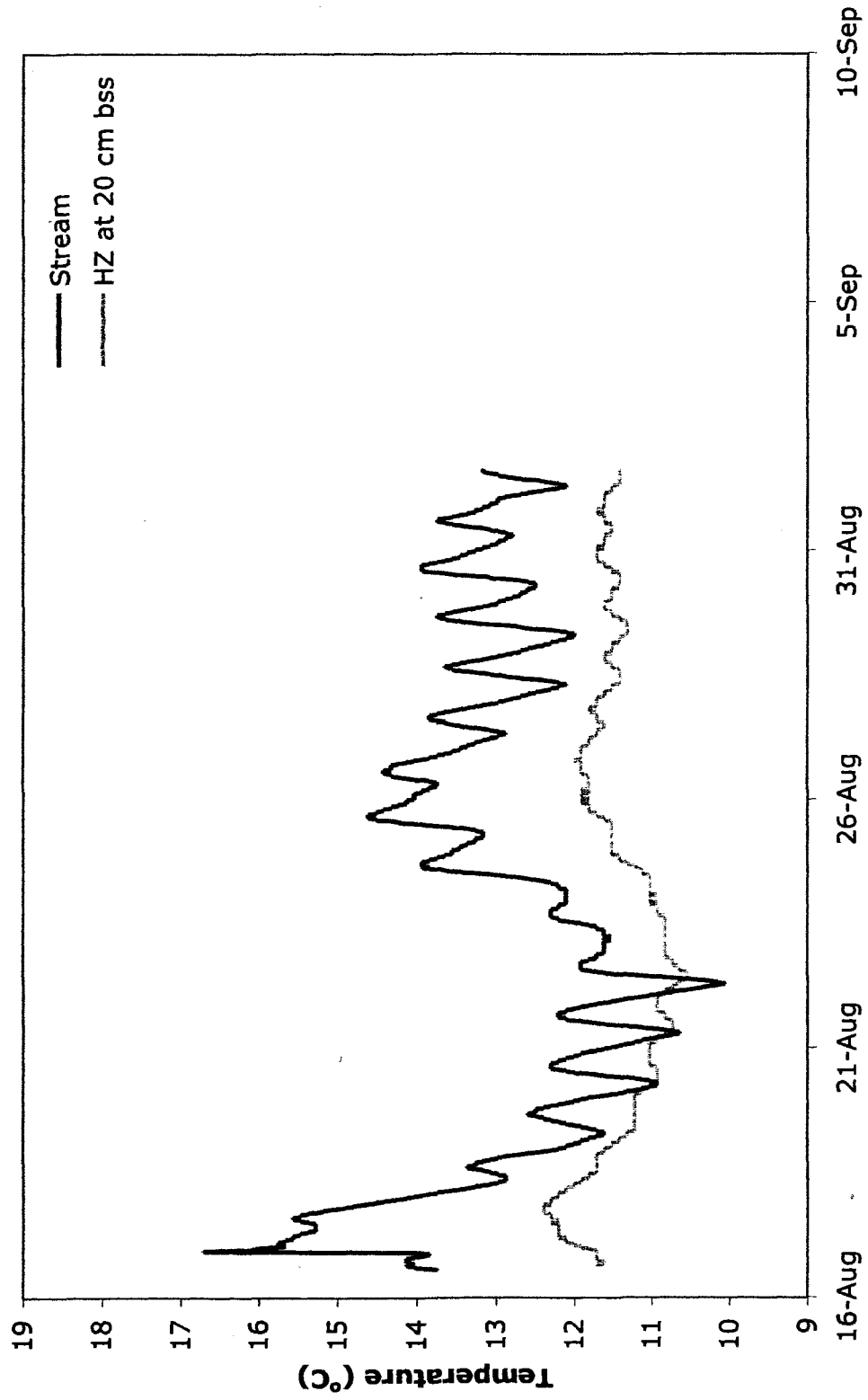
Stream and hyporheic zone temperatures at 413 m, August to September 2007
 Wednesday Hill Brook in Lee, NH



Stream and hyporheic zone temperatures at 422 m, August to September 2007
 Wednesday Hill Brook in Lee, NH

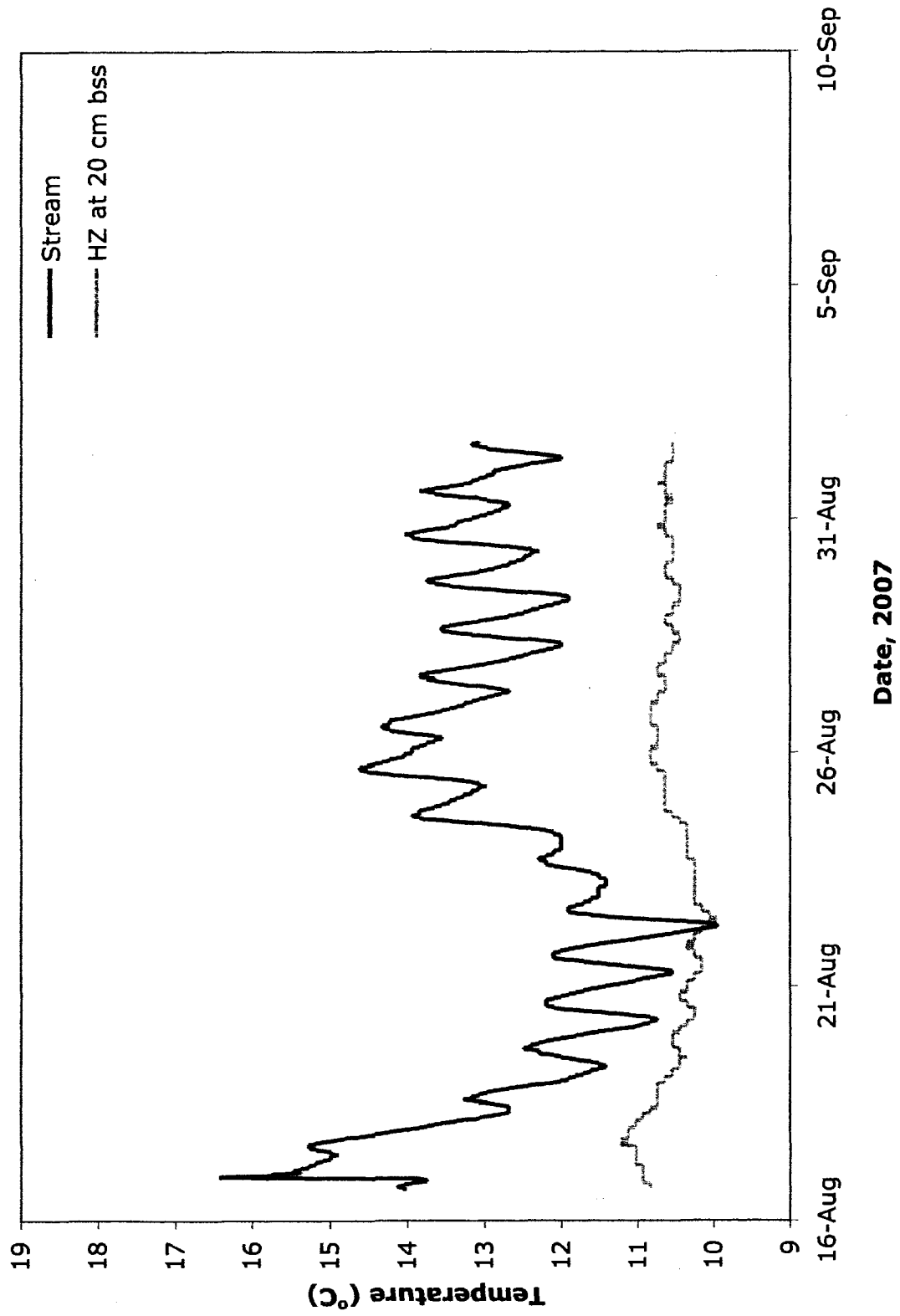


Stream and hyporheic zone temperatures at 430 m, August to September 2007
 Wednesday Hill Brook in Lee, NH

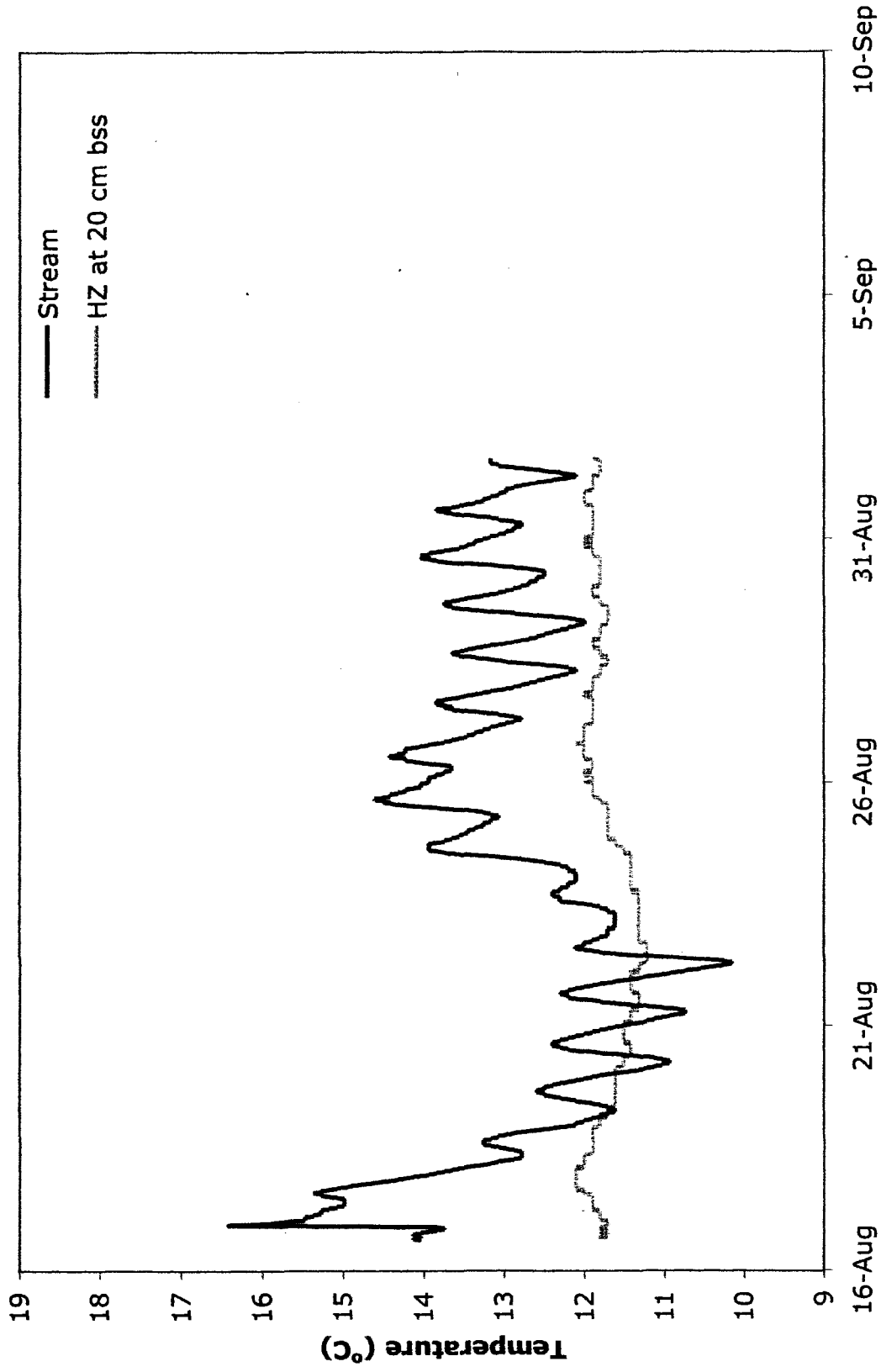


Date, 2007

Stream and hyporheic zone temperatures at 430 m, August to September 2007
 Wednesday Hill Brook in Lee, NH

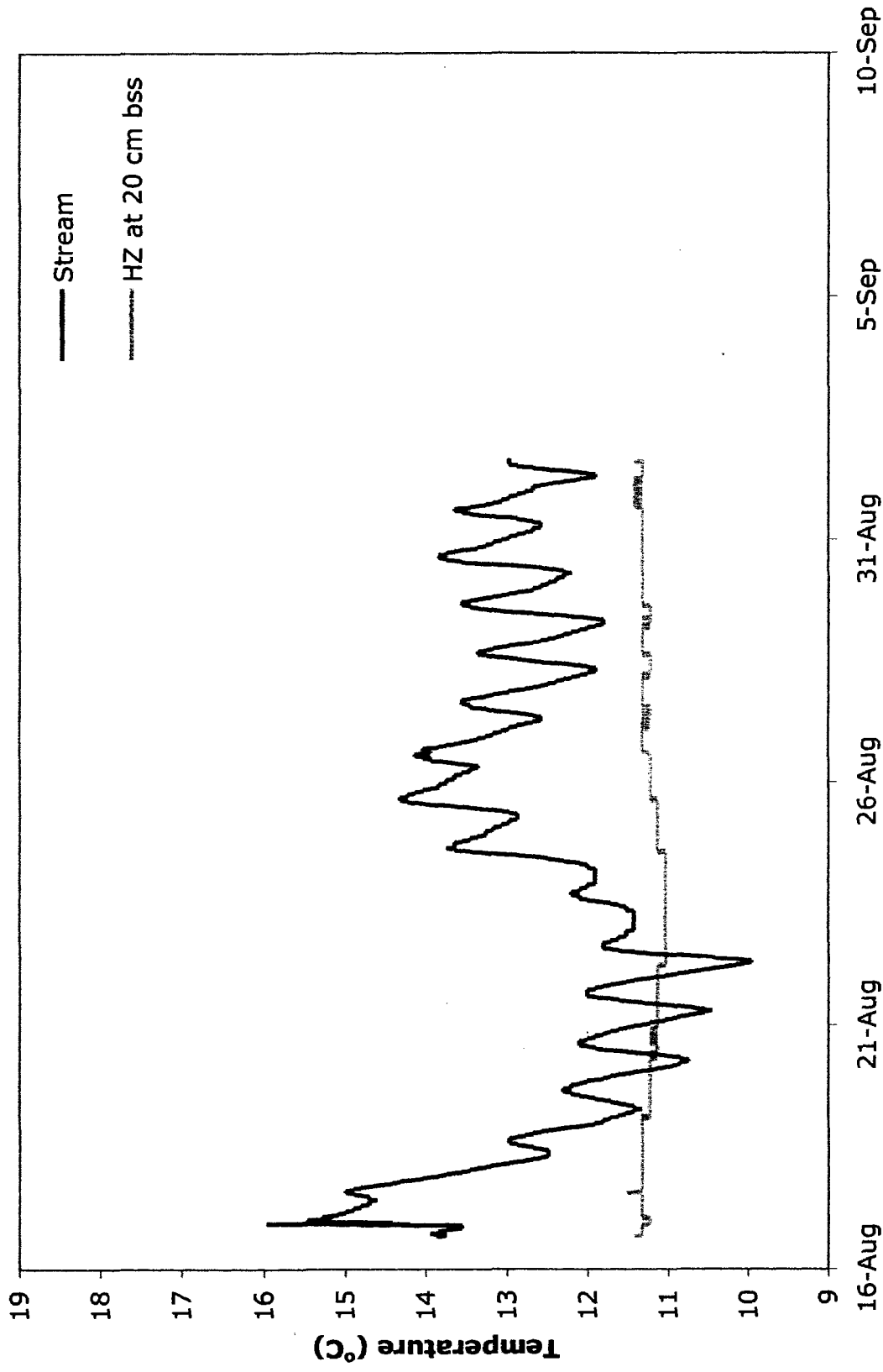


Stream and hyporheic zone temperatures at 461 m, August to September 2007
 Wednesday Hill Brook in Lee, NH

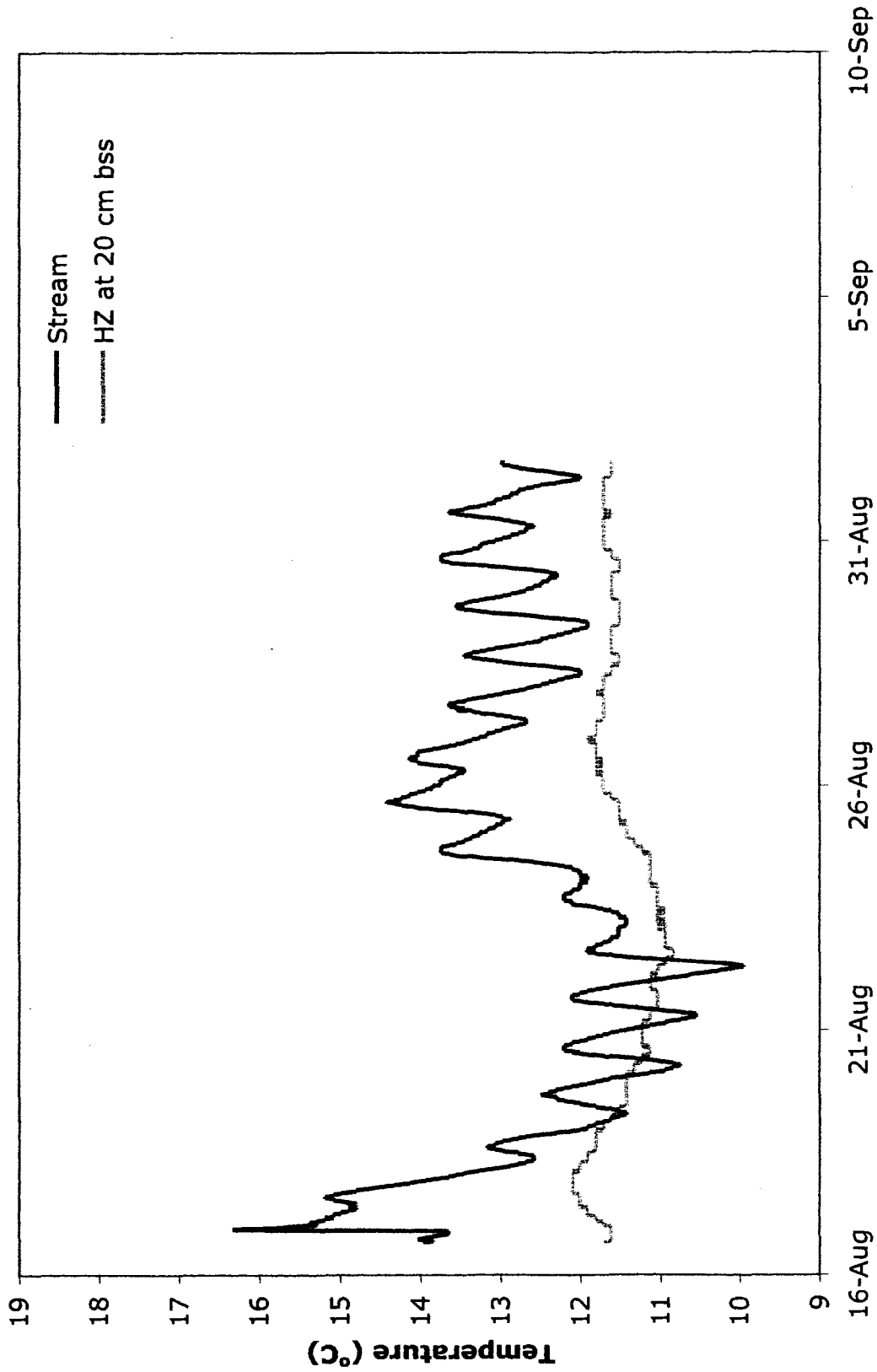


Date, 2007

Stream and hyporheic zone temperatures at 480 m, August to September 2007
 Wednesday Hill Brook in Lee, NH

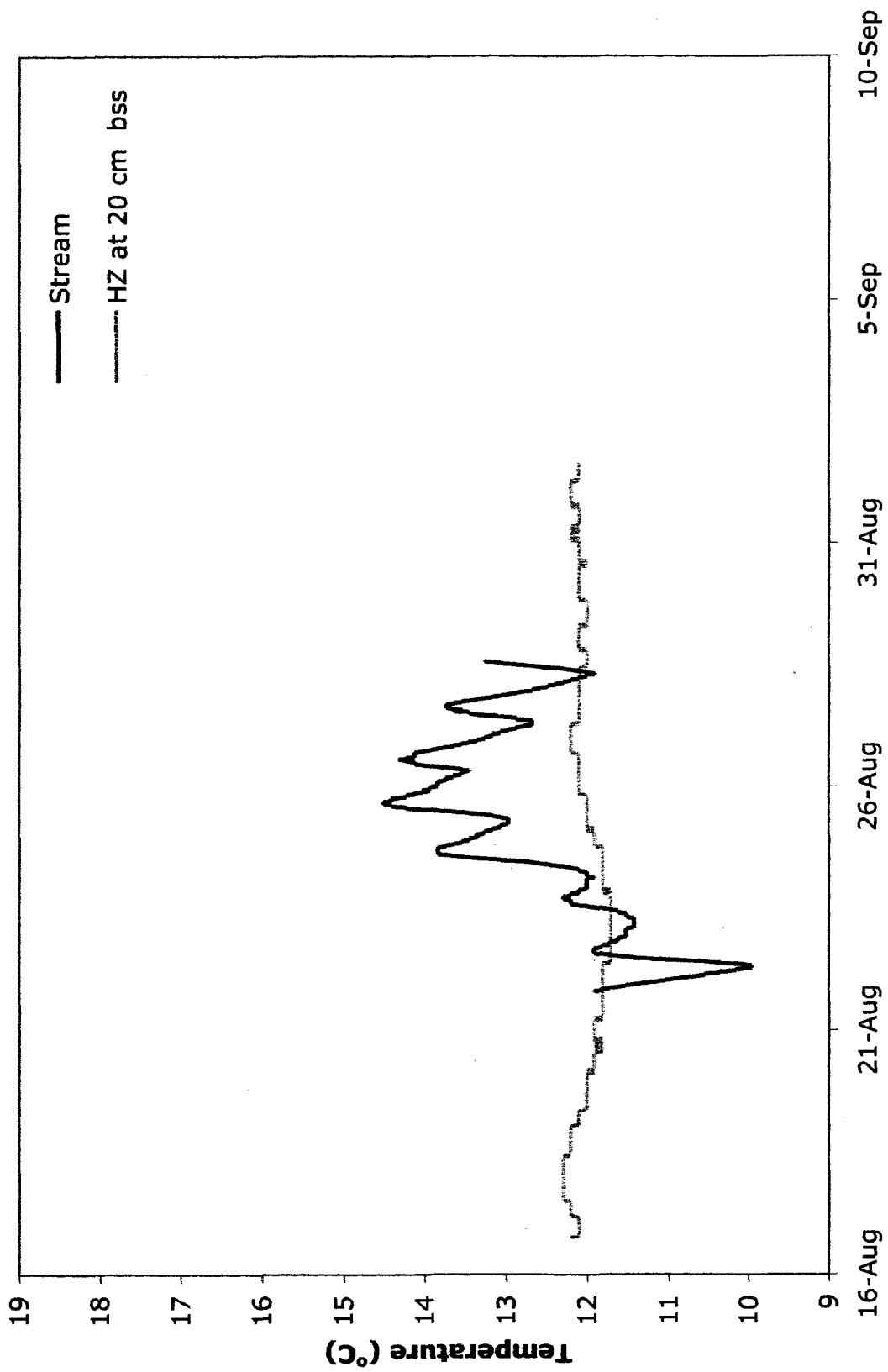


Stream and hyporheic zone temperatures at 486 m, August to September 2007
 Wednesday Hill Brook in Lee, NH



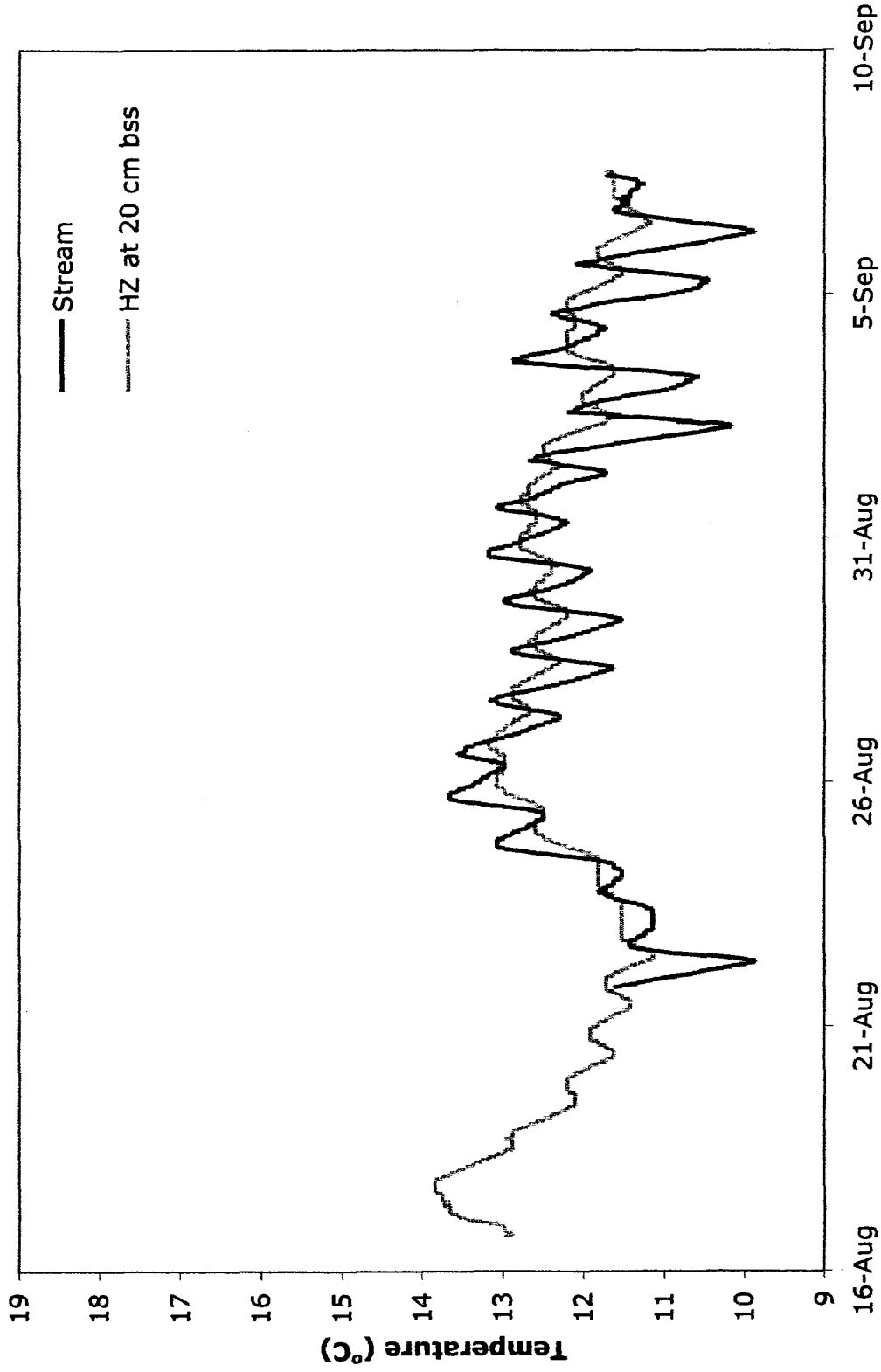
Date, 2007

Stream and hyporheic zone temperatures at 491 m, August to September 2007
 Wednesday Hill Brook in Lee, NH



Date, 2007

Stream and hyporheic zone temperatures at 525 m, August to September 2007
 Wednesday Hill Brook in Lee, NH



Stream and hyporheic zone temperatures at 634 m, August to September 2007
 Wednesday Hill Brook in Lee, NH